Exploring New and Emerging Mechanisms to Target Difficult to Treat Cancers

AUTHOR(S)

Catherine Richards

CITATION

Richards, Catherine (2019): Exploring New and Emerging Mechanisms to Target Difficult to Treat Cancers. Royal College of Surgeons in Ireland. Thesis. https://doi.org/10.25419/rcsi.10764086.v1

DOI

10.25419/rcsi.10764086.v1

URL

https://repository.rcsi.com/articles/thesis/Exploring_New_and_Emerging_Mechanisms_to_Target_Difficult_to_Treat_Cancers/10764086/1

RCSI

Exploring new and emerging mechanisms to target difficult to treat cancers

---

Catherine Richards BSc

Supervised by Dr. Ann Hopkins

Department of Surgery

Royal College of Surgeons in Ireland

A thesis submitted to the School of Postgraduate Studies, Faculty of Medicine and Health Sciences, Royal College of Surgeons in Ireland, in fulfilment of the degree of Doctor of Philosophy

Contents

Dedication

To my daughter Alyssa, forever my ray of sunshine

Acknowledgements

First and foremost, I would like to express my deepest, heartfelt thanks to my supervisor Dr Ann Hopkins, for your continual support, compassion and guidance throughout my PhD studies. I have had the pleasure to learn a great deal from you and I am grateful to you for your confidence in my ability to do well, even when my own seemed lost. I would like to thank Science Foundation Ireland for affording me the opportunity to conduct this research (grant number 13/IA/1994; to AMH).

I would also like to thank past and present members of the Hopkins group, who offered advice, support, and life-lasting friendships. Special thanks to Dr Yvonne Smith and Dr Emily Rutherford, who provided strength at times when I had none and celebrated all the successes with me – thank you for the many laughs! I would also like to extend those thanks to all those in the ERC, RCSI, particularly Molecular Medicine, Pathology and Respiratory groups for all their guidance, support and friendship during my time in the ERC, Beaumont Hospital.

To my family, thank you for all you have done to help me during what felt like a mammoth task. For all the childcare duties you each took on, the last-minute pick-ups and the party runs. I am unbelievably lucky and eternally grateful to you all.

To my partner Shane, without you this would not have been possible. Thank you for your unwavering support and love. I am truly blessed to have had you with me on this journey, celebrating my victories and wiping my tears. Thank you for pretending you understood what I was saying these past four years, and for being a willing practice audience for presentations. You have been my tower of strength.

Finally, I would like to thank my daughter Alyssa, for sharing me with the words written across these pages. For her patience and love, and her ability to put a smile on my face, often when I needed it most. Alyssa, you are my star.

Abbreviations

ADAM	A Disintegrin and Metalloproteinase domain-containing protein
APS	Ammonium persulphate
ATCC	American Type Culture Collection
ATP	Adenine triphosphate
BCA	Bichinchoninic acid
BSA	Bovine serum albumin
Cas-3	Caspase-3
cJAM-A	Cleaved JAM-A
CQ	Chloroquine
DAPI	4,6,-diamidino-2-phenylindole
DCIS	Ductal carcinoma *in situ*
ddH_2O	Distilled water
DMEM	Dulbecco's modified Eagle's medium
DMSO	Dimethylsulphoxide
DNA	Deoxyribonucleic acid
DTT	Dithiothreitol
ECL	Enhanced chemiluminescence
ECM	Extracellular matrix
EDTA	Ethylenediamene tetracetic acid
EGF	Epidermal Growth Factor
EGFR	Epidermal Growth Factor Receptor
ELISA	Enzyme-linked immunosorbent assay
EMT	Epithelial to mesenchymal transition
ER	Estrogen Receptor
ERK	Extracellular signal-regulated kinases
EtOH	Ethanol
FBS	Foetal Bovine Serum
FFPE	Formalin-fixed paraffin embedded
FISH	Fluorescent *in situ* hybridisation
H&E	Haematoxylin and Eosin
HCL	Hydrochloric acid
HER	Human Epidermal Growth Factor Receptor
HRP	Horseradish Peroxidase
JAM-A	Junctional Adhesion Molecule-A
Lap	Lapatinib
mAb	Monoclonal Antibody
MAPK	Mitogen-associated protein kinase
NGS	Normal goat serum
PCR	Polymerase chain reaction
PDX	Patient derived xenograft
PI3K	Phosphatidylinositol-3-Kinase
PR	Progesterone Receptor
rcJAM-A	Recombinant Cleaved JAM-A

RNA	Ribonucleic acid
RPPA	Reverse phase protein array
RTK	Receptor Tyrosine Kinase
SDS	Sodium dodecyl sulphate
siRNA	Short interfering RNA
TBS	Tris buffered saline
TEMED	N,N,N,N-tetramethylethylenediamine
TMA	Tissue Microarray
TNBC	Triple Negative Breast Cancer
TNM	Tumour, Node, Metastasis
Tras	Trastuzumab
UV	Ultraviolet

Summary

Gastro-oesophageal cancers are associated with poor survival in patients, due to their aggressive nature, late-stage diagnosis, and a lack of specific targeted therapies. The development of new therapeutics will prove crucial to improve mortality rates. This thesis discusses two novel potential approaches which merit further investigation towards this goal.

Firstly, natural compounds have previously found several uses as chemotherapeutic agents. We found a diterpenoid compound in the same class as Taxol, Crassin, to have significant anti-cancer effects in both gastro-oesophageal cell lines and triple negative breast cancer cell lines. Specifically, Crassin reduced cell viability in a manner dependent on reactive oxygen species, and demonstrated bioefficacy in an *in ovo/semi-in vivo* model. Interestingly, Crassin did not activate any known cell death mechanisms but rather induced cell stasis through cell-cycle shifts from G1 to G2/M. Since research is highlighting cytostatic inducers as powerful agents in combatting cancer growth, particularly when combined with cytostatic compounds, we suggest that Crassin is a candidate for further development as an anti-cancer agent.

Secondly, we examined other potential therapeutic targets in gastro-oesophageal cancers. Previous work in our lab has shown that overexpression of the adhesion molecule Junctional Adhesion Molecule-A (JAM-A) drives proliferation and tumorigenic behaviour in breast cancer. We hypothesised that the overexpression of JAM-A in gastro-oesophageal cancers may play a similar role in driving cancer progression. Furthermore, our group has highlighted a regulatory role of JAM-A for receptor tyrosine kinases (RTKs), including HER and Eph family members. Since gastro-oesophageal cancers are also known to overexpress HER2, we also hypothesised that JAM-A may play an important role driving HER2 overexpression and downstream cell survival. Gastro-oesophageal cell lines demonstrated varied responses to JAM-A loss, but no universal effects on cell

viability, colony-forming potential or tumour development and invasion in an *in ovo/semi-in vivo* model. We could find no apparent mechanism of regulation between JAM-A and three RTKs examined, though some correlations between JAM-A and HER2 and JAM-A and EphB4 expression were discovered in gastro-oesophageal cancer full-face sections. We suggest this is representative of aggressive tumour phenotypes. Excitingly, in JAM-A reduced cells, we identified a 'primed' state characterised by increased apoptosis efficacy of HER2 targeting therapies *in vitro*. Hence, we propose JAM-A targeting in this setting, in combination with pro-apoptotic chemotherapies merit future investigation as a "priming" mechanism for treatment of oesophageal cancers

In summary, we have examined potential mechanisms for targeting gastro-oesophageal cancers and have also highlighted a complex role for the adhesion protein JAM-A in that setting. Given the accessibility of JAM-A at the surface of cells, we suggest that targeting JAM-A in this setting could prove beneficial in priming cells for other drugs.

Chapter 1: Introduction

1.1 Introduction to Cancer

Cancer Overview

After cardiovascular disease, cancer is the second leading cause of mortality worldwide (1). Normally, cellular growth and differentiation is subject to tight homeostatic regulation that ensures normal functioning of cells. In cancer, cells undergo a series of genetic mutations which change cellular functions and allow them to develop one or more survival or growth advantages (2). These changes can occur as germ-line mutations, or can be acquired sporadically via external influences including environmental, lifestyle (i.e. tobacco and alcohol use) and dietary factors (3). The cocktail of changes usually occur in genes referred to as oncogenes or tumour suppressor genes (4). The term oncogene refers to genes that undergo some form of gain of function (GOF) which drives cancer-promoting characteristics and allows for continued growth, evasion of cell death and promotion of invasion. Some well-known oncogenes that are mutated in cancer include *erb-b2* receptor tyrosine kinase 2 (ErbB2, neu or Human Epidermal Growth Factor Receptor-2 (*HER2*)) and phosphoinositide 3-kinase (*PI3K*) (4-6). Tumour suppressors are genes whose mutation induces a loss of function (LOF) preventing them from performing key roles in inhibiting proliferation and/or inducing cell death mechanisms (4, 6). There are several tumour suppressor genes which are commonly mutated in cancer, including *TP53* (the gene encoding p53 protein), phosphatase and tensin homolog (*PTEN*) and retinoblastoma protein (*RB*); all of which play a role in regulating genomic instability of cells (4-6).

Hallmarks of Cancer

There are several functional changes that confer tumorigenic phenotypes upon cells. These phenotypes have been established as the 'hallmarks of cancer', which classify the different mechanisms that cells use to continue their growth and survival (2). To date, 11 well-defined hallmarks have been so described **(Figure 1.1) (2)**. These are: sustaining proliferative signalling, resisting cell death, activating invasion and metastasis, avoiding

immune destruction, inducing angiogenesis, tumour-promoting inflammation, deregulation of cellular energetics, genomic instability, evading growth suppressors, and enabling replicative immortality (2). When a cell has acquired one, or several, of these hallmarks it then replicates and passes the phenotype to its daughter cells, initiating tumourigenesis. Following several replications, these cells undergo expansion and are then referred to as a tumour (7). The aggressiveness of tumours can vary based on the phenotypic characteristics they retain, which influences the severity of cancer in patients, and will be discussed in more detail in the following section.

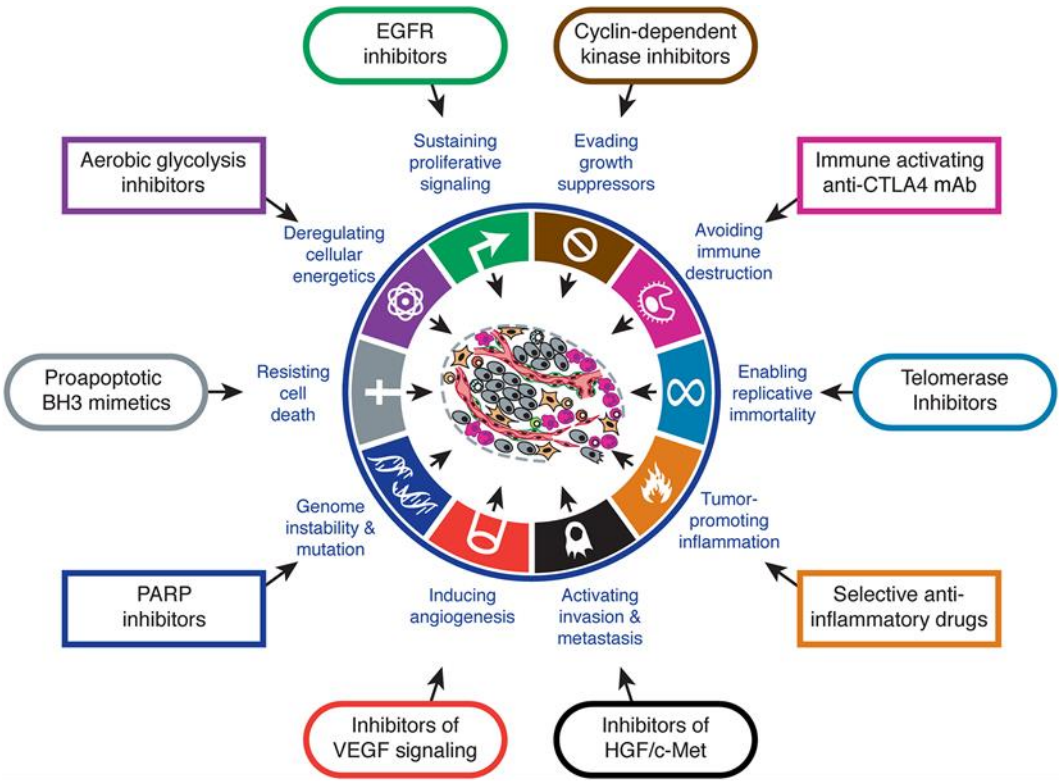

Hanahan & Weinberg (2011)

Tumour Aggressiveness

Tumour development and progression can be categorised and disease severity assessed by a number of approaches; towards enabling healthcare professionals to make informed decisions regarding treatment management for patients (8, 9). Most cancers are assessed histologically which provides prognostic information and establishes the stage of the disease (10-12). Using haematoxylin and eosin (H&E) stains, pathologists can assess and grade tumours based on the level of cellular differentiation observed; where poor differentiation indicates higher grade tumours (10). The standard approach for estimating tumour aggressiveness in many cancers is the TNM (tumour-node-metastasis) staging system. This tri-partite approach assesses the location of the primary tumour and its level of invasion (T), examines whether local lymph nodes have been invaded (N), as well as evidence whether the primary tumour has metastasised to distant sites (M) (8, 13).

1.2 Introduction to Breast Cancer

Breast Cancer Epidemiology

There are >20,000 new cases of cancer in Ireland each year and, while survival rates continue to increase, there are still ~10,000 cancer-related deaths per year (14). In fact breast cancer is the second leading cause of cancer-related deaths in women in Ireland, with over 3,000 new cases diagnosed and over 700 deaths annually (15). Recent improvements in survival have been attributed to improved early detection methods and expansion in the availability of targeted therapies (16). Current treatments for cancer patients comprise standard approaches including surgery, radiation, chemotherapy, targeted therapies, immunotherapy and hormone therapy (17). The hallmarks of cancer and the cellular characteristics that enable cancer progression have been extensively described (2), and now act as a markers for targeted therapies. However at the core of breast cancer biology is a need to understand the basic physiological structure and functions of the breast in order to guide a better understanding of the pathophysiology.

Breast Cancer Initiation and Progression

The normal function of the breast is lactation, the production of milk for neonatal and infant development. Accordingly the breast consists of epithelial structures which are specialised to perform this function: ducts and lobules **(Figure 1.2)**. Lobular structures contain epithelial milk-producing glands, which are hormonally activated during late stage pregnancy and post-natal periods (18). Milk then drains from the lobules to the nipple via a network of simple epithelial ducts supported by the connective and adipose tissue of the breast **(Figure 1.2)** (18).

There are two main types of breast cancer initiation sites: ductal or lobular. Cancers at either site arise when cells begin to grow at an increased rate, or develop genetic or epigenetic mutations enabling them to avoid cell death (2). If the tumour cells remain confined within the space of the original duct or lobule, this is referred to as *in situ* carcinoma. When the cancer cells move into the surrounding tissue, this is then referred to as invasive carcinoma (19) **(Figure 1.2)**. Invasive ductal carcinoma and invasive lobular carcinoma are the most common histological subtypes of breast cancer, accounting for ~80% and ~15% of cases respectively (20).

Breast Cancer Molecular Classification

Recent advancements in scientific technology have allowed the definition of

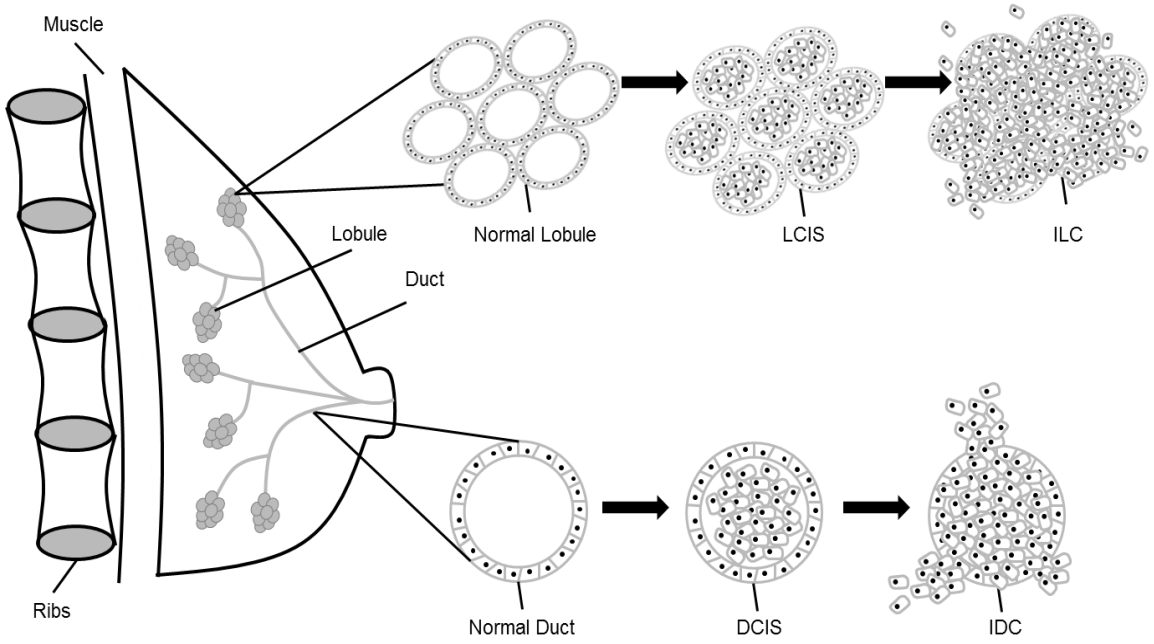

Figure 1.2: Anatomy of the breast and the progression from physiological to pathophysiological phenotypes, in both ductal- and lobular-type breast cancers. *This diagram denotes the normal structure of the breast and the predicted progression to either invasive lobular carcinoma (ILC) or invasive ductal carcinoma (IDC).*

genomic signatures for individual patient tumours, and represent improvements on diagnosis over histological features alone. This 'fingerprinting' of tumours is also i professionals to treat patients with the most suitable therapies for their subtype of tumour. Breast cancer has five established genomic subtypes based largely on protein expression of the following markers: estrogen receptor (ER), progesterone receptor (PR) and the human epidermal growth factor receptor-2 (HER2). ER- and PR-positive cancers are termed luminal A and luminal B or hormone receptor (HR)-positive, and make up two thirds of diagnosed breast cancers. Luminal B is additionally associated with increased expression of pro-proliferative genes and an increased risk of relapse (21, 22). Up to 25% of breast cancer patients have HER2-positive cancers (23, 24), a gene amplification first described in 1987 (25). Claudin-low and basal-like are triple-negative breast cancers, which describes their lack of ER, PR and HER2 expression (26, 27). Basal-like/triple-negative breast cancers (TNBC) account for 12-20% of all cases and are typically associated with poor prognosis and higher risk of early recurrence (26). Accordingly they are insensitive to many targeted therapies, so their treatment frequently relies upon conventional chemotherapeutic drugs (27).

Table 1.1: Molecular Subtypes of Breast Cancer. Hormonal, HER2 and Ki67 status in the molecular subtypes of breast cancer

Molecular Subtype	Hormonal Status	HER2	Ki67
Luminal A	ER+ and/or PR+	-	Low
Luminal B (HER2-negative)	ER+ and/or PR+	-	High
Luminal B (HER2-positive)	ER+ and/or PR+	+	Low or High
HER2/neu+	ER- and PR-	+	Low or High
Basal-like/Triple-negative	ER- and PR-	-	Low or High
Claudin-low	ER- and PR-	-	Low

Breast Cancer Treatments

Breast cancer treatment is dependent on the molecular subtype of breast cancer and the stage of disease progression. Surgery, radiation, chemotherapy and targeted therapies are standard treatment practices. In cancers that show a triple-negative phenotype, surgery, radiotherapy and chemotherapy are standard treatment approaches, as the lack of cell-surface markers limits targeted therapy options (28). This lack of appropriate targeted therapies also means that 30-40% of TNBCs progress to metastatic disease (29). Due to the aggressive phenotype of TNBCs, chemotherapies are used to target DNA repair and sometimes act as p53 substitutes (28). Taxanes, anthracycline and platinum agents are all commonplace in TNBC treatment regimens (28). More recently, androgen signalling has been shown to be an important player in some subtypes of TNBC, and it is now suggested that

androgen receptor-inhibiting therapies may prove beneficial in the TNBC setting (29).

Approximately 70% of breast cancers are HR-positive, and the presence of either ER or PR recommends them for targeted hormonal therapies. Along with surgery, radiation and chemotherapy, selective estrogen receptor modulators and down regulators (SERMs and SERDs respectively), as well as aromatase inhibitors, all work to block signalling capabilities through hormone receptors and to prevent tumour growth (30, 31).

The growth factor receptor HER2 has had several targeted therapies directed against it, which work effectively to block the downstream signalling cascades of HER2 that drive tumour growth (32). Therapies such as Trastuzumab, Pertuzumab, lapatinib and afatinib are all approved HER2-directed therapies; however resistance to therapy still remains an issue within this subtype of breast cancer (32).

1.3 Introduction to Gastro-oesophageal Cancers

The Normal Gastro-oesophageal Tract

The main function of the oesophagus is to transport swallowed food to the stomach, via a network of striated and smooth muscles. The oesophagus has a secondary function, which is to block the contents of the stomach from being able to flow back up into the oesophagus via the lower oesophageal sphincter **(Figure 1.3)**. This 'backflow' is referred to as ga(33). Once the oesophagus has successfully transported the food bolus into the stomach, the main function of the stomach is to prepare this food for digestion and its later absorption by the intestine (34). Gastric acid production by the stomach ensures that the food is broken down enough to be released into the small intestine (34). Structurally, the oesophageal epithelium consists of stratified squamous epithelium versus simple columnar epithelium in the stomach. This change in nature is facilitated at the gastro-oesophageal junction, where both epithelial cell types are found (35).

Gastro-oesophageal Cancer Epidemiology

Gastric cancers are the fourth most common cancer worldwide and have the second-highest associated mortality rate (36, 37).

Both genetic and environmental risk factors have been linked to the incidence and progression of gastric cancers, with dietary factors having a large impact. High fruit and vegetable intake; particularly those with higher levels of antioxidants; low-sodium diets and lower alcohol consumption are all thought to decrease the risk of gastric cancer development (37-39). In contrast, poor socioeconomic backgrounds, smoking and *Helicobacter pylori (H. pylori)* infections all increase gastric cancer development risk (38, 39). Genetic risk factors include germline mutations of the *CDH1* gene (the gene encoding E-cadherin) (40-42), and *TP53* (42, 43).

There has been a steady decline in incidence worldwide, which has often been attributed to improved levels of hygiene and diet, as well as the

eradication treatment now available for *H. pylori (37, 39)*. In Europe, five-year survival rates for gastric cancers are poor at only 20%, whereas in Japan survival is as high as 90% due to superior screening methodologies (38, 39).

Oesophageal cancers are the eighth-most commonly diagnosed cancer worldwide and the sixth leading cause of cancer-related deaths, with five-year survival rates as low as ~10% (44, 45). Risk factors include environmental factors such as alcohol, smoking and obesity, as well as genetic influences such as mutations to genes involved in cell-cycle regulation and growth factor receptors (45).

Interestingly, obesity and neoplastic inflammatory conditions (such as gastro-oesophageal reflux disease (GERD) and *H.pylori* infections) increase both gastric and oesophageal cancer development risk (39, 46-48), suggesting inflammatory responses could play an important role in the progression of this cancer type. Specifically, obesity is thought to increase the production of inflammatory mediators and cytokines (i.e. TNF-α and IL-6) (49, 50). Furthermore, an association between obesity and disrupted mitochondrial function has been highlighted, suggesting that obesity can alter energy metabolism, creating a suitable environment for cancer development (51).

Gastro-oesophageal Cancer Classification

Gastric cancers are typically classified by their anatomical location. Gastric cancers tend to be referred to as either cardial, when they originate in the uppermost part of the stomach; or non-cardial, when they arise in the mid or distal regions including the body, pylorus etc. **(Figure 1.3)** (39). Interestingly, *H. pylori* infections are significantly correlated with non-cardial gastric cancers at a rate of ~65-80% (37). There has been a longstanding appreciation for the relationship between infection-associated inflammation and increased cancer risk, not just in the gastrointestinal tract but also in other organ locations (52).

Oesophageal cancers are also distinguished from each other based upon their location. Oesophageal cancers originating higher in the oesophagus are usually squamous cell carcinomas (SCCs), whereas those which occur in the lower oesophagus are adenocarcinomas (44). These subtypes have different risk factors. While SCCs are mainly associated with lifestyle risk factors, including high levels of alcohol consumption, frequent hot drink intake and smoking, oesophageal adenocarcinomas are often related to GERD, which

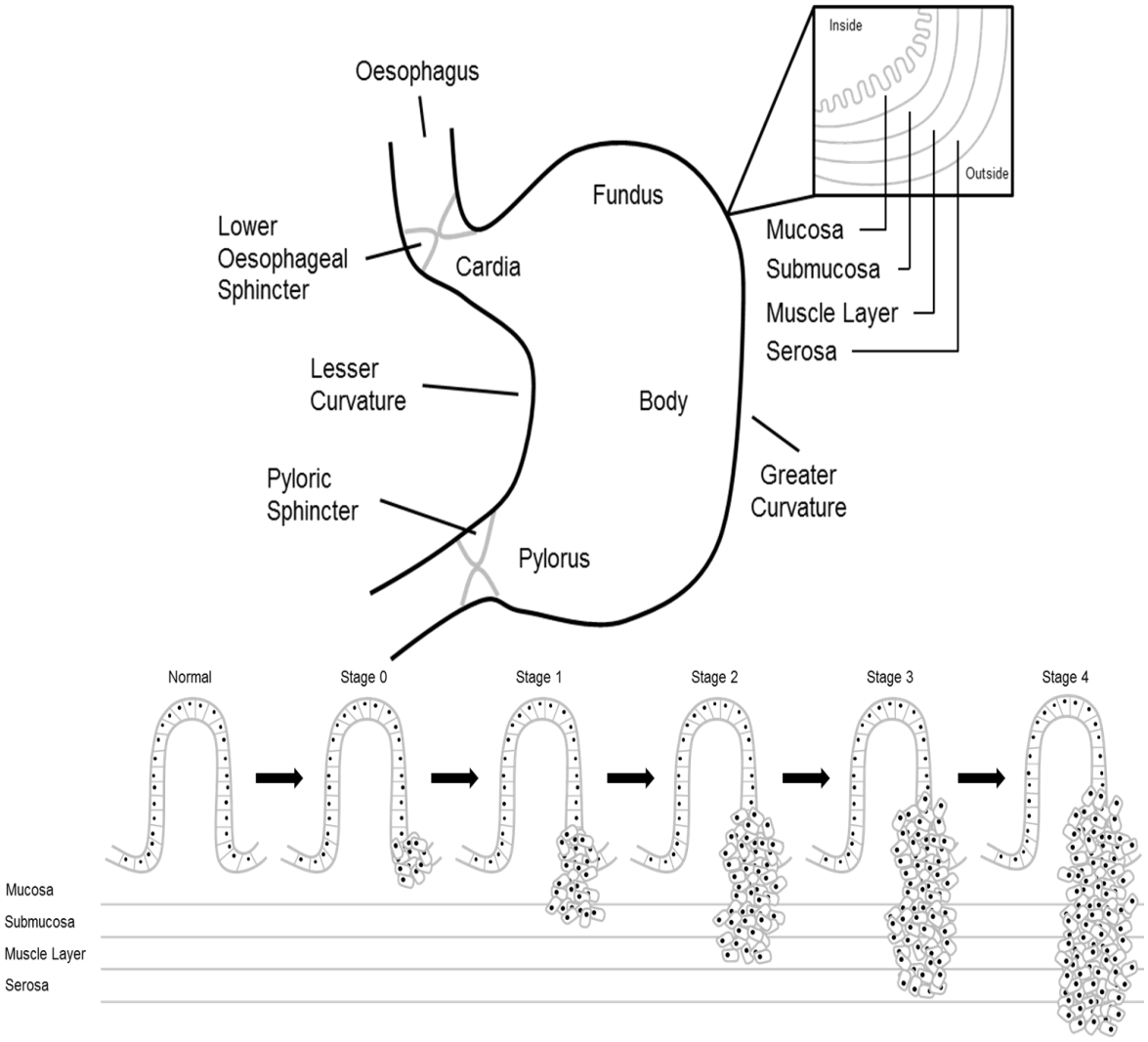

Figure 1.3: Anatomy of the normal human stomach, and a schema for progression from normal physiology to cancer pathophysiology. *This diagram represents the normal anatomical structure of the stomach and the progression of normal tissue to invasive gastric cancers with assigned staging.*

can progress to Barrett's oesophagus; a risk factor for oesophageal cancer development linked to inflammation-induced progression (44, 53-56). Interestingly, obesity; a known risk factor for oesophageal cancer progression; has been highlighted to significantly increase the risk of GERD in patients (57), and in creating molecular changes which result in the development of both GERD and Barrett's oesophagus, a pre-requisites of adenocarcinomas, prevalent found within the region (58, 59).

Due to the close physical proximity of gastric, gastro-oesophageal and oesophageal adenocarcinomas, an anatomical classification method known as the Siewert classification was devised (60). Type I tumours are defined as distal oesophageal adenocarcinomas, Type II describes adenocarcinomas of the cardia immediately at the gastro-oesophageal junction, and Type III status is allocated to adenocarcinomas that are subcardial but also infiltrate the gastro-oesophageal junction and distal oesophagus (60). Overall, Type I adenocarcinomas are classified as oesophageal, whereas Types II and III are considered gastric.

Another diagnostically-useful way of distinguishing gastric cancers from each other is to use histopathological criteria to distinguish between intestinal- or diffuse-type cancers (61). This system separates cancers based on the morphological appearance of the tissues. Intestinal-type cancers tend to be well differentiated and grow slower in glandular forms with abundant cell-cell contact, whereas diffuse-type cancers are poorly differentiated, lack extensive cell-cell contact and are much more aggressive in comparison (61, 62). While intestinal-type cancers appear more frequently in older males, diffuse-type cancers occur equally in both genders but at a younger age (61, 62). The aggressiveness of both subtypes is defined according to the level of invasion of tumour cells into deeper surrounding tissues, using the TNM (tumour-node-metastasis) staging system (63). The World Health Organisation (WHO) further differentiates gastric cancers into adenocarcinomas, signet-ring cell carcinomas and undifferentiated carcinomas, but their classification is not universally accepted and is preferred (38). Signet-ring carcinomas are classed as diffuse-type under the

Lauren classification system, and are named due to their appearance, where the nucleus is visibly pushed to the outside edge of cells by cytosolic mucins, giving cells a 'signet ring' appearance (64).

Gastric cancers are also classified based on their initiating factor. Most commonly (~80%), gastric cancers are sporadic in nature and referred to as sporadic gastric cancers (SGCs). This cancer type is most frequently associated with environmental risk factors and more frequently occurs in older males (~60-80yrs) (38). Other gastric cancer subgroups include early onset gastric cancers (EOGCs), gastric stump cancers and hereditary diffuse gastric cancers (HDGCs), occurring at a rate of ~10%, ~7% and ~3%, respectively. EOGCs occur more frequently in females, are often diffuse in nature and hormonal regulation is believed to be an important factor in their progression (38). HDGCs are associated with germline mutations, particularly those in *CDH1* (which encodes E-cadherin), and generate poorly-differentiated and diffuse-type gastric cancers (38, 40, 42).

Gastro-oesophageal Cancer Treatments

A multidisciplinary approach is required for the treatment of gastric and oesophageal cancers. Like in breast cancer; surgery, chemotherapy, radiotherapy and more recently targeted therapy are all utilised for the best patient survival outcomes. In gastroesophageal cancers, early stage cases require less invasive surgeries, and endoscopic resection can often be used. However, a risk of relapse still remains, so other measures are taken in combination. Late stage cancers require much more radical intervention, including both sub- and total gastrectomy or oesophagectomy (60, 63).

Chemotherapy is often administered peri-operatively, meaning it is given both pre- and post-surgery; also referred to as neo-adjuvant (pre) and adjuvant (post). Some studies have shown increased survival for patients who received chemotherapy regimens pre- and post-surgery, as opposed to surgery alone (65, 66). There is currently no worldwide standardised regimen practiced, however combinations of platinum-based drugs (e.g. cisplatin),

fluoropyrimidines (e.g. 5-fluorouracil) and Taxanes (e.g. paclitaxel) are often utilised for both first- and second-line therapies (65, 67, 68).

Furthermore, radiotherapy is often received by patients in a neo-adjuvant setting in combination with chemotherapy schedules and has been shown to increase overall survival of patients. More recently, neoadjuvant radiotherapy has also shown promising benefits for overall patient survival (69).

As in breast cancer, gene amplification of the oncogene *HER2* is emerging as an area of significant interest in the field of gastric and gastro-oesophageal cancers. HER2 is known to be overexpressed in ~10-35% of gastric and gastro-oesophageal cancers (70), hence the anti-HER2 therapy Trastuzumab has been approved as a targeted therapy for use in HER2-positive gastric and gastro-oesophageal cancers (71, 72). Current trials are examining whether multi-targeting HER2 therapies may prove beneficial in order to overcome associated resistance (73, 74). Section 1.4 will describe in more detail the contribution of HER2 overexpression/signalling to cancer initiation and progression.

Unlike breast cancer, gastro-oesophageal cancers have few known molecular subtypes and hence there is a lack of targeted therapies available in the neo-adjuvant setting (75). However, knowledge of the genetic makeup of these cancer types is ever evolving and given the recent advances in immuno-scoring in this setting, future research may even highlight immunotherapies as greatly beneficial for patients. Immuno-scoring is a complex process based on tumour immunophenotyping, which shows enormous promise in predicting clinical outcomes and patient chemotherapy responses (76). The method assesses tumour T lymphocyte populations; cytotoxic and memory T cell (76). This method has been shown to predict gastric cancer patient survival outcomes, as well as identify those at risk of reoccurrence (77, 78). PD-L1 positivity was also highlighted as a predictor of worsened survival in oesophageal cancer patients (79, 80). Since immunotherapies often utilise PD-L1 and its receptor (PD-1) expression, it is possible that this method of treatment may have great efficacy in this cancer setting.

1.4 The role of HER2 in cancers

HER2

HER2 belongs to a family of four type 1 transmembrane growth factor receptors (81) (**Figure 1.4)**; Epidermal Growth Factor Receptor (EGFR/HER1), HER2, HER3 and HER4. HER receptors undergo dimerization upon activation, leading to transphosphorylation and upregulation of downstream signalling pathways associated with proliferation, invasion, metastasis and cell survival (82). The *HER2* gene is located on chromosome 17 and encodes a 185 kDa protein with an extracellular, transmembrane and intracellular tyrosine kinase domain (81). HER2 has no known ligand, so it relies on activation by either heterodimerisation with other HER family members or homodimerisation when overexpressed (81). HER2/HER3 dimers have been shown to drive signalling through the PI3K/AKT pathway, a key player in tumour survival, as well as the Mitogen-Activated Protein Kinase (MAPK) pathway (81, 83, 84).

HER2 possesses the strongest downstream signalling capabilities of the four HER family members (81), and has been shown to be overexpressed in a variety of different cancers including breast, gastroesophageal, ovarian, non-small cell lung, head and neck, as well as pancreatic and colon cancers (85, 86). Both breast and gastroesophageal cancers have been approved for targeted therapy with anti-HER2 drugs, as HER2 overexpression is reportedly present at rates of ~25% and ~10-35% in breast and gastro-oesophageal cancers respectively (24, 70, 72).

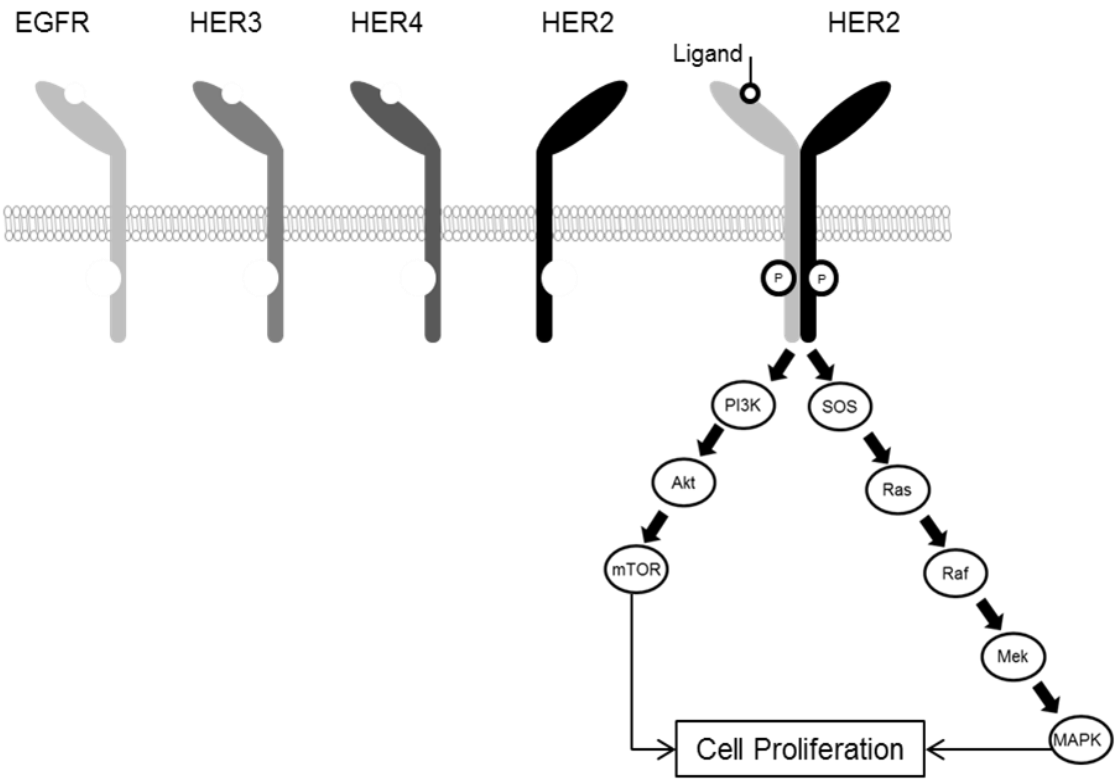

Figure 1.4 The Human Epidermal Growth Factor Family. *HER2 activation occurs following heterodimerization with another HER family member, in the presence of a ligand, leading to autophosphorylation of their tyrosine kinase domains and activation of the PI3K (phosphoinositide-3-kinase) and MAPK (mitogen-activated protein kinase) downstream signalling pathways which drive cellular proliferation and anti-apoptotic signalling.*

The Phosphoinositide 3-kinase (PI3K) Pathway

The PI3K enzymatic pathway was discovered in the 1980s and is known to be a key player in cell survival, proliferation and differentiation. The various PI3K family members become activated in response to ligand/growth factor binding to receptors including HER family members and Insulin-like growth factor-I Receptor (IGF1R) (87-90). There are three classes of PI3Ks: Class I, II and III; of which Class I forms are frequently mutated in cancers (91). Class I PI3Ks have two subunits, a regulatory (p85) and a catalytic (p110) subunit. The p85 regulatory subunit has three different p110 catalytic subunit has four forms (p110α, p110β and p11

where α and β ubiquitously while γ and δ are more common found in immune cells (87, 92).

The p85 subunit of Class I PI3K enzymes is responsible for interacting with the tyrosine phosphate motifs on activated receptors (including the HER family members), either directly or through adapter proteins (87). This interaction catalyses activation of the p110 subunit, which in turn results in the addition of a phosphate molecule to phosphatidylinositol (4,5)-bisphosphate (PIP2), transforming it to phosphatidylinositol (3,4,5)-trisphosphate (PIP3), which activates downstream signalling (87) **(Figure 1.5)**. The active PI3K pathway is terminated by means of the tumour suppressor protein phosphatase and tensin homolog (PTEN), which converts PIP3 back to PIP2 by dephosphorylation and accordingly inhibits downstream signalling effects. Hence, loss of function mutations to PTEN have been commonly described in a range of different cancers, including breast and gastric (93). Mutations to PTEN alone are often enough to account for the cancer burden associated with PI3K pathway disruption, however a synergistic effect of mutations to both PTEN and PI3K in the same tumour has previously been shown (94, 95).

Following the conversion of PIP2 to PIP3, Akt (or protein kinase B) is phosphorylated and activated. Akt is an important member of the PI3K pathway, responsible for the phosphorylation-induced inhibition of several tumour suppressor genes. For example, Akt-mediated phosphorylation of the tuberous sclerosis complex 2 (TSC2; tuberin) protein displaces the protein tuberous sclerosis complex 1 (TSC1) protein bound to TSC2 (96). TSC1 is responsible for stabilising and preventing the proteasomal degradation of TSC2. When no longer bound to TSC1, TSC2 is then free to bind 14-3-3 protein, activate Rheb and in turn the mechanistic target of rapamycin (mTOR) complex, which is responsible for promoting cellular proliferation and growth as well as inhibiting autophagy (97). Akt is also known to inhibit PRAS-40, a negative regulator of mTOR. Specifically, Akt phosphorylates PRAS-40, rendering it inactive and allowing mTOR signalling (97). Another important target of Akt is the transcription factor Forkhead box protein O (FoxO), which is phosphorylated and inhibited by active (phosphorylated) Akt, thereby

preventing the transcription of several genes that induce apoptosis, reduce cell cycle progression or inhibit growth (97). Active Akt also phosphorylates and inhibits glycogen synthase kinase 3 (GSK3), which is responsible for downregulating the important oncogene c-Myc through the inh catenin (97).

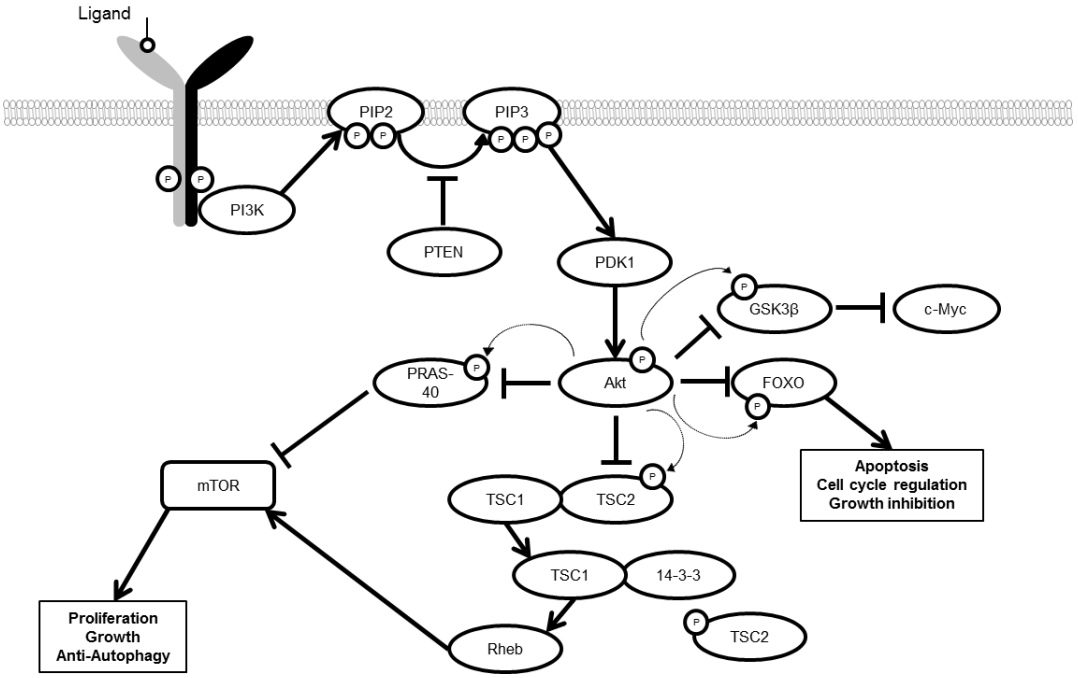

Figure 1.5 The PI3K pathway. *Activation of PI3K results in the addition of a phosphate molecule to PIP2 (phosphatidylinositol 4,5-bisphosphate), transforming it to PIP3 (phosphatidylinositol 3,4,5-trisphosphate), which begins a cascade of downstream signalling events resulting in proliferation and anti-apoptotic effects in cells. This signalling pathway is inhibited in the presence of PTEN (phosphatase and tensin homolog), which reverses the PIP2 to PIP3 pathway via removal of a phosphate molecule.*

The mitogen-activated protein kinase (MAPK) pathway

The MAPK pathway is another important signalling pathway responsible for driving cellular proliferation in cancers overexpressing HER2. Following the autophosphorylation of tyrosine residues in HER2 homo- or hetero-dimers, the adapter protein growth-factor receptor bound protein-2 (GRB-2) binds to a receptor tyrosine kinase (RTK) (e.g. HER family dimers) and recruits the small GTP-binding protein son of sevenless (SOS) (98). SOS then binds RAS, activating the kinase, which phosphorylates and activates RAF kinase (99). Upon RAF activation, MAPK kinase (MEK) is then phosphorylated and, in turn, phosphorylates ERK. Once activated via phosphorylation, ERK translocates to the nucleus and upregulates the expression of several transcription factors targeting genes involved in cellular proliferation and growth (including c-Jun, c-Fos and Elk1) (98, 99).

Upstream regulation of both the PI3K and MAPK pathways is known to occur through several diverse cellular proteins. One such category of proteins of particular interest for this thesis, adhesion proteins, has previously been shown to affect Akt activation (100-102). The structure and function of adhesion proteins in both normal physiology and cancer pathophysiology will be discussed in more detail in the next section.

1.5 Cell Adhesion in Cancers

Tight Junctions

Epithelial cells attach to each other along their lateral intercellular membranes via multi-protein complexes termed intercellular adhesive junctions. Tight junctions are the apical-most intercellular junctions, and play an essential role in maintaining barrier function and controlling paracellular diffusion and the movement of solutes (103-106). Following their assembly, tight junctions play a key role in the maintenance of cell polarity, which is essential for tissue differentiation and development (107).

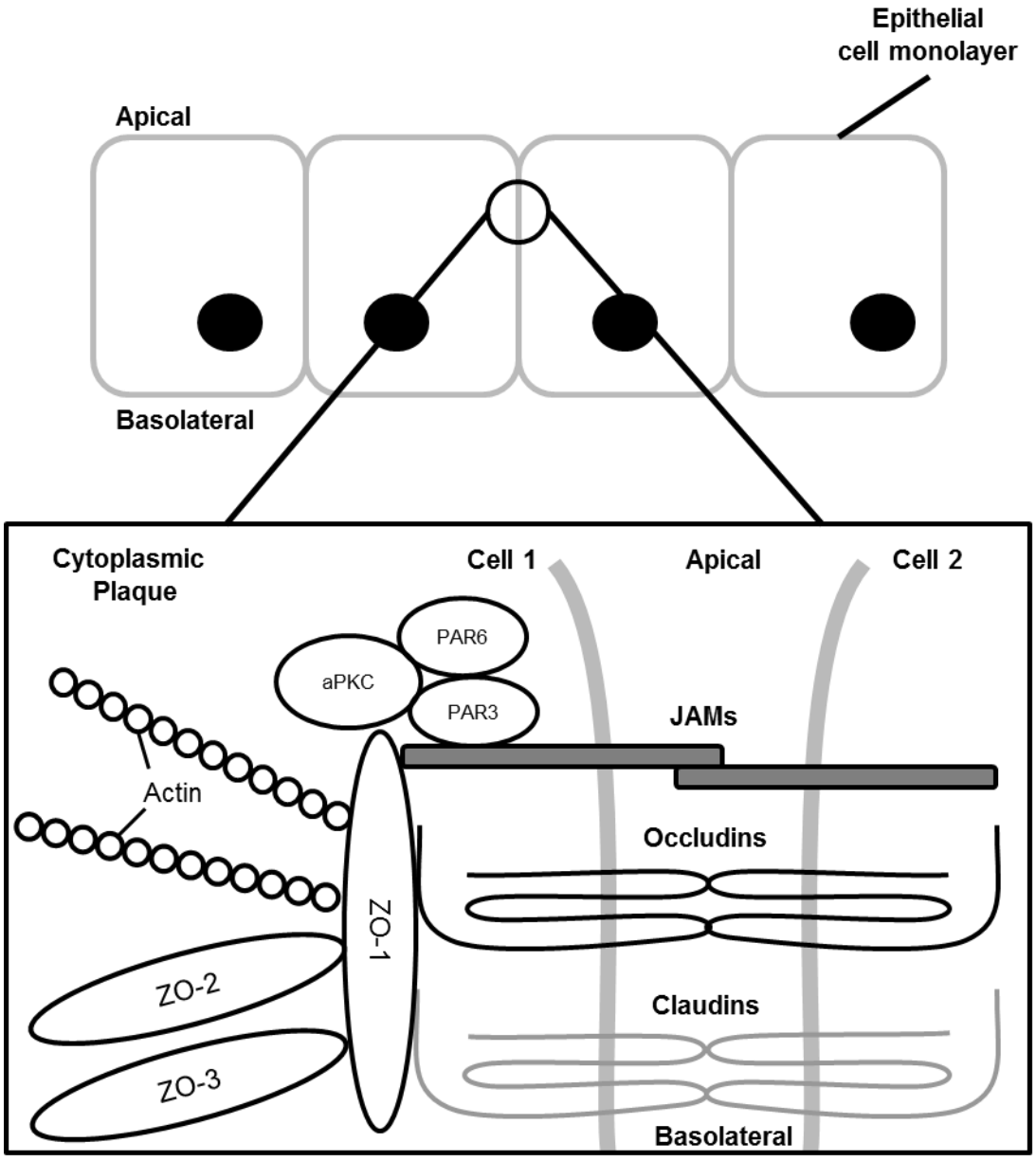

Figure 1.6: Tight Junction Location and Composition. *This diagram denotes the position of the tight junction in delineating the apical versus basolateral domains of epithelial cells. It also illustrates the 3 types of proteins found within this complex, specifically transmembrane, scaffolding and signalling proteins.*

There are several different classes of proteins found at the tight junction, including transmembrane, scaffolding and signalling proteins **(Figure 1.6)** (108, 109). The transmembrane proteins encompass both tetra-span and single-span proteins. Tetra-spanning protein families include claudins and the myelin and lymphocyte and related proteins for vesicle trafficking and membrane link (MARVEL)-domain containing proteins occludin, tricellulin and MARVELD3 (103, 104, 107). Single-spanning proteins include the junctional adhesion molecule family (JAM: JAM-A, -B, -C and –4), Coxsackievirus and Adenovirus receptor (CAR), as well as crumbs protein homolog (CRB3) (103, 104, 107, 110, 111).

Such proteins are linked to adapter protein complexes found within the cytoplasmic plaque, which act as connectors and signal transducers between the transmembrane or scaffolding proteins and the cytoskeleton (103, 107). Zona occludens (ZO)-1 is one such example with important roles in the tight junction. It has several protein-interacting domains, including a PSD-95, discs large, ZO-1 (PDZ)-domain and a guanylate kinase (GUK)-domain, which allow for interactions with transmembrane proteins like occludin as well as with actin within the cytosol (**Figure 1.5)** (103, 107). Studies have highlighted the importance of PDZ-binding domains and PDZ binding motif-containing proteins in forming the connections found at intercellular junctions (112).

Despite the many important physiological functions of tight junction proteins, a role for their expressional or functional alterations has been emerging in the pathophysiology of several diseases including cancer. Several tight junction proteins were originally connected with the pathophysiology of various infections, by virtue of their actions as receptors for viruses including reovirus, coxsackievirus and adenovirus (103, 106, 107). In addition, disruption to tight junction proteins has also been associated with hypertension (113, 114) and deafness (115, 116). However of most interest to this thesis is the fact that both LOF and overexpression of various different tight junction proteins has been recently associated with the pathophysiology of cancer. Of particular relevance is the TJ protein JAM-A, which will be described in more detail in the following section.

Junctional Adhesion Moleculeï A

JAM-A (also known as JAM-1, CD321, PAM-A or F11R) belongs to the immunoglobulin (Ig) protein superfamily of proteins and is widely expressed on both epithelial and endothelial cells (110, 112).

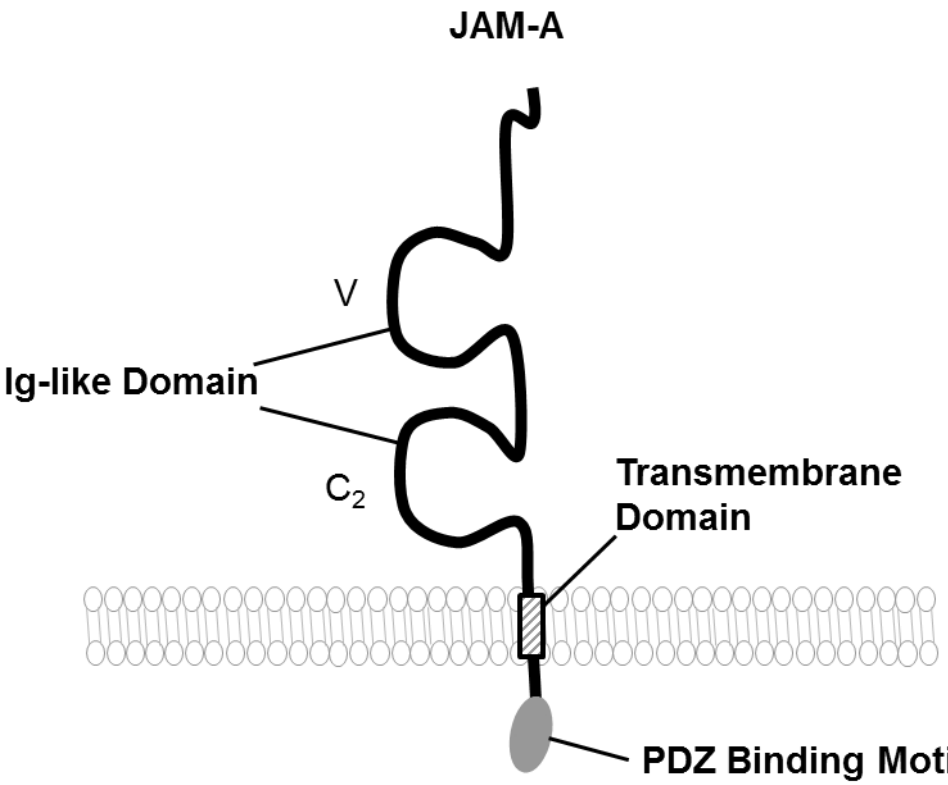

Figure 1.7: Junctional Adhesion Molecule A. *Schematic diagram of the structure of JAM-A, including the Ig-like domains, transmembrane domain and PDZ binding motifs.*

JAM proteins undergo homophilic interactions with JAM proteins on neighbouring cells, helping to create the paracellular barrier **(Figure 1.6)** (110, 112, 117). Its structure is characterised by two Ig-like domains found in the extracellular domain, a single-pass transmembrane domain and a canonical Type II PDZ binding motif located in its short C-terminal tail **(Figure 1.7)** (112, 118, 119).

JAM-A has been demonstrated as a key player in regulating and maintaining cellular polarity through interactions with adapter proteins, including ZO-1, afadin-6 (AF-6) and PDZ-containing polarity-related protein-3 (PAR3) via its PDZ-binding motif (112, 120, 121). During the early formation of cell-to-cell contacts, JAM-A has also been shown to recruit a complex containing PAR3, aPKC and PAR-6, which is known to regulate cellular migration and to dictate cell polarity (120).

JAM-A in Cancer

Aberrant expression of JAM-A has been shown to be involved in several different carcinomas, though it is often debated as to whether LOF or overexpression is more important in certain tissue settings. Loss of JAM-A has been associated with poorer survival of patients with either gastric or renal cancer (122, 123), as well its downregulation being reported in breast metastases (124). JAM-A overexpression leading to poor prognosis and cancer cell growth has since been established in other solid tumour types, including gastric, nasopharyngeal and lung, as well as suggestions that JAM-A may be an important player in cancer stem cell maintenance (102, 125-129).

1.5.1.1 JAM-A and Breast Cancer

Pathophysiologically, JAM-A *downregulation* was first reported as driving cancer invasion in breast cancer models (130). However research using larger scale models rather demonstrated JAM-A *upregulation* in invasive breast cancers to be associated with poor patient prognosis (131, 132). Furthermore, JAM-A overexpression has been associated with HER2-positive subtypes of breast cancer, and JAM-A has been proposed as a novel regulator of HER2 expression via influencing its protein degradation (100). JAM-A silencing has also been shown to be involved in reducing cell motility, as well as reducing the expression of the β1-integrin (131), itself a marker for poor prognosis in breast cancer patients. This highlights a potential mechanism of driving cancer progression via upstream regulation of HER2. In addition, JAM-A-targeting with either miRNA or antagonists reduced tumour

progression (126, 133) The discrepancies regarding oncogenic properties of JAM-A may have occurred through differences in scientific methodologies, including patient selection and *in vitro* models, or more likely it reflects a complex role for JAM-A in different spatial and temporal settings associated with tumour growth and metastasis.

1.5.1.2 JAM-A and Gastro-oesophageal Cancers

As previously discussed, HER2 is now known to be overexpressed and clinically-targetable in cancers other than breast, including those in the gastroesophageal tract. However there is ongoing debate as to whether JAM-A overexpression also plays an important role in gastro-oesophageal cancer progression and its potential as a therapeutic target in the gastro-oesophageal cancer setting (122, 127).

In support of a possible role, JAM-A has previously been shown as a key player in *H. pylori* infection via its recruitment by cytotoxin-associated gene A (CagA) protein. CagA is translocated by the bacteria into gastric epithelial cells, where it recruits JAM-A and impairs assembly of tight junctions at bacterial contact sites (134-136). In light of the known disruption of tight junctions during infection, as well as the previously-mentioned links between infection, inflammation and increased cancer risk, this could potentially place tight junctions as key players in cancer. However there is a paucity of studies on the role of JAM-A in either gastric or oesophageal cancer. The one published study in oesophageal cancer saw no increase in JAM-A protein expression in oesophageal tumour tissue samples compared to normal controls (133). Furthermore, studies in gastric cancer have been controversial, suggesting both JAM-A protein loss and overexpression as potential biomarkers for poor patient prognosis (122, 127). Specifically, one study revealed low JAM-A protein expression in gastric tissue sections had a significant correlation with increased tumour size and lymph node metastasis (122). In contrast, *in vitro* work across gastric normal and cancer cell lines revealed a significant reduction in proliferation and invasion following JAM-A silencing. Furthermore, the same study showed correlations between the

expression of JAM-A and an anti-apoptotic protein, Bcl-XL, following reduction of JAM-A (127). These disparate studies highlight the need for a deeper understanding of the mechanisms that drive JAM-dependent tumour-promoting properties in this tissue setting. Complementary to this would be to uncover if regional differences in JAM-A expression exist within the gastro-oesophageal spectrum, thereby allowing for the differential promotion or suppression of local cancers.

2. Statement of Hypothesis

2.1 Hypothesis

In light of the novel evolving relationship between HER2 and JAM-A in breast cancer, we hypothesise that the same relationship occurs in other cancers featuring HER2 overexpression. We further hypothesise that JAM-A acts as an upstream regulator of HER2 expression and signalling.

3. Aims of This Thesis

3.1 Aims

As expressional changes in JAM-A represent a potential biomarker of poor prognosis in cancers, the global aim of this PhD project is to evaluate the mechanistic role of JAM-A in invasive cancers. In particular the thesis will focus on examining whether JAM-A acts as a predictor of poor prognosis or a novel therapeutic target in cancers outside of the breast, and in determining whether the JAM-A/HER2 crosstalk established in breast cancer is mirrored in other cancers known to overexpress HER2. With that in mind, the specific aims of the work are as follows:

Specific Aim 1: To elucidate the mechanism of a novel natural compound in gastro-oesophageal and breast cancers.

Specific Aim 2: To establish whether there is a correlation between the expression of JAM-A and HER2 in HER2-positive gastro-oesophageal cancers.

Specific Aim 3: To uncover mechanisms of crosstalk between JAM-A and HER2 in both breast and gastro-oesophageal cancers.

Specific Aim 4: To explore whether JAM-A is responsible for regulating other receptor tyrosine kinases in gastro-oesophageal cancer settings.

Chapter 2: Materials and Methods

2.1 Cell Culture

2.1.1 Aseptic Technique

All cell culture was performed in a class II laminar flow hood using aseptic technique. Laminar flow cabinets were swabbed with 70% ethanol (EtOH) or 70% industrial methylated spirits (IMS) before and after use, and all items brought inside were thoroughly sterilised. Only one cell line was manipulated at a time in the cabinet, after which time the hood would undergo 15 mins disinfection with ultraviolet light (UV). Liquid waste was disposed of in chlorine-based disinfectant (Presept tablets VWR, 330773N;1 x 2.5 g tablet/500 ml waste). The hood underwent monthly cleaning using industrial Virkon, followed by sequential water EtOH or IMS wipe-downs. Incubators were maintained with 10 ml of microbiocidal agen Acryl Aqua Clean (WAK Chemie Medical, WAK-AQA-250) diluted to a volume of 2 L in sterile distilled water and were routinely cleaned in the same manner as flow hoods. A separate laboratory coat was kept for aseptic work.

MDA-MB-231, 4T1, SKBR3, NCI-N87 cells were obtained from the American Type Culture Collection; OE33 cells were a kind gift of Dr. Anne Marie Byrne, Trinity College Dublin. ESO26, OE19, SNU16 and KATO III cells were a kind gift from Dr. Sinead Toomey, RCSI. Cell line characteristics described in **Table 2.1.** Human primary breast cancer cells (198T) were isolated from a triple-negative breast cancer patient as described (137) with ethical approval from the Beaumont Hospital Medical Ethics (Research) Committee. MDA-MB-231 cells were cultured in Dulbecco's (Sigma-Aldrich, Poole, UK) supplemented with 10% Foetal Bovine Serum (FBS), 50 U/mL penicillin, 50 µg/mL streptomycin and 2 mM L-glutamine. 4T1, NCI-N87, ESO26, OE19 SKBR3, SNU16 and OE33 cells were maintained in RPMI 1640 cell culture medium (Sigma) supplemented with 10% FBS, 50 U/mL penicillin and 50µg/mL streptomycin. KATO III cells were maintained in Iscove's Modified Dulbecco's Medium (Sigma) supplemented with 20% FBS, 50 U/mL penicillin and 50 µg/mL streptomycin. Primary cells (198T) were maintained in DMEM/HAMS F12 (Sigma) supplemented with EGF (Peprotech,

#AF-100-15, 10 ng/mL), Hydrocortisone (Sigma #H-4001, 0.5 µg/mL), Insulin (Sigma, #I-5500, 5 µg/mL), Bovine Pituitary Extract (BPE; Sigma, #p1476, 70 µg/mL), Transferrin (Sigma, #T-2252 5 µg/mL), Ethanolamine (Sigma, #E9508, $1x10^{-4}$ M) and O-phosphoethanolamine (Sigma, #P-0503, $1x10^{-4}$ M).

Table 2.1 Characteristics of Cell Lines

Cell Line	M/F	Tumour Site	Differentiation	Td (h)	Mutation Status	Tumourigencity	Histopathology
Gastric Call Lines							
N87	M	Stomach (Liver Metastasis)	Well	47	ERBB2, TP53	+	Intestinal-type Adenocarcinoma
OE33	F	Lower Oesophagus (Barrett's)	Poor	33	TP53	+	Adenocarcinoma
ESO26	M	GEJ	Not Known	35-50	ERBB4, PIK3CA, TP53	+	Adenocarcinoma
OE19	M	GEJ	Moderate	50-60	ADAM10, CDH1, TP53	+	Adenocarcinoma
KATO III	M	Gastric /Pleural Effusion Metastasis	Not Known	36	CDH1, PIK3CA	+	Diffuse type - Adenocarcinoma
SNU16	F	Gastric/ Ascites Metastasis	Poor	27	KRAS, TP53	+ (in semi-solid medium)	Adenocarcinoma
Breast Cell Lines							
MDA-MB-231	F	Breast/Pleural Effusion Metastasis	Poor	38	KRAS, TP53	+	Adenocarcinoma
4T1		Mouse Mammary Gland	Not Known	22.9	-	+	Adenocarcinoma

2.1.2 Mycoplasma Testing

MycoAlert mycoplasma detection kits (Lonza LT07-418) were used four times/year (or more frequently, if indicated) to test cell lines for mycoplasma. MycoAlert is a colorimetric assay which measures the ratio of ADP/ATP conversion in supernatant samples extracted from conditioned medium. According to the manufacturer's protocol, readings of >1.2 indicated mycoplasma-positive samples and cells were discarded. Negative samples returned a ratio of <1. Borderline samples were retested with fresh supernatant samples 24h post initiall read.

2.1.3 Cell Culture Subculturing

Cell culture media was warmed to 37°C. Cells were grown to ~80% confluency in T75-cm^2 tissue culture flasks and washed with sterile Phosphate Buffered Saline (PBS). Following the removal of PBS, 2mL of trypsin-EDTA (concentration of 1x (0.05% Trypsin in 0.02% EDTA) for all breast cancer cell lines or 10x (0.5% trypsin and 0.2% EDTA) for all gastro-oesophageal cancer cell lines) was then added to cells, which were incubated at 37°C until fully detached, as observed under a light microscope. 10mL of fresh cell culture medium was added, whereupon cells were transferred to a 15mL tube and centrifuged at 300 x relative centrifugal force (rcf)/3mins.

2.1.4 Cell Culture Freezing Stocks

Following detachment and centrifugation of confluent cells, cell pellets were re-suspended in freezing medium (the appropriate cell culture media plus 5% dimethylsuphoxide (DMSO) as a cytoprotective agent). Cells collected from one T75-cm^2 flask were re-suspended in 3mL freezing medium and aliquoted at 1mL into cryovials, where they were placed at -80°C for 24h in a cryo 1°C freezing container. After 24h, cryovials were placed into a liquid nitrogen tank for long term storage.

2.1.5 Cell Culture Cell Stock Recovery

For cell recovery, cell aliquots in liquid nitrogen were removed from liquid nitrogen and rapidly thawed at 37°C. Cells were then placed into a 15 mL tube and spun at 300 rcf/3mins. The DMSO-containing supernatant was removed, whereupon cells were re-suspended in 10mL fresh cell culture medium and placed in a T75-cm^2 tissue culture flask. The cells were then maintained in a humidified tissue culture incubator at 5% CO_2 and 37°C.

2.1.6 Cell Counting

Following subculturing, cells were re-suspended in 3 mL cell culture medium. 10 µL of cells was added to 10 µL of trypan blue (Sigma, #T8154, 0.4%) (1:1) and loaded onto a haemocytometer. Cells were counted across four of the haemocytometer quadrants using a light microscope (as shown in **figure 2.1)**. In order to calculate the mean number of cells per mL, the mean of the quadrants was calculated and multiplied by two (dilution factor of trypan blue) and then multiplied by a factor of 10^4.

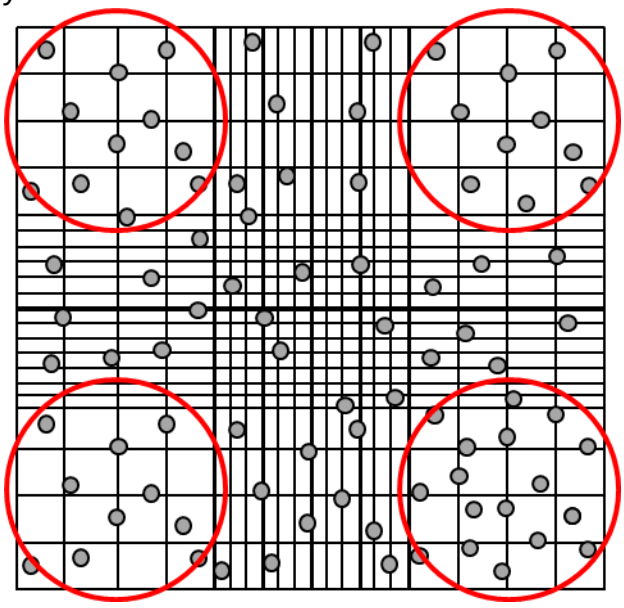

Figure 2.1 Representation of a Haemocytometer

Cells are counted in the four outer quadrants (circled). Cells on the out edges within these quadrants, falling into the inner space are discounted from the final tally.

2.2 Pharmacological Treatments

2.2.1 Drug Treatments

The coral-derived diterpenoid compound Crassin (Crassin/S-Benzyl-N-malonylcysteine) was kindly donated by the US National Cancer Institute (NCI) Developmental Therapeutic Programme (DTP; www.dtp.cancer.gov; compound reference NSC-210236) and dissolved in DMSO (20mM stock). Cells were treated following their specific doubling periods with a range of Crassin concentrations (0.3, 0.6, 1.25, 2.5, 5, 10, 20 µM). All treatments were in complete media. DMSO at the concentration corresponding to matched Crassin treatments (0.0015625, 0.003125, 0.0625, 0.0125, 0.025, 0.5, 0.1 % v/v) was used as vehicle control.

The antioxidant N-acetyl-L-cysteine (NAC; Sigma, #A7250) was made fresh before each treatment (10mg/mL in sterile PBS pH7.4, sterile-filtered) then added to the desired concentration (3mM) in complete media and incubated for 1h before the addition of Crassin. Fresh NAC was re-added in parallel with Crassin.

2.2.2 HER2-Targeting Drugs

Trastuzumab (21mg/mL) was donated by Beaumont Hospital Pharmacy, and dissolved in sterile ddH_2O. Cells were treated with a concentration of 10µg/mL, with sterile ddH_2O (0.0475% v/v) as vehicle control. Lapatinib (Lap; Sequoia Research #SRP01211l) and dissolved in DMSO to a stock concentration of 10.8mM. Cells were treated with a concentration of 2µM, with DMSO (0.0185% v/v) as vehicle control.

2.2.2 Cell death Inhibitors and Inducers

Necrostatin-1 (Sigma, #N9037) was dissolved in DMSO (10mg/mL) and used at 100µM, Ferrostatin-1 (Sigma, #SML0583) was dissolved in DMSO (10mg/mL) and used at 5µM, and Doxorubicin (Dox) was dissolved in DMSO (4µg/mL) and used at 2.5µM. These were incubated +/- Crassin or NAC for 24/48 hours at 37°C. In the same manner as NAC treatments, cells were pre-

treated with either Nectrostatin-1 or Ferrostatin-1 and compounds re-added following 1 hour incubation +/- Crassin or NAC. DMSO (0.025% v/v) was used as vehicle control. The pro-apoptotic agent staurosporine (Staur) was dissolved in H_2O (1mg/mL) and used at 10µM/3h or 1µM/48h for western blot or flow cytometric positive controls (respectively).

2.2.3 RNA Synthesis Inhibition

Actinomycin-D (Actino-D) (Calbiochem #114666) stabilises topoisomerases I and II, inducing RNA synthesis inhibition. Actino-D was reconstituted in DMSO (2mg/mL) and cells were treated at 4µM/6h. Cleaved caspase-3 antibody was used as a positive control for western blotting.

2.2.4 Lysosomal Protein Degradation Inhibition

Chloroquine (CQ) is an anti-malarial therapy shown to inhibit lysosomal degradation of proteins *in vitro.* CQ was reconstituted in ddH_2O (5mg/mL) and used at 30µg/mL. LC3BI/II antibody was used as a positive control for western blotting.

2.3 Protein Expression Analysis

2.3.1 Whole Cell Lysate Preparation

Cell lysates were prepared by washing confluent cells on 6-well plates 3 times with ice-cold PBS, before being scraped in 200µL of extraction buffer. RIPA and Relax buffer (Appendix D) were used in breast and gastro-oesophageal cancer cell lines respectively. Cells were then triturated 20 times through a 26-gauge needle. Cells extracted using RIPA buffer were stored on ice for 10 minutes and incubated at -80°C for 24h. Thawed samples were centrifuged (15300 rcf, 20 minutes, 4°C) and supernatants stored at -20°C. Cells extracted using Relax buffer were centrifuged at 1500rcf/5min following trituration, and the supernatant collected and stored at -20°C.

2.3.2 Protein Quantification

The protein concentration within cell lysates was determined using a highly sensitive and selective colorimetric detection of the cuprous cation (Cu^{1+}) by bicinchoninic acid (BCA). Bovine serum albumin (BSA) was dissolved in ddH_2O to a stock concentration of 5mg/mL, whereupon serial dilutions (5, 2.5, 1.25, 0.625, 0.3125, 0 mg/mL) were then used as assay standards. 10µL of each sample (and standard) was added in duplicate to 96-well cell culture plates. 200µL of freshly-mixed, light-protected BCA reagent A and B (1:50 dilution) (Pierce, 23225) was then added to each sample. Plates were incubated in the dark (30min/37°C) and absorbance measured at 560nm using a VICTOR™ X3 Multilabel Plate Reader (Perkin Elmer). A standard curve was generated based on the BSA serial dilution concentrations and the unknown protein concentrations of samples calculated based on a linear curve fit.

2.3.3 SDS-Polyacrylamide Gel Electrophoresis (SDS-PAGE)

Proteins for western blot analysis were separated using SDS-PAGE. Resolving and stacking gels were prepared according to requirements (Appendix E). Resolving gels were cast using 10cm x 8cm gel cassettes consisting of glass front and spacer plates (BioRad) and 0.75mm plastic separating combs (BioRad). Resolving gels were cast first and left to set for 20min-1h, covered by 70% EtOH. The layer of 70% EtOH was then poured off, the stacking gel poured on top and the separating comb inserted to generate wells for sample loading. Equivalent protein concentrations (calculated via BCA assay) were mixed with 6x Laemmeli sample buffer (Appendix D), whereupon they were heated at 100°C/5min and placed on ice. Samples and 10µL of protein ladder (pre-stained broad range molecular weight markers) were then loaded and electrophoresed (40mA/gel, or 35V/gel for caspase-3 gels), using a Bio-Rad Mini-Protean II gel system in Tris-glycine running buffer (Appendix D).

2.3.4 Western Blot Analysis

Proteins were wet-transferred to nitrocellulose membranes using the Bio-Rad Mini-Protean blotting system (100V/75 min or 200mA/2h for caspase-3). Membranes were then stained with Ponceau S (Appendix D) and photographed, before being de-stained with TBS washes. Membranes were blocked for 1h with 5% (w/v) milk or BSA in 1xTBS containing 0.1% (v/v) Tween-20 (TBS-T), then incubated with primary antibody (Appendix A) overnight at 4°C. Following 3x 5min washes in TBS-T, horseradish peroxidase (HRP)-tagged anti-mouse or anti-rabbit secondary antibody was incubated for 1 hour at room temperature (RT). After incubation, membranes were washed a further 3x 5min in TBS-T, after which membranes were immersed in enhanced chemiluminescence solution (ECL; Millipore Immobilin Western #WBKLS0050) for 1 minute before being imaged in a Bio-Rad ChemiDoc MP imager.

2.3.4 Stripping of Membranes

In order to remove previously probed membranes of bound antibody, membranes were washed 3 times for 5 min in TBS-T and then stripped in either β-mercaptoethanol-based buffer (Appendix D) (65°C/15 min), or Restore Western Blot Stripping Buffer (Thermo Scientific) (RT/10-15min) prior to being washed and Western blotted for a second antigen. Densitometry for actin was used as an internal reference point for signal intensities between treatment groups.

2.3.5 Statistical Analysis of Protein Expression

Volume intensity of western blot bands was calculated using Image lab software 5.2.1 where the protein of interest intensity was calculated relative to the loading control. Average mean data (± standard error of the mean (SEM)) values from western blot experiments were calculated and graphed using Graphpad Prism 7, Experimental data (n=3) were statistically tested with one-tailed, unpaired t-tests (*$p<0.05$, **$p<0.01$, ***$p<0.001$)

2.4 Viability Assays

2.4.1 Alamar Blue

Cellular viability was measured via Alamar Blue-Resazurin (Invitrogen DAL1025) assays as follows. Various cell numbers were plated in 96-well plates (see individual figures). After drug incubations, media was aspirated and Alamar blue solution added to a final concentration of 10% Cell were incubated in the dark (5h/37°C), and fluorescence measured at 610nm using a VICTOR™ X3 Multilabel Plate Reader. performed using Graphpad Prism-6 software, and statistical significance (*p<0.05, **p<0.01, ***p<0.001) calculated following software-recommended tests and post-tests and described in individual figure legends.

2.5 Microbiology

2.5.1 Transient JAM-A Overexpression

Luria-Bertani broth (LB) (Fisher BioReagents #BP1426) and LB agar (Fisher BioReagents #BP1425) were prepared with distilled H_2O and autoclaved. Ampicillin (Amp) was then added to each preparation to a final concentration of 100µg/mL. LB-Amp agar was poured onto sterile plates in a class II laminar flow hood. Following setting and cooling of LB-Amp agar plates, inoculation loops were sterilised and used to streak plates with bacteria from commercially-available agar stabs containing Amp-resistant vectors. The vectors were as follows: empty backbone vector (EV) (FLAG-HA-pcDNA3.1 Plasmid #52535 addgastro-oesophagealne.org) or full-length human JAM-A vector (J+) (hJAM-A pcDNA3.1 Plasmid #70073 addgastro-oesophagealne.org). Cultures were incubated at 37ºC overnight in a shaking incubator.

2.5.2 Single Colony Selection

Single colonies were selected from either EV or J+ containing plates, inoculated into 5mL LB-Amp broth and incubated overnight at 37ºC in a

shaking incubator. Cultures were then inoculated into 45mL fresh LB-Amp broth and incubated overnight at 37ºC in a shaking incubator. 1mL of the LB-Amp broth containing either EV or J+ plasmid was then added to 1mL glycerol (Sigma, #G5516) and placed into long-term storage at -80ºC.

2.5.3 Plasmid Purification

Using a commercially-available plasmid plus prep kit (Qiagen), bacteria were centrifuged as per manufacturer instructions and plasmid DNA purified using the QIAvac 24 plus vacuum system. Collected samples were then assessed using the Nanodrop8000 spectrophotometer for DNA quantification at OD_{260nm}.

2.6 Transient siRNA-Mediated Gene Silencing or Overexpression

2.6.1 Transient siRNA-Mediated Gene Silencing of JAM-A

To determine the effect of JAM-A silencing on cell viability/proliferation and downstream protein expression, a pool of siRNAs targeting the F11R (JAM-A) gene were transiently transfected into various cell types using DharmaFECT-I (Dharmacon, USA #T-2001-02) transfection reagent according to the manufacturer's instructions. Non-targeting siRNA control siRNA pool [siNeg] (ON-TARGETplus non-targeting pool, Dharmacon #D-001810-10-05) or JAM-A siRNA ([siJAM-A1] - SASI_Hs01_00049785, Sigma-Aldrich, [siJAM-A11] - (see Appendix G), Dharmacon, Lafayette, USA), were pooled (siJp) and transfected into gastro-oesophageal cell lines at a final concentration of 25nM, whereupon both cell viability and protein expressional changes were analysed via Alamar blue assays and Western blotting respectively.

Briefly, cells were either plated at 2 x 10^5 cells per well in 6-well plates or at 5 x 10^3 cells per well in 96-well plates, and allowed to undergo one population doubling prior to transfection. siRNAs were diluted sterile ddH_2O to give final concentrations of 25nM, combined with DharmaFECT-I transfection reagent in 400µl additive-free medium and incubated at RT for 10 minutes. Antibiotic-free

media was made up by adding 10% FBS and 1% L-glut to the volume of medium required prior to adding it to each transfection plate (160µl / well for 96-well plates; 1.6mL/well for 6-well plates). Subsequently 40µl (96-well plate) or 400µl (6-well plate) of siRNA-DharmaFECT mixture was added to corresponding wells. Cells were incubated at 37°C with 5% $C0_2$ and extracted 96h post-transfection (unless otherwise stated in individual figures).

2.6.2 Transient JAM-A Overexpression

ESO26 cells were plated 72h prior to transient transfections, whereas NCI-N87 and OE19 cells were plated 24h prior to transfection (2 x 10^5 cells / well for 6-well plates; 5 x 10^3 cells / well for 96-well plates). For the transfections, 3µL of GeneJuice (Novagen) was added to 100µL of additive free media and vortexed briefly. 1µg of either EV or J+ vector was added to the mix and incubated for 10mins at RT. Either 1900mL or 190µL was then added to 6-well or 96-well plates (respectively), to which 100µL or 10µL of transfection mix was added to either 6-well or 96-well plates respectively. The transfection mix was replaced with fresh medium on ESO26 cells following 24h incubation; and on NCI-N87 and OE19 cells at 72h post-transfection. All cells were extracted for either RNA **(Section 2.8.1)** or protein analysis at 72h post-transfection.

2.7 Phenotypic Evaluation

2.7.1 Invasion Assay

Following transient JAM-A gene silencing or overexpression, invasive potential was assessed using a commercially available 96-well basement membrane extract (BME) cell invasion assay (Cultrex). Before invasion assessment, ESO26 and OE19 cells were transiently modified for both JAM-A overexpression and gene silencing (as previously described) in 6-well plates for either 72h or 96h (as stated) in triplicate. 4h prior to the assay being carried out, the 96-well plate was coated with 0.5X BME solution in the top chamber of assay plates and incubated at 37ºC in a humidified CO_2 Incubator. Next, transiently modified cells were trypsinised, each treatment condition counted, and 5 x 10^5 cells in 50µL additive-free media made up in triplicate.

The BME coat was aspirated and triplicate technical replicates placed in additive-free media in the top chamber of the assay plate, with either serum-containing or additive-free media placed in the lower chamber. Following a 24h invasion period, the top and bottom chambers were aspirated and washed using PBS wash buffer. Calcein-AM and cell dissociation solution were then added to the lower chamber (as per the manufacturer's instruct and incubated for 1h at RT. The top chamber was then removed and the bottom plate read for changes in fluorescence at 485nm excitation and 520nm emission. A standard curve of serial dilutions of both ESO26 and OE19 cell number (50,000, 25,000, 12,500, 625, 312.5, 0) was also generated in separate curves to extrapolate cell numbers from fluorescent outputs.

2.7.2 Colony Forming Assays

ESO26, N87 and OE19 cells were plated at 1 x 10^3 cells per well in 6-well plates. Following 7 days of establishment, cells were treated with various treatments/transient transfections (see individual figures). Following 72h incubation, treatments/transfections were removed from the cells, which were placed in additive-containing media. Cells were left to form colonies for a further 10 days, with a single media change given on the 7^{th} day post-treatment/transfection removal.

Upon completion of incubation, colonies were washed in PBS and fixed in 100% ice-cold EtOH at -20ºC for 20mins. Following fixation, plates were washed with PBS. 0.5% (v/v) Crystal Violet solution in ddH_2O was then added and incubated at RT for 20mins. Crystal violet was removed and each well was then washed 3x in PBS. Plates were left to dry. Plates were kindly photographed by Julie Workman (Department Molecular Medicine, RCSI) using a Canon EOS 7D camera, after which 1mL methanol was added to solubilise each well with gentle rocking for 30mins (138). Absorbance was then read at 595nm on a VICTOR™ X3 Multilabel Plat

2.8 qRT-PCR

2.8.1 RNA Extraction

In order to determine mRNA expression of JAM-A and other target genes in gastro-oesophageal cell lines, 2 x 10^5 cells per well were plated in 6-well plates and transfected after 96h with a final concentration of 25nM of either non-targeting siRNAs (siNeg) or JAM-A pooled (siJp) siRNA targeting JAM-A. Following 96h of transfection, total RNA was extracted by adding 1mL of TRI-Reagent (Sigma-Aldrich) to each well and transferring into 1.5ml tubes. Following 5mins incubation at RT, 100µL of chloroform was added to each sample, vortexed for 15s and incubated for 10mins at RT. The samples were centrifuged at 12,000 × g for 15mins at 4°C. The aqueous phase was then added to 250µl isopropanol. Following another 5min incubation at RT, samples were centrifuged at 12,000 × g for 15 minutes at 4°C, supernatants discarded and the RNA pellet re-suspended and washed in 75% ethanol, centrifuged at 12,000 × g for 5 minutes at 4°C, air-dried for 5–10 minutes and finally resuspended in 25 µL nuclease-free water.

2.8.2 RNA Quantification

RNA was quantitated using a NanoDrop8000 Spectrophotometer (Thermo Scientific, Waltham, USA) using the following formula: OD_{260nm} x Dilution factor x 40 = ng/ml RNA. Pedestals (upper and lower) were cleaned before and after use with nuclease free H_2O and Kim-wipes. Using the NanoDrop8000 software, “nucleic acid” was selected and the instrument blanked using 2 µL nuclease-free H_2O (or equivalent matched vehicle control for RNA samples). Pedestals were then wiped clean, samples loaded (1 µL) onto pedestals and read at ng/µL. A_{260}/A_{280} ratio of 1.8 is indicative of pure RNA when diluted in nuclease free water, but samples between 1.6-2.0 were observed and used. RNA samples were stored at -80ºC.

2.8.3 cDNA generation

Based on quantification, samples were calculated to give 500ug RNA in nuclease free H_2O. Using the QuantiTect Reverse Transcription Kit (Qiagen, Venlo, Netherlands) according to manufacturer's instructions, genomic DNA sequences were removed and reverse transcription carried out for cDNA generation.

2.8.4 Primer Design

Primers were designed under specific guidelines using the online tool Primer-BLAST (https:www.ncbi.nlm.nih.gov/tools/primer-blast) based on required gene sequence. Primers were selected to have GC content of between 40-60%, span 2 exons with an ideal product size of 100-200bp and T_m of ~60ºC. Primer sequences and final concentrations can be found in Appendix H.

2.8.5 qRT-PCR Analysis

Real time qPCR reactions were performed using a LightCycler 480 SYBR Green I Master Kit (Roche, Basel, Switzerland) according to the manufacturer's instructions, and analysis / System (Roche). The SYBR Green qRT-PCR programme measures fluorescent emission when the SYBR dye is incorporated into the DNA helix and hence fluorescent reads are proportional to the amount of double-stranded DNA generated during the programme. Samples first underwent a pre-incubation at 95ºC x 5 min. Amplification, annealing of primers and the elongation programme was set as follows: 95ºC x 10 sec, 56ºC x 10 sec (or 55ºC in some instances) and 72ºC x 10 sec (25 bases/sec), respectively. This 3 step cycle was repeated 40-45 times and cycle threshold (Ct) values generated based on the amount of DNA amplified. Experimental data then underwent analysis as follows: Average Ct values for all gene replicates, Delta Ct value between gene of interest and housekeeping gene for each experiment, average Delta Ct values between experiments (replicates), Delta-Delta Ct values (Delta Ct experiment - Delta Ct control) and finally Fold Change [2^(-Delta Delta Ct)].

2.9 Immunohistochemistry

2.9.1 Tissue Microarray Staining

Gastric cancer Tissue Microarrays (TMAs) (kindly donated by Prof. Karin Jirstrom, Lund University, Sweden) were stained for JAM-A (Abnova) (Appendix B) by Dr. Joanna Fay (Biobank Technician, Beaumont Hospital) and scored for membranous JAM-A expression with the assistance of Dr. Kathy Sheehan (Consultant Histopathologist, Beaumont Hospital). Analysis was conducted using a 0, 1+, 2+, 3+ semi-quantitative scoring system; where 0 denoted no staining, 1+ denoted weak, non-complete membranous staining, 2+ denoted weak complete membranous staining and 3+ was given for strong complete membranous staining. All images were obtained using an Olympus CKx41 microscope with Cell B imaging software at 20x magnification.

2.9.2 Full-Face Gastric Cancer Tissue Staining

Gastric cancer tissues from n=11 patients were kindly sectioned and stained for JAM-A or EphB4 by Dr. Tony O'Grady (Chief Med
Hospital) (Appendix B). Scoring of both JAM-A and EphB4 membranous staining was completed individually and with the assistance of Dr. Kathy Sheehan and Professor Elaine Kay (Consultant Histopathologists, Beaumont Hospital). Analysis was accomplished using a weighted ranking system, allocating 0.25 for every % graded 1, 0.5 for every % graded 2 and 1 given for every % graded 3. Based on this the overall score was then calculated per tissue section and ranked either low (<33), moderate (33-66) or high (>66) for JAM-A staining based on overall score. All images were obtained using an Olympus CKx41 microscope with Cell B imaging software at 20x magnification.

2.9.3 Cell Pellet Staining

The cell lines ESO26, NCI-N87 and OE19 were pelleted following sub-culturing, all trypsin was removed with a sterile PBS wash followed by re-centrifugation at 300rcf/3min, after which point PBS was removed. Cells were

re-suspended in formalin, then agar, then paraffin-embedded and sectioned to be stained for JAM-A, HER2 and HER3.

2.10 Immunofluorescence

ESO26 cells were plated at $5x10^4$ per well onto sterilised 13mm round glass coverslips in 24-well plates. After the indicated treatment incubation periods, cells were washed 2 times in 1mL PBS. Cells were then fixed in 500 µL ice-cold 100% ethanol at -20°C for 20 minutes. Cells were again washed twice in PBS before the inserts were removed and placed cell side down on 100µl of blocking buffer (5% goat serum in PBS). The primary antibody was then made up using the same diluent as blocking buffer (Appendix C). Inserts were placed into a humidity chamber onto 100µl drops of primary antibody and incubated overnight at 4°C. The next day, inserts underwent 3 x PBS washes in drops of PBS. The secondary antibody with fluorescent tag (either Alexa-fluor-488 goat anti-mouse IgG or Alexa-fluor-568 goat anti-rabbit IgG), was then made up using the same diluent and specific to primary antibody species at 1:200. Cells were incubated in 100µl drops for 1 hour at RT and then washed 3 times in PBS. The inserts were then placed cell side down onto slides using 5µl Vectashield mounting medium with DAPI (Vector Laboratories, Cat # H-1200). Images were then acquired using an LSM510 confocal microscope connected to a charge-coupled device camera.

2.11 Annexin-V Apoptosis Assay

Cell death was assessed using the BD FITC Annexin-V Apoptosis Detection Kit I (Becton Dickinson, #556547). Cells were plated at 300,000 cells/well in 6 well plates for 48 hours then treated with either vehicle control, Crassin (5µM) or Staur. (1µM) as a positive control. Cells were washed using chloride- and magnesium-free PBS (CMF-PBS) and trypsinized. Tubes were centrifuged (670 rcf/5 minutes) and washed 3x in CMF-PBS, following which the cell pellet was resuspended in 200µl incubation buffer and 5µl Annexin-V and 5µl propidium iodide (PI) dyes and incubated at RT for 15 minutes. Cells were gated and 20,000 analysed on a Beckman Coulter FC500 flow cytometer; and

% gated were recorded in order to generate mean ± SEM of experimental data (n=3) for analysis of cell death using Graphpad Prism 6 (conditions relative to vehicle control (DMSO 0.025% v/v)).

2.12 Cycle Cycle Analysis

Cytostasis of cells was assessed using the same method as Annexin-A Apoptosis Assay (without the staurosporine positive control). Cells were plated at 300,000 cells per well and treated with either vehicle control, Crassin (5µM) ± NAC (3mM). Cells were washed using chloride- and magnesium-free PBS (CMF-PBS) and trypsinized. Tubes were centrifuged (670 rcf/5 minutes) and washed 3x in CMF-PBS, following which the cell pellets were resuspended in 200µl incubation buffer and 5µl propidium iodide (PI) dye and incubated at RT for 15 minutes. Cells were gated and 20,000 analysed on a Beckman Coulter FC500 flow cytometer for peaks of G1/G2 of cell cycle staging; and % gated were recorded in order to generate mean ± SEM of experimental data (n=3) for analysis of cell death using Graphpad Prism 6 (conditions relative to vehicle control (DMSO)).

2.13 Lactate Dehydrogenase (LDH) Assay

Necrosis was assessed using Sigma LDH Assay Kits (#MAK066). MDA-MB-231 cells were plated at 5,000/well in 96-well plates and treated 36h later with Crassin or vehicle for 48h. Incubation with 1% (v/v) 10x Triton-X100 (45 minutes/37°C) was used as a positive control for maximum cell lysis. Plates were centrifuged (670 rcf/5 minutes) and the supernatant transferred to new plates. LDH Assay buffer and substrate mix were added as per product manual and incubated for 2 minutes. Following incubation, plates were spectrophotometrically read at 450nm on a VI Reader.

2.14 Bromodeoxyuridine (BrdU) Assay

Proliferation was assessed using Roche Cell Proliferation ELISA, BrdU kit (#11647229001, Sigma). Following Crassin treatment, cells were labelled with

BrdU labelling solution (per kit instructions) for 2h/37°C. The labelling solution was replaced with FixDenant solution (30 minutes/RT). This solution was then replaced by anti-BrdU-POD antibody for 90 minutes at RT, after which the cells were washed and incubated with substrate solution (10 minutes/RT) followed by stop solution (1M H_2SO_4). Plates were read at 450nm (reference 690nm) using a VICTOR™ X3 Multilabel Plate Reader

2.15 Chick Chorio-Allantoic Membrane (CAM) Assay

2.15.1 Xenograft Generation

Fertilised chick eggs were obtained from Shannonvale Hatcheries (Co. Cork) and gently washed with sterile ddH_2O in a primary culture hood. Eggs were then marked on top with a pencil line, to ensure they remain the correct way up throughout the assay and then stored in a cotton wool-padded incubator at 37°C (Day 0). On day 3, eggs were removed from the incubator, a small puncture wound made in the bottom right hand corner of the egg using an 18G needle and ~3mL of albumin was withdrawn **(Figure 2.2)**. A small window was then cut on the top of the egg and re-covered with a semi-permeable membrane. On day 7, T-75 flasks were treated with either siNeg or siJp (final concentration 25nM). On day 8, the semi-permeable window was re-opened, and a silicon ring (removed from cyrovials and washed in EthOH, followed by ddH_2O) was placed on top of each CAM. $2x10^6$ ESO26 cells (either untreated or 24h-treated siNeg or siJp), previously pelleted, were resuspended in 50µL of additive-free RPMI-1640 plus 50µL Matrigel and slowly added (dropwise) into the centre of the silicon rings. The window was re-covered using fresh semi-permeable membrane and eggs replaced at 37°C. On days 10 and 12, untreated ESO26- containing eggs were treated with either Crassin (1.15µM) or vehicle control (DMSO) at a total volume of 15µL dropped directly onto the model xenografts sitting on the silicon rings. On days 10 and 13, siNeg- and siJp-treated eggs were re-treated with siRNA (25nM final concentration) in 15µL final volume dropped directly onto cell mass within silicon rings. The eggs were then replaced at 37°C. On day 14,

the embryos were sacrificed and the tumour xenografts extracted by removal of surrounding CAM (cutting 1cm diameter around silicon ring).

2.15.2 Xenograft Fixation and Immunohistochemical Analysis

Xenografts were fixed overnight in formalin and transferred to 70% EthOH the following day. Tumours were then paraffin-embedded, sectioned by Lance Hudson (Department of Surgery, RCSI) and immunohistochemically stained for Ki67, cytokeratin, JAM-A and HER2 (by Dr. Joanna Fay, Histopathology). Ki67 was scored as either positive or negative based on the presence of Ki67-positive cells. Cytokeratin staining was observed and noted as either present or absent; evidence of invasion beyond the Matrigel plug was also noted. Both JAM-A and HER2 were scored as previously described, as either 0,1+, 2+ or 3+ based on intensity and completeness of membranous staining.

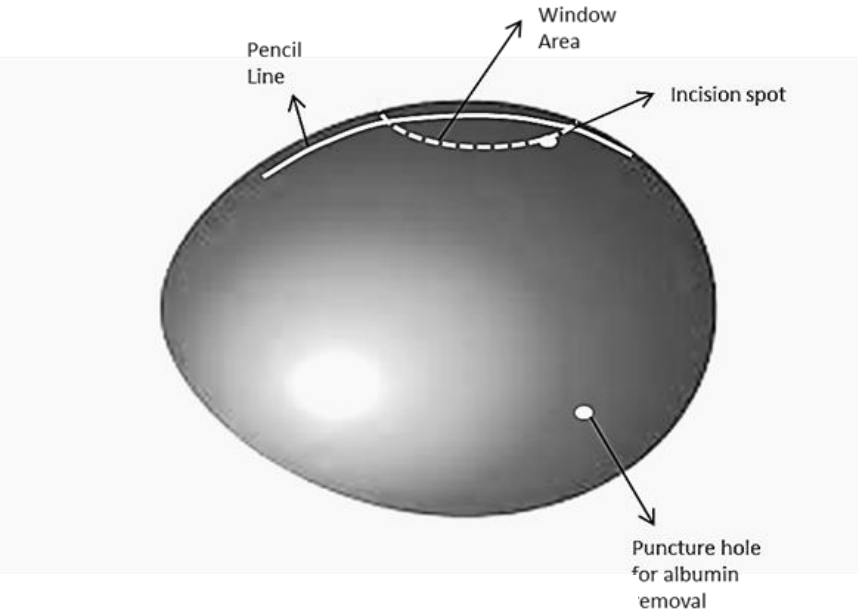

Figure 2.2 Representation of a CAM Assay Day 0

2.16 Kaplan Meier Curve Online Generator

An online tool was used to generate Kaplan Meier curves examining patient survival data in the context of publicly-available gene expression datasets. This online tool, which allows users to select probes for their genes of interest, was used to examine the expression levels of several genes of interest in different cancers. The generator was found at www.kmplot.com and the green colour coded boxplots were generated as described in figure legends. The breast cancer generator is referenced in this paper (139) and the gastric cancer generator is referenced here (140).

2.17 JAM-A ELISA Analysis for Cleaved JAM-A

RayBiotech ELISA (enzyme- linked, immunosorbent assay) kits were used to quantify levels of cleaved human JAM-A in cell culture supernatants via coating of a specific human JAM-A antibody onto 96-well plates. Supernatants were extracted from ESO26, NCI-N87 and OE19 cells in which JAM-A had been transiently silenced (siJp versus negative control siNeg; 96h) overexpressed (EV or J+; 72h). Samples were then flash frozen at -80ºC pending the collection of n=3 experimental replicates. Samples were then thawed on ice and BCA assays performed to ensure adequate levels of protein for all samples. The JAM-A ELISA was performed by Dr. Emily Rutherford in order to assess the levels of cleaved JAM-A found in cell line supernatants. Standards of recombinant JAM-A were generated via serial dilution ranging from 50ng/mL-13.72pg/mL JAM-A. 100µL of each cell line supernatant condition was added in duplicate to 96-well plates coated with JAM-A antibody and incubated with gentle shaking for 2.5h at RT. Solutions were then discarded and washed 4x using 1x wash buffer. Following the complete removal of wash buffer, 100µL of biotinylated antibody was added to each well and incubated for 1h at RT while gently shaking, The solution was then again discarded and washed as before. 100µL of HRP-streptavidin was added to each well and incubated for 45mins whilst gently shaking. The solution was again discarded and washed as previously described. 100µL of TMB one-step substrate was added to each well and the plate was incubated

in the dark at RT for 30mins whilst shaking. Following this incubation, 50µL stop solution was added and the plate read immediately at 450nm using a VICTOR™ X3 Multilabel Plate Reader.

2.18 Statistical Analysis

Statistical analysis between groups was carried out using unpaired student t-tests (unless otherwise stated in figure legends). All analysis was completed using GraphPad Prism 7 or SPSS statistical software, where data was either tabulated or graphed as mean ± standard error of the mean (SEM). Experiments requiring different statistical analysis are described in more detail within individual figure legends.

Chapter 3: Coral-Derived Crassin Treatment for Gastro-oesophageal and Triple-negative Breast Cancers

3.1 Introduction

As the second most common cancer in the world, breast cancers are responsible for approximately 25% of all cancer-related deaths. Triple negative breast cancers (TNBC) comprise ~20% of all breast cancers (26). TNBC tumours fail to express three common receptors: estrogen receptor (ER), progesterone receptor (PR) and human epidermal growth factor receptor-2 (HER2) (26, 27). Accordingly, TNBCs do not benefit from many currently available targeted therapies and make use of more conventional chemotherapeutic therapies as their main treatment type (27). However TNBCs are not the only type of cancer lacking successful targeted therapy approaches. For example, as discussed in Section 1.3; gastro-oesophageal cancers are also typically difficult to treat and are associated with poor prognosis for patients. These cancers illustrate the growing need to develop drugs which are beneficial in 'difficult to' settings. Although expecting targeted therapies to be the solution in all settings, it could be argued that a broader approach to treatment will prove critical to improve recovery rates in certain cancers and to overcome the development of *de novo* and acquired resistance.

So what is an ideal broad-spectrum anti-cancer drug? Conventional cancer therapies such as cisplatin, doxorubicin and 5-flourouracil personify the "broad" treatment approach, but often have many off-target effects (141-143). Therefore there is an argument for drug discovery which takes a step back from conventional chemical synthetic approaches. Compounds derived from natural sources have been proposed to exhibit improved toxicity profiles when compared with purely synthetic compounds; hence natural compound screening libraries have been employed as tools to discover anti-cancer agents with minimal side effects (144, 145). One important compound discovered in this manner, Taxol, a diterpenoid compound which derives from the bark of the Pacific yew tree, has become a key component of front-line combination therapy in several cancers including breast and prostate (146). The ability of taxol to halt cell division through G2/M

cell cycle arrest exhibits powerful synergies with cytotoxic drugs. Other diterpenoid compounds such as Crassin A-H have recently been shown to induce cytotoxicity in leukemic and lung cancer cell models (147).

Cytotoxicity, however, is but one paradigm to explain the anti-cancer properties of some drugs. Chemotherapies can work through cytotoxic or cytostatic mechanisms, or even a combination of both. Cytotoxic compounds induce cell death, either accidentally (ACD) or in a regulated fashion (RCD) (148). ACD is caused by severe insults induced through physical, chemical or mechanical injuries experienced by the cells; whereas RCD usually results from modification of the molecular machinery utilised by cells, often in response to immune or stress activation (148). Once these pathways are activated, the mechanisms of cell death can include (but are not limited to) apoptosis, autophagy, necrosis, necroptosis or ferroptosis (149-152).

Apoptosis occurs through two mechanisms; intrinsic and extrinsic (153). Intrinsic apoptosis describes the upregulation of pro-apoptotic proteins like p53, which upregulate BH3 only proteins, which aggregate at mitochondrial membranes and permit the release of cytochrome c, the formation of the apoptosome, the proteolytic cleavage of procaspase-9 and apoptotic induction (153-155). Extrinsic apoptosis utilises a ligand-presenting cell; often a lymphocyte or natural killer cell; which binds and activates a cell-surface receptor containing a death domain, recruitment of pro-caspase 8 and 10 and the downstream proteolytic cleavage of caspases and activation of apoptosis (153, 156).

Autophagy translates as 'self-eating' and refers to cellular response to nutrient stress or lack of energy production (157). The cell utilises autophagosomes which engulf entire organelles within the cell and join with lysosomes to complete the degradation of its content, which is then recycled (157, 158). In contrast, necrosis, unlike apoptosis and autophagy, is often referred to as an ACD (159) in response to unexpected trauma or insult (160). Reductions to cellular ATP levels induce membrane permeabilisation and

leakage of the cytoplasm into the surrounding area. This leaky phenotype promotes inflammatory responses around the dying cell (160).

Necroptosis, aptly named for its crossover between necrotic morphology but extrinsic apoptotic mechanisms, is initiated when a presenting ligand activates necrosome formation (161, 162). The necrosome then reduces cellular ATP and generates Reactive Oxygen Species (ROS) within the cell, increasing membrane permeability which causes swelling and the appearance of necrosis prior to ultimate death by apoptosis (163). Ferroptosis is an iron-dependent form of cell death, where System Xc (responsible for cysteine uptake within the cell), is inhibited and glutathione levels become reduced (164-166). The cell then becomes vulnerable to ROS and lipid peroxidases. Lipid peroxidases require iron in order to destroy mitochondria within the cell, hence iron chelators and ferrostatin have been shown to inhibit ferroptosis (164, 166, 167).

In contrast to the above mechanisms, cytostatic agents do not induce ACD or RCD, but instead inhibit cellular proliferation through mechanisms such as oxidative stress, DNA damage and cytoskeletal inhibition. Interestingly, some chemotherapeutic agents have the capacity to induce both cytotoxic and cytostatic phenotypes, depending on drug dosage and timing. Activation of oxidative stress may be one factor which influences the outcome in favour of either cytotoxicity or cytostasis (168, 169). Specifically, while early work settled upon oxidative stress as a tumour-promoting environmental factor (170, 171), more recent research is showing that oxidative stress can also act as a switch to push tumours towards cytotoxicity or cytostasis (170).

In an attempt to help develop increased treatments for cancers', our laboratory has screened a natural compound library (US National Cancer Institute Developmental Therapeutics Program, www.dtp.cancer.gov) for potential candidates with bioactivity against cancer cells *in vitro*. Having screened the panel, we found a diterpenoid coral-derived compound, Crassin (Crassin/S-Benzyl-N-malonylcysteine, compound

reference NSC-210236), to exert significant bioactivity across a number of cancer cell types. The focus of this chapter, therefore, was in beginning to explore the utility of this compound in models of "difficult to

3.2 Aims of this Chapter

The broad aim of this chapter was to explore the potential anti-cancer effects of a coral-derived compound Crassin and to elucidate its mechanism of action. The specific aims were as follows:

Specific Aim 1: To confirm the bioactivity of Crassin in gastro-oesophageal and triple-negative breast cancer cell models.

Specific Aim 2: To identify whether Crassin has the ability to reduce functional behaviours associated with tumour aggressiveness in gastro-oesophageal and triple-negative breast cancer cell models.

Specific Aim 3: To elucidate the mechanism of action of Crassin in cell line models.

3.3 Results

In-house screening via cell viability analysis was undertaken, examining the effect of novel compounds donated by the US National Cancer Institute (www.dtp.cancer.gov) in cancer cell lines using Alamar blue metabolic assays. Reduced viability of cancer cell lines following treatment with novel natural compounds was indicative of an anti-cancerous agent. Using this approach, one promising compound, coral-derivedCrassin (NSC-210236) emerged.

3.3.1 Crassin treatment significantly decreases cellular viability across a panel of gastro-oesophageal cancer cell lines.

A panel of gastro-oesophageal cell lines was treated with Crassin at varying concentrations or matched vehicle controls (DMSO). As illustrated in **Figure 3.1**, concentration-dependent reductions in cell viability of ESO26, N87 and OE19 cell lines were observed following Crassin treatment for either 24h or 48h. The IC_{50} of Crassin was thus established as 2.27µM (24h) and 1.15µM (48h) in ESO26 cells, as 6.05µM (24h) and 4.52µM (48h) in N87 cells, and as 7.58µM (24h) and 2.68µM (48h) in OE19 cells. Furthermore, reductions in cell viability were statistically significant across all three cell lines following 5µM Crassin treatment for 48h. Specifically, cell viability was reduced in ESO26 by 89 ±2%, N87 by 55 ±11% and OE19 by 62 ±13%.

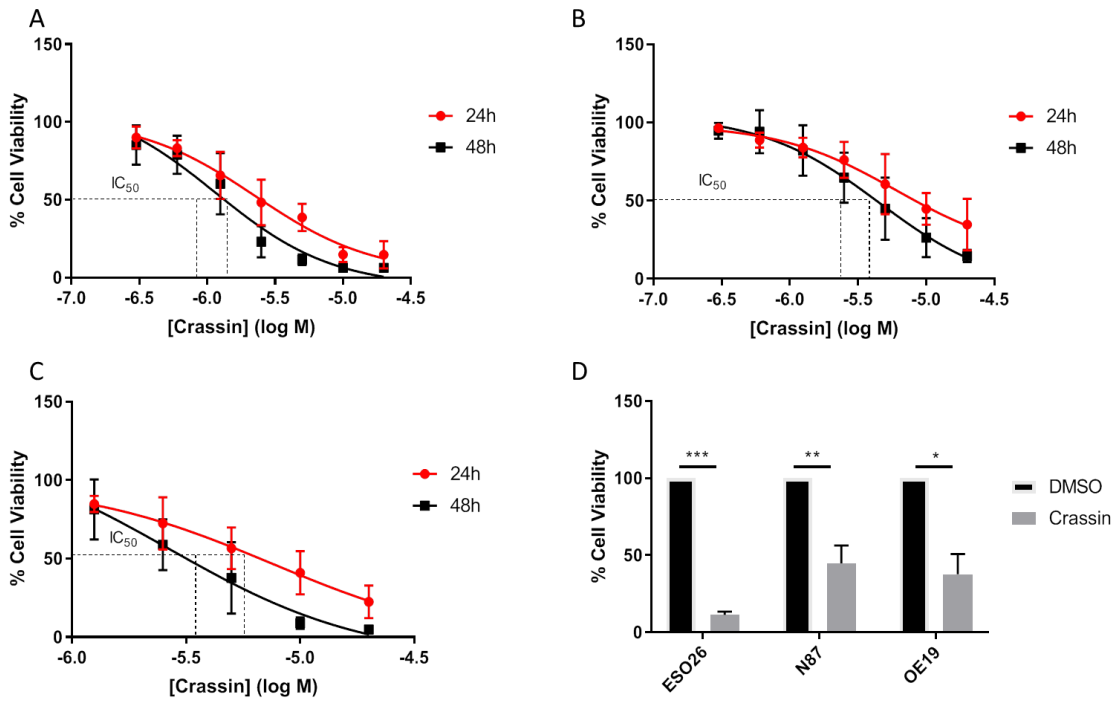

Figure 3.1: Crassin significantly decreases cellular viability across a panel of GE cancer cell lines. *ESO26* ***(A)****, N87* ***(B)*** *and OE19* ***(C)*** *cells were plated at 5,000 cells per well and treated with serial dilutions of Crassin (20-0.325μM) for 24 or 48h. Cell viability was assessed spectophometrically using Alamar Blue metabolic assays and expressed as % optical density relative to that of a matched vehicle control (DMSO;* 0.0015625, 0.003125, 0.0625, 0.0125, 0.025, 0.5, 0.1% v/v*). Data from n=3 independent experiments are represented, and expressed as mean ±SEM. IC_{50} values were calculated using Graphpad Transform function and curve fitted using non-linear regression. ESO26, N87 and OE19* ***(D)*** *cells were plated at 5,000 cells per well and treated with 5μM crassin or DMSO (0.025% v/v). After 48h cell viability was assessed spectophometrically using Alamar Blue metabolic assays and expressed % optical density relative to that of a matched vehicle control. Data (n=3 independent experiments) are expressed relative to vehicle control (DMSO) as mean ±SEM. Statistical analysis was calculated using paired, two-tailed Student's t-test (*p < 0.05, **p < 0.01, ***p < 0.001, ****p < 0.0001).*

3.3.2 Crassin significantly decreases colony-forming ability of gastro-oesophageal cell lines

As Alamar blue assays only establish whether cellular metabolism is affected following treatments, we sought to investigate the phenotypic effects of Crassin on gastro-oesophageal cancer cell lines using colony-forming assays.

As shown in **Figure 3.2,** Crassin successfully inhibited colony formation when compared to vehicle control- (DMSO-) treated wells. Relative to matched vehicle control wells, ESO26 cells exhibited significant reductions in colony forming capabilities (by 86 ± 4%; $p<0.0001$, that in N87 cells significantly decreased by 68 ± 8% ($p<0.0012$), while colony-forming capabilities were significantly reduced in OE19 cells by 94 ± 2% ($p<0.0001$).

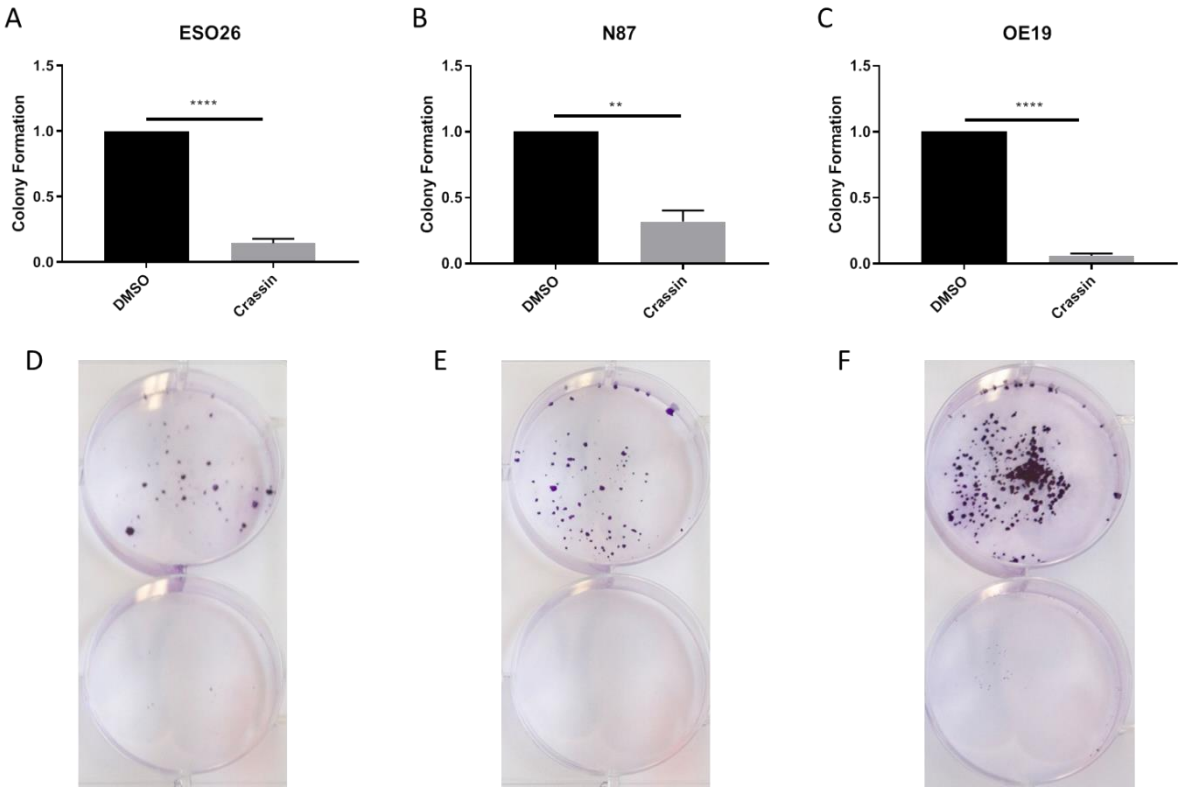

Figure 3.2: Crassin treatment decreased colony-forming capabilities across a panel of gastro-oesophageal cancer cell lines. *ESO26* ***(A, D)****, N87* ***(B, E)*** *and OE19* ***(C, F)*** *cells were plated at 1,000 cells per well and treated with Crassin or vehicle (DMSO) at their established* IC_{50} *(ESO26; 1.15εM (DMSO 0.00006% v/v) N87; 4.52εM (DMSO 0.00023% v/v) OE19; 2.68 (DMSO 0.000134% v/v)). Colony formation was assessed following crystal violet staining and solubilisation in methanol and read at 595nm on a VICTORÊ X3 Multilabel Pl. Data (n=3 independent experiments) are expressed relative to vehicle control (DMSO) as mean ±SEM. Statistical analysis was calculated using unpaired, two-tailed t-tests* (*p < 0.05, **p < 0.01, ***p < 0.001, ****p < 0.0001).

As previously discussed, we suspected that this natural compound may have an improved toxicity profile when compared to other chemotherapeutics available. However, Crassin is a relatively novel compound which (to the best of our knowledge) has not been tested in an *in vivo setting*. We therefore wanted to extend studies on the bioefficacy of Crassin past *in vitro* settings and into a chick embryo model. This *in ovo/semi-in vivo* approach allows tumour formation through the 'hijacking' developing chorioallantoic membrane (CAM) of fertilised chick embryos (172).

3.3.3 Crassin reduces xenograft tumour burden in CAM Assays

Fertilised hen eggs were incubated at 37°C and underwent procedural steps described in **Figure 3.3**. Following implantation of ESO26 cells onto the chick CAM on day 8, windows were re-covered with a semi-permeable membrane and left to develop. On days 10 and 12 eggs were re-opened at their window and treated with either the IC_{50} of Crassin (1.15µM) or with matched vehicle control (DMSO, 0.00006% v/v) Initially, there were 10 eggs allocated per treatment group, but with ongoing issues throughout the procedure maintaining chick embryos, only 6 chick embryos survived for each condition (Vehicle control and Crassin). We also saw the loss of three eggs on the final night of incubation (2 DMSO and 2 Crassin-treated), however the xenografts were still believed to be viable and were extracted, sectioned, stained and included in the results presented.

As illustrated in **Figure 3.4**, DMSO-treated eggs had more grossly-visible tumours (VT) at the endpoint of the study (80%), whereas in contrast, Crassin treated tumours had more non-visible tumours (NVT) (67%). This suggested that Crassin has the ability to reduce tumour development in a *semi-in vivo* setting. However, two Crassin-treated tumours did continue to develop tumours **(Appendix J - Supplementary Figure 1)**. We speculate that this may be as a result of the method of the treatment; ensuring correct placement locally over developing xenograft tumours by hand; rather than a statement on Crassin bioefficacy. We saw no evidence of decreased embryonic viability across the Crassin-treated groups, rather the loss of viable eggs across both

treatment groups likely reflected procedural issues rather than overt toxicity of any of treatment.

We next tested whether Crassin had the ability to reduce proliferation and invasion in the *semi-in vivo* setting by examining Ki67 and cytokeratin localization by immunohistochemistry.

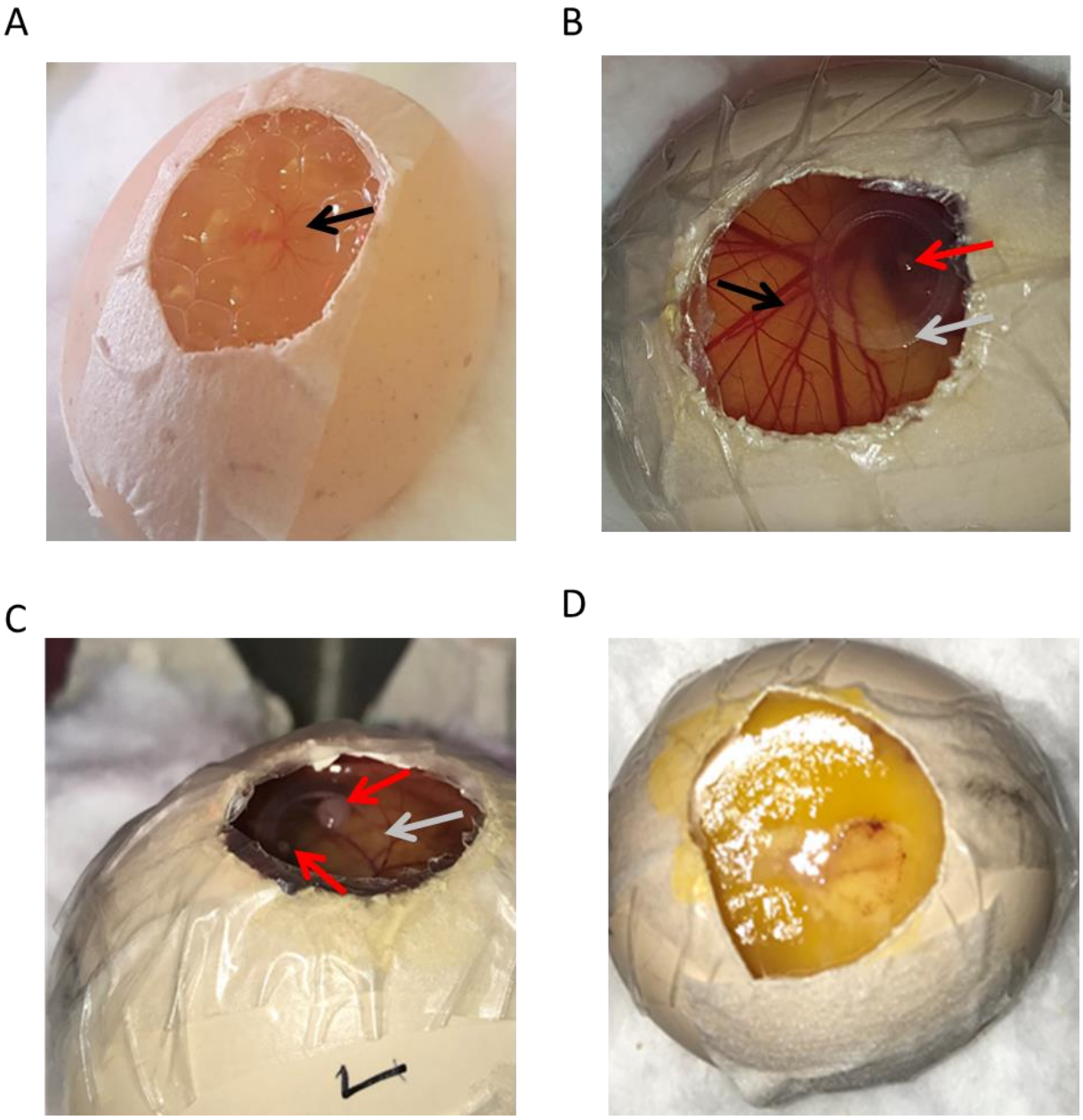

Figure 3.3: Establishment of the in ovo CAM assay. *Egg windows were opened on day 3 (A) and inspected for vascularisation (denoted by black arrow) as evidence of living embryos. On Day 8 windows were re-opened and silicon rings gently placed on the CAM (denoted by grey arrow), 2 x* 10^6 *ESO26 cells were then mixed 1:1 with Matrigel and slowly dropped within the silicon ring (xenografts denoted by red arrow) (B). In situ treatments were added as per method described in Section 2.15 and eggs were monitored for vascularisation on each occasion. On the final day, evidence of tumours was noted for each condition (C). Throughout the process, eggs that did not survive the process and showed loss of vascularisation were discarded appropriately (D).*

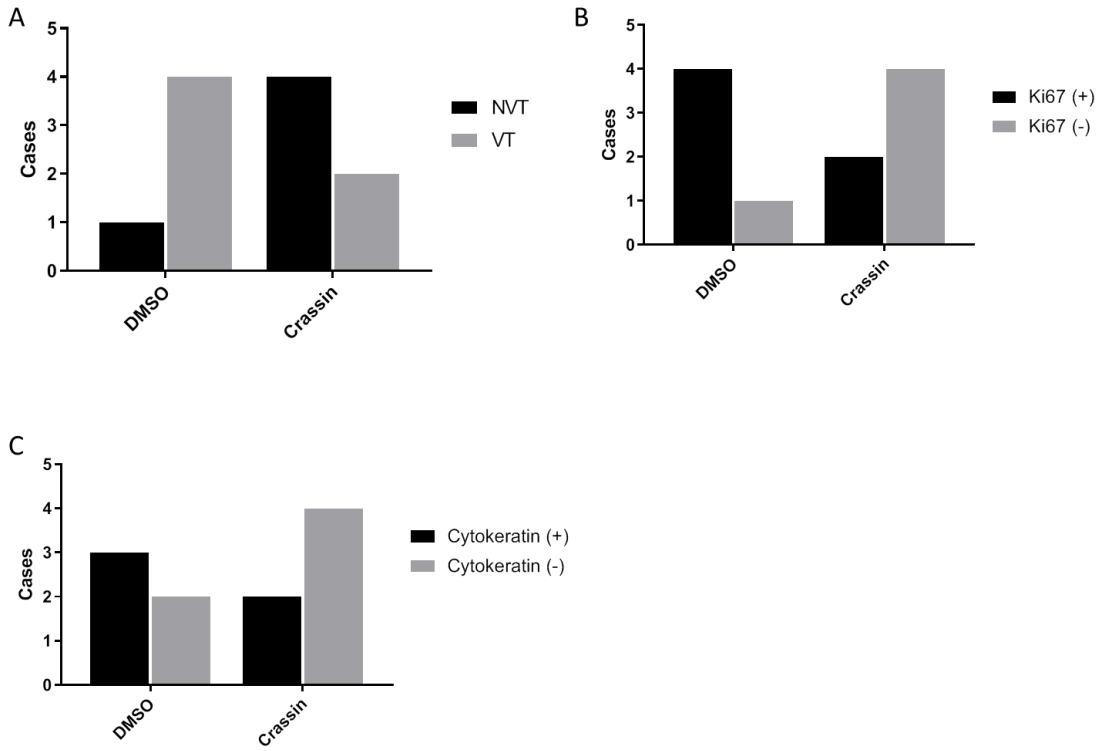

Figure 3.4: Crassin reduces visible development of gastro-oesophageal xenograft tumours on the CAM. *Following implantation of ESO26 cells onto CAM membranes and treatment with either Crassin (1.15µM) or matched vehicle control (DMSO), gross tumour visibility* ***(A)*** *was noted on the final day prior to extraction and Ki67* ***(B)*** *and cytokeratin* ***(C)*** *positivity/negativity was assessed following immunohistochemical staining. Data for Crassin (n=6) and for DMSO (n=5) are displayed throughout and Fisher's exact test was performed. Reflecting the small numbers, no statistical significance was found for either treatment group.*

3.3.4 Crassin treatment effects on proliferation and tumour markers

Crassin- (n=6) and DMSO- (n=6) treated xenograft tumours were immunohistochemically stained for key tumour-associated proteins to assess the extent of growth and to visualise invasion. Interestingly, 67% of Crassin-treated xenografts were negative for cytokeratin and Ki67 following binary visual quantification (presence or absence of positive staining) **(Figure 3.4).** However, due to the small numbers, no significant correlation was found by Fisher's exact testing and further quantification of staining was not undertaken. In the DMSO-treated control group there was evidence of

invading tumour cells, which had moved out from the containment of the Matrigel and into the surrounding CAM tissue **(Figure 3.5;** black arrow**)**. One egg within the vehicle control (DMSO)-treated group was not viable on the final day of extraction and failed to show any sign of tumour development. This may have been a failure within the chick embryo or incorrect implantation of cells within the silicon ring, as all other negative control tumours successfully formed. It was also evident that implanted cells appeared in the Matrigel area of Crassin-treated xenografts, indicating that cells were correctly implanted, but that Crassin was successful in diminishing tumour establishment. Although some tumours did develop in the Crassin-treated group, overall these results indicated that Crassin was effective in a *semi-in vivo* setting in reducing tumour growth and proliferation and concurrently had the ability to reduce the invasive phenotypes demonstrated within the negative control (DMSO)-treated group. Furthermore, lack of overall toxicity to developing embryos suggests Crassin may have potential as a candidate for further drug development.

To further explore the bioactivity of C
next examined the effect of Crassin in TNBC cells *in vitro.*

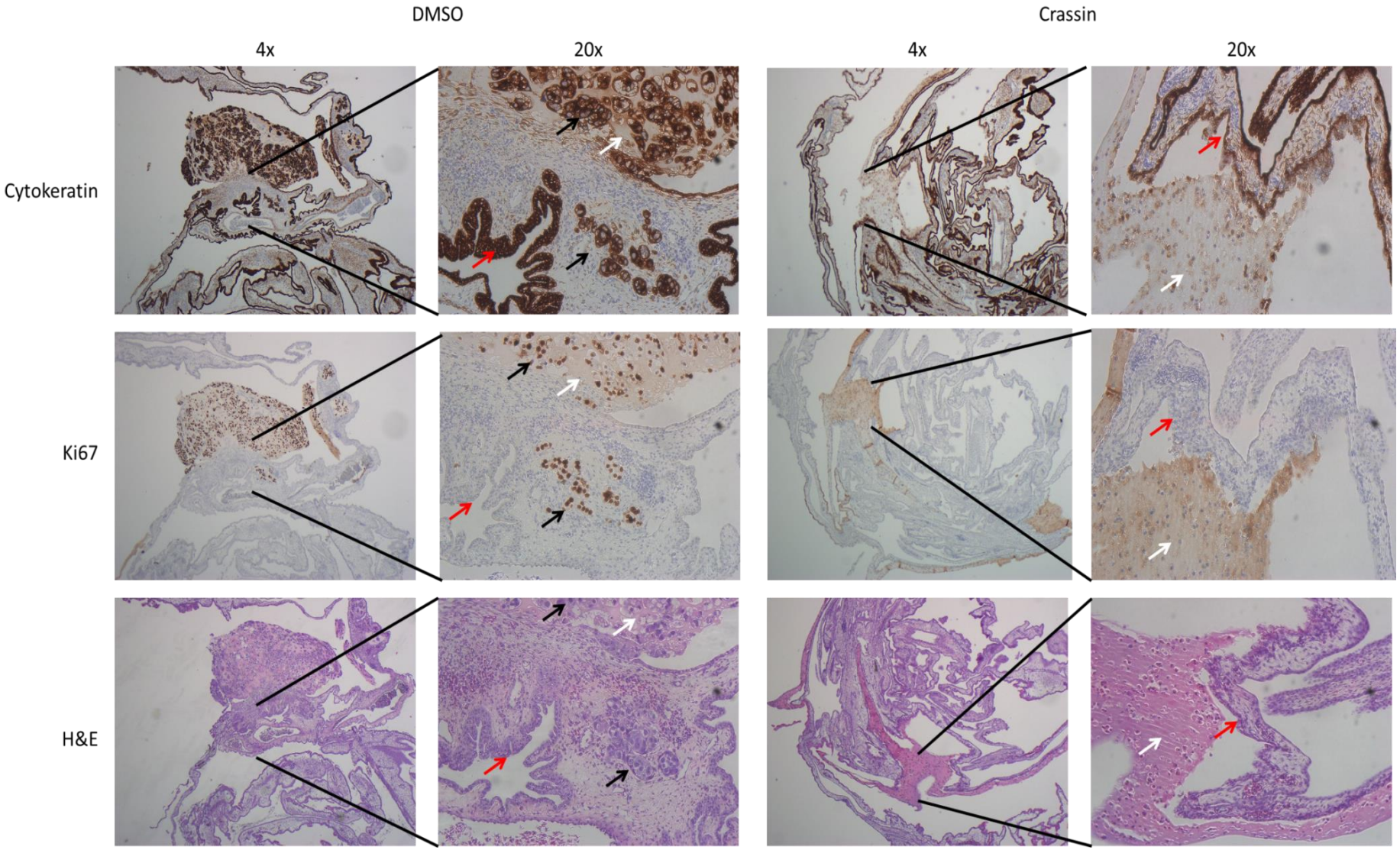
DMSO
Crassin
4x
20x
4x
20x
Cytokeratin
Ki67
H&E

Figure 3.5: Crassin-treated gastro-oesophageal xenografts showed evidence of inhibited proliferation. *2 x ^{6} ESO26 cells were grafted onto the CAM of fertilised hen's eggs on day 7 post-fertilisation (v.e.) and treated with either Crassin (vehicle control (DMSO) and 12. On silicon rings 1 and 4, surrounding areas of the CAM were excised, formalin-fixed and stained for cytokeratin, Ki67 or haematoxylin and eosin (H&E). Stained sections were then imaged on an Olympus CKx41 microscope at 4x or 20x with Cell B imaging software. Areas of tumour are denoted by black arrows, areas of Matrigel are denoted by white arrows and areas of CAM are denoted by red arrows. All images were obtained using an Olympus CKx41 microscope with Cell B imaging software at 20x magnification.*

3.3.5 Crassin reduces the viability of TNBC cells

Having demonstrated the ability of Crassin to halt aggressive cancer phenotypes in gastro-oesophageal cancer cell lines and in a *semi-in vivo* setting, we next explored whether the bioactivity of Crassin could be demonstrated in another 'difficult' cancer. We established the IC_{50} of Crassin in the TNBC cell line MDA-MB-231 as 9.16 µM (24 hours) and 4.65 µM (48 hours), respectively, using Alamar Blue - Resazurin assays **(Figure 3.6)**. In addition to this concentration sensitivity, we also established time sensitivities to Crassin in two TNBC cell lines and in a primary TNBC cell culture **(Figure 3.6)**. We found that MDA-MB-231 cells exhibited Crassin-induced time-dependent reductions in viability of 38 ± 6.3% and 63.5 ± 4.1% at 24 hours and 48 hours, respectively **(Figure 3.6)**. Similar time-dependent reductions in cell viability were observed following Crassin treatment in TNBC 4T1 cells, namely 58.3 ± 9.9% and 86 ± 3.8% at 24 hours and 48 hours, respectively **(Figure 3.6)**. A single biological replicate of the primary TNBC cell culture 198T also yielded similar data, with a significant reduction in viability (52 ± 0.02%) in Crassin-treated cells compared to vehicle control (DMSO) treated cells **(Figure 3.6).**

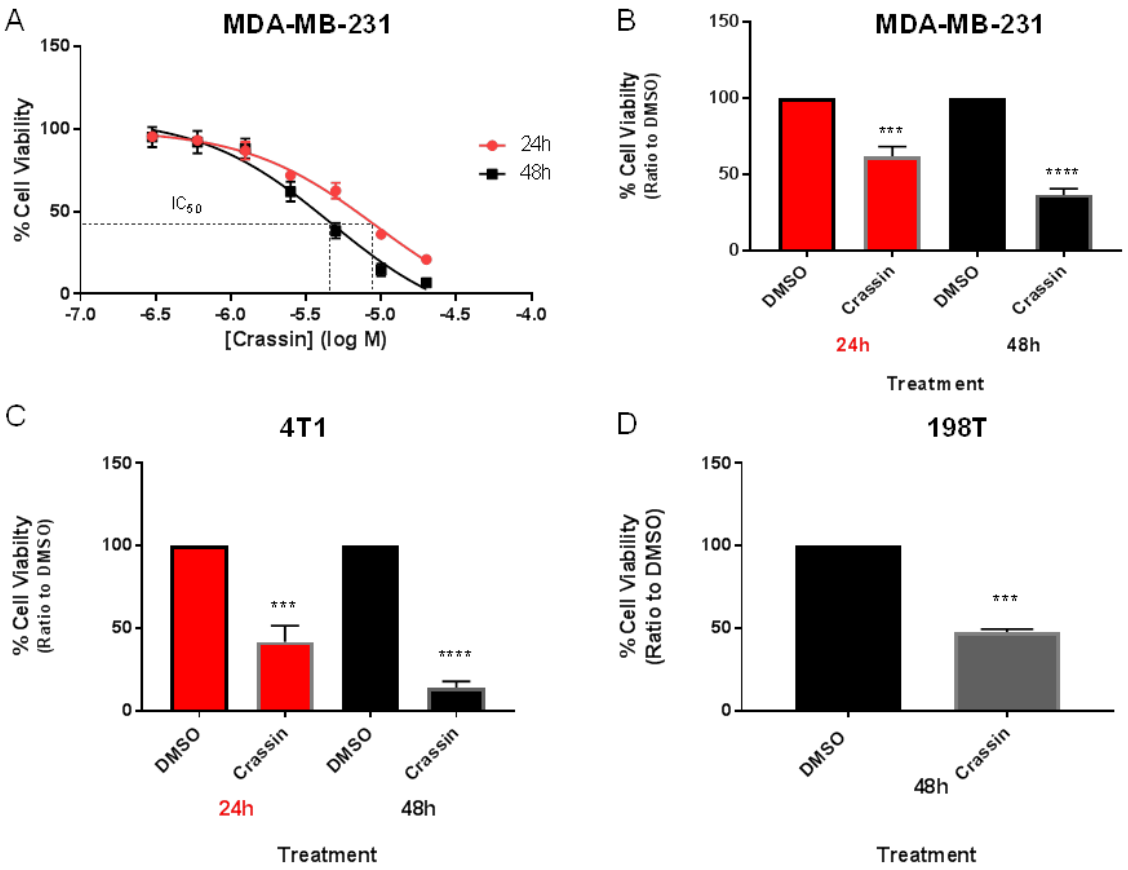

Figure 3.6: Crassin dose and time-dependently reduces the viability of TNBC cells *MDA-MB-231 cells were seeded at a density of 5,000 cells per well in 96-well plates and treated 48 hours later with Crassin at concentrations ranging from 0.325 to 20 µM. Cell viability was assessed spectophotometrically using Alamar Blue metabolic assays, and expressed as % optical density relative to that in vehicle (DMSO) treated cells. Data (n = 3 independent experiments) are expressed as X=log(X) mean ± SEM. IC50 values were calculated using the Graphpad Transform function and curve fitted using non-linear regression. MDA-MB-231 cells **(B)** were seeded at a density of 5,000 cells per well, 4T1 cells **(C)** at 1,000 per well and primary breast cells at 5,000 per well **(D)** in 96-well plates and treated after one doubling time with Crassin (5µM) or vehicle control (DMSO). Viability was assessed at 24 hours and 48 hours for MDA-MB-231 and 4T1 cells and at 48 hours for 198T cells using an Alamar Blue assay, and expressed as % of the DMSO vehicle control. Data (n = 3 independent experiments) are expressed as mean ± SEM, with statistical significance determined using one-way ANOVA correcting for multiple comparisons adjusted p values (MDA-MB-231, 4T1 cells) or unpaired two-tailed Student's t tests (primary cells)* (*p < 0.05, **p < 0.01, ***p < 0.001, ****p < 0.0001).

3.3.6 Crassin increases pAkt and pERK levels in an antioxidant-sensitive manner.

Having established that C4 reduces viability in three (primary and established) TNBC cell models, we next set out to assess its effect on known cell survival signalling pathways. Unexpectedly, we found that expression of the cell survival effector phosphorylated Akt (pAkt) (173-176) increased significantly after 24 and 48 hours of Crassin treatment **(Figure 3.7)**. Since Akt signalling has also been associated with cell death downstream of the release of reactive oxygen species (ROS) (177-179), we next examined the viability of cells pre-treated with the antioxidant N-acetyl-cysteine (NAC;3 mM) prior to treatment with Crassin (5 µM) for 24 or 48 hours. We found that NAC significantly counteracted the negative effects of Crassin on the viability of both MDA-MB-231 and 4T1 cells **(Figure 3.7)** and, in addition, restored pAkt levels to those of Crassin-untreated controls **(Figure 3.7)**. Interestingly, we also observed a reduction in total Akt in 4T1 cells, but not in MDA-MB-231 cells, following Crassin treatment. This reduction may be attributed to cell density, potentially reflecting better access of Crassin to the cell surfaces of loosely growing 4T1 cells than the more densely growing MDA-MB-231 cells. In light of the observed Crassin-dependent increases in pAkt levels, we next set out to explore whether ERK phosphorylation (also known to play a key role in cell survival (180)) was similarly affected by Crassin treatment. By doing so, a small but statistically insignificant increase in pERK levels was observed after Crassin treatment of MDA-MB-231 cells **(Figure 3.8)**.

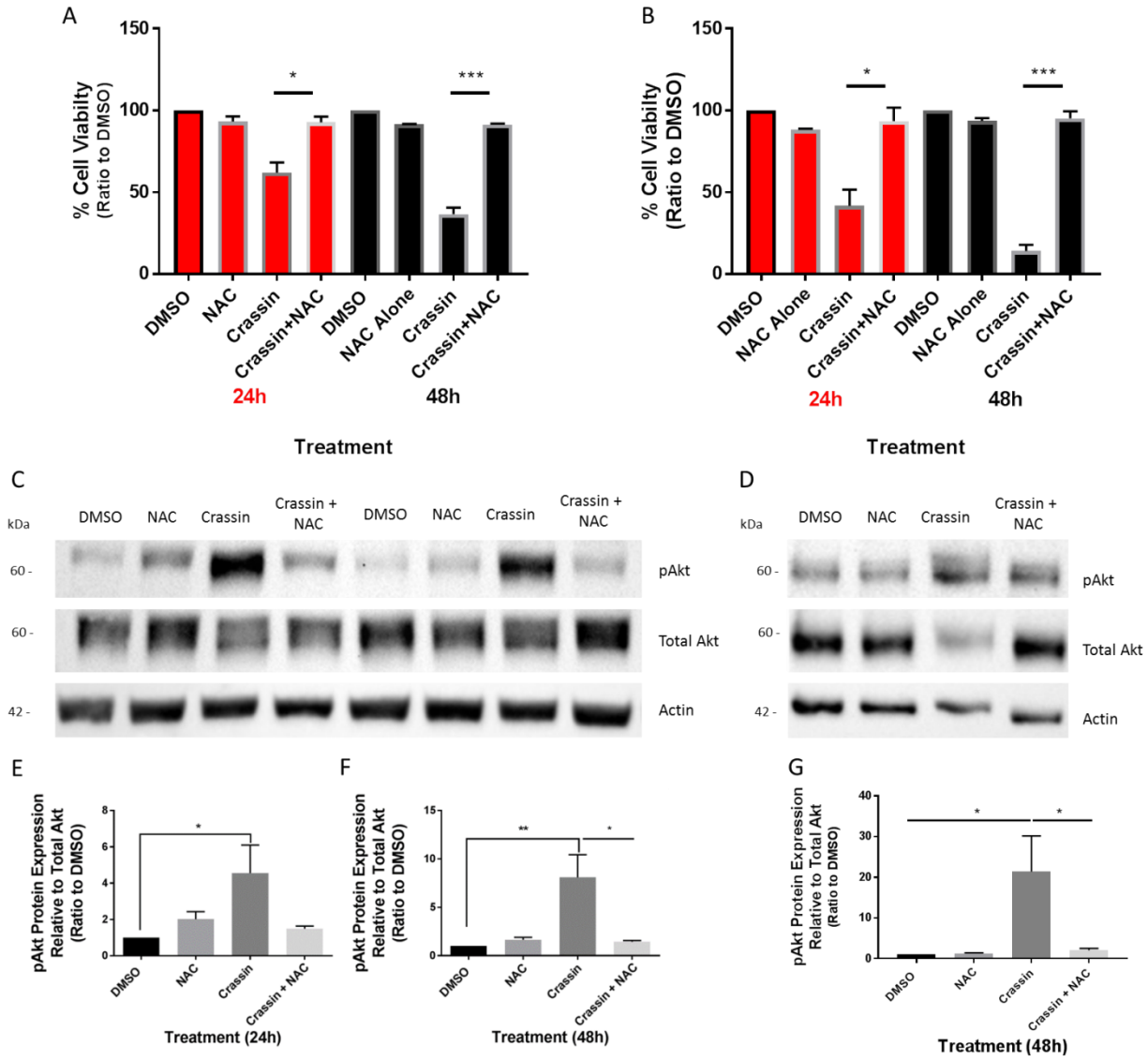
A
% Cell Viabilty (Ratio to DMSO)
150
100
50
0
*
***
DMSO
NAC
Crassin
Crassin+NAC
DMSO
NAC Alone
Crassin
Crassin+NAC
24h
48h
Treatment
B
% Cell Viability (Ratio to DMSO)
150
100
50
0
*
***
DMSO
NAC Alone
Crassin
Crassin+NAC
DMSO
NAC Alone
Crassin
Crassin+NAC
24h
48h
Treatment
C
kDa
DMSO
NAC
Crassin
Crassin + NAC
DMSO
NAC
Crassin
Crassin + NAC
60 -
pAkt
60 -
Total Akt
42 -
Actin
D
kDa
DMSO
NAC
Crassin
Crassin + NAC
60 -
pAkt
60 -
Total Akt
42 -
Actin
E
pAkt Protein Expression Relative to Total Akt (Ratio to DMSO)
8
6
4
2
0
*
DMSO
NAC
Crassin
Crassin + NAC
Treatment (24h)
F
pAkt Protein Expression Relative to Total Akt (Ratio to DMSO)
15
10
5
0
**
*
DMSO
NAC
Crassin
Crassin + NAC
Treatment (48h)
G
pAkt Protein Expression Relative to Total Akt (Ratio to DMSO)
40
30
20
10
0
*
*
DMSO
NAC
Crassin
Crassin + NAC
Treatment (48h)

Figure 3.7: Crassin reduces cell viability and increases pAkt expression in a ROS-dependent fashion *MDA-MB-231 cells* ***(A)*** *were seeded at a density of 5,000 cells per well and treated 48 hours later with Crassin (5 µM) or vehicle control (DMSO) +/- NAC (3 mM) for 24 or 48 hours. 4T1 cells* ***(B)*** *were seeded in 96-well plates at a density of 1000 cells per well and treated 24 hours later with Crassin (5 µM) or vehicle control (DMSO) +/- NAC (3 mM) for 24 or 48 hours. Cell viabilities were assessed using Alamar Blue assays, and expressed as % of DMSO vehicle control. Data (n = 3 independent experiments) are expressed as mean ± SEM, with statistical significance determined using unpaired two-tailed S t u d e t-tests. MDA-MB-231 cells were seeded in 6-well plates at a density of 300,000 per well and treated 48 hours later with Crassin (5 µM) or vehicle control (DMSO) +/- NAC (3 mM) for 24 or 48 hours* ***(C)****. 4T1 cells were seeded at a density of 50,000 per well and treated 24 hours later with Crassin (5 µM) or vehicle control (DMSO) +/- NAC (3 mM) for either 24 or 48 hours* ***(D)****. The expression of pAkt* ***(C, D)*** *was analysed using Western blotting, and densitometrically quantified using ImageLab software 5.2.1 in MDA-MB-231* ***(E, F)*** *and 4T1* ***(G)*** *cells (volume intensity of band relative to matched total Akt band and displayed relative to DMSO). Results are expressed as mean ± SEM (n = 3). Statistical significance was calculated by unpaired one-tailed S t u d e t-tests (*p < 0.05, **p < 0.01, ***p < 0.001, ****p < 0.0001).*

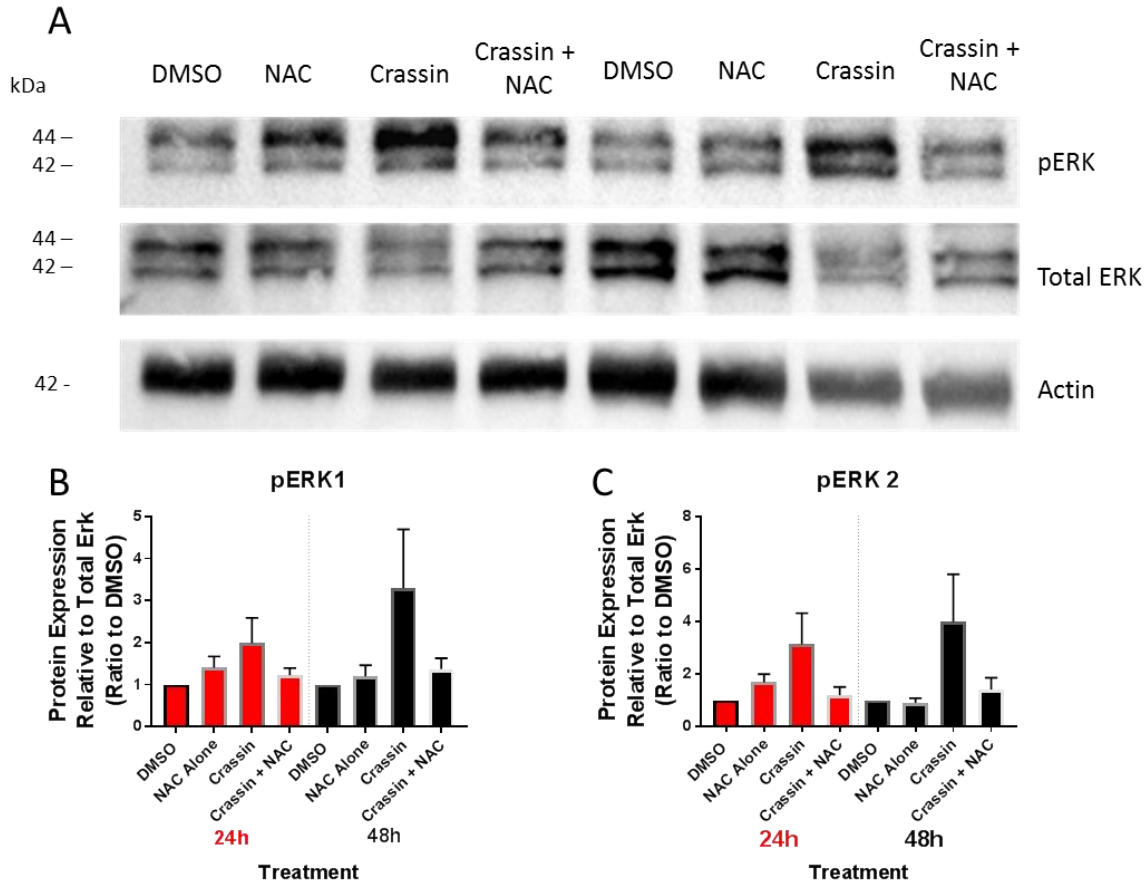

Figure 3.8: Crassin increases pERK expression in a ROS-dependent fashion MDA-MB-231 cells were seeded in 6-well plates at a density of 300,000 per well and treated 48 hours later with Crassin (5 µM) or vehicle control (DMSO) +/- NAC (3 mM) for 24 or 48 hours **(A)**. The expression of pERK **(A)** was analysed using Western blotting, and densitometrically quantified using ImageLab software 5.2.1 in MDA-MB-231 **(B,C)** (volume intensity of band relative to matched total ERK band and displayed relative to DMSO). Results are expressed as mean ± SEM (n = 3 independent experiments). Statistical significance was calculated by unpaired one-tailed S t u d e -tests (*p < 0.05, **p < 0.01, ***p < 0.001, ****p < 0.0001).

3.3.7 Crassin-induced reductions in cell viability are not accounted for by apoptotic mechanisms of cell death

Having established that Crassin reduces cell viability across three TNBC cell models, in conjunction with ROS-mediated Akt and ERK activation (phosphorylation), we next set out to examine potential downstream cell death pathways. To this end, we first examined Caspase-3 (Cas-3) cleavage to assess a possible contribution of apoptosis to cell death (181, 182). Upon Western blotting, cleaved Cas-3 bands were only observed under positive control (staurosporine-treated) but not under Crassin-treated conditions **(Figure 3.9)**. This apparent lack of apoptosis involvement was subsequently confirmed using flow cytometric Annexin-V assays. Specifically, we found that MDA-MB-231 cells treated with the positive control reagent staurosporine showed increased Annexin-V positivity compared to DMSO treated cells ($p < 0.001$), whereas Annexin-V staining was not significantly increased above negative control levels in Crassin-treated cells, even after 48 hours **(Figure 3.9)**.

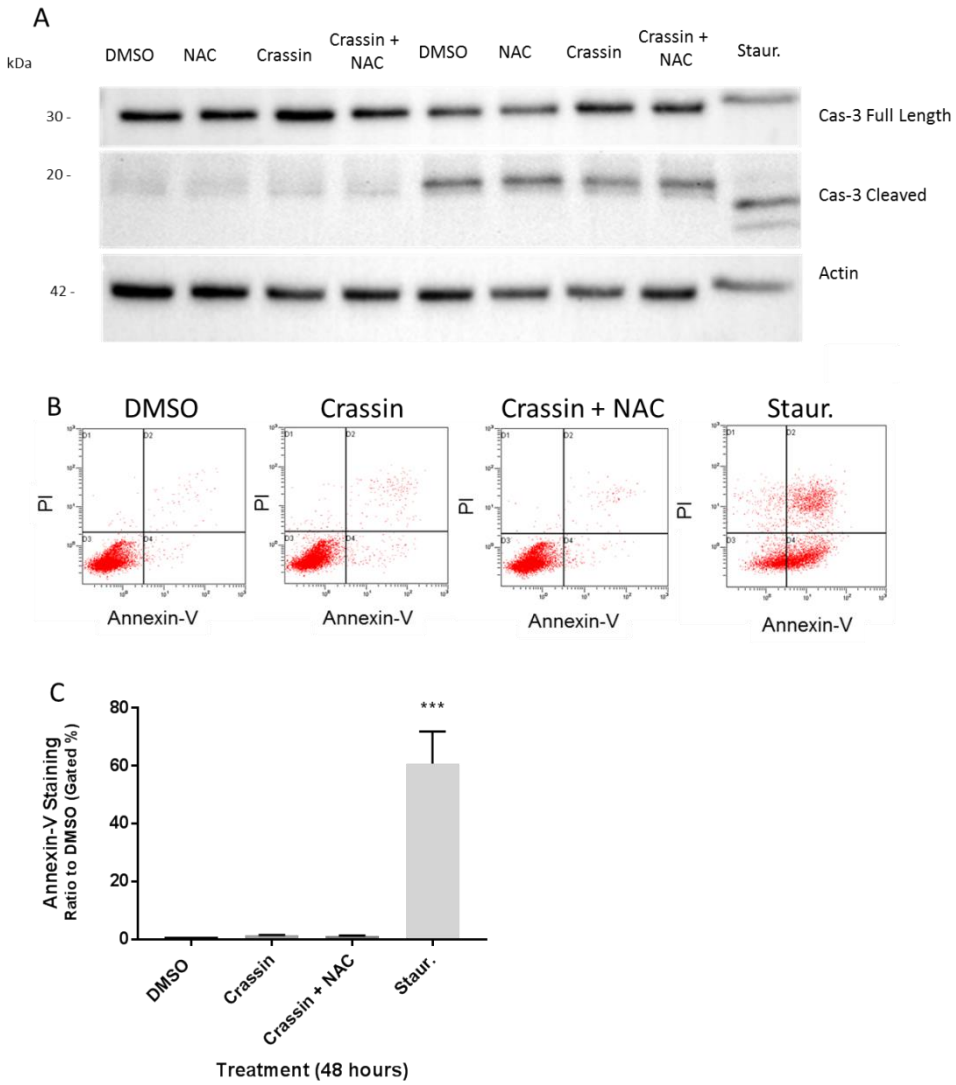

Figure 3.9: Crassin does not induce apoptotic cell death. *MDA-MB-231 cells were seeded in 6 well plates at a density of 300,000 per well and treated 48 hours later with Crassin (5 µM) or vehicle control (DMSO) +/- NAC (3 mM) for either 24 or 48 hours [using Staurosporine/(staur.; 10 µM/3 hours or 1 µM/48 hours) as a positive inducer of apoptosis]. Caspase-3 expression was analysed using Western blotting* ***(A)****. Cells were flow cytometrically analyzed after staining with a BD Annexin-V kit* ***(B)****. The gated % of the treatment groups were analysed for Annexin-V positivity/apoptosis (quadrant D4)* ***(C)*** *using one-way ANOVA, correcting for multiple comparisons and Dunnett's post-hoc test. Data (n = 3 independent experiments) are expressed as mean ± SEM and statistical significance was found relative to the matched vehicle control % ratio.* (*p < 0.05, **p < 0.01, ***p < 0.001, ****p < 0.0001)

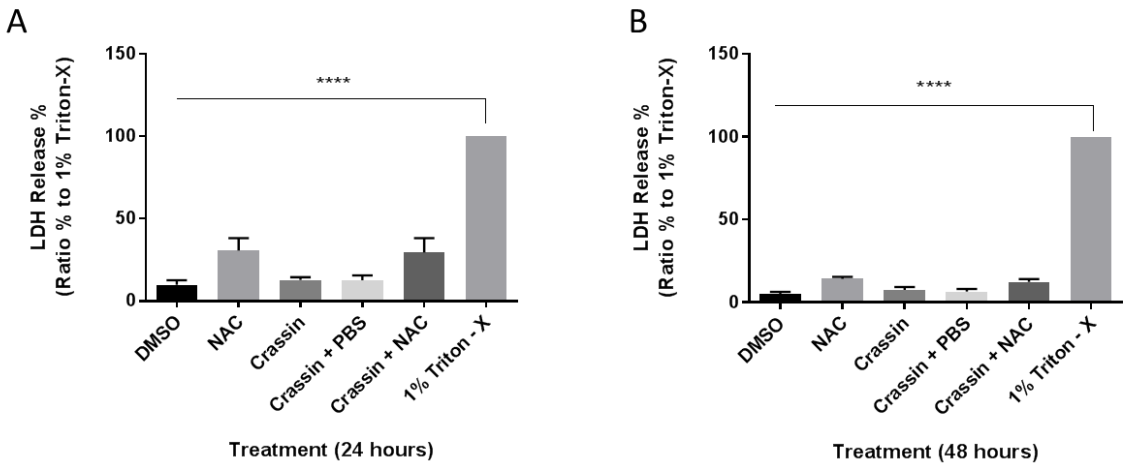

Figure 3.10: Crassin does not induce necrotic death. *MDA-MB-231 cells were seeded at a density of 5,000 cells per well in 96-well plates and treated 48 hours later with Crassin (5 µM) in the presence or absence of NAC (3 mM) for 24 and 48 hours* ***(A),*** *at which points positive control wells were treated with 1% Triton-X for 45 minutes. Necrosis was measured using an LDH Assay kit. Data (n = 3 independent experiments) are expressed as mean ± SEM. Statistical significance* (*p < 0.05, **p < 0.01, ***p < 0.001, ****p < 0.0001*) was determined using one-way ANOVA correcting for multiple comparisons using Dunnetôs test reporting a DMSO-treated controls for all groups.*

3.3.8 Crassinï induced cell viability reductions are not induced by other common mechanisms of cell death

The possibility that Crassin may activate necrotic cell death was next explored using lactate dehydrogenase (LDH) assays in Crassin-treated cells (with Triton-X100-treated cells as a positive control). We found that LDH release was not different between control DMSO- or Crassin-treated cells, i.e., 10% (± 3) and 13% (± 2) at 24 hours, respectively, and 5% (± 1) and 8% (± 2) at 48 hours, respectively, compared to positive control cells **(Figure 3.10)**. This suggests that membrane permeabilisation is not a feature of Crassin-treated cells even after 48 hours. Interestingly, we noted a significant increase in LDH release by NAC-treated cells, but this may be due to a transient NAC-induced permeabilisation of the cell membranes, as this release was seen to tail off at

48 hours (31 ± 8% at 24 hours, reduced to 14 ± 2% at 48 hours). Given the sensitivity of each assay to the ROS inhibitor NAC, we next set out to explore other modes of cell death putatively involving ROS induction.

3.3.9 Crassin-induced reductions to cell viability were not induced by cell death mechanisms.

Both necroptosis and ferroptosis are apoptosis-independent mechanisms of cell death associated with increased ROS levels (161, 164, 166, 183). To test these possibilities, MDA-MB-231 cells were treated with Crassin (5 µM) in the presence or absence of necroptosis or ferroptosis inhibitors (Necrostatin-1 and Ferrostatin-1, respectively). We found that neither Necrostatin-1 (100 µM) nor Ferrostatin-1 (5 µM) were able to block the Crassin-induced decreases in cell viability **(Figure 3.10)**, whereas Crassin-induced cell viability effects could still be rescued by NAC (3 mM). Erastin (10 µM) was used as a positive control inducer of ferroptosis. A positive control inducer of necroptosis in MDA-MB-231 cells could not be found (data not shown). Next we explored autophagic cell death by examining LC3B II protein expression in Crassin-treated MDA-MB-231 cells. Significant increases in LC3B II conjugation were observed compared to controls at both 24 hours **(Figure 3.10)** and 48 hours **(Figure 3.10)** ($p = 0.0001$ and $p = 0.0494$, respectively). However we found that the morphology of cells following Crassin treatment was not consistent with autophagy **(Appendix J - Supplementary Figure 2**; which suggests that reductions in cell viability after Crassin treatment may reflect cytostasis rather than overt autophagic toxicity.

3.3.10 Crassin induces cytostasis in TNBC cells

To determine whether Crassin induces cell cycle arrest, flow cytometric cell cycle analyses were conducted in propidium iodide-stained MDA-MB-231 cells following Crassin treatment. By doing so, we observed a significant shift in the Crassin-treated cells from G1 to G2/M (**Figure 7A**). Specifically, we found that 37 ± 12% fewer Crassin-treated cells were in the G1 phase of the cell cycle than in DMSO-treated control cells, whereas 30 ± 4% more Crassin-treated cells were in the G2/M phase. Subsequently, BrdU assays were carried out to

examine the proliferative capabilities of the cells following treatment with Crassin (**Figure 7B**). Our data indicate diminished proliferative capabilities even after a 24 hour treatment with Crassin (5 µM; reductions of 90.6 ± 4.7% and 95.9 ± 2.9% at 24 hours and 48 hours, respectively). Taken together, we conclude that our data are consistent with a cytostatic mode of action of Crassin, reflecting a reduced capability to metabolize resazurin to resorufin in Alamar Blue - Resazurin assays.

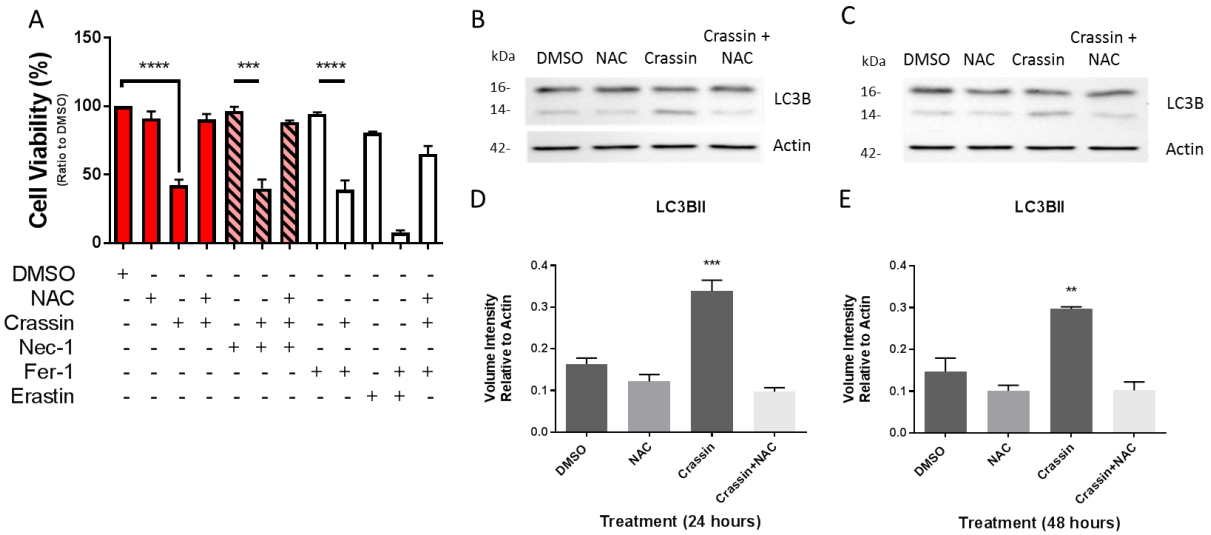

Figure 3.11: Crassin does not induce conventional cell death mechanisms. *MDA-MB-231 cells were treated with Crassin (5 µM) or vehicle control (DMSO) +/- NAC (3 mM) for 48 hours in the presence or absence of necrostatin-1 (nec-1; 100 µM), or ferrostatin-1 (fer-1; 5 µM) with Erastin (10 µM) as a positive control for ferroptosis, prior to performing Alamar Blue cell viability assays* ***(A).*** *Data (n = 3 independent experiments) are expressed as mean ± SEM. Statistical significance was determined using one-way ANOVA correcting for multiple comparisons using Dunnett's test relative to DMSO. MDA-MB-231 cells were seeded at a density of 300,000 per well and treated 48 hours later with Crassin (5 µM) or vehicle control (DMSO) +/- NAC (3 mM) for 24 or 48 hours. LC3B II expression was analysed using Western blotting at 24 hours* ***(B)*** *and 48 hours* ***(C)****, and densitometrically quantitated using ImageLab software 5.2.1* ***(D,E)*** *(volume intensity of band relative to matched Actin band). Results are expressed as mean ± SEM (n = 3 independent experiments). Statistical significance was calculated relative to DMSO by one-way ANOVA using Dunnett multiple comparisons and reporting adjusted p-values.* (*p < 0.05, **p < 0.01, ***p < 0.001, ****p < 0.0001)

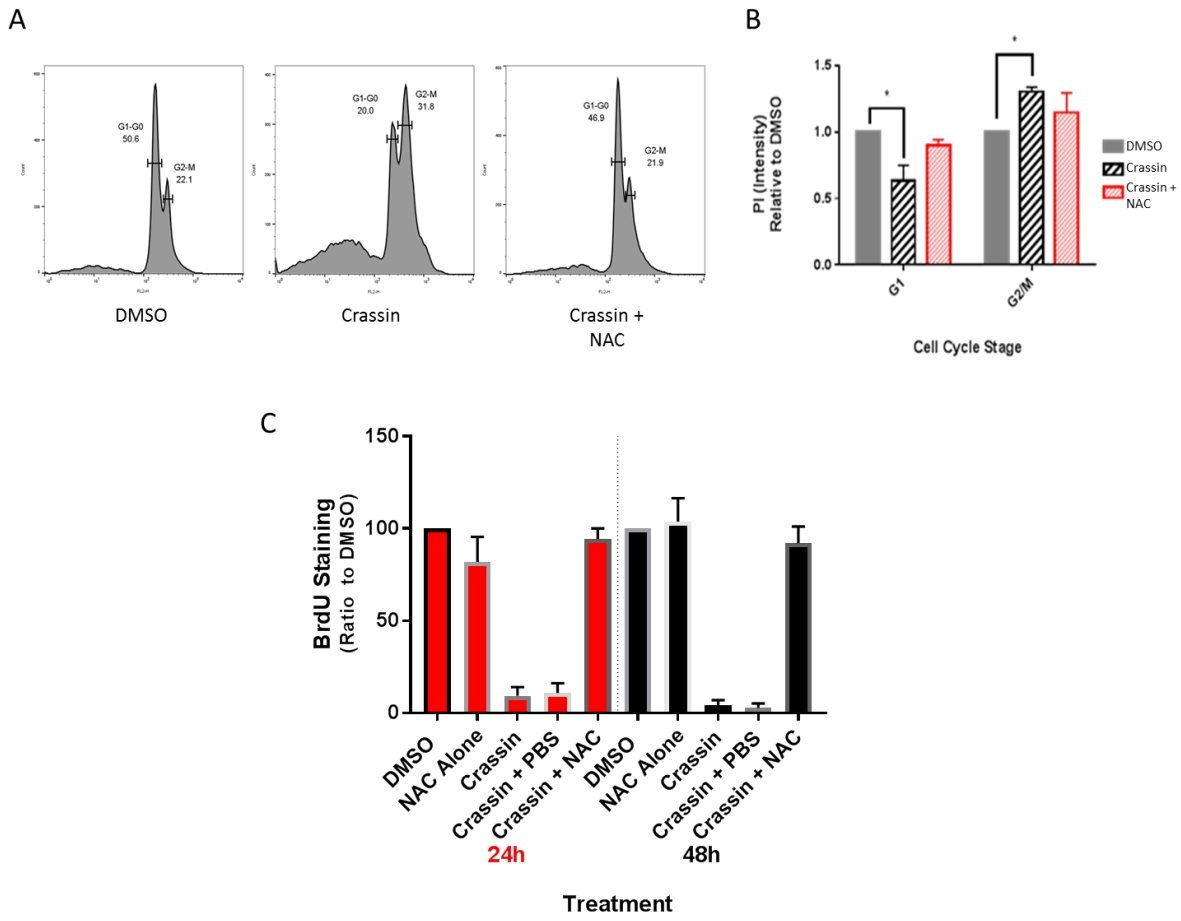

Figure 3.12: Crassin induces cell cycle arrest in a ROS-sensitive manner. *MDA-MB-231 cells were plated at 300,000 cells per well and treated 48 hours later with Crassin (5 µM) for 24 or 48 hours, +/- 1 hour pre-treatment with NAC (3 mM). Cells were flow cytometrically analysed after staining with PI dye and assessed for G1/G2 peaks. MDA-MB-231 cells were seeded at a density of 2,500 cells per well in 96-well plates and treated 48 hours later with Crassin (5 µM) for 24 or 48 hours, +/- 1 hour pre-treatment with NAC (3 mM). Next, a BrdU colorimetric assay was performed* ***(C, D)****. Data (n = 3 independent experiments) are expressed as mean ± SEM. Statistical significance was assessed by comparing Crassin to the pre-treated NAC group* (*p < 0.05, **p < 0.01, ***p < 0.001, ****p < 0.0001)*; one-way ANOVA performed using Prism 6 software with multiple comparisons and co reporting adjusted p-values calculated using DMSO treated control for all groups).*

3.3.11 Crassin synergises with Doxorubicin in targeting TNBC cell viability

Finally, the potential usefulness of a cytostatic compound like Crassin in combination with an established chemotherapeutic drug (doxorubicin) was investigated in TNBC cells. We found that the combination of Crassin and doxorubicin synergistically reduced cell viability over the responses to either compound alone (**Figure 3.13**, Dox. 2.5 µM; reductions of 30 ± 2% and 69 ± 2% at 24 hours and 48 hours, respectively; Crassin 5 µM; reductions of 37 ± 3% and 66 ± 2% at 24 hours and 48 hours, respectively; Crassin and Dox combination reductions of 58 ± 3% and 82 ± 2% at 24 hours and 48 hours, respectively).

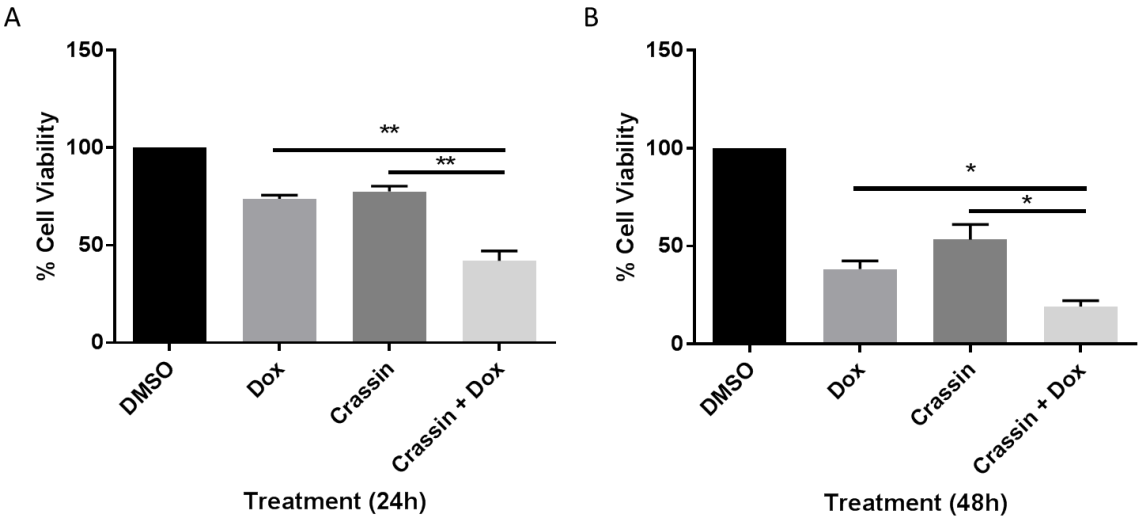

Figure 3.13: Crassin- and doxorubicin-induced reductions in cell viability are synergistic. *MDA-MB-231 cells were seeded at a density of 5,000 cells per well in 96-well plates and treated with Crassin/Dox 48 hours after seeding (5 µM or 2.5 µM, respectively). Cell viabilities were assessed using Alamar Blue assays after 24* ***(A)*** *or 48* ***(B)*** *hours and expressed as % optical density of that in vehicle control (DMSO)-treated cells. Data (n = 3 independent experiments) are expressed as mean ± SEM. Statistical significance (*p < 0.05, **p < 0.01, ***p < 0.001, ****p < 0.0001) was determined using unpaired two-tailed Student's t-tests calculated using DMSO treated control for all groups).*

3.4 Discussion

Gastro-oesophageal cancers and triple-negative breast cancers (TNBC) are both associated with poor patient survival (27, 28, 36, 37, 44, 45, 184-186). Despite recent advances, specifically for HER2-positive gastro-oesophageal cancers (71, 72), few targeted therapies are available and, therefore, the treatment options are often limited to surgery, radiation or conventional chemotherapy (28). Here, we identified a natural compound, Crassin, which effectively reduces the viability of three gastro-oesophageal cell lines *in vitro* and demonstrated promising bioactivity against a gastric cell line in a *semi-in vivo* setting.

In light of the fact that Crassin exerted significant reductions on the viabilities of cancer cell lines ESO26, N87 and OE19, this led us to speculate that Crassin may also have the capability to inhibit other aggressive phenotypes associated with cancer development. Hence we tested the ability of Crassin to inhibit colony formation across three gastro-oesophageal cell lines. Quantification of colony forming assays revealed that Crassin significantly reduced the ability of gastro-oesophageal cancer cell lines to form colonies in this setting. Importantly, the ESO26 cancer cell line had an overall lower level of colony formation in control conditions, and hence this limited our ability to extrapolate data from this cell line for this assay. Future work should asses other phenotypical changes better suited to the ESO26 cell lines (e.g. migration and invasion assays). However, we believe that Crassin may merit further exploration in pre-clinical settings.

We further examined both the efficacy and toxicity profile of Crassin in this setting using a *semi-in vivo* chick embryo model. The chick chorioallantoic membrane (CAM) assay has been extensively utilised by cancer researchers, as an effective tool to study the invasive nature and angiogenic properties of cancer cells (172, 187, 188). Treatment of tumours with Crassin on the CAM of developing chick embryos showed a reduced ability to develop through negative Ki67 and cytokeratin staining, commonly used for proliferation and invasion assessment (189, 190). This was supported by both evidence of

dead cancer cells within the Matrigel of Crassin-treated tumours and also through the invasive nature of DMSO-treated negative control tumours. The ability of DMSO-t r e a t e d c e l l s t o i n v a d e i n t o t h that the cells were indeed effective in utilising host systems, and comments on the naturally invasive nature of the cell line selected. While we are aware that two of six of the Crassin-treated xenografts did show similar aggressive phenotypes to control (DMSO) treated groups, we suggest that the manner in which cells are implanted and treated leaves a wider margin for error than other *in* vivo models. Since the treatments are given at small volumes across the silicon ring, cells which have dispersed from within the Matrigel plug may not be targeted by the treatment (191). We also note that one of the DMSO control-treated CAMs failed to develop a tumour and did not have a viable embryo upon extraction.

Having firmly established that Crassin had the potential to reduce tumour establishment both *in vitro* and *in vivo* in gastro-oesophageal cancer cells, we also demonstrated that Crassin exerts similar properties in breast cancer.

Based on this result, we assessed the expression levels of the survival effectors pAkt and pERK in TNBC cells following Crassin treatment. Akt in its activated (phosphorylated) form has been shown to promote cell survival and to inhibit apoptosis (180, 192, 193). With the expectation that the pAkt and pERK levels would decrease following Crassin treatment, we surprisingly noted significant *increases* in pAkt and pERK expression levels. Accordingly, we considered the involvement of reactive oxygen species (ROS) as a possible explanation to this conundrum. ROS are generated due to a partial reduction of oxygen, resulting in molecules with unpaired electrons (194). ROS can oxidise members of the PI3K/Akt signalling pathway (194) and specifically activate ERK (195-197). This phenomenon may occur naturally during mitochondrial oxidative metabolism, but can also be induced in response to external stimuli (198). The unstable nature of ROS means they are highly reactive and can cause a further instability of cellular macromolecules, including lipids, proteins and DNA (198, 199). If this process o f ‘ e l e c t r o n s t e a l i n g ’ i s l e f t u n c h e c k

structures continues to deteriorate, a cell may enter the process of programmed cell death (199, 200). Therefore, we used an anti-oxidant (NAC) in an attempt to prevent Akt and ERK activation (phosphorylation). Anti-oxidants have the ability to donate an electron to unstable free radicals, without compromising their own stability (198), and hence may prevent damage caused by ROS seeking or donating electrons. Strikingly, we found that NAC treatment prevented Crassin-induced increases in pAkt and pERK, indicating that this phenotype is mediated by an oxidant environment. Furthermore, NAC treatment prevented Crassin-induced reductions in cell viability in TNBC cells compared to C4 treatment alone. This is consistent with Crassin inducing oxidative stress upstream of Akt activation, resulting in reduced cell viability.

Previous work had attempted to elucidate ROS levels post-Crassin treatment, however the assay selected (Dichloro-dihydro-fluorescein diacetate; DCFH-DA) did not reveal oxidative stress states in Crassin-treated cells (data not shown). Alternative ROS measurement assays may prove useful in highlighting ROS activation in Crassin-treated cells, since ROS-protective NAC clearly reduces cell viability loss.

Since Crassin treatment significantly reduced the viability of TNBC cells, we next attempted to identify the cell death mechanism known to involve ROS. Caspase-3 (Cas-3) is a key member of the apoptotic pathway (182), and its cleavage activates a downstream cascade of events leading to cytochrome c release and cell death (181). However, no Cas-3 cleavage was observed in Crassin-treated samples. Furthermore, no evidence of Annexin-V positivity was noted in Crassin-treated cells, suggesting that the Crassin-induced reductions in cell viability were independent of traditional apoptotic pathways. To next test whether Crassin could induce necrosis, we measured LDH release in TNBC cells and found that the Crassin-decreases in cell viability occurred independently of necrosis. Also, links between ROS activation and necroptotic or ferroptotic mechanisms of cell death have recently been reported (161, 164, 166), but we failed to obtain any evidence for necroptosis or ferroptosis in response to Crassin treatment of TNBC cells. Interestingly,

increases in LC3B cleavage (indicative of activation of an autophagic mode of cell death) were observed, but our morphologic observations suggest that these increases in expression may not reflect autophagy, or at most may indicate that Crassin-treated cells are in a primitive stage of cell death. Extended treatment times may uncover a shift from cellular stasis to induced autophagy, though significantly diminished cell numbers at later treatment time points may pose an inevitable concern for result validation.

While it is possible that the later (48 hour) Crassin treatment time point represents a premature state of cell death, cell cycle analysis revealed a significant shift from G1 to G2/M in these cells compared to controls. Furthermore, BrdU assays revealed diminished proliferative capabilities of TNBC cells following Crassin treatment, supporting a role for Crassin in cytostasis induction. The induction of cell cycle arrest by Crassin may prove to be an important mechanistic effect of the non-cytotoxic natural compound, similar to the cytostatic effects exerted by Taxol (201). Our data showing synergism of Crassin with the chemotherapeutic drug doxorubicin may indicate a potential future use in clinical settings. At this point in time, however, it is not known whether (and how) Crassin synergises with the anti-tumorigenic effects of other chemotherapeutic compounds (i.e., anti-metabolites, alkylating agents etc.). Nonetheless, supportive literature demonstrates benefits of anti-cancer cytostatic therapies when used in combination with cytotoxic chemotherapies (202), and this approach is now commonly employed in the design of chemotherapy protocol algorithms (203). Such algorithms have shown, both *in vivo* and *in silico*, that cytostatic/cytotoxic combinations may improve the efficacy of treatment and the overall efficiency of chemotherapy (203). It is also of interest to note that compound Crassin belongs to the same broad chemical class as the widely used cytostatic chemotherapeutic drug, Taxol (the diterpenoid class). Whilst both compounds are of natural origin, they exhibit chemical differences that likely affect their bioactivities. Crassin has the following formula and molecular weight: $C_{20}H_{30}O_4$, MW 334.456, while Taxol is a nitrogenous alkaloid with the following formula and molecular weight: $C_{47}H_{51}NO_{14}$ /MW 853.918. Similar to

Crassin, Taxol has been shown to induce G_2/M cell cycle arrest, but under certain circumstances Taxol has also been found to act as a pro-apoptotic agent in a p53-independent manner (201, 204). We found, however, that Crassin exhibited no cytotoxicity at the tested concentrations. However, given the similarities between these compounds, it is possible that the mechanism by which they bind and are taken up into the cell may also be similar, and future work investigating the role of Crassin could investigate this. Taken together, we found that Crassin may induce cell cycle arrest via the sensitisation of cancer cells to ROS, thereby increasing Akt and ERK activation and decreasing cell proliferation. Our data, already published (Richards et al., 2017 (205)), warrant a further investigation of the therapeutic efficacy of Crassin in combination with other cytotoxic agents for both gastro-oesophageal and TNBC and perhaps other cancer types.

Chapter 4: Elucidating the importance of Junctional Adhesion Molecule-A in non-breast cancers

4.1 Introduction

Previous work in our laboratory has reported that JAM-A gene and protein expression positively correlates with poor prognosis in breast cancer patients, and highlighted the link between JAM-A and integrin-mediated migratory events in this cancer type (131). Further work by our laboratory and others has further shown key links between JAM-A, Rap1 GTPase and integrin signalling (206, 207), which may underlie migratory events associated with the early stages of metastasis.

As previously described in Chapter One, there are conflicting publications relating to the role of JAM-A in gastro-oesophageal cancers; with some studies reporting low levels of JAM-A as a biomarker for poor survival (122) and others supporting a role for JAM-A overexpression in poor prognosis (127). Similar conflicting evidence has been observed in other cancer types. In light of the ambiguity surrounding the role of JAM-A in gastro-oesophageal cancers, there is a need to elucidate whether JAM-A expressional changes occur at all and merit its consideration as a putative drug target for this cancer type.

As JAM-A is an important tight junction protein, physiologically responsible for cellular adhesion, morphology and polarity (106, 107, 118, 121), it is conceivable that its loss may reduce cell-cell anchorage, driving local invasion in cancers. However the work by our group (100, 131, 206) and others (125, 126, 133) to date suggests that JAM-A overexpression is more likely to drive pathophysiological events through downstream activation of cell migration and invasion. It is therefore interesting to speculate that the same dichotomies exist for JAM-A expression in gastro-oesophageal cancers, whereby either loss or overexpression could play critical roles in driving cancer in different spatial and temporal contexts. Cellular switches suggest a "Janus" function for JAM-A expression in cancers. Understanding the balance between JAM-A loss and overexpression in pathophysiological settings could be the key to underpinning JAM-A as a therapeutic target.

If JAM-A overexpression were to play an important role in gastro-oesophageal cancers, we would expect to see similar increases to proliferative and migratory capacities as described in breast cancer cell lines (131) in gastro-oesophageal cancer cell lines *in vitro*. Our group has previously shown siRNA-mediated silencing of JAM-A decreases invasion, migration, colony forming capabilities and proliferation *in vitro* in breast cancer cell lines (131), and likewise cell lines altered to stably overexpress JAM-A were shown to be more aggressive and to have higher proliferation rates (Rodrigo Cruz, personal communication). JAM-A-overexpressing cells were also shown to possess higher migratory and invasive phenotypes. It is, however, currently unknown whether the same functional changes would be demonstrated in gastro-oesophageal as well as breast cell settings.

Furthermore, our previous work has highlighted that cleavage of JAM-A (cJAM-A) by A disintegrin and metalloproteinase (ADAM) proteases may play an important role in driving force for migration and invasion in breast cancer. A recombinant form of this cJAM-A (rcJAM-A) applied to cells was recently shown to increase invasive properties of breast cancer cells in *in vitro and semi-in vivo* settings (208). JAM-A cleavage has also been shown to play a role in inhibiting neutrophil transmigration, as well as serving as a biomarker for inflammation, with cJAM-A levels increasing in the presence of pro-inflammatory cytokines indicating cJAM-A may have other functions in other settings relevant to cancer (207, 209). Specifically, elevated levels of cJAM-A were shown in patients with coronary heart disease, which also correlated with levels of tumour necrosis factor-α (TNF-α) (209). Furthermore it was suggested that cJAM-A levels were directly influenced by increased TNF-α, driving platelet aggregation and increasing the burden of plaque formation in atherosclerosis patients, placing JAM-A at the centre of an inflammatory-driven disease . Since cJAM-A has also featured in diverse pathophysiologies associated with the heart, including coronary heart disease and hypertension (210, 212), it is possible that it could play a role in cancer-associated thrombosis. Another potential mechanism of action for cJAM-A is as a communicator between cells. It has been speculated that cJAM-A may act as

a ligand, shed into the extracellular space as a communicator with both the microenvironment and neighbouring cells, in order to initiate downstream signalling pathways that drive the functional phenotypes associated with increased invasion (208). It is therefore important to investigate whether the same role for cJAM-A exists in gastro-oesophageal cancers, and whether rcJAM-A has the ability to promote an invasive phenotype.

Further to this, our laboratory has recently shown that targeting JAM-A with a small peptide JAM-A-inhibitor in an *in vivo* mouse model of mammary ductal carcinoma significantly decreased tumour growth and invasion (Yvonne Smith, personal communication). The JAM-A inhibitor was designed using molecular modelling software to block the *cis*-dimerisation site of JAM-A, which is hypothesised to inhibit potential pathogenic downstream effects. This work further solidified our working theory that JAM-A represents a druggable target in cancers. Knowing this, it is important to investigate whether JAM-A is targetable across other cancers, or if its role is limited to specific cancer types. If JAM-A were to play a decisive role in gastro-oesophageal cancers, it may then offer an alternative target in this setting.

4.2 Aims of this Chapter

The primary aim of this chapter was to elucidate whether JAM-A overexpression is associated with aggressive phenotypes in gastro-oesophageal cancers. Given published discrepancies to date, it is important to clarify whether JAM-A is a potential target in those cancers as well as that of the breast. The specific aims where therefore as follows:

Specific Aim 1: To compare JAM-A protein expression across non-breast cancers and a subset of gastro-oesophageal cancers.

Specific Aim 2: To establish whether loss or gain of JAM-A affects the tumourigenic properties of gastro-oesophageal cancers *in vitro* or *semi-in vivo.*

Specific Aim 3: To investigate the role of cleaved JAM-A in gastro-oesophageal cancers, given the recent indication it may play an important role in breast cancer.

4.3 Results

4.3.1 JAM-A expression across a multi-organ cancer tissue microarray

In order to explore the differential expression of JAM-A reported in different cancers, a multi-organ tissue microarray (TMA) was stained for JAM-A protein expression **(Figure 4.1)**. Based on semi-quantitative scoring of membranous JAM-A staining intensity, cancer types such as nasal, breast, lung, stomach and oesophageal all demonstrated moderate/high (2+/3+) levels of JAM-A whereas lymph and cerebral cancers were classified as having low/absent (0/1+) expression **(Figure 4.1)**.

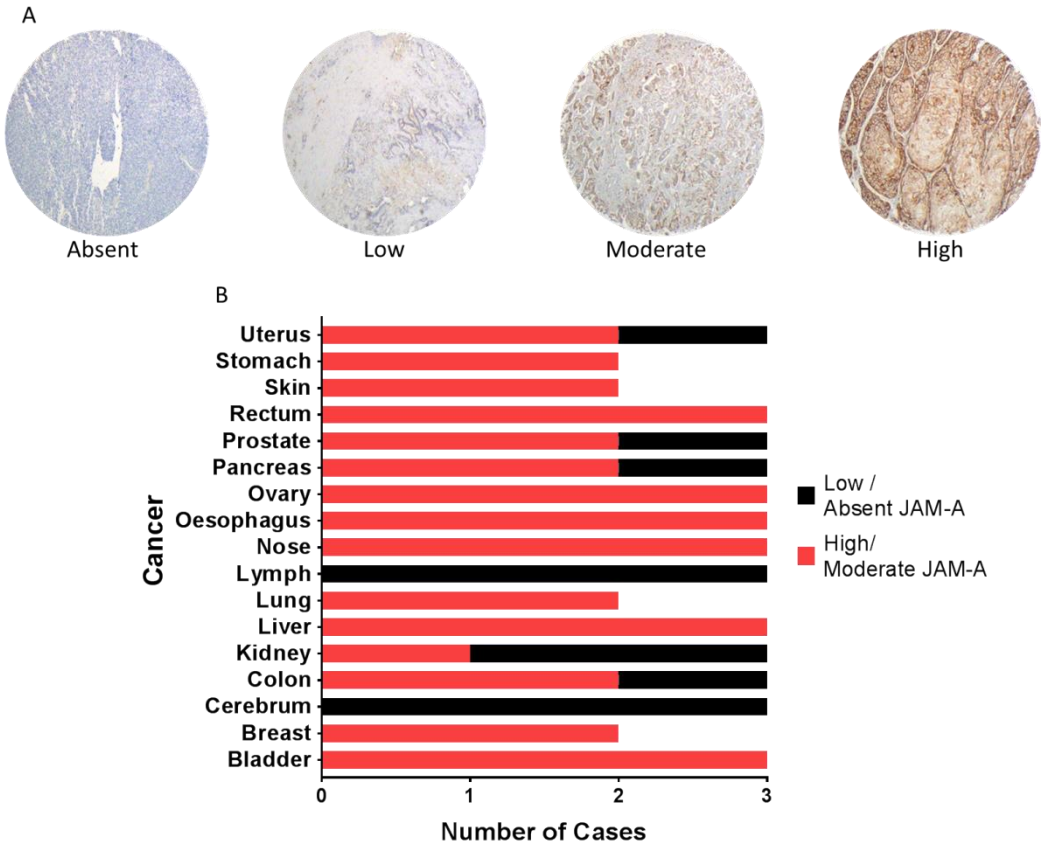

Figure 4.1: High levels of JAM-A are associated with several cancer types. *Immunohistochemical staining of JAM-A in a commercial TMA was scored as absent (0), low (1+), moderate (2+) or high (3+)* ***(A)*** *based on complete/incomplete membranous staining. JAM-A protein expression was then correlated with cancer type and grouped as either being absent/low or moderate/high in* ***(B).*** *Representative images were obtained at 20x magnification on an Olympus CKx41 microscope with Cell B software (****A).***

Given that both gastric and oesophageal cancers showed moderate/high levels of JAM-A staining across the multi-organ cancer TMA, we next wanted to investigate whether this correlation was seen on a larger scale, and whether JAM-A overexpression correlated with worsened prognosis.

4.3.2 JAM-A associates with poor prognosis in gastric cancer patients

In order to establish whether JAM-A played a role in gastro-oesophageal cancers, we first utilised publicly-available gene expression data from patient databases (www.kmplot.com) (140). As shown in **Figure 4.2**, recommended probes and exclusions for the JAM-A gene F11R were selected as described in Section 2.15, and correlated with both overall survival and tumour progression in gastric cancer patients. High levels of F11R significantly correlated with poorer overall survival in 140 gastric cancer patients ($p=0.0067$), 33 of whom expressed high levels of F11R. There was also a correlation between high F11R expression and shorter time to first progression in gastric cancer cases, but this correlation was not statistically significant ($p=0.099$). However the latter sample size was small at only 59 patients (of which 15 had high levels of F11R), therefore we suspect that the finding would be statistically significant in a larger population. Given these results, we next set about to establish suitable *in vitro* models to study JAM-A expression in gastro-oesophageal cancers.

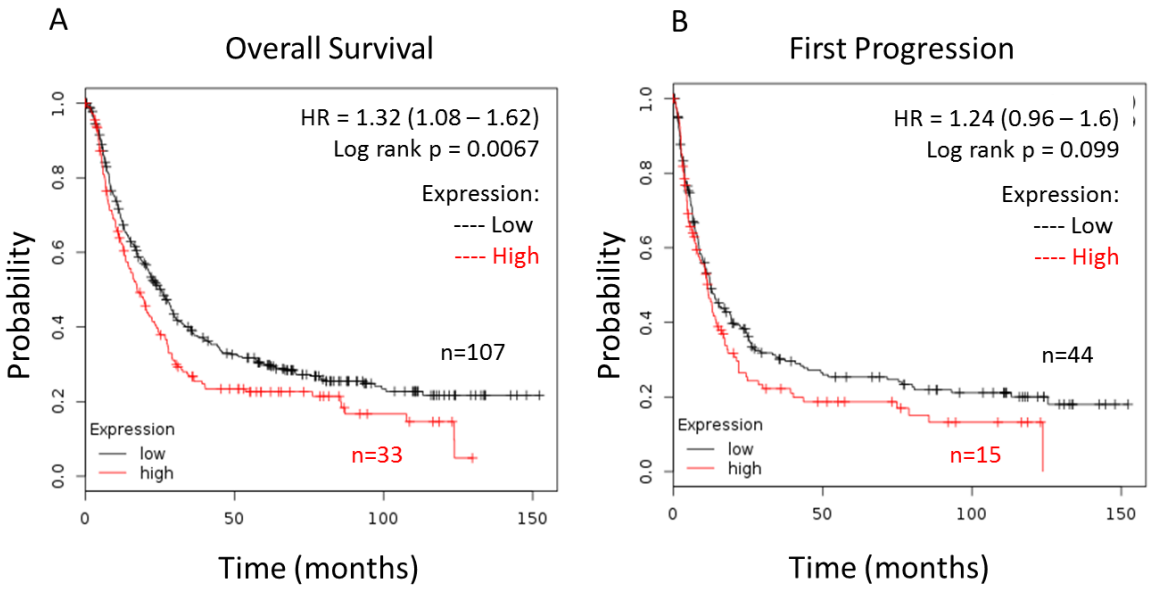

Figure 4.2: JAM-A overexpression is related to poor prognosis in gastric cancer patients. *The Kaplan Meier Plotter platform (http://kmplot.com/analysis/) was used to correlate JAM-A gene expression with indices of prognosis in gastric cancer patients, using the F11R jetset probe excluding GSE62254 as recommended. This revealed that high mRNA expression of F11R (JAM-A) was associated with worsened overall survival* ***(A)*** *and shorter time to first progression* ***(B).***

4.3.3 JAM-A Expression Profile in GE Cancer Cell Lines

To establish representative *in vitro* models for the study of JAM-A in gastro-oesophageal cancers, a panel of GE cancer cell lines was cultured and probed for JAM-A and HER2 expression under baseline conditions. Via Western blotting, JAM-A protein expression was detected to be high in N87, OE33, OE19, ESO26, SNU16 and low in KATO III cells. HER2 expression was high in N87, OE19 and ESO26 cells, but low in OE33 and negligible in SNU16 and KATO III cells (**Figure 4.3**). Thus ESO26, N87 and OE19 cells were selected as the models for on-going studies due to their high levels of both JAM-A and HER2 expression.

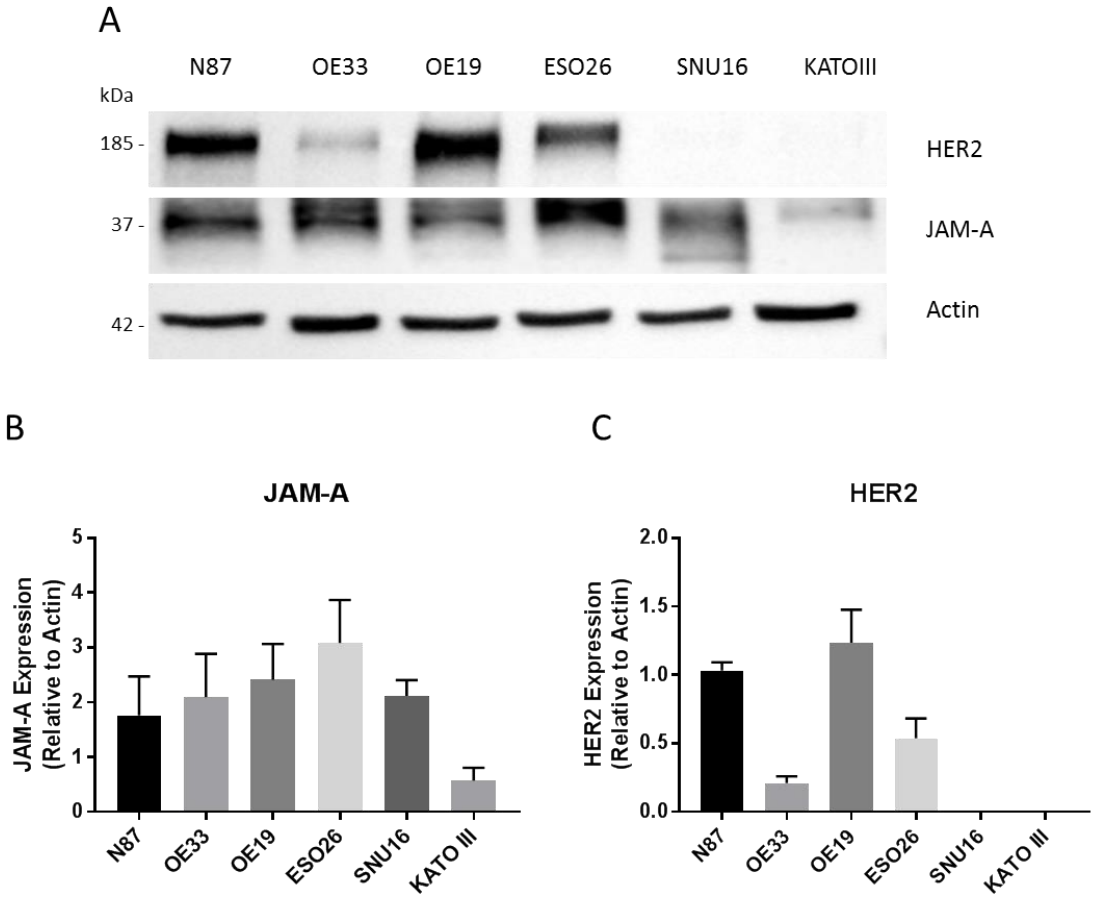

Figure 4.3: Basal levels of JAM-A and HER2 protein in a panel of GE cell lines. *N87, OE33, OE19, ESO26, SNU16 and KATO III cell lines were Western blotted for basal levels of JAM-A and HER2 expression* ***(A).*** *Densitometric analysis of three independent experiments was used to compare the basal expression of both JAM-A* ***(B)*** *and HER2* ***(C)*** *across the cell lines.*

4.3.4 Modulating JAM-A expression through transient silencing and overexpression *in vitro*

Our group has previously examined the potential role of JAM-A in breast cancer cells by undertaking classic gene silencing and overexpression methods. In order to begin investigating the potential importance of JAM-A expression in gastro-oesophageal cancer cells, we set about optimising the methods used previously. As shown in **Figure 4.4**, both JAM-A mRNA and protein expression levels were significantly reduced across all three cell lines following transient JAM-A gene silencing. Specifically, in ESO26 cells JAM-A mRNA expression was reduced by 58 ± 8% (p=0.0017) while protein levels were reduced by 44 ± 16% (p=0.0471) **(Figure 4.4)**. In N87 cells, JAM-A mRNA and protein levels were significantly reduced by 53 ± 7% and 39 ± 7% respectively (p=0.0017 and p=0.0043) **(Figure 4.4)**. In OE19 cells, JAM-A mRNA and protein expression were significantly reduced by 36 ± 1% and 56 ± 17%, respectively (p=0.0335 and p=0.0317) **(Figure 4.4)**.

Similarly, transient overexpression of JAM-A elicited increased JAM-A expression at both mRNA and protein levels for all three gastro-oesophageal cell lines tested (ESO26, N87 and OE19; **Figure 4.5)**. However, inter-experiment variability reduced the significance of some results. For example, JAM-A mRNA expression increased from 3-23-fold in ESO26 cells across experimental replicates. Despite such a wide standard deviation, the positive point to note was that JAM-A was consistently overexpressed across all conditions. We were satisfied that the JAM-A overexpression levels achieved were sufficient for proof-of-principle studies. ESO26 cells demonstrated a fold increase of 9 ± 7 for JAM-A mRNA expression, and protein expression significant increases of 137 ± 35% **(Figure 4.5;** p=0.0181**)**. A significant average fold increase of 100 ± 31% was seen in N87 JAM-A mRNA expression (p=0.0338), and largely variable protein increases of 50 ± 40% **(Figure 4.5)**. OE19 cells had almost significant increases in JAM-A mRNA (130 ± 53 fold; p=0.0594), while protein expression of JAM-A was significantly) overexpressed by 138 ± 24% **(Figure 4.5;** p=0.0046**)**.

Since JAM-A has a similar molecular weight to some housekeeping proteins used as controls, Ponceau S staining was sometimes used to demonstrate equal protein loading. Having established successful silencing and overexpression protocols for JAM-A in the three chosen gastro-oesophageal cancer cell lines, we next set about to uncover whether modulation of JAM-A expression therein elicited any functional changes.

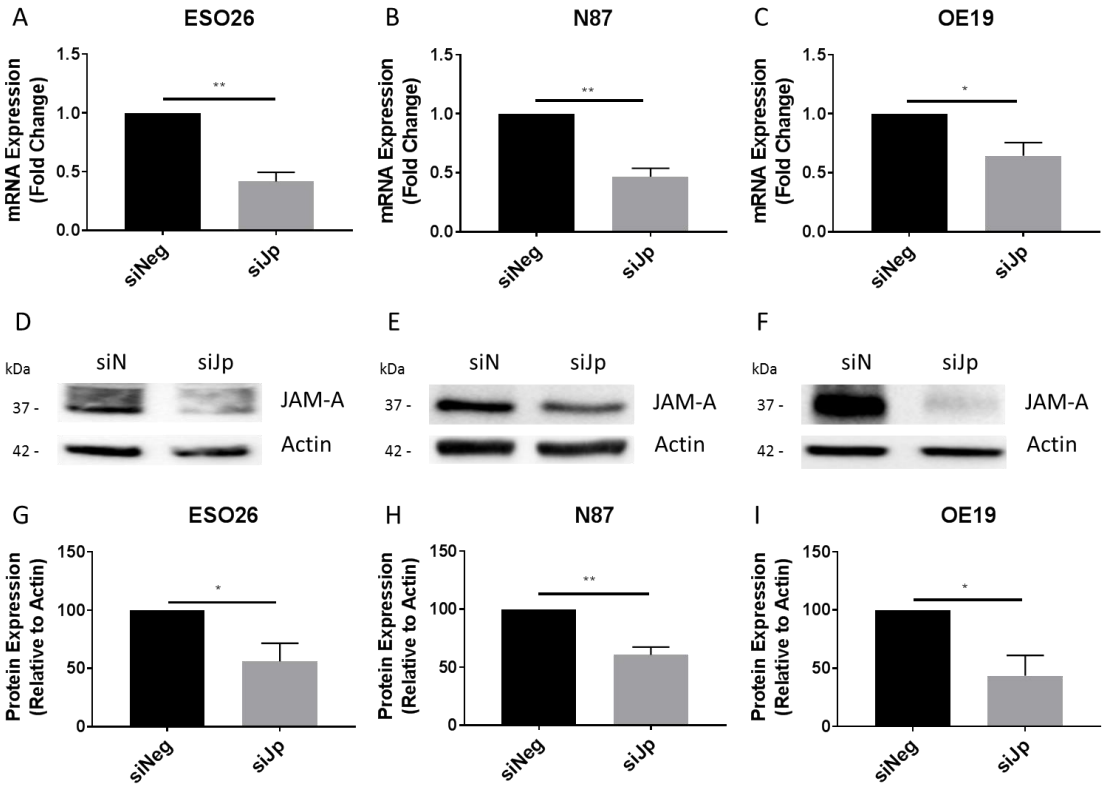

Figure 4.4: JAM-A mediated silencing induced significant reductions to JAM-A expression in gastro-oesophageal cell lines. *Gastro-oesophageal cancer cells lines were plated at 2x10^5 in 6-well plates and allowed to undergo one doubling time before being transiently transfected with either non-targeting siRNA (siNeg) or a JAM-A targeting siRNA pool (siJp) (final concentration 25nM). RNA was extracted and reverse-transcribed to cDNA, whereupon qRT-PCR was performed to detect JAM-A expression in ESO26* ***(A)*** *N87* ***(B)*** *and OE19* ***(C)*** *cells. Ct values of samples were set relative to matched Ct values of the housekeeping gene (RPLP0). Pooled data from three independent experiments (n=3) was displayed as mean ± SEM and statistically compared using unpaired two-tailed Student's t test. In parallel, total cellular protein was extracted and immunoblotted for JAM-A expression. ESO26* ***(D)****, N87* ***(E)****, and OE19* ***(F)****. Densitometric analysis (ESO26* ***(G)****, N87* ***(H)****, and OE19* ***(I)****) (n=3 independent experiments) was performed relative to a loading control (Actin) and displayed relative to siNeg as mean ± SEM. Significance was tested using unpaired, two-tailed student's t test (*p<0.05, **p<0.01, ***p<0.001, ****p<0.0001).*

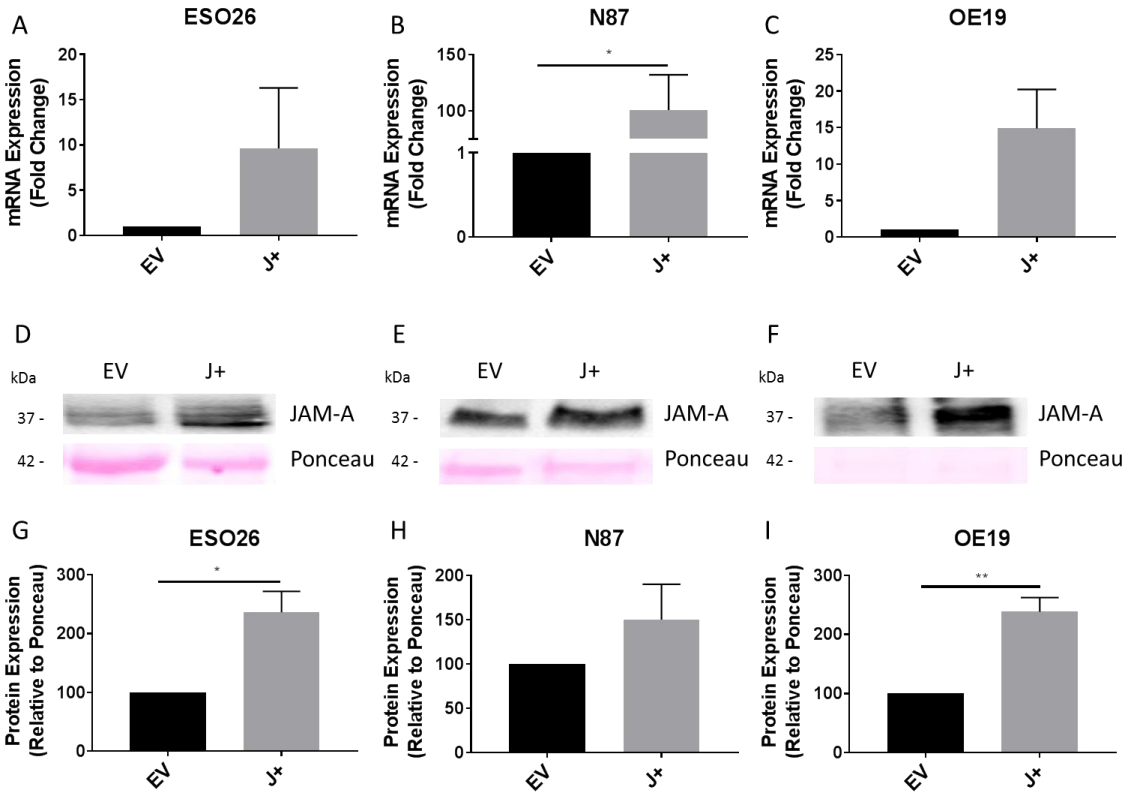

Figure 4.5: Transient JAM-A overexpression significantly increased JAM-A expression in gastro-oesophageal cell lines. *Gastro-oesophageal cancer cell lines were plated at 2x10^5 in 6-well plates. ESO26 cells were allowed to undergo one doubling time and N87 and OE19 cells were incubated for 24h before cells were transiently transfected with either control (EV) or hJAM-A (J+) plasmid (1µg). RNA extractions of samples were completed, cDNA generated and qRT-PCR performed to assess JAM-A mRNA expression in ESO26* ***(A)*** *N87* ***(B)*** *and OE19* ***(C)*** *cells. Ct values of samples were set relative to matched Ct values of the housekeeping gene (RPLP0) Pooled data from three independent experiments (n=3) was displayed as mean ± SEM and statistically compared using unpaired two-tailed t-tests. In parallel, total cellular protein was extracted and immunoblotted for JAM-A expression. ESO26* ***(D)****, N87* ***(E)****, and OE19* ***(F)****. Densitometric analysis (ESO26* ***(G)****, N87* ***(H)****, and OE19* ***(I)****) (n=3 independent experiments) was performed relative to a loading control (Actin) and displayed relative to siNeg as mean ± SEM. Significance was tested using unpaired, two-tailed student's t-tests (*p<0.05, **p<0.01, ***p<0.001, ****p<0.0001).*

4.3.5 Induced changes in JAM-A expression differentially impact cell viability in gastro-oesophageal cancer cell lines.

As shown in **Figure 4.6**, JAM-A silencing reduced the cellular viability of two gastro-oesophageal cell lines (ESO26 and N87). Interestingly, however, it *increased* the viability of OE19 cells. Proliferation was assessed over five days following initial transfections period (72h). Cells transfected with siRNA were re-silenced every 72h to ensure JAM-A levels remained reduced; and Alamar blue assays used to compare treated cells to their negative control counterparts. Surprisingly, cells induced to transiently overexpress JAM-A did not show any significant changes in cell viability when compared to EV controls **(Figure 4.6)**. This may reflect the fact that cells were only transfected once with JAM-A overexpressing plasmids, in contrast to repeated transient siRNA transfections. Regardless, we hypothesised that any overt changes to proliferative rates would be demonstrated during the first few days of assessment.

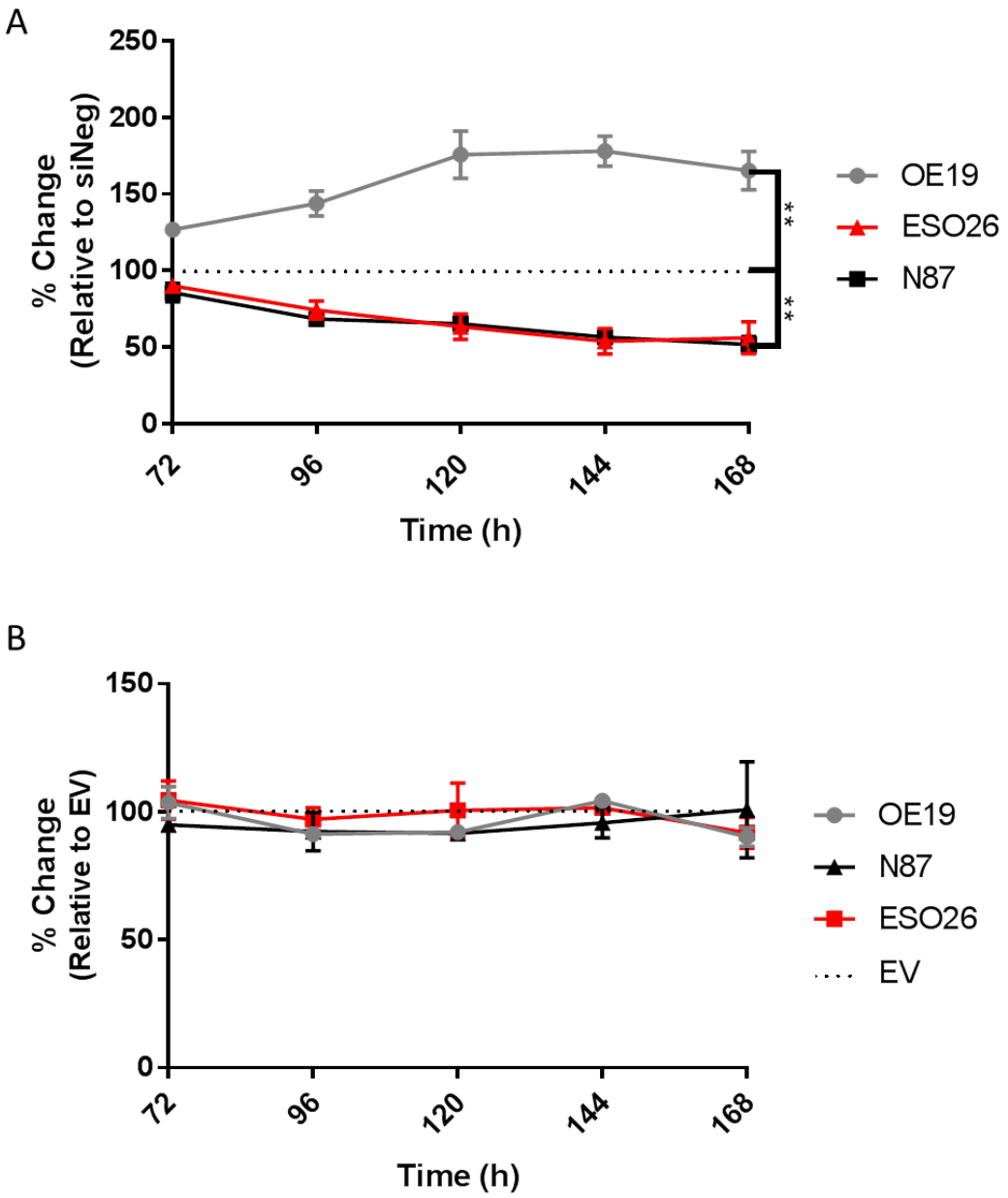

Figure 4.6: JAM-A silencing reduces cell viability in two gastro-oesophageal cancer cell lines. *Three gastro-oesophageal cell lines (5,000 cells per well) were transfected with either a pool of JAM-A-targeting siRNA (siJp) or non-targeting siRNA (siNeg;* ***A****); in parallel with Empty Vector control plasmid (EV) or JAM-A overexpressing plasmid (J+;* ***B****). Cell viability/proliferation was measured using Alamar blue assays 72h to 168h post-transfection* ***(A, B).*** *To maintain gene silencing status, siNeg and siJp were re-transfected every 72h during the assessment period. Experiments were performed three times and data shown as mean ± sem compared using two-tailed, paired Student's t-tests (*p<0.05, **p<0.01, ***p<0.001, ****p<0.0001).*

We also examined whether JAM-A silencing or JAM-A overexpression drove invasive phenotypes in gastro-oesophageal cells. ESO26 and OE19 cells were selected for their differential response to JAM-A targeting (data not shown). Unfortunately, however, levels of invasion fell well below detectable limits from the standard curve generated for each cell line. This suggested that alternative approaches may in future need to be tested to explore invasion in such slow-growing cell lines.

4.3.6 JAM-A silencing, but not overexpression, altered colony-forming ability in two gastro-oesophageal cell lines

Colony-forming ability is often assessed as a means of establishing whether treatments can reduce aggressive functional phenotypes associated with cancer cells *in vitro (213)*. Having already established that JAM-A silencing induced different viability outcomes in different cell lines, we next set out to monitor colony-forming potential post-transfection with JAM-targeting reagents. As shown in **Figure 4.7,** both ESO26 and N87 cells exhibited reductions in colony-forming potential following JAM-A silencing. Specifically, that in ESO26 cells was significantly reduced by 28 ± 3% **(Figure 4.7**; p=0.0005**)** while that in N87 cells was significantly reduced by 24 ± 4% **(Figure 4.7**; p=0.0056**)**. In support of our previous findings showing that OE19 cells had increased cell viability following JAM-A silencing, OE19 cells also had an increased capacity for colony formation following JAM-A silencing with an increase of 37 ± 21%. However this was not statistically significant **(Figure 4.7)**. We also noted that ESO26 cells did not respond consistently in this assay, as their semi-adherent nature was incompatible with the low plating densities required for the assay.

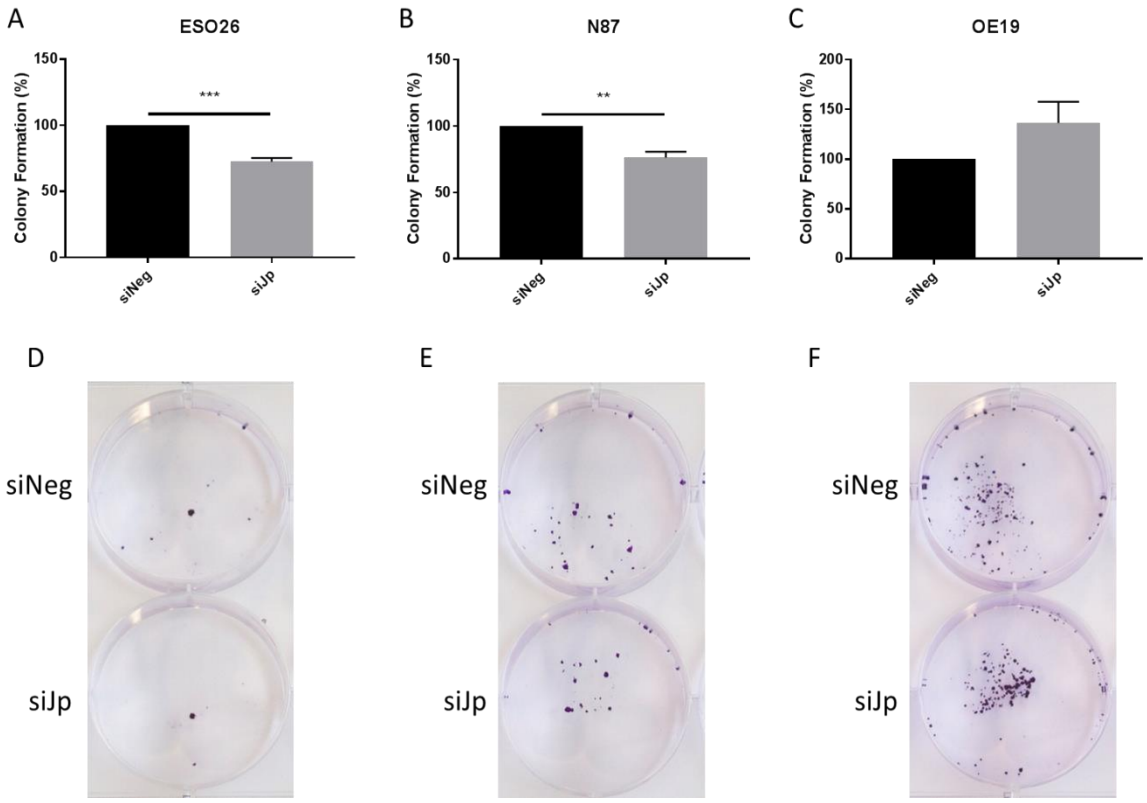

Figure 4.7: Differential colony forming abilities in response to JAM-A silencing in gastro-oesophageal cancer cell lines. *ESO26* ***(A, D)****, N87* ***(B, E)*** *and OE19* ***(C, F)*** *cells were plated at 1,000 cells per well and treated with either non-targeting siRNA (siNeg) or a pool of JAM-A targeting siRNA (siJp) (final concentration 25nM). Colony formation was assessed using crystal violet staining and read spectrophotometrically at an optical density of 595nm following solubilisation of the stain in methanol. Data (n=3 independent experiments) are expressed relative to vehicle control (siNeg) as mean ±SEM. Statistical analysis was calculated using unpaired two-tailed Student's t-test* (*p < 0.05, **p < 0.01, ***p < 0.001, ****p < 0.0001).

Taking this into account, and since unpublished evidence from our laboratory had found that breast cancer cells stably overexpressing JAM-A had increased colony-forming potential (Rodrigo Cruz, personal communication), we tested whether the same was the case for JAM-A transient overexpression in the three gastro-oesophageal cancer cell lines.

4.3.7 JAM-A overexpression does not alter colony formation in gastro-oesophageal cancer cells

As illustrated in **Figure 4.8,** gastro-oesophageal cancer cell lines were transiently transfected to overexpress JAM-A for 72h after a 7-day establishment period. Following transfection, cells were placed back into serum-positive medium and incubated for a further 10 days whereupon colonies were fixed, stained and spectrophotometrically quantified as described. As previously discussed, colony formation in ESO26 cells was not as successful as that in N87 and OE19 cells, but outputs were still analysed. There was no significant change in the colony-forming abilities of gastro-oesophageal cancer cell lines following JAM-A overexpression **(Figure 4.8)**.

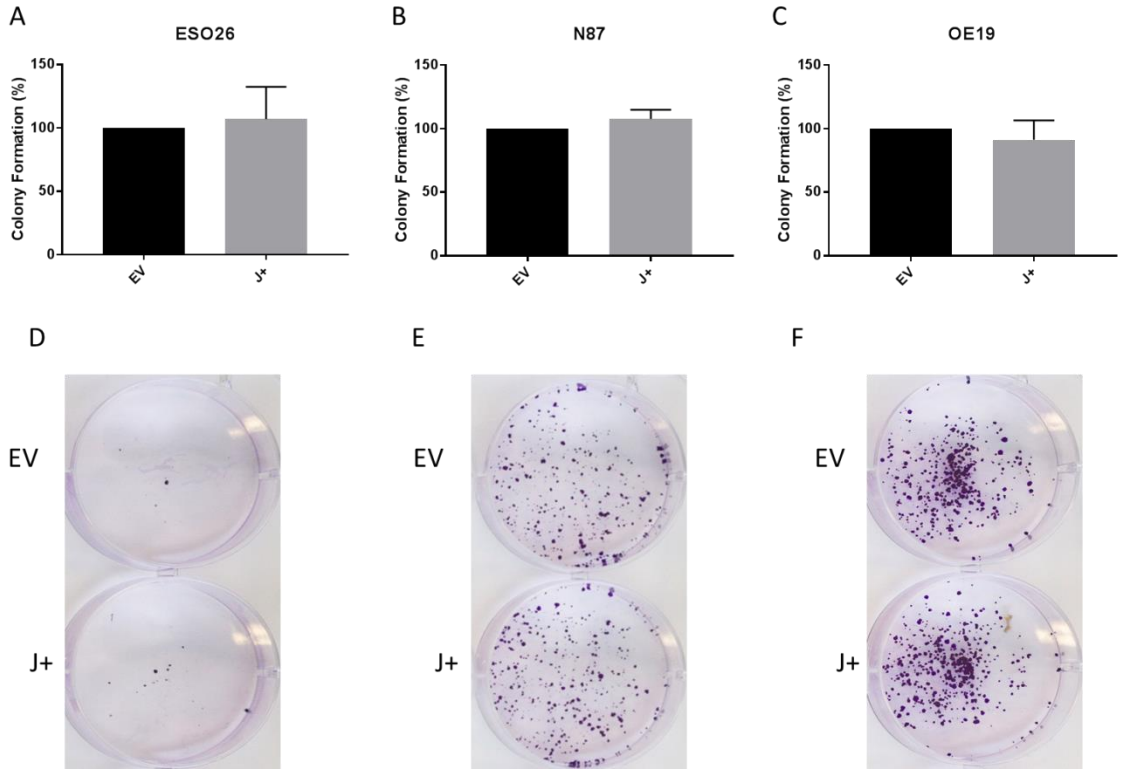

Figure 4.8: JAM-A overexpression does not alter colony-forming potential in gastro-oesophageal cancer cell lines. *ESO26* ***(A, D)****, N87* ***(B, E)*** *and OE19* ***(C, F)*** *cells were plated at 1,000 cells per well and transfected with either Empty Vector (EV) or JAM-A overexpressing (J+) plasmids (1µg). Colony formation was assessed using crystal violet staining and read spectrophotometrically at an optical density of 595nm following solubilisation of the stain in methanol. Data (n=3 independent experiments) are expressed relative to vehicle control (EV) as mean ±SEM. Statistical analysis was calculated using unpaired two-tailed Student's t-test (*p < 0.05, **p < 0.01, ***p < 0.001, ****p < 0.0001).*

4.3.8 Recombinant soluble JAM-A treatment in gastro-oesophageal cancer cells has no impact on proliferation

Since JAM-A overexpression was insufficient to alter the proliferation or colony-forming potential of gastro-oesophageal cell lines, yet JAM-A silencing results suggested that the protein had a functional role in driving tumorigenic properties, we next considered other possibilities. Our group recently reported that JAM-A is cleaved from the membrane of breast cancer cells (cJAM-A), and may play a role in driving resistance to HER2-targeted therapies (208). Therefore we hypothesised that simple upregulation of JAM-A protein expression may not by itself drive poorer survival for patients and enhance cell viability as noted *in vitro* for two of our gastro-oesophageal models. First we confirmed by Western blotting that cJAM-A could be detected in gastro-oesophageal cancer cell lines (**Supplementary Figure 3).** Next we examined the levels of cJAM-A following either transient JAM-A silencing (siJp) or overexpression (J+) relative to controls (siNeg and EV, respectively) using a commercially available ELISA kit, in order to establish differences in cJAM-A levels (data not shown). Unfortunately, we were unable to detect any changes between control and JAM-A targeted samples, as all sample cJAM-A level outputs fell below the threshold of the standard curve and were not quantifiable.

Since the role of cJAM-A was still unclear in this setting, we next utilised a commercially-available recombinant form of cleaved JAM-A (rcJAM-A) and treated all three cell lines at varying concentrations (0.5, 2, 5 ng/mL) to assess its impact on their viability. Treatment with rcJAM-A did not alter viability in any of the three cell line models at any of the concentrations selected **(Figure 4.9)**.

We next sought to test whether rcJAM-A exerted changes on colony-forming potential. N87 and OE19 gastro-oesophageal cancer cell lines were selected for their differential responses to JAM-A targeting and previous knowledge that these cell lines performed better in colony forming assays.

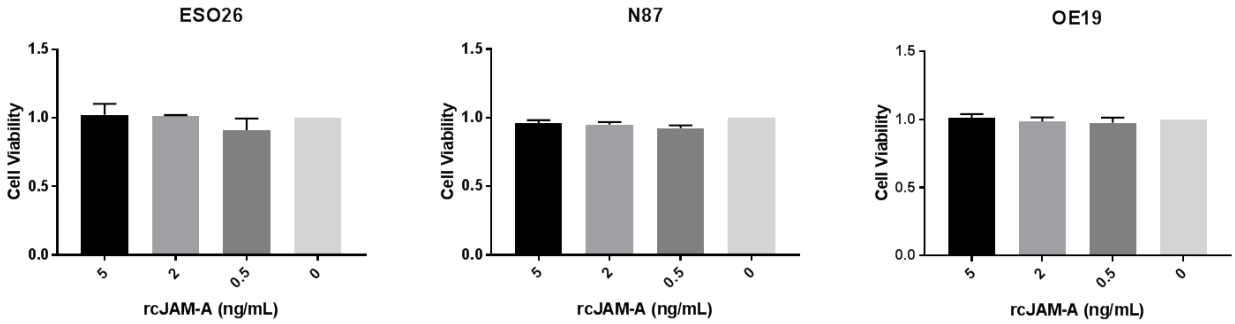

Figure 4.9: Recombinant JAM-A treatment does not affect cell viability in gastro-oesophageal cancer cell lines. *ESO26* ***(A),*** *N87* ***(B)*** *and OE19* ***(C****) cells were plated at 5,000 cells/well in 96-well plates. Following 72h cells were treated with varying concentrations of rcJAM-A or matched vehicle control (PBS-/-) and left for 72h in serum-free media. Cell viability was then measured via Alamar Blue assays. Experiments were performed three times and data shown as mean ± SEM.*

4.3.9 Recombinant JAM-A decreases colony-forming ability in gastro-oesophageal cell lines

We tested to see whether rcJAM-A treatment, at varying concentrations (2, 5ng/mL) increased the number of colonies formed by gastro-oesophageal cancer cells post-treatment. rcJAM-A treatment decreased the colony-forming efficiency of gastro-oesophageal cancer cell lines. N87 cells demonstrated reductions in colonies by 20 ± 15% and 27 ± 10%, at 2ng/mL and 5ng/mL respectively **(Figure 4.10)**, though these reductions were not statistically significant. However, rcJAM-A significantly reduced colony formation in OE19 cells by 54 ± 9% and 78 ± 4%, at 2ng/mL and 5ng/mL respectively **(Figure 4.10**; $p < 0.01$, $p < 0.0001$, respectively**)**.

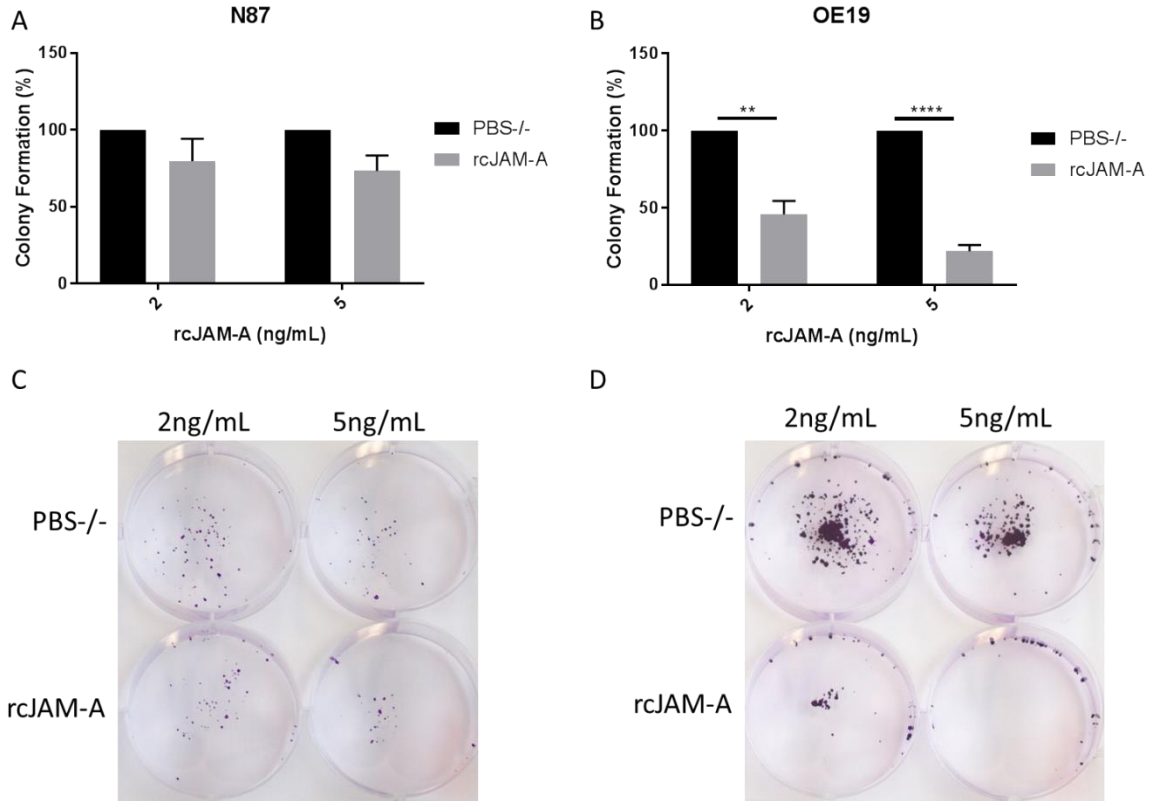

Figure 4.10: Recombinant JAM-A decreases colony formation in gastro-oesophageal cancer cells. *N87* ***(A, C)*** *and OE19* ***(B, D)*** *cells were plated at 1,000 cells/well in 6-well plates, treated 7 days cells later with varying concentrations of rcJAM-A or matched vehicle control (PBS-/-) and incubated for 72h in serum-free medium. Treatments were then removed and cells incubated in serum-positive medium for a further 10 days. Colony formation was assessed using crystal violet staining and read spectrophotometrically at an optical density of 595nm following solubilisation of the stain in methanol. Data were (n=3 independent experiments) are expressed relative to vehicle control (EV) as mean ±SEM. Statistical analysis was performed using multiple t-tests (correcting for multiple corrections using Holm-Sidak post-test)* (*p < 0.05, **p < 0.01, ***p < 0.001, ****p < 0.0001).

4.3.10 Targeting JAM-A *semi-in vivo* does not impact tumour growth

Given the ability of JAM-A silencing to reduce both proliferation and colony formation in some gastro-oesophageal cancer cell lines, we utilised a chick embryo xenograft model (described in Section 3.3.3) to investigate the role of JAM-A in ESO26 cell xenografts. Our previous experience with gene silencing in the CAM xenograft model indicated that *in situ* transfection was insufficient to significantly reduce gene expression (Rodrigo Cruz, personal communication). Hence, we silenced JAM-A *in vitro* 24h prior to implantation of cells onto the CAM and again while *in situ* **(Figure 4.11)**. Via immunoblot analysis, JAM-A was verified to be reduced by approximately 30% **(Figure 4.11)** at the time of implantation, which was encouraging since protein losses would not normally manifest themselves as early as 24h. Since transient silencing of JAM-A has been shown to be effective beyond 96h (data not shown), we hypothesised that JAM-A protein levels would continue to decrease. Nonetheless, xenografts on the CAM were re-transfected every 72h with JAM-A siRNA. On the final day, before tumour extraction, grossly visible tumours were observed. However, we noted no gross differences between tumour growth or development between siJp and control (siNeg) treated groups **(Figure 4.11)**.

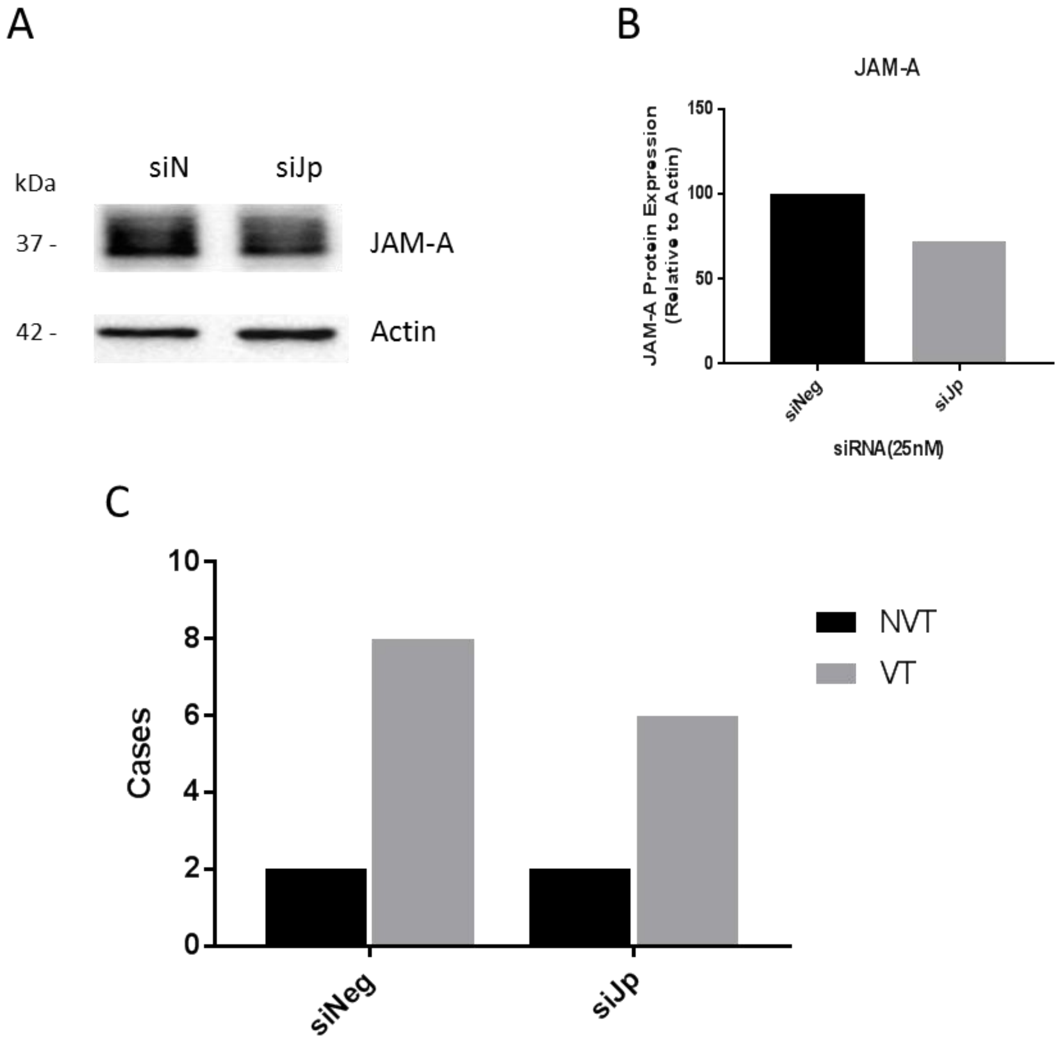

Figure 4.11: JAM-A mediated silencing did not alter visible tumour development in chick embryo xenograft model. *Before imp, ESO26 T75 cm² flasks at 80% confluence wer or siJp (25nM fi The remaining cells ... t lysed and protein extracted. Samples were used* ***(A)*** *f and the individual biological repl i loading control-A* ***(B)*** *Before (n) model JAM tumour visibility was recorded for each two tailed Fisher's exact test* ***(C)****.*

4.3.11 JAM-A silencing did not elicit functional changes in a chick embryo xenograft model.

Following tumour excision and fixation, tumours and their surrounding CAMs were immunohistochemically stained for various protein markers. To ensure we could correctly asses invasion in implanted tumours, sections were stained for pan-cytokeratin to highlight epithelial cells and monitor invasion from the Matrigel into the CAM. Ki67 staining was also used to establish whether cells were proliferating at the time of extraction. Finally, sections were stained for JAM-A to verify if JAM-A silencing was effective. Haematoxylin and eosin (H&E) staining was used for morphological reference.

As illustrated in **Figure 4.12**, both control and JAM-A-silenced tumours invaded past the CAM (denoted by black arrows). Ki67-positivity also confirmed proliferative activity in both siNeg and siJp treated cells. Unexpectedly, it appeared that JAM-A-silenced xenografts disseminated across the CAM to a greater extent than control xenografts. However this was not easily quantified due to inter-section and inter-treatment differences.

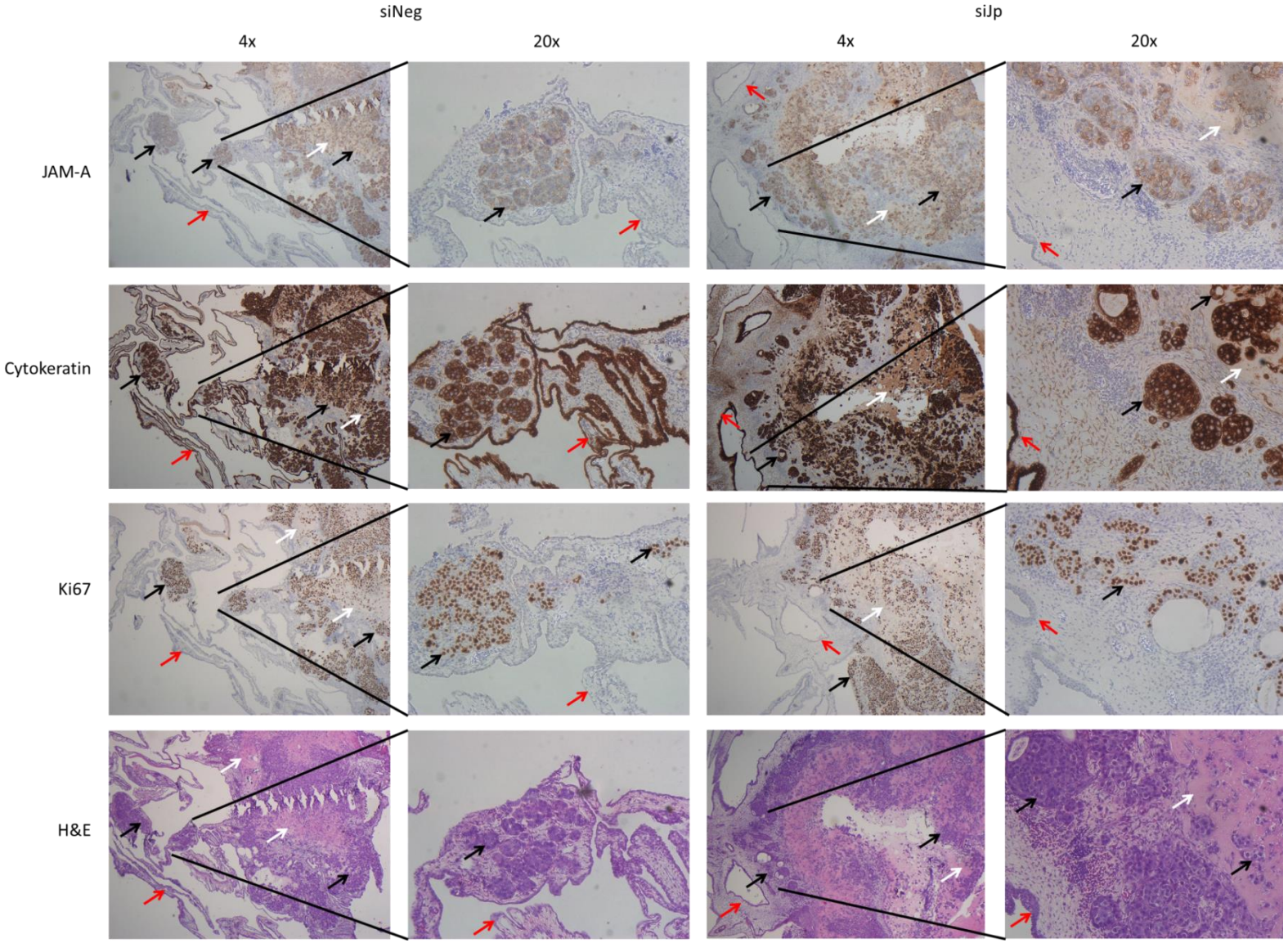
siNeg
siJp
4x
20x
4x
20x
JAM-A
Cytokeratin
Ki67
H&E

Figure 4.12: JAM-A silencing did not alter model tumour formation or invasion in a chick embryo xenograft model. *2 x 6 E1S0O2 6 c e l l i m p l a n t e d o n t o t h e CAM o n d a y v B n g p f b s i l e n c e d 2 4 h - A e a (r s i i R N A - A f t o w e r J A M - A m g e n t i n g 2 5 n M) . X e n o g r a f a t n s s f w e c r t e d r i e n s i t u o n x e n o g r a f t s l i c o r i m g s t h e s u r o u n d i n g CAM were excised, formalin-fixed and stained for JAM-A, pan-cytokeratin, Ki67 and H&E. Areas of tumour are denoted by black arrows, areas of Matrigel are denoted by white arrows and areas of CAM are denoted by red arrows. All images were obtained using an Olympus CKx41 microscope with Cell B imaging software at 20x magnification.*

A

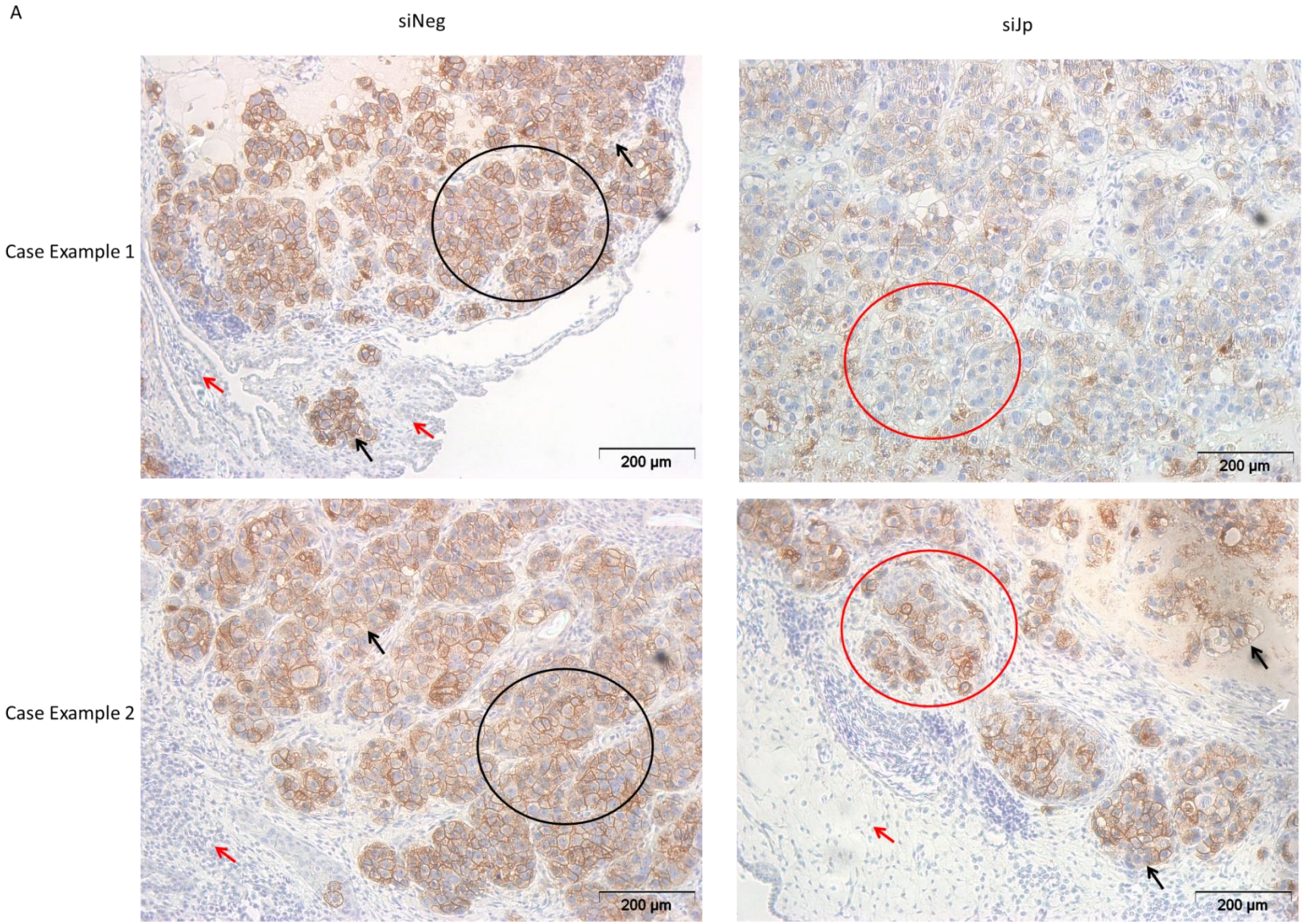
siNeg
siJp
Case Example 1
Case Example 2
200 µm
200 µm
200 µm
200 µm

Figure 4.12: JAM-A was successfully silenced in model tumours xenografted onto the CAM. J A M *Stained sections analysed and imaged. Areas of tumour are denoted by black arrows, areas of Matrigel are denoted by white arrows and areas of CAM are denoted by red arrows. Areas of homogenous (black) and heterogeneous (red) staining patterns are encompassed in circles. All images were obtained using an Olympus CKx41 microscope with Cell B imaging software at 20x magnification.*

4.3.112 JAM-A silencing elicited expressional heterogeneity across cases

As illustrated in **Figure 4.13**, JAM-A expression in tumours silenced with JAM-A-targeting siRNA showed a high level of heterogeneity across samples (illustrated by red circles) compared to the uniform expression demonstrated in the siNeg control group (denoted by black circles). While a uniform reduction in JAM-A expression may have helped confirm whether JAM-A drives pathogenesis in tumours in this *in ovo/*semi-*in vivo* model, we feel this result is extremely reflective of the JAM-A staining pattern across gastro-oesophageal cancer tumour samples we have seen previously (discussed in later chapter). Our group has often discussed the possibility that JAM-A expression may require a threshold for pathogenesis, rather than an explicit loss or gain as a cause of functional changes. Importantly, regardless of heterogeneity, we were successful in altering JAM-A expression in the siJp cases compared to control treated (siNeg) cases. However, quantifying the level of JAM-A present was extremely challenging in siJp cases. Standard measurements would denote >10% 3+ as an overall 3+, since levels of 3+ were still evident in siJp cases, scoring this way would be unable to discriminate any differential expression patterns between groups. We therefore chose not to score sections, particularly when cases did not appear to show differences in Ki67 positivity and invasion, and instead illustrate the heterogeneous nature of JAM-A for further discussion. Areas where JAM-A was successfully reduced did not demonstrate visible differences in invasion or proliferation compared to control treated (siNeg) groups, indicating that

JAM-A reductions had no impact on the aggressive nature of ESO26 cells *in ovo/semi-in vivo*.

4.4 Discussion

Aberrant expression of the adhesion protein Junctional Adhesion Molecule-A has been shown across different cancer types, with both loss (122-124) and gain (100, 131, 133) being hypothesized to drive pathogenesis. The lack of unifying role for JAM-A in cancer has translated into a lack of clarity on a potentially viable therapeutic target and biomarker in cancer. Furthermore, given the high rate of resistance to targeted therapies in many cancers, breast and gastro-oesophageal cancers for example, elucidating upstream targetable regulators could prove key in combating poor survival rates among particular patient cohorts.

Our laboratory has previously reported that high levels of JAM-A protein expression correlated with poor survival in breast cancer patients (131), but have been aware of the discrepancies surrounding JAM-A loss vs gain in both breast and other cancer types (122, 124, 127, 128). While this may be as a result of different methodologies, it is conceivable that JAM-A may play different roles in different cancer types or even across individual patients. This may be the result of a number of different factors, including differential micro-environments (214-216), gene expression patterns of tumours etc (217-219). However, given evidence that JAM-A may be a poor prognostic biomarker in certain settings (122), it is essential that the mechanisms surrounding JAM-A driving pathogenesis are better defined in order to evaluate whether it may be a therapeutic target or not.

In light of the pre-existing conflict surrounding JAM-A in gastro-oesophageal cancers (122, 127), we verified its expression as moderate-high in a small commercially-available TMA of gastric and oesophageal cancer cases. Furthermore, we validated suitable *in vitro* models and selected three JAM-A-expressing gastro-oesophageal cell lines to test whether JAM-A had the ability to drive pathogenesis in these cancer cell lines. Optimisation of transient

transfections to alter JAM-A levels proved much more challenging in gastro-oesophageal cancer cell lines, compared to breast cancer cell lines (100, 131). Among other concerns, due to the slow growing, clustering nature of the cell lines selected, cell plating density became a major consideration for optimal extraction. Seeding densities too low, and cells transfected too soon after plating, meant that cell numbers on extraction were low to unreadable via protein quantification assays and Western blotting (data not shown). Conversely, due to the clumped colony nature of the gastro-oesophageal cell lines, high seeding densities or transfections at higher confluency also hampered transfection efficiency and consistency transfection mix to the cells.

Moreover, issues surrounding JAM-A-mediated silencing and its impact on cytoskeletal proteins (used as loading controls) became apparent. Following expression analysis in a PCR screening panel (Sri Vellanki, personal communication), our group was aware that expressional alterations in JAM-A induced corresponding changes in many potential downstream targets including common loading controls like actin and GAPDH. Given the challenges of ensuring high levels of protein within samples, immunoblotting of low protein concentrations (~5-10µg) of samples exacerbated the signal to noise ratio in loading control proteins, making it extremely difficult to use appropriate densitometry methods. All in all, JAM-A proved a difficult protein to modulate in this cancer setting, though we did manage to elicit significant changes to JAM-A across all three cell lines at both gene and protein levels.

Following validation of techniques, we examined the proliferative and colony forming capabilities of cells after either silencing or overexpression of JAM-A. We showed that JAM-A reductions resulted in decreased viability and colony forming of two of three of the gastro-oesophageal cancer cell lines, while the third increased. JAM-A overexpression did not appear to alter functional cellular behaviours associated with tumorigenesis in any of the cell lines, though we note that these cells already express high levels of JAM-A.

Currently, to the best of our knowledge, no body of research conducted has highlighted JAM-A as playing a potentially complex role across one cancer type. Given the proliferative differences across cell lines following JAM-A loss, it is possible that JAM-A expression directly relates to spatial and temporal settings of individual tumours. As previously mentioned, we hypothesise that JAM-A may act as a 'molecular switch' where expressiona functional changes are induced. We suggest that this is the case for differential responses across the three gastro-oesophageal cancer cell lines, complicated in part by differential transfection efficiencies between them. Specifically, if a particular threshold for amount of loss or gain of JAM-A required is met, we speculate that only then is a pathophysiological role for JAM-A activated. If this were to be true, uncovering the exact point of such a ' prove key for future work implicating JAM-A as a player in cancer pathogenesis.

Our group has previously shown extracellular JAM-A cleavage and its regulation by ADAMs as playing an novel potential role in resistance to HER2-targeted therapies in breast cancer patients (208). We have also highlighted that recombinant cleaved JAM-A (rcJAM-A) promotes invasive properties *in vitro* and *in vivo* in breast cancer models (208). However, rcJAM-A seems not to exert similar effects in gastro-oesophageal cancer cell lines *in vitro.* While there was no effect on cellular proliferation, surprisingly, colony forming abilities were reduced following treatment with a recombinant form of cJAM-A. It may be the case that cJAM-A plays a role in micro-environmental communication rather than cell survival and, like other soluble proteins released by primary tumours, could prime metastatic niches (220). It would be interesting to see if inhibition of cJAM-A release at varying levels via ADAM inhibition (208, 209) elicited differential outcomes to colony forming abilities of gastro-oesophageal cancer cells and whether rcJAM-A had the ability to drive invasion of gastro-oesophageal cells *in vivo*, where micro-environment of primary tumours are replicated.

Finally, having demonstrated JAM-A silencing had the ability to reduce tumorigenic properties of cells *in* vitro, we investigated whether the same held true in *in vivo* settings, and utilised chick embryo xenograft assays to assess the

impact of JAM-A silencing on tumour development and invasion . No evidence was found to suggest that JAM-A expressional decreases could reduce tumour burden and hence quantification of Ki67 and cytokeratin levels was not undertaken as no differences were apparent However, given the strong heterogeneity in JAM-A staining both within and across JAM-silenced experimental replicates, it is possible that the threshold for reducing tumour burden was not met, or it is also possible that regardless of JAM-A expression levels, tumours retain their invasive properties and hence their ability to disseminate across the CAM (172, 187, 221).

Overall, we have shown that JAM-A does not behave in the same way in gastro-oesophageal cancer cell lines as previously described in breast cancer cells and that given the lack of consistency across gastro-oesophageal cell lines, further work is required to underpin whether JAM-A functions as a switch for pathogenesis in this setting.

Chapter 5: Probing a relationship between JAM-A and HER2 in gastro-oesophageal cancer cells

5.1 Introduction

Previous work in our laboratory has focused on the role of JAM-A in specific molecular subtypes of breast cancers, particularly the emerging relationship between JAM-A and HER2 expression (100) and the role of JAM-A in developing resistance to HER2-targeted therapies in HER2-positive breast cancer settings (208). In addition, our cell biological investigations have shown that silencing JAM-A expression in breast cancer cells reduces cellular behaviours associated with tumorigenesis (100, 131). Furthermore, our recent investigations in a mouse model of breast ductal carcinoma *in situ* (DCIS) revealed that dual inhibition of both JAM-A and HER2 shortened the interval to reach maximal efficacy of a HER2-targeted therapy (Yvonne Smith, personal communication). This thesis has so far demonstrated that in some instances JAM-A silencing alters viability in gastro-oesophageal cells; but it suggests that the role of JAM-A in gastro-oesophageal cancers is more complex than that in breast cancer. We therefore sought to investigate in more detail whether JAM-A plays a role in the regulation of HER2 in the gastro-oesophageal setting.

As discussed in Section 1.4, HER2 belongs to a family of receptor tyrosine kinases, which upon phosphorylation activate a cascade of downstream signalling pathways relating to proliferation, metastasis and survival (81, 82). Gastro-oesophageal cancers were approved for the clinical use of HER2-targeted therapies in 2010 (71), but the same issues surrounding *de novo* and acquired resistance seen in HER2-positive breast cancers also exist in gastro-oesophageal cancers (222-225). Hence a need to uncover valid upstream targets within the HER2 pathway has presented itself, so that cancer progression induced via HER2 signalling can still be inhibited in resistant settings. Resistance to HER2-targeted therapies has been described to occur through different mechanisms, including post-translational modifications of HER2, which, despite attempted inhibition, allow HER2 to remain constitutively activated (226, 227). Resistance has also been demonstrated in cases where other HER family members are activated in the absence of

HER2 (227, 228). It is possible that JAM-A could play a role in promoting HER2 activation through post-translational modifications.

Furthermore, understanding how HER2 is recycled within cells has proven challenging since HER2 has no known ligand. However some research involving HSP90 inhibitors has highlighted a possible role for lysosomal regulation and demonstrated the presence of HER2/Trastuzumab-HRP conjugates within lysosomes (229). Hence, synthetically inhibiting lysosomal function may result in increased levels of HER2 at the cell surface and warrants investigation. Unpublished data from our group has shown both proteasomal and transcriptional regulation of HER2 downstream of JAM-A expression, relating to tumour progression in breast cancers. Given these results, it is important to elucidate whether a similar role for HER2 regulation by JAM-A is seen in the HER2-positive gastro-oesophageal cancer setting. Furthermore, since common mechanisms of protein regulation occur at either transcriptional or post-transcriptional levels, It will be important to explore both mechanisms in this cancer setting if JAM-A is found to alter HER2 expression.

If JAM-A *were* to play a role in either the stabilisation of HER2 or the compensatory increased expression of other HER family members during HER2 inhibition, then JAM-A could prove to be a valid target in this setting.

5.2 Aims of this Chapter

Having optimised JAM-A mediated silencing and overexpression of JAM-A in three gastro-oesophageal cell lines (Chapter 4), the primary aim of this chapter was to elucidate whether JAM-A is involved in the regulation of HER2 expression levels in HER2-positive gastro-oesophageal cancer settings. The specific aims were as follows:

Specific Aim 1: To determine whether JAM-A silencing reduces HER2 expression in gastro-oesophageal cancer cell lines and, if so, to examine underlying transcriptional or post-transcriptional regulatory pathways.

Specific Aim 2: To examine whether JAM-A silencing alters HER2 expression in a *semi-in vivo* gastro-oesophageal xenograft model.

Specific Aim 3: To probe a possible correlation between HER2 positivity and high JAM-A expression in gastro-oesophageal cancer patient tissues.

5.3 Results

5.3.1 High JAM-A and HER2 expression are related to poor prognosis in gastric cancer patients

To establish the clinical significance of JAM-A expression in HER2-positive gastric cancer patient cases we used an open-source online gene expression data resource (http://kmplot.com) (140). Analysis revealed that high expression of both JAM-A and HER2 in gastro-oesophageal cancers carried a significantly greater risk of both poorer overall survival in patients (p=0.033) and poorer survival in patients whose cancers progressed (p=0.036) **(Figure 5.1)**. However, high JAM-A expression in HER2-positive cases did not significantly impact on gastric cancer progression/metastatic risk **(Figure 5.1)**. This may suggest that in this cancer setting, JAM-A does not drive metastatic phenotypes, but instead may impact other phenotypes, perhaps cell death mechanisms or even responsiveness to therapies.

To examine the correlation between JAM-A and HER2 expression in gastric cancer patients, we also used another open-source online data resource (http://xenabrowser.net). Analysis revealed that high JAM-A and high HER2 gene expression were moderately, positively correlated in a gastric cancer patient cohort (r=0.4, p=<0.001) **(Figure 5.1).** This indicates that high JAM-A expression is associated with higher levels of HER2 and supports our hypothesis that JAM-A may be a potential candidate for therapeutic targeting, requiring validation, in HER2-positive gastro-oesophageal cancers.

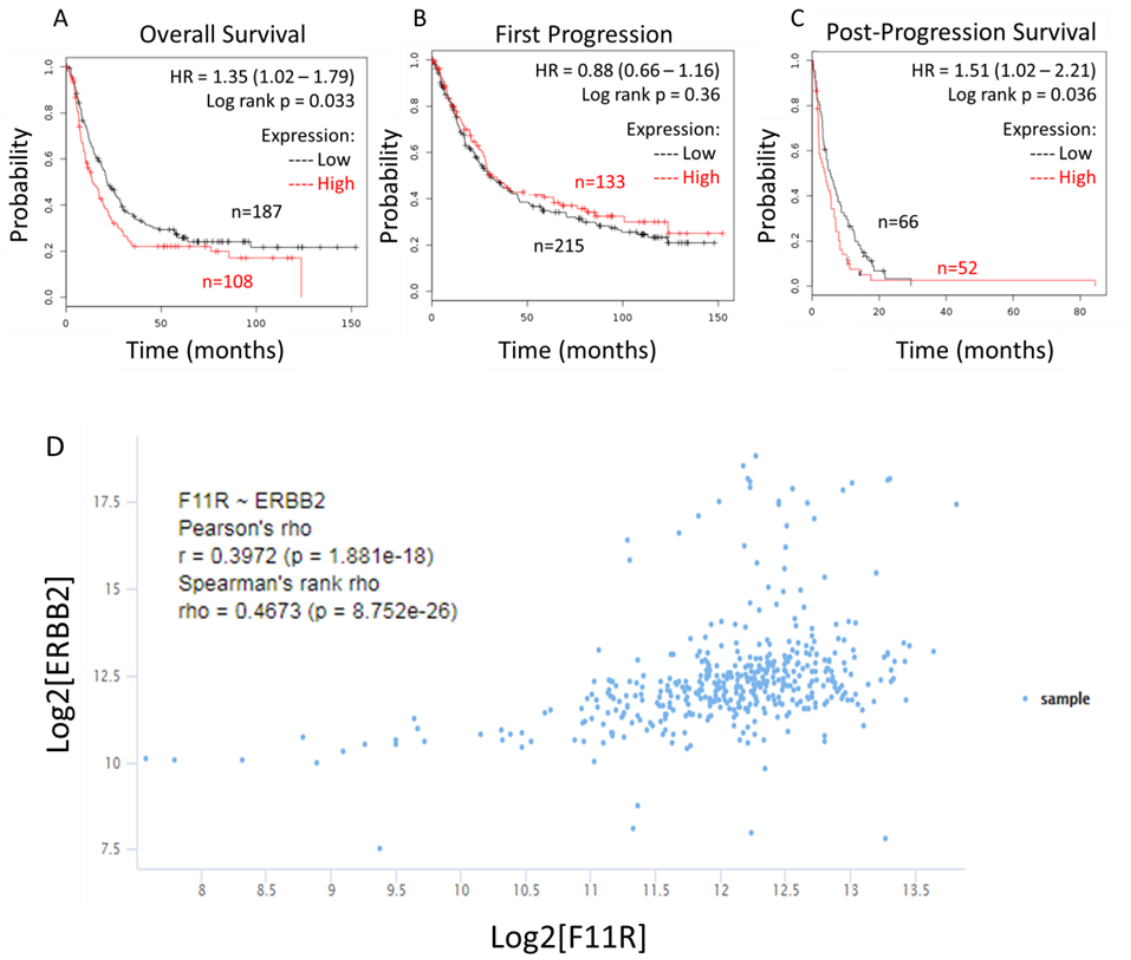

Figure 5.1: High JAM-A and HER2 expression predict worsened survival in gastric cancers. *The Kaplan-Meier Plot platform (http://kmplot.com/analysis/) was used to generate survival curves showing associated JAM-A and HER2 expression in gastric cancer patients. Using F11R jetset probes (excluding GSE62254 as recommended) in HER2-positive cases revealed high mRNA expression of F11R (JAM-A) is associated with worsened overall survival (A) and post-progression survival (C), but not risk of progression (B). Xenabrowser platform (https://xenabrowser.net/) was used to generate a scatter plot (D) showing correlations between JAM-A and HER2 mRNA expression in gastric cancer patients. Using F11R and ERBB2 genes as variables in the TCGA Stomach Cancer cohort, revealed a statistically significant moderately positive correlation (D).*

5.3.2 Basal expression of HER2 in JAM-A expressing cell lines

Having already established dual JAM-A-/HER2-expressing GE cancer cell lines, we sought to confirm that these results could be confirmed by a separate, clinically-utilised method. Accordingly, cell pellets were prepared from cultured ESO26, N87 and OE19 cell lines and immunohistochemically stained for JAM-A and HER2. As illustrated in **Figure 5.2**, all three cell lines expressed high levels of both JAM-A (3+ staining) and HER2 (3+ staining).

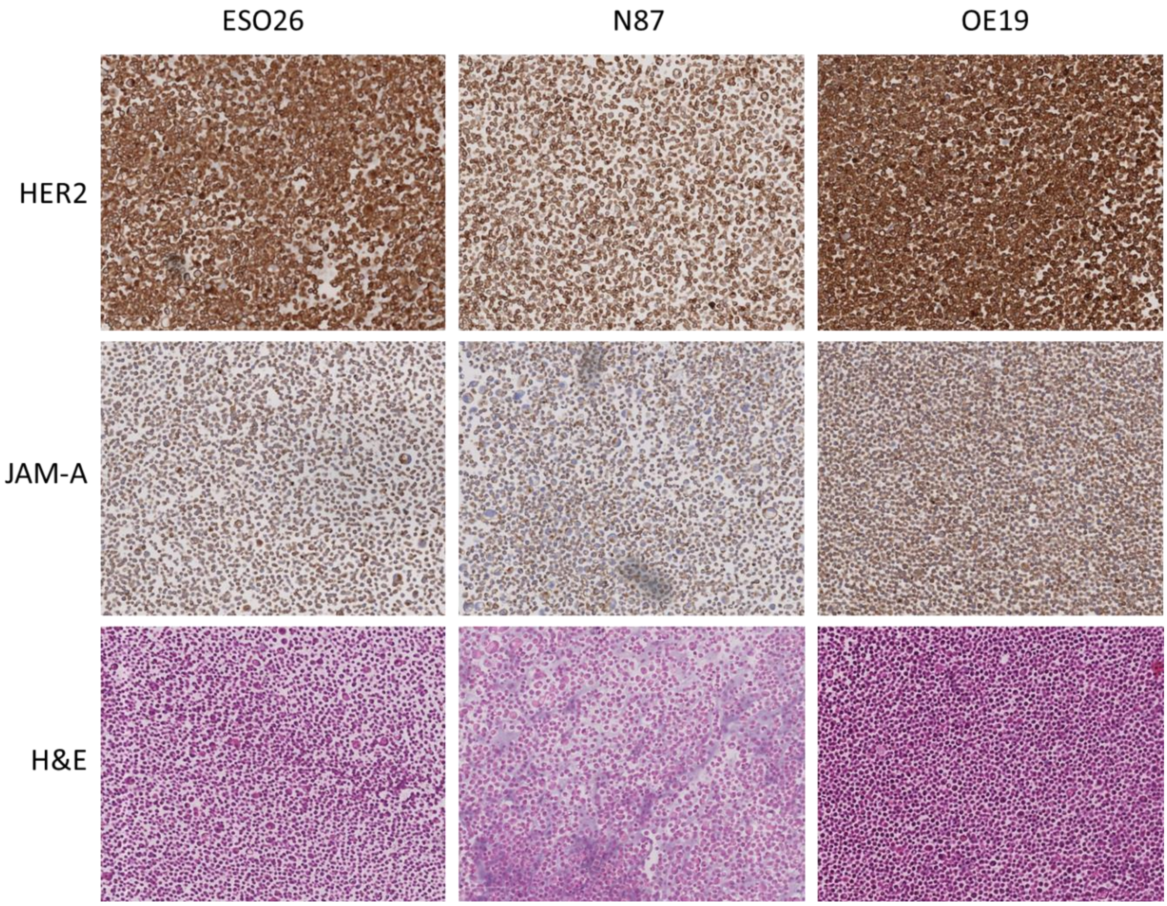

Figure 5.2: JAM-A and HER2 basal expression in gastro-oesophageal cancer cell lines. *Formalin-fixed cell pellets from ESO26, N… gastro-oesophageal cell lines were embedded and paraffi… immunohistochemically analysed for JAM-A and HER2 (H&E) stained sections. JAM… were imaged and formatted using Qupath software at 9.66x magnification.*

5.3.3 JAM-A silencing significantly increases HER2 mRNA expression

Our laboratory had previously shown that JAM-A regulated both HER2 mRNA and protein levels (Rodrigo Cruz, personal communication), so we examined HER2 mRNA expression following JAM-A silencing. Surprisingly, we saw significant increases in HER2 mRNA expression in two of our cell line models following JAM-A silencing, opposing previous work completed in breast cancer cell lines. Specifically, HER2 mRNA expression was significantly increased (by 1.16 ± 0.3-fold; p=0.0166) in ESO26 cells following JAM-A silencing (to 0.58 ± 0.08-fold of control levels; p=0.0017) **(Figure 5.3)**. N87 cells saw significant reductions in HER2 mRNA expression (to 0.31 ± 0.06 relative to control levels; p=0.077) following JAM-A reductions (to 0.53 ± 0.07 of control levels; p=0.0017) **(Figure 5.3)**. Further to our surprise, the cell line that had shown increased proliferation following JAM-A silencing in the previous chapter, OE19, exhibited significantly lower HER2 mRNA levels (reduced to 0.65 ± 0.2 of control levels; p=0.0168) after JAM-A mRNA reductions (0.36 ± 0.11) **(Figure 5.3)**. While these results appear counter-intuitive given the functional responses to JAM-A reductions demonstrated in the previous chapter, it is possible that cells with reduced HER2 mRNA expression may activate compensatory mechanisms to increase proliferation. It is also possible that ESO26 and N87 cell lines may upregulate mRNA expression of HER2 in response to JAM-A loss, but are met with translational issues evoking fluctuating protein expressions downstream.

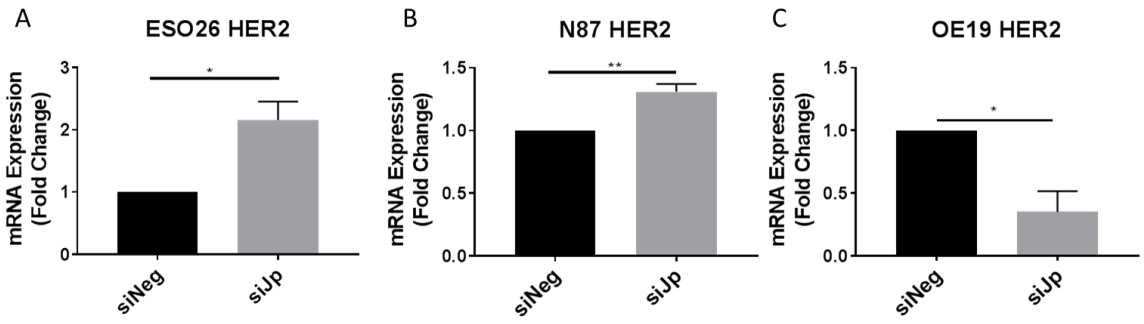

Figure 5.3: JAM-A expressional reductions variably alter HER2 expression across cell line models. *Gastro-oesophageal cancer cells were plated at 2x10^5 in 6-well plates and allowed to undergo one doubling time before cells were transiently transfected with either non-targeting siRNA (siNeg) or JAM-A targeting siRNA pool (siJp) (final concentration 25nM). RNA was extracted, cDNA generated and qRT-PCR performed to determine HER2 expression for ESO26* ***(A)*** *N87* ***(B)*** *and OE19* ***(C)*** *cells. Ct values of samples were set relative to matched Ct values of the housekeeping control gene (RPLP0). Analysis of three independent experiments (n=3) was displayed as mean ± SEM and statistically compared using unpaired, two-tailed Student's t-test (*p<0.05, **p<0.01, ***p<0.001).*

5.3.4 JAM-A silencing does not significantly alter HER2 protein expression

Previous work in our laboratory has demonstrated that JAM-A silencing decreases HER2 expression in several breast cancer cell lines (131). Knowing that gastro-oesophageal cancers sometimes overexpress HER2, we wanted to elucidate whether the same mechanism of regulation was demonstrated across a panel of gastro-oesophageal cancer cell line models. Furthermore, we wanted to probe any functional differences between the models, given that JAM-A silencing did not elicit uniform functional responses across the cell lines (as demonstrated in Section 4.3.5).

As shown in **Figure 5.4** ESO26, N87 and OE19 cells were transfected with either control siRNA (siNeg) or a pool of two siRNAs targeting JAM-A (siJp). Upon cell harvesting at 96h post-transfection, JAM-A protein expression was reduced by 44 ± 16% in ESO26 cells, by 39 ± 7% in N87 cells and by 56 ± 17% in OE19 cells; yet there was no evidence of significant changes in HER2 protein expression. However the individual HER2 expressional responses in biological replicates varied greatly from each other, as did the levels of JAM-A silencing. This may support our idea of an expressional threshold, whereby a specific level of JAM-A loss must be achieved before any downstream functional changes become evident.

Specifically, following significant reductions to JAM-A in ESO26 cells ($p=0.0471$; 44 ± 16%) there were no significant changes to HER2 protein levels (to 55 ± 47% in JAM-silenced versus control conditions). HER2 expression changes in N87 were not significant and varied greatly (8 ± 38%) following significant JAM-A reductions (39 ± 7%; $p=0.0043$). OE19 cells had a similar response following statistically significant reductions in JAM-A by (56 ± 17%; $p=0.0317$), with insignificant changes to HER2 expression (12 ± 18%).

Since we had previously hypothesised that JAM-A-induced changes in functional behaviour may require an expressional threshold, we next sought to test whether the same was the case for JAM-A-dependent regulation of HER2 expression levels. We used a compilation of biological and technical replicates

of JAM-A-silenced samples in ESO26 cells previously probed for JAM-A and HER2 via Western blotting, and densitometrically analysed. We then performed correlation analysis using Pearson's no significant correlation between expressional changes of two proteins **(Figure 5.5)**. This suggested that there was no expressional threshold of JAM-A for regulating HER2 expression.

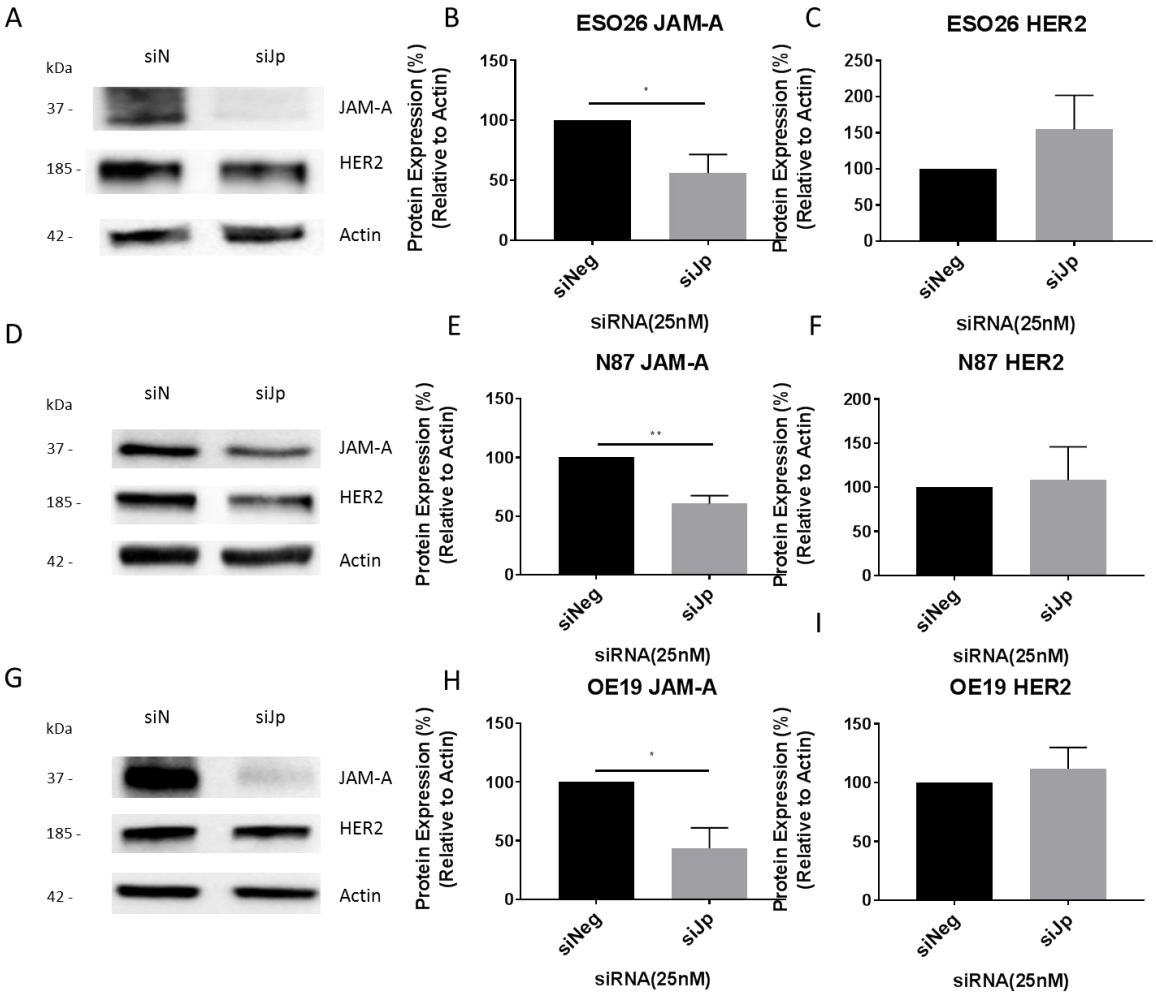

Figure 5.4: JAM-A silencing did not change HER2 protein expression in gastro-oesophageal cell lines. *Gastro-oesophageal cancer cells lines were plated at 2x10^5 in 6-well plates and allowed to undergo one population doubling before cells were transiently transfected with either non-targeting siRNA (siNeg) or a JAM-A targeting siRNA pool (siJp) (final concentration 25nM). Lysates were then subjected to immunoblot analysis for JAM-A and HER2. ESO26* ***(A)****, N87* ***(D)*** *and OE19* ***(G)****. Densitometric analysis (ESO26* ***(B,C)****, N87* ***(E,F)*** *and OE19* ***(H,I)****) (n=3 independent experiments) was performed relative to a loading control (Actin) and displayed relative to siNeg as mean ± SEM. Statistical significance was tested using unpaired, two-tailed Student's t-test (*p<0.05, **p<0.01, ***p<0.001).*

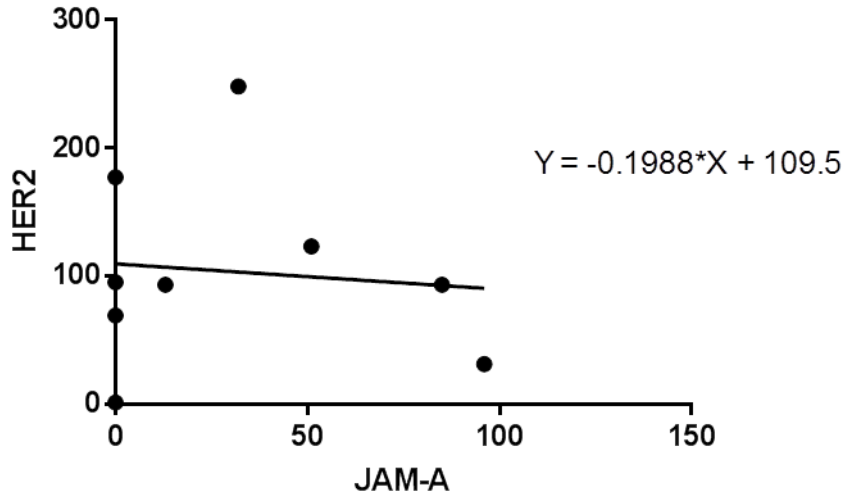

Figure 5.5: JAM-A expressional reductions do not correlate with induced changes in HER2 expression. *The gastro-oesophageal cancer cell line ESO26 was plated at 2x10^5 in 6-well plates and allowed to undergo one population doubling before cells were transiently transfected with either non-targeting siRNA (siNeg) or a JAM-A targeting siRNA pool (siJp) (final concentration 25nM). Lysates were subsequently immunoblotted for JAM-A and HER2; and densitometrically represented relative to the band size of the loading control protein (Actin). Statistical significance was tested using Pearsonôs correlation coefficient*

5.3.5 Increased JAM-A expression does not significantly alter HER2 expression

To summarise our findings to date, JAM-A silencing in gastro-oesophageal cancer cell lines had elicited greatly varied expressional changes in HER2 levels, which did not correlate with expressional changes previously observed in breast cancer cell lines or support our hypothesis that JAM-A levels exerted a parallel regulation on those of HER2. However, since JAM-A *overexpression* rather than loss in patients is the feature of most interest, we therefore set out to examine HER2 expression in a JAM-overexpressing microenvironment. Accordingly, JAM-A was transiently overexpressed in gastro-oesophageal cell lines in order to search for knock-on consequences for HER2 protein expression. We hypothesised that, given the complexity of JAM-A expressional thresholds in GE cancers, HER2 may increase in correlation with JAM-A.

However, high levels of variation in HER2 expression following transient JAM-A overexpression across three cell lines resulted in no significant changes to HER2 mRNA expression **(Figure 5.6A-C)**. HER2 protein expression also varied greatly following JAM-A overexpression, but was not statistically significant despite a trend for parallel increases in both ESO26 and OE19 cells. Specifically, HER2 expression in ESO26 cells was increased by 94 ± 61% following JAM-A overexpression **(Figure 5.6G)**, while that in OE19 cells increased by 23 ± 12% under similar circumstances **(Figure 5.6I)**. Variability was even higher in N87 cells, with two biological replicates showing HER2 reductions of approximately 15%, while the third replicate showed increases of almost 100% (used as representative image in **Figure 5.6H)**.

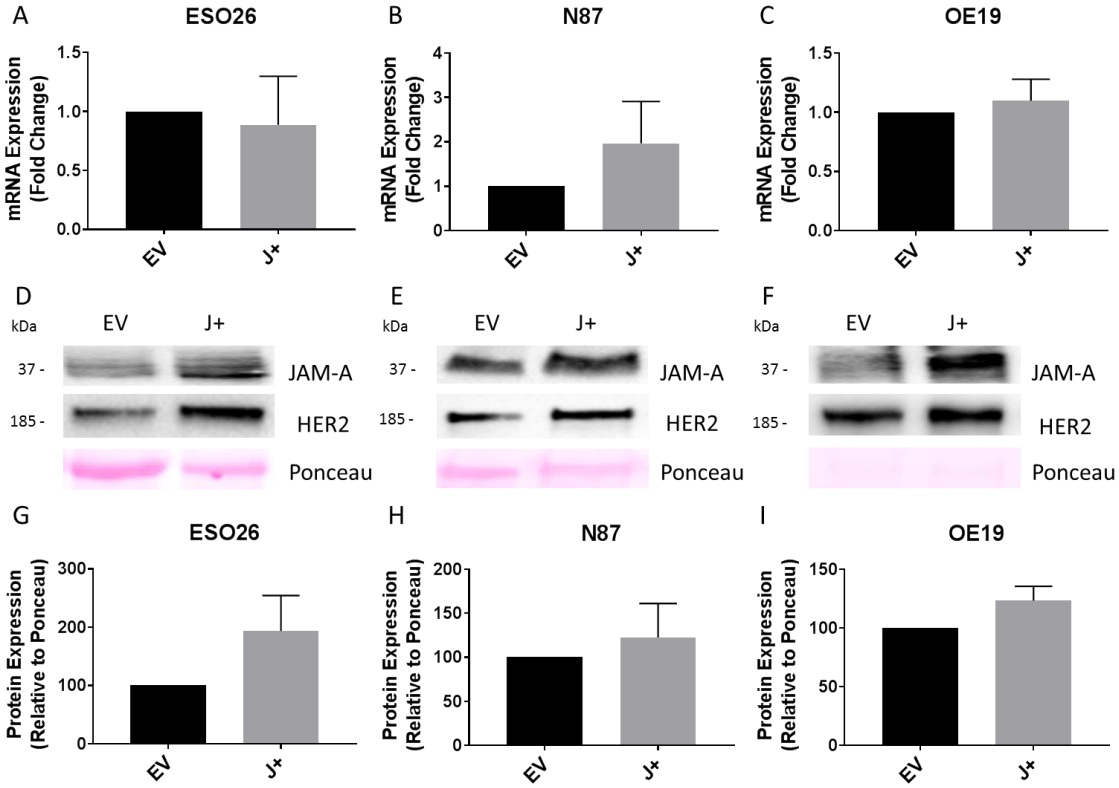

Figure 5.6: Transient overexpression of JAM-A does not change HER2 gene or protein expression. *Gastro-oesophageal cancer cells lines were plated at 2x10^5 in 6-well plates. ESO26 cells were allowed to undergo one population doubling and N87 and OE19 cells incubated for 24h before cells were transiently transfected with either control (EV) or hJAM-A (J+) plasmid (1µg). RNA was extracted, cDNA generated and qRT-PCR performed to determine HER2 expression for ESO26* ***(A)*** *N87* ***(B)*** *and OE19* ***(C)*** *cells. Ct values of samples were set relative to matched Ct values of the housekeeping control gene (RPLP0). Lysates were then subjected to immunoblot analysis for JAM-A and HER2. ESO26* ***(A)****, N87* ***(D)****, and OE19* ***(G)****. Densitometric analysis (ESO26* ***(B,C)****, N87* ***(E,F)****, and OE19* ***(H,I)****) (n=3 independent experiments) was performed relative to a loading control (Actin) and displayed relative to siNeg as mean ± SEM. Statistical significance was tested using unpaired, two-tailed Student's t tests (*p<0.05, **p<0.01, ***p<0.001).*

5.3.6 Reductions in JAM-A alter HER2 membranous staining

Having seen such variability of HER2 expression following both JAM-A silencing and overexpression across gastro-oesophageal cancer cell lines, we tested whether JAM-A alterations correspondingly altered HER2 in ways that could not be appreciated by simple expression analysis. Specifically, immunofluorescence microscopy was conducted on ESO26 cells following JAM-A silencing to visualise any changes in HER2 localisation. Interestingly, HER2 membranous staining was punctate or incomplete in several spatial areas where JAM-A was reduced **(Figure 5.7)**; with some suggestion of cytoplasmic uptake of the protein; in comparison to the membranous staining of HER2 across control treated (siNeg) cells (white arrows). It was however not uniform across all replicates.

Since this outcome was based on visualised changes to structure, rather than loss or gain of HER2 staining, quantitative analysis was notundertaken. It is, however, suggestive that further work elucidating cellular stabilisation changes following JAM-A silencing may prove beneficial.

Given the variability in HER2 expressional changes following manipulation of JAM-A levels in gastro-oesophageal cancer lines, it was likely that no direct regulation by JAM-A was occurring in this setting. However, it was still possible that JAM-A was indirectly regulating HER2 through transcriptional or post-transcriptional methods. Hence we next sought to discover whether the variations in HER2 disruptions following JAM-A silencing could be stabilised using known mRNA and lysosomal inhibitors.

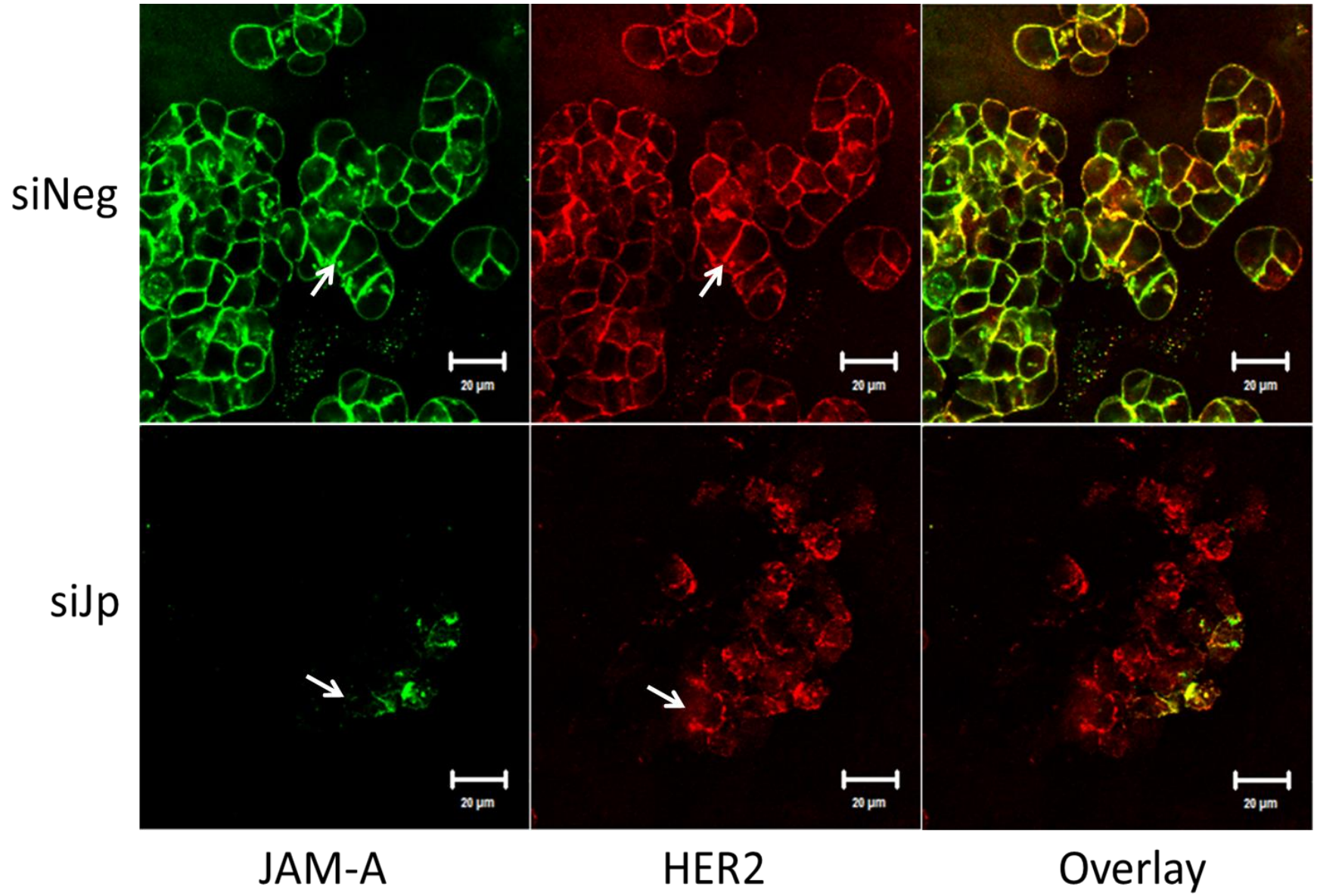
siNeg
siJp
20 µm
JAM-A
HER2
Overlay

Figure 5.7: JAM-A silencing alters HER2 localisation in gastro-oesophageal cells. *The gastro-oesophageal cancer cell line ESO26 was plated at 5x10^4 cells onto coverslips and allowed to undergo one population doubling before cells were transiently transfected with either non-targeting siRNA (siNeg) or a pool of siRNA targeting JAM-A (siJp) (final concentration 25nM). Following fixation and ESO26 cells were subjected to immunofluorescence double-labelling and analysed using Zeiss LSM-510 confocal microscopy. Green staining denotes JAM-A, red staining denotes HER2 and yellow staining denotes co-localisation. Areas of interest are denoted by white arrows. Scale bar 20ε M.*

5.3.7 JAM-A silencing does not alter HER2 expression through inhibition of RNA synthesis.

Work in our lab has previously shown JAM-A as a regulator of HER2 expression at both transcriptional and post-transcriptional levels (100, 208). We therefore set out to examine whether effects on HER2 expression induced by JAM-A silencing were related to transcriptional pathways.

As a tool to investigate the impact of JAM-A silencing on transcriptional control of HER2, we used Actinomycin D (ActinoD) to stabilise topoisomerases I and II and thereby inhibit RNA synthesis. Accordingly, ESO26, N87 and OE19 cells silenced for JAM-A were subsequently treated with ActinoD to determine whether JAM-A exerted pre-translational control over HER2 expression. ActinoD failed to block HER2 expressional changes induced by JAM-A gene silencing **(Figure 5.8)**, indicating that transcriptional pathways were not involved.

As ActinoD induces apoptosis in cancer (230, 231), cleaved caspase-3 (cas-3) was used as a positive control to verify ActinoD bioactivity. While cleaved cas-3 was predictably increased in ActinoD treated conditions, it was interesting to note enhanced cas-3 cleavage in JAM-A-silenced cells treated with ActinoD **(Figure 5.8)**. Previous research has shown that JAM-A removal increases apoptotic potential in gastric cancer cells (125, 127), but it was encouraging that this observation was consistent across all three cell lines (even in OE19 cells which had previously exhibited increased growth following JAM-A silencing). Further negative controls (siNeg + Actino D.) would have been ideal, however, since comparisons were only to be made between siJp and siJp + ActinoD and given the difficulties surrounding protein levels upon extractions for all siJp treated samples; other negative controls were not utilised within this experiment.

Since JAM-A was not controlling HER2 expression at RNA synthesis level, we next looked to other mechanisms of protein regulation.

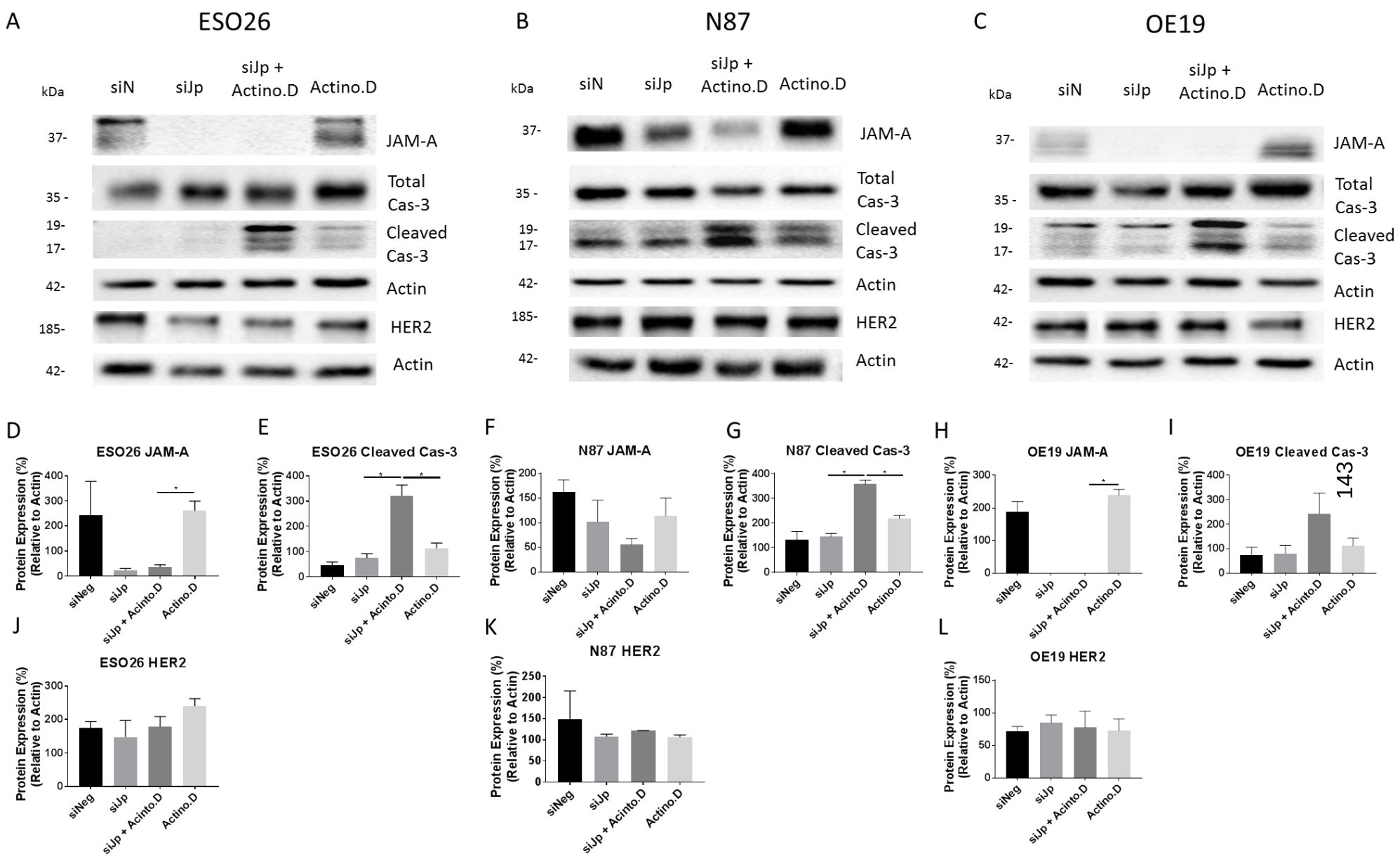
A
ESO26
B
N87
C
OE19
kDa
siN
siJp
siJp + Actino.D
Actino.D
37-
JAM-A
35 -
Total Cas-3
19-
17-
Cleaved Cas-3
42-
Actin
185-
HER2
D
ESO26 JAM-A
E
ESO26 Cleaved Cas-3
F
N87 JAM-A
G
N87 Cleaved Cas-3
H
OE19 JAM-A
I
OE19 Cleaved Cas-3
Protein Expression (%) (Relative to Actin)
siNeg
siJp
siJp + Acinto.D
Actino.D
J
ESO26 HER2
K
N87 HER2
L
OE19 HER2
143

Figure 5.8: HER2 expression variations following JAM-A silencing are not regulated at RNA synthesis level. *Gastro-oesophageal cancer cell lines were plated at 2x10^5 in 6-well plates and allowed to undergo one population doubling before being transiently transfected with either control siRNA (siNeg) or a JAM-A targeting siRNA pool (siJp) (final concentration 25nM). Following 66h transfection, the RNA synthesis inhibitor ActinoD (4µM) was added to cells for 6h. Proteins were extracted and samples used for immunoblot analysis: ESO26* ***(A)****, N87* ***(B)****, and OE19* ***(C)****. Densitometric analysis (ESO26* ***(D,E,J)****, N87* ***(F,G,K)****, and OE19* ***(H,I,L)****) (n=3 independent experiments) was expressed relative to loading control (Actin) and displayed as mean ± SEM. Significance was tested using paired t-test (*p<0.05, **p<0.01, ***p<0.001).*

5.3.8 Lysosomal inhibition does not alter HER2 expression following JAM-A silencing

As lysosomes play a crucial role in cell surface receptor degradation and have been shown to regulate the recycling of HER2 (229), we next sought to investigate whether JAM-A played a regulatory role upon HER2 lysosomal turnover. Specifically, we hypothesised that if the lysosome was involved in degrading HER2 secondary to JAM-A silencing, lysosomal inhibition would protect against this event. Lysosomal function was inhibited using chloroquine, a known inhibitor of autophagosome-lysosomal fusion (232) (CQ; 30μg/mL) during the final 6h of 72h JAM-A silencing in ESO26, N87 and OE19 GE cancer cell lines.

As shown in **Figure 5.9**, successful inhibition of lysosomes was evidenced in the positive control condition by increased levels of LC3B II (indicating an accumulation of autophagosomes (233)). As expected, JAM-A silencing evoked altered HER2 expression responses which were different among cell lines, but these were not significantly altered by lysosomal inhibition. This suggested that lysosomal proteolytic regulation is unlikely to be involved in regulation of HER2 levels by JAM-A.

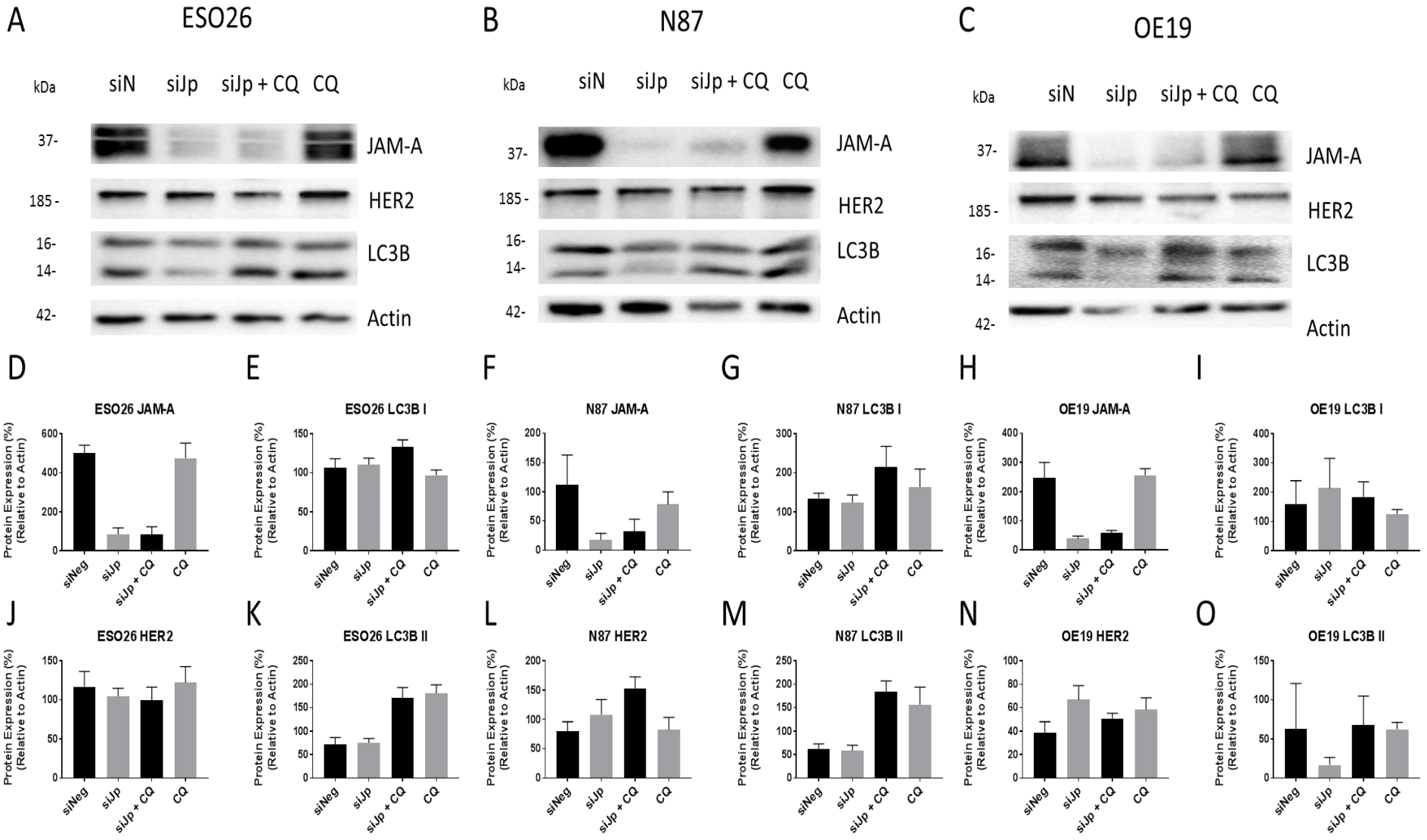
A
ESO26
kDa
siN
siJp
siJp + CQ
CQ
37-
JAM-A
185 -
HER2
16-
14-
LC3B
42-
Actin
B
N87
C
OE19
D
ESO26 JAM-A
E
ESO26 LC3B I
F
N87 JAM-A
G
N87 LC3B I
H
OE19 JAM-A
I
OE19 LC3B I
J
ESO26 HER2
K
ESO26 LC3B II
L
N87 HER2
M
N87 LC3B II
N
OE19 HER2
O
OE19 LC3B II
Protein Expression (%)
(Relative to Actin)
siNeg
siJp
siJp + CQ
CQ

Figure 5.9: HER2 expressional variations following JAM-A silencing are not dependent on lysosomal degradation. *Gastro-oesophageal cancer cell lines were plated at 2x10^5 in 6-well plates and allowed to undergo one population doubling before being transiently transfected with either control siRNA (siNeg) or a pool of JAM-A targeting siRNA (siJp) (final concentration 25nM). Following 66h transfection, the lysosomal inhibitor (CQ) (30µg/mL) was added to cells for 6h. Proteins were extracted and samples used for immunoblot analysis: ESO26* ***(A)****, N87* ***(B)****, and OE19* ***(C)****. Densitometric analysis (ESO26* ***(D,E,J,K)****, N87* ***(F,G,L,M)****, and OE19* ***(H,I,N,O)****) (n=3 independent experiments) was expressed relative to loading controls (Actin) and displayed as mean ± SEM. Significance was tested using paired Student's t-tests (*p<0.05, **p<0.01, ***p<0.001).*

5.3.9 *In vitro* HER2 targeting is more effective in JAM-A silenced cells

With accumulating evidence that JAM-A does not regulate HER2 expression in gastro-oesophageal cancer cell lines as it does in breast cells, we were nonetheless intrigued by the fact that JAM-A loss may prime cells to undergo apoptosis (**Figure 5.8**). Since common HER2 therapies activate apoptotic pathways (234-237), we therefore questioned whether JAM-A loss may have the ability to increase responsiveness to HER2 therapies *in vitro*. We also predicted that the OE19 cell line may respond differently given that OE19 cells had increased growth following JAM-A loss, in contrast to ESO26 and N87 cell lines (Section 4.3.5).

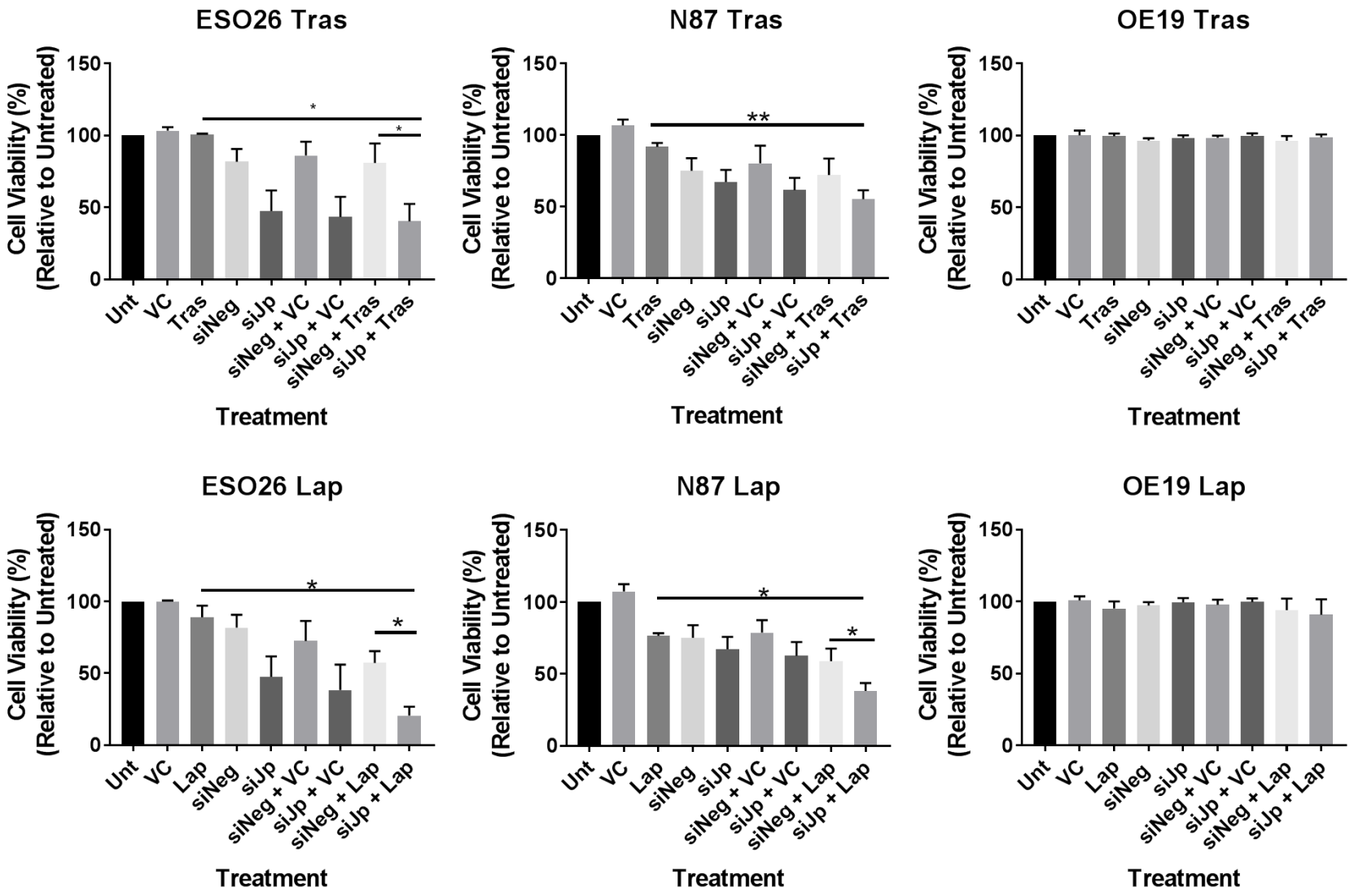
ESO26 Tras
N87 Tras
OE19 Tras
ESO26 Lap
N87 Lap
OE19 Lap
Cell Viability (%)
(Relative to Untreated)
150
100
50
0
Unt
VC
Tras
Lap
siNeg
siJp
siNeg + VC
siJp + VC
siNeg + Tras
siJp + Tras
siNeg + Lap
siJp + Lap
Treatment
*
**

Figure 5.10: JAM-A silencing sensitises gastro-oesophageal cells to anti-HER2 drugs. *ESO26, N87 and OE19 cells were plated in triplicate wells of 96-well plates (5,000 cells/well) and transfected after 72h with either control siRNA (siNeg) or pooled siRNA to JAM-A (siJp) (final concentration 25nM). After 72h, ESO26 and N87 cells were then treated with either Trastuzmab (Tras; 10µg/mL) or Lapatinib (Lap; 2µM) for 24h, while OE19 cells were treated at the same concentrations of both Tras and Lap for 72h. Control cells were treated with matched vehicle controls (VC) (Trastuzumab VC: H_2O 0.05% v/v; Lapatinib VC: DMSO 0.02% v/v). Cell viability was assessed using Alamar Blue assays and experiments performed three times. Data shown represent mean ± SEM, and statistical significance was tested using paired, two-tailed Student's t-tests (*p<0.05, **p<0.01, ***p<0.001).*

As shown in **Figure 5.10**, JAM-A silencing sensitised cells to the anti-viability effects of Trastuzumab (Tras). Comparing the means between Tras alone vs JAM-A silenced cells plus Tras treatment, there was a significant reduction in cell viability in ESO26 cells, with reductions of 60 ±13% (p=0.0422). Importantly there were also significant differences between siRNA control + Tras and siJp + Tras treatment groups, ensuring that the additive effect of Tras was induced by JAM-A silencing and not by the transfection process. N87 cells also saw significant reductions of 37 ± 3% between siJp + Tras and Tras alone treatment groups (p=0.0089), however the difference between negative control siRNA treated + Tras and siJp + Tras was insignificant. This may therefore represent an artefact of the transfection process. Knowing that JAM-A silencing increased the proliferation of OE19 cells (Section 4.3.5), we did expect to see differences in responsiveness to anti-HER2 drugs in siJp-treated groups across the gastro-oesophageal cell lines. However we saw no significant reductions in viability of Tras treated OE19 cells compared to untreated groups, suggesting that the cells did not respond to the treatment at this timepoint.

These results were also recapitulated with the dual EGFR/HER2 kinase inhibitor Lapatinib (Lap), where **Figure 5.10** illustrates significant additive effects of Lap on JAM-A silenced groups in gastro-oesophageal cancer cell lines *in vitro*. Using the same method of mean comparison, ESO26 cells showed significant reductions of 69 ± 8% in cell viability between siJp + Lap treated vs Lap alone (p=0.0133). Significant (p=0.0340) reductions in cell viability between siRNA control and siJp + Lap groups (37 ± 7%) confirmed that the effect was not due to transfection artefacts. Similar additive effects in cell viability loss were observed in JAM-A-silenced N87 cells vs Lap alone with significant (p=0.0272) reductions between groups (38 ± 6%). We also saw additive reductions in siJp + Lap treated cells when compared to siNeg + Lap treatments (p=0.0308) (21 ± 4%), indicating additive reductions in siJp + Lap groups were not due to the transfection process.

Given that OE19 cells did not respond to either anti-HER2 treatment at the 24h timepoint, we extended exposure times to both Tras and Lap to 72h. As shown in **Figure 5.11**, the longer treatment with HER2-targeted therapies successfully reduced cell viability following JAM-A silencing in OE19 cells.

While OE19 cells did not exert significant cell viability losses to Tras treatments at the given concentrations, there were no significant differences in cell viability reductions between any of the groups with Tras treatment. In contrast, OE19 cells responded well to Lap treatment. However, as there were no differences in reductions to cell viability between siNeg/siJp + Lap treated groups, the reduced cell viability response was considered independent of JAM-A **(Figure 5.11)**.

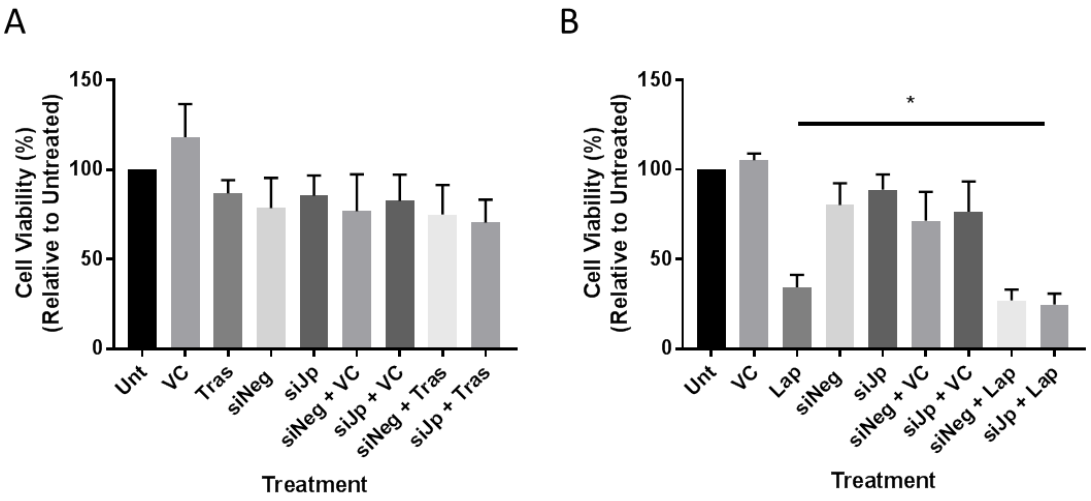

Figure 5.11 Responsiveness to HER2-targeted drugs is not influenced by JAM-A expression in OE19 cells. *OE19 cells were plated in triplicate wells of 96-well plates (5,000 cells/well) and transfected after 72h with either control siRNA (siNeg) or pooled siRNA to JAM-A (siJp) (final concentration 25nM). After 72h ESO26 and N87 cells were then treated with either Trastuzmab (Tras; 10µg/mL) or Lapatinib (Lap; 2µM) for a further 72h. Control cells were treated with matched vehicle controls (VC; Trastuzumab VC: H_2O 0.05% v/v; Lapatinib VC: DMSO 0.02% v/v). Cell viability was assessed using Alamar Blue assays. Experiments were performed three times and data shown as mean ± SEM. Statistical significance was tested using paired, two-tailed Student t-tests. (*p<0.05, **p<0.01, ***p<0.001).*

5.3.10 JAM-A silencing did not impact HER2 protein expression in a *semi-in vivo* model.

We next sought to confirm that JAM-A was not regulating HER2 in higher-order settings, using the semi-*in vivo* chick embryo model employed in previous chapters. In xenografted tumours composed of JAM-A-silenced ESO26 cells (siJp) vs control cells (siNeg), tumours and their surrounding CAM were immunohistochemically stained for HER2 expression in order to examine whether local JAM-A reductions altered HER2 staining patterns. In light of the previous discussion around the heterogeneity of JAM-A expression in JAM-silenced tumours, and the possibility that a specific threshold of JAM-A loss is required before HER2 changes are evident, we chose to visually inspect the cases rather than obtain a heterogeneous overall score per section.

No significant loss of HER2 was observed across the tumours extracted from siJp compared to control groups. Closer examination of focal areas of JAM-A loss across heterogeneous samples revealed no impact on HER2 staining at these points. Specifically, HER2 staining remained consistently membranous **(Figure 5.12)**, contrasting with earlier (simpler) fluorescent immunocytochemistry on the same target areas **(Figure 5.8).**

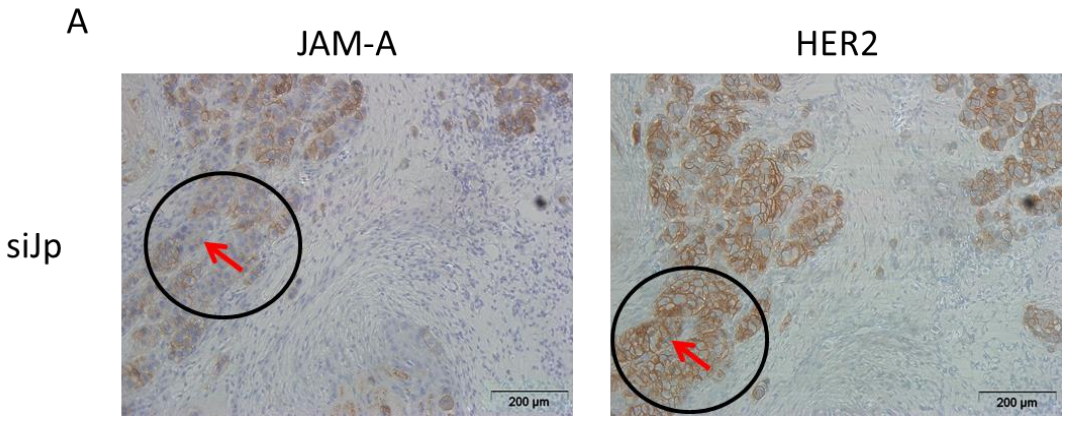

Figure 5.12: JAM-A silencing elicited no changes to HER2 expression in xenografts extracted from the CAM assay. *JAM-A immunohistochemistry (IHC) was performed on tumour xenografts which had been grown on the CAM of developing chick embryos. JAM-A-heterogeneous areas were identified and JAM-A-low areas were matched to HER2 expression of the same area. Representative images* ***(A)*** *show matched areas of stained sections, with heterogeneous areas circled in black and specific areas highlighted by red arrows. All images were obtained using an Olympus CKx41 microscope with Cell B imaging software at 20x magnification.*

5.3.11 Tissue Microarray Analysis of JAM-A in HER2-positive gastro-oesophageal cancers

Since JAM-A overexpression had correlated with HER2 positivity and poorer survival through online gene expression datasets from gastric cancer patients **(Figure 5.2)**, we thought it likely that our *in vitro and* semi-*in vivo* models were not capturing the pathophysiological complexities of clinical cases. Therefore to independently search for a potential correlation between JAM-A and HER2 expression in gastric cancer patients, we scored 150 sections from a 174-primary tumour bank donated by Prof. Karin Jirström (Lund University, Sweden) (238). Membranous staining of JAM-A was assessed as either absent (0), weak incomplete (1+), weak complete (2+) and strong complete (3+); where scores of 0-2+ indicated low/moderate while 3+ indicated high JAM-A staining **(Figure 5.13)**. Patient cores were in duplicate, and in the event of a discordant score between patient-matched cores, the higher score was recorded. The relationship between JAM-A and clinicopathological features was then examined using SPSS crosstabulation and χ^2 and asymptotic significance calculated. Analysis revealed that JAM-A had no significant correlation with overall survival, tumour grade, proliferation (Ki67 staining), Lauren classification, differentiation or TNM-staging (**Table 5.1**). Furthermore, no significant correlation existed between high JAM-A expression and HER2 positivity **(Table 5.1)**. Interestingly, however, significant ($p<0.05$) correlations were seen between JAM-A expression and the primary tumour location, showing that high JAM-A levels were significantly likely in oesophageal cases than those originating from the stomach.

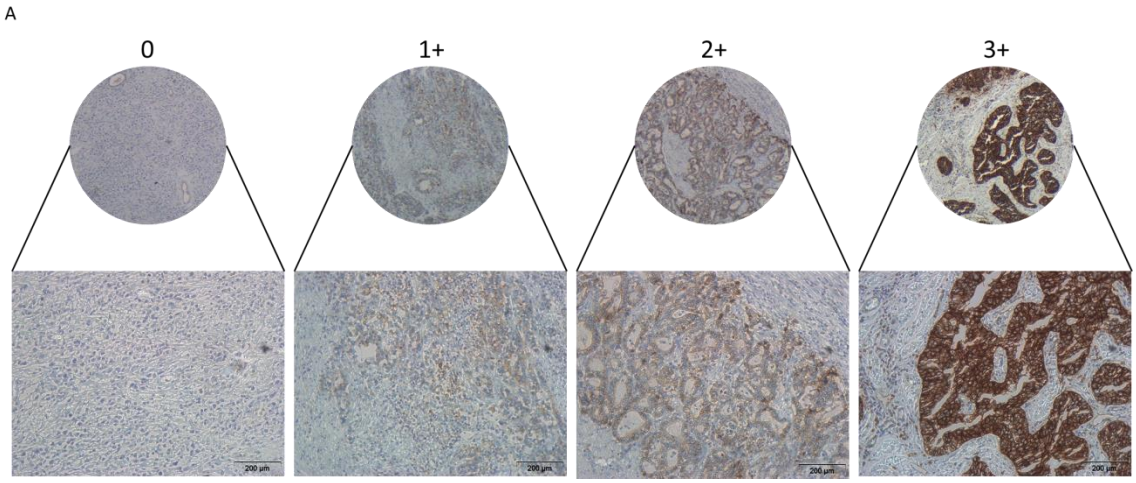

Figure 5.13 JAM-A expression does not correlate with HER2 expression in a gastro-oesophageal tissue microarray. *JAM-A immunohistochemistry (IHC) was performed on 4µm sections across a TMA of gastro-oesophageal cancers totalling 174 primary tumour cases. Membranous JAM-A expression was scored 0, 1+, 2+, 3+ based on completeness and intensity of staining; with 150 scorable cases. JAM-A results were scored in conjunction with a histopathologist. Scale bar; 200µm.*

Table 5.1- Clinicopathological Features of TMA with known HER2 status.

A TMA of 174 primary tumours from gastro-oesophageal cancer patients was stratified based on either High or Low/Moderate JAM-A expression based on intensity and completeness of JAM-A membranous staining. Statistical analysis was carried out using the χ^2 test comparing JAM-A expression with clinicopathological parameters on SPSS version 24 software. Comparisons were considered significant at $p<0.05$.

Variable	N	Low/Moderate	High	P-Value
Sex	150			0.596
Female		23	9	
Male		79	39	
Overall Survival	150			0.735
Living		25	13	
Decease		77	35	
T-Stage	150			0.843
1		9	5	
2		18	11	
3		57	25	
4		18	7	
N-Stage	150			0.981
0		29	15	
1		20	9	
2		28	12	
3	150	25	12	
M-Stage				0.107
0		89	47	
1		13	1	
Differentiation	150			0.664
High		5	1	
Moderately		32	17	
Low		65	30	
Lauren Classification	150			0.359
Intestinal		72	39	
Diffuse		25	7	
Mixed		5	2	
Location	150			*0.049
Oesophagus + Carc		62	37	
Stomach		40	11	
Ki67	149			0.545
0-1%		2	1	
2-10%		14	4	
11-20%		17	11	
21-50%		29	18	
>50%		39	14	
HER2 Positivity	96			0.396
Negative		54	24	
Positive		9	4	
Unspecified		2	3	
HER2 Positivi				

JAMA Expression: Low/Moderate = 2+ High = 3+
HER2 Positive IHC3+

We also sought to examine whether any changes to JAM-A expression were demonstrated between primary tumours and metastases. There was a significant correlation between JAM-A expression in primary tumours and metastatic lesions in 66 cases, specifically in low/moderate cases. This is an important finding given the difficulty of finding viable targets suitable for both primary and metastatic forms of the disease (239) and suggests that, perhaps irrespective of HER2 status, JAM-A may by itself be a targetable protein in the metastatic setting.

.

Table 5.2 JAM-A staining correlated in Primary and Metastatic Tumours

± l· NJ ƛ l· ō f Ŝ	b [ƨ ǿ к a ƨ Ř Ŝ	l ƛ Ǝ K	t- ± l· f
W ! -ɑ { ű l· ƛayŜƛűyƚ·Ǝă	c		Ғ Ғ л ϙ
[ƨ ǿ к a ƨ	o y	p	
l ƛ	м o	м л	
W ! -ɑ 9 È LJNJ Ŝ ă ă ƛ ƨ ỿ Ɏ н Ŧ [ƨ ł ǿ ƛ к Ǝ ɑ ƙ ƨ Ř ĺ Ŝ NJ d· ŧ ű Ŝ Ґ	л		

However, a significant limitation of the TMA was there was a lack of consistency between duplicate cores. We saw that out of 45 cases which were classified as being JAM-A-high, 30 of the replicate cores (scored blindly) had different scores. In some instances a core within the sample may have only received 1+ score, but if its second core received 3+ because there were areas of 3+ in the tumour; hence the overall case was rated as having high JAM-A expression. Given the diversity between cases in this setting, and recent discussions on the importance of intra-tumour heterogeneity in tumour progression (239), we were concerned that the lack of consistency across duplicate cores meant our JAM-A scoring may not reflect the cancer cases. This may explain why we were unable to uncover any correlations between JAM-A and HER2 expression.

5.3.12 JAM-A expression is extremely heterogeneous in GE cancer cases

In order to test whether JAM-A expression is more reproducibly analysed on larger tissue surfaces, we undertook a pilot study using 11 full-face gastro-oesophageal sections with known HER2 status. Scoring of JAM-A was then undertaken in parallel with a clinical histopathologist. Since significant heterogeneity of JAM-A staining was displayed across individual cases, a specific scoring method was developed in order to best stratify the cases. Using a weighted ranking system, sections were given a percentage for each score (0, 1+, 2+, 3+) **(Figure 5.15)** across the tumour within the section. We used a weighted ranking system based on the percentage of the scores within each case **(Table 5.3)**.

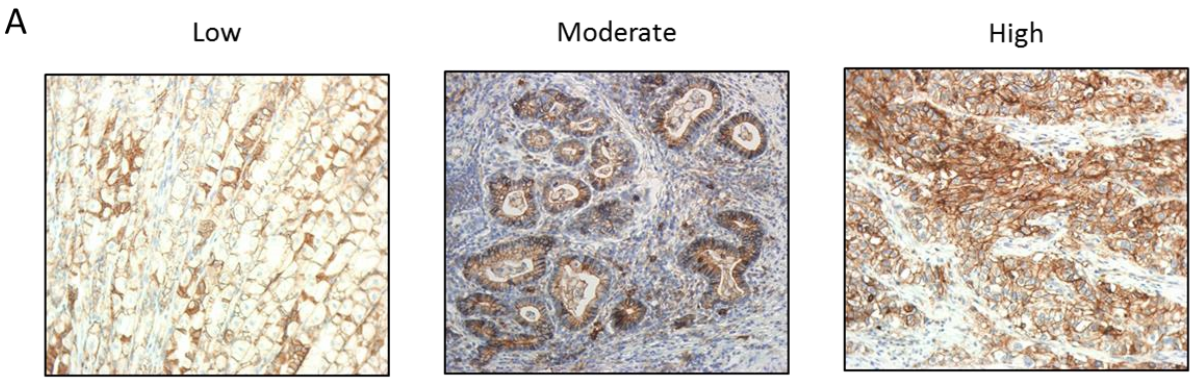

Figure 5.15: JAM-A Immunohistochemical staining in gastro-oesophageal cancer full-face sections. *JAM-A immunohistochemistry (IHC) was performed on 4µm sections across 11 primary gastro-oesophageal cancer cases. Membranous JAM-A expression was scored 0, 1+, 2+, 3+ based on completeness and intensity of staining; with each score given a % value for each section. JAM-A results were scored in conjunction with a histopathologist.*

Table 5.3: JAM-A expression weighted ranking system for immunohistochemical analysis of full-face sections. *A novel weighted ranking system was developed in order to stratify cases based on JAM-A expression which was extremely heterogeneous across cases. A percentage of each score was allocated, and that percentage weighted based on intensity and quantity. This was used to assign an overall JAM-A score to individual sections.*

Gastric Tissue Section Overall Score Calculation									
Case	% of Score			Grade Calculation			Accumulated Grade Score	JAM-A Staining Intensity	HER2
	1	2	3	1	2	3			
1	20	50	30	5	25	30	60	Moderate	-
2	-	40	60	-	20	60	80	High	+
3	5	55	40	1.25	27.5	40	68.75	High	+
4	33	33	33	8.25	16.5	33	57.75	Moderate	-
5	5	55	40	1.25	27.5	40	68.75	High	+
6	30	40	30	7.5	20	30	57.5	Moderate	-
7	10	60	30	2.5	30	30	62.5	Moderate	+
8	10	20	70	2.5	10	70	82.5	High	+
9	75	25	-	18.75	12.5	-	31.25	Low	-
10	10	40	50	2.5	20	50	72.5	High	+
11	30	30	40	7.5	15	40	62.5	Moderate	-

Grade 1 = each % is worth 0.25
Grade 2 = each % is worth 0.5
Grade 3 = each % is worth 1

Low = < 33
Moderate = 33 - 66
High = > 66

Table 5.4: JAM-A staining significantly correlates with HER2 status in gastro-oesophageal cancer full-face Sections. *Full-face sections of gastro-oesophageal cancer patient tissue (n=11) were stratified based on either High or Low/Moderate JAM-A expression based on intensity and completeness of JAM-A membranous staining. Statistical analysis comparing JAM-A expression with clinicopathological parameters on SPSS version 24 software. Comparisons were considered significant at p<0.05.*

Variable	N	Low/Moderate	High	P-Value
T-Stage	11			0.497
1		0	1	
2		0	0	
3		4	3	
4		2	1	
N-Stage	11			0.246
0		2	3	
1		1	1	
2		3	0	
3		0	1	
Differentiation	11			0.382
High		0	0	
Moderately		0	1	
Low		3	3	
Both Moderately/Low		3	1	
Lauren Classification	11			0.547
Intestinal		3	2	
Diffuse		2	2	
Mixed		1	0	
Location	11			0.088
OG Junction + Lesser Curvat		4	0	
Gastric Bod		0	2	
Gastric Body + Lesser Curvat		0	1	
OG Junctio		0	1	
OG Junction and Gast		1	0	
Gastric Cardi		1	0	
Gastric Pyloru		0	1	
HER2 Positivity	11			**0.006
Negative		5	0	
Positive		1	5	
Unspecifie		0	0	

JAM-A Expression: Low/Moderate = 0/1+ High = 3+
HER2 Positive IHC3+, OG = Oesophageal Gastric

Having assessed the evident heterogeneity of JAM-A staining across full-face sections **(Figure 5.16),** we were able to further investigate whether JAM-A intensity correlated with a number of limited clinicopathological features. While JAM-A intensity saw no correlation with T and N staging, Differentiation, Lauren classification or localisation of tumour, statistically significant correlations were noted between JAM-A intensity and HER2 positivity **(Figure 5.17**; χ^2 test, p<0.01**)**. We also analysed this data set using a Fisher's exact test and observed that 100% of HER2-negative cases had low/moderate JAM-A staining; whereas 83% of HER2-positive cases had high JAM-A expression **(Figure 5.18**; p=0.0152**).**

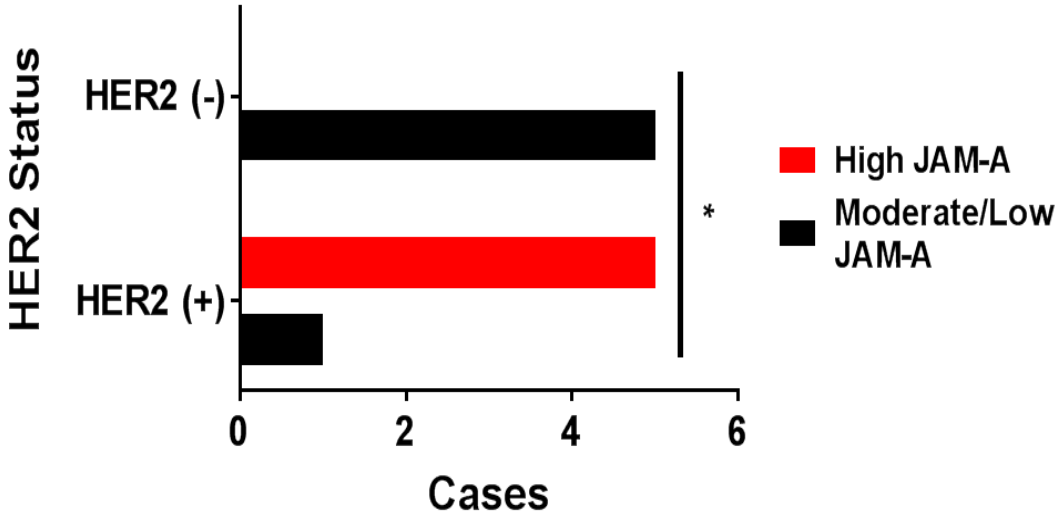

Figure 5.18: High JAM-A expression in gastro-oesophageal cancer cases correlates with HER2 positivity. *JAM-A expression in eleven primary tumours from* gastro-oesophageal *cancer patients was correlated with HER2 status, based on either high or low/moderate JAM-A expression. Statistical analysis was a* χ^2 *test comparing JAM-A output expression with clinicopathological parameters on SPSS version 24 software. Comparisons were considered significant at *p<0.05, **p<0.01, ***p<0.001.*

5.4 Discussion

JAM-A has recently been highlighted as a regulator of HER2 expression in breast cancer settings (100). Our group has also recently highlighted JAM-A as a potential treatment target using an *in vivo* DCIS mouse model (Yvonne Smith, personal communication). Hence we hypothesised that, in HER2-overexpressing gastro-oesophageal cancers, JAM-A may also play an important role. We selected three HER2-positive gastro-oesophageal cancer cell lines and tested to see whether alterations to basal JAM-A expression (both loss and gain) could induce mirrored changes in HER2 expression, as previously described in breast cancer cell lines.

There was no uniformly-consistent response in any cell line, with HER2 expression fluctuating even within biological replicates. Hence, we could provide no concrete evidence proving that JAM-A regulates HER2 expression in the gastro-oesophageal cancer setting. However, considering the discussion in Chapter 4 regarding the ability of JAM-A to impact a myriad of downstream targets, including those of the cytoskeleton, it is possible that the changes to HER2 documented may be consequential, and reflect cytoskeletal changes induced by JAM-A loss.

One thing which can be taken from these studies is that it is important to consider varied responses between cancer cell lines *in vitro*. Perhaps, had other cell lines been selected, we may have replicated the responses we expected based on prior evidence gathered in breast cancer settings. Model selection may also explain the discrepancies already existing in the literature prior to this study, showing conflicting roles for JAM-A as being either protective or a driving factor in cancer progression. Though this may offer an explanation for discrepancies between cancer types (100, 122, 124, 126, 127, 131, 133), it offers a wider commentary on the use of single *in vitro* models as validation of mechanisms within cancer types.

Overexpression of JAM-A across all three cell lines did show a trend for HER2 expressional levels to increase, though this was not statistically significant.

This may reflect a limitation of the model (240, 241). It is possible that more efficient techniques, and perhaps longer time points (given the slow growth of these cell lines) may elicit more convincing results. For example, stable transfections of JAM-A using crispr-cas9 methods may reveal more consistent increases to downstream proteins (241, 242). Of note, stable transfections were attempted for the purposes of this thesis, however attempts to develop successfully JAM-A-overexpressing or -mutated cell lines were unsuccessful and could not be included in this body of work.

If HER2 changes were indeed dependent of JAM-A increases (rather than loss), as in the breast tumour setting, this may suggest that an intermediary protein(s) is responsible for JAM-mediated regulation of HER2 expression (rather than direct regulation by JAM-A of HER2). In support of this hypothesis, publicly-available gene expression data revealed a significant correlation between JAM-A and HER2 positivity in gastric cancers. It is possible that JAM-A acts upstream of HER2 in these cases; either directly or indirectly. It is also conceivable that intermediary proteins may regulate HER2 downstream of JAM-A signalling. If this were to be true, then the intermediary proteins themselves could potentially act as novel therapeutic targets.

Since JAM-A has been shown previously to induce apoptotic priming in cells (127) as well as in this thesis, we showed that JAM-A silencing in gastro-oesophageal cancers potentiates the cell viability deficits induced by HER2 targeted therapies. It also suggested that, irrespective of the role of JAM-A in individual cancer cell lines, its loss was specifically highlighted in the OE19 cell line responses to both ActinoD and Lapatinib following JAM-A silencing. This is an exciting finding, as it suggests that JAM-A targeting may have a significant effect in gastro-oesophageal HER2-positive cancers resistant to HER2-targeted therapies, whereby targeting JAM-A could see cancers re-sensitize to apoptosis-inducing therapies. This would also be exciting to test across a series of resistant cancer types, and not just in HER2 cases, as JAM-A is known to be ubiquitously expressed across epithelial and endothelial cells (110, 208).

Since molecular analysis revealed no direct regulation of HER2 by JAM-A we hypothesised that immunohistochemical studies may reveal correlations between the JAM-A and HER2 expression in gastro-oesophageal cancers. Analysis of a 174 primary tumour TMA did not reveal any significant correlations between JAM-A expression and clinicopathological features; with the exception of location, where high JAM-A expression occurred more frequently in oesophageal than gastric cancers. Although this was surprising, we feel the work illustrates an extremely important commentary on the use of TMAs for validating proteins known to be expressed heterogeneously. We were able to show correlations between JAM-A and HER2 expression in full-face sections when heterogeneity levels were accurately assessed, which correlated with gene data available online, but this correlation had not been demonstrated through TMA analysis. It seems even more essential that heterogeneity is accounted for in any validation study; in order to capture the most information available about a given protein in specific tissues and to relay the recent importance being placed on intra-tumour heterogeneity and the role it may play in disease pathogenesis (239). Hence, we developed a novel weighted ranking system which quantified the level of JAM-A staining intensity present based on visual assessment of the amount (%) of 1+. 2+. 3+ staining. Each % score was then weighted; each % of 1+ given 0.25, each % of 2 given 0.5, each % of 3+ given 1. We then assessed overall intensity by ranking weighted scores as either low (<33%), moderate (33-66%), or high (>66%). Once overall scores had been allocated, we re-examined sections and tested whether our assessment had accurately captured JAM-A expression for the case. To our knowledge, this is the first example of a weighted ranking assessment method for heterogeneous proteins.

Overall, we speculate that JAM-A reductions do not directly impact HER2 in this cancer setting, however JAM-A overexpression may play a role in the indirect increases in HER2 via intermediary protein(s) which could act to increase HER2 stabilisation. HSP90, a known regulator of HER2 (229), may be one potential candidate in this setting. Previous work by our group did examine whether HSP90 inhibition could alter HER2 expression in JAM-A

silenced breast cancer cells. However the results suggested that JAM-A regulated HER2 independently of HSP90, since HER2 reductions were additive under combination treatments (data not shown). It is also conceivable that this proposed intermediary protein(s) is inconsistently unaffected by JAM-A loss, explaining the variations in HER2 expressional responses detailed in this thesis. However, given that JAM-A has the ability to prime apoptotic activation, it may be a potentially useful player in drug-resistant settings and a potential candidate for developing targeting treatments.

Chapter 6 Elucidating the role of JAM-A in regulating other RTKS

6.1 Introduction

Receptor tyrosine kinases (RTKs) are crucial players in diverse cellular processes. They have many physiological roles, activating downstream signalling cascades that drive cell growth, differentiation, motility and metabolism (243, 244). However aberrant expression of RTKs through hyperactivation or dysregulation has also been associated with many pathophysiologies including cancer progression (243). In general, RTKs are activated by ligand presentation which induces dimerization, autophosphorylation and downstream signalling (243, 245). This process is tightly regulated by several different mechanisms including negative regulation by ligand antagonists, switching off autophosphorylation via tyrosine phosphatases, and receptor endocytosis leading to lysosomal degradation (244).

In cancer, RTKs have been found to undergo chromosomal translocation, gain of function mutations, overexpression or autocrine activation resulting in aberrant expression driving pathogenesis (244, 245). The role of the RTK HER2 has been discussed in previous chapters of this thesis, however dysregulation of many other RTKs has also been highlighted as playing roles in cancer progression.

As previously discussed, HER family members have long been implicated in breast cancer and more recently gastro-oesophageal cancers (32, 70, 82, 238, 246-257). However HER3 is increasingly being recognised as a prominent driving force in breast cancer progression by virtue of its ability to act as the most potent signalling partner of HER2. Like HER2, HER3 is activated through heterodimerisation and phosphorylation of its tyrosine kinase domain. Unlike HER2, however, HER3 lacks an intracellular protein kinase domain, and hence relies on other HER family members for activating downstream signalling events (258).

HER3 overexpression is thought to occur in ~10% of breast cancer patients and its aberrant expression has been reported in ~12% of gastric cancers

(255, 259, 260). HER3 has also been linked with poor survival in gastric cancers, where its expression significantly associated with invasion and progression of tumours as well as more aggressive phenotypes such as metastasis and recurrence (246, 250). Interestingly, HER3 has been shown to play a role in Trastuzumab resistance in oesophageal tumours. In one study, ADAM-10 dependent release of the HER3 ligand heregulin was increased in response to Trastuzumab therapies, promoting HER3 signalling and downstream activation of AKT in a classic tumour progression pathway (261). The same mechanism of resistance conferral has also been established in lapatinib-resistant gastro-oesophageal cancers (262). Given the recent report by our laboratory that ADAM-dependent release of cleaved JAM-A (cJAM-A) also acts as a biomarker in patients resistant to HER2-targeted therapies (208), it is exciting to speculate that JAM-A may also play a role in gastro-oesophageal cancer resistance via HER3 activation.

Our group has also recently highlighted a novel mechanism where JAM-A regulates HER3 via expressional changes in FOXA1 (Rodrigo Cruz, personal communication). FOXA1 is a transcription factor which has been shown to bind to the promoters of many genes, including HER3 (263). Aberrant overexpression of FOXA1 has been demonstrated in oesophageal tumours (264). Our group has highlighted a linear mechanism of HER3 regulation by JAM-A in breast cancer cells involving modulation of β-catenin cellular location, which in turn dictates β-catenin localisation in the nucleus and its consequent activation of FOXA1 transcription (Rodrigo Cruz, personal communication). If the same mechanism were active in gastro-oesophageal cancers, it may suggest novel therapeutic targets in both HER3-overexpressing cancers as well as in cancers resistant to HER2-targeted therapies induced through aberrant HER3 activation. But first a pathway of regulation between JAM-A and HER3 must be established in gastro-oesophageal cancers

While HER3 provides a rational target for investigation downstream of JAM-A expressional changes, accumulating evidence suggests that JAM-A may also regulate RTKs independent of the HER family. For example, unpublished

preliminary data from our laboratory has uncovered a potential role for JAM-A in regulating EphB4 expression in breast cancer (Sri Vellanki, personal communication). EphB4 belongs to the largest family of RTKs and binds to the ligand EphrinB2, driving downstream physiological and pathophysiological angiogenic, proliferative and migratory phenotypes (265). Interestingly, like JAM-A, overexpression is not the only reported mechanism for oncogenic signalling from EphB4; and accordingly its loss has also been linked with tumorigenesis in some settings (266). This may suggest a threshold or 'molecular switch' expression role as we

EphB4 expression has been shown to correlate with tumour grade in breast cancers (267) and worsened prognosis in gastric cancers (268), hence we hypothesise that JAM-A may play correlate with EphB4 gene expression and potentially correlate with JAM-A expression levels in patient tissues.

6.2 Aims of this Chapter

The primary aim of this chapter was to elucidate whether JAM-A is involved in the expressional regulation of RTKs other than HER2 in gastro-oesophageal cancers. The specific aims were as follows:

Specific Aim 1: To determine whether JAM-A silencing regulates HER3 or EphB4 gene expression in gastro-oesophageal cancer cell lines;

Specific Aim 2: To examine whether JAM-A expression correlates with HER3 or EphB4 expression in tumour tissue from gastro-oesophageal cancer patients;

Specific Aim 3: To elucidate whether downstream linear pathways of regulation of HER3 by JAM-A through FOXA1 and β-catenin were evident in gastro-oesophageal cancers, as previously found in breast cancer cell lines.

6.3 Results

As described in preceding chapters, the simple relationship between JAM-A and HER2 which we previously reported in breast cancer (100) does not seem to hold true in gastro-oesophageal cancers. In light of unpublished screening data from our laboratory suggesting that JAM-A regulates RTKs other than HER2, we first wanted to investigate if a relationship between HER3 and JAM-A could be established in the gastro-oesophageal cancer setting.

6.3.1 JAM-A and HER3 gene expression do not correlate in gastro-oesophageal cancer cases.

We first tested if there was any correlation between gene expression levels of JAM-A, HER3 and prognosis in gastric cancer patients, using an open-access online tool (https//:kmplot.com) (140).

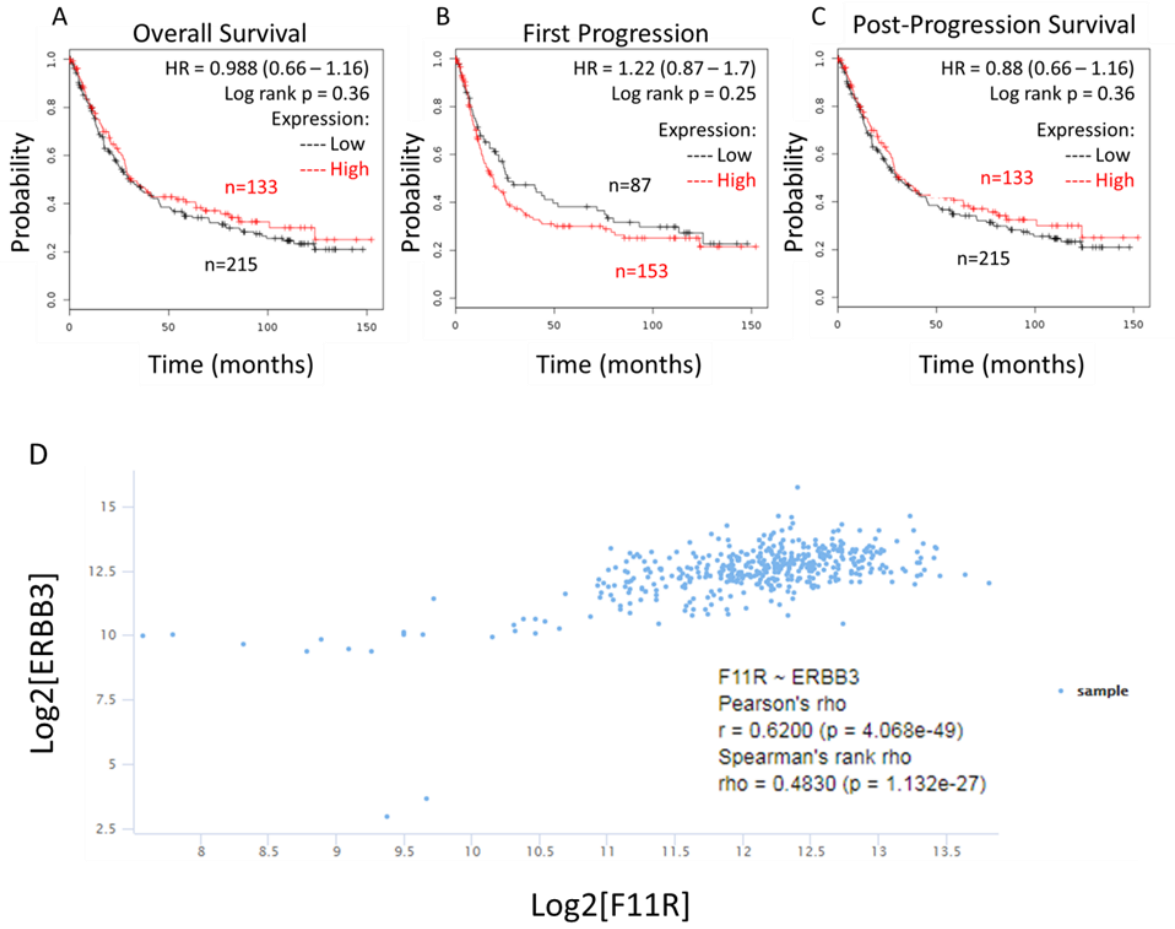

Figure 6.1: High co-expression of JAM-A and HER3 mRNA does not predict poor prognosis in gastric cancer patients. *Kaplan-Meier Plot platform (http://kmplot.com/analysis/) was used to generate survival curves correlating JAM-A and HER3 expression in gastric cancer patients. Using F11R and ErbB3 jetset probe (excluding GSE62254 as recommended) revealed no significant correlations between F11R and ErbB3 mRNA expression with worsened overall survival (A), risk of progression (B) or post-progression (C). Xenabrowser platform (https://xenabrowser.net/) was used to generate a scatter plot (D) showing correlations between JAM-A and HER3 mRNA expression in gastroesophageal cancer patients. Using F11R and ERBB3 genes as variables in the TCGA Stomach Cancer cohort revealed a significant positive correlation (D).*

As shown in **Figure 6.1**, there was no significant association between JAM-A, HER3 and patient prognosis in this setting. However, surprisingly there was evidence that low levels of both JAM-A and HER3 correlated at gene level (r=0.6, p=<0.001), hence we next investigated whether any linear regulatory relationship between JAM-A and HER3 existed at protein level in gastro-oesophageal cancers.

6.3.2 JAM-A protein expression correlates with low HER3 expression in a cohort of gastro-oesophageal cancer cases

To uncover whether JAM-A and HER3 protein expression was correlated in gastro-oesophageal cancer cases, a second TMA of 166 patients was kindly donated to us by Dr. Karin Jiström (Lund University, Sweden) with available data on HER3 expressional changes in gastro-oesophageal cancers pre- and post-treatment with pre- and post-neoadjuvant chemotherapies (251). This TMA was stained for JAM-A in a cohort of 144 patients, 83 of which were successfully scored with the assistance of a clinical histopathologist (Dr. Kathy Sheehan, RCSI). As previously described, JAM-A staining was scored based on the intensity and continuous membranous staining of JAM-A as follows: no staining (0), weak and incomplete membranous staining (1+), weak and complete staining (2+) and strong and compete staining (3+). Cases were grouped as Low/Moderate (0-2+) or High (3+) JAM-A expression, and correlated with clinicopathological features of each case. Statistical significance was tested using χ^2 tests in conjunction with

± l· NJ ƛ l· ō f Ŝ	b	l ƛ Ǝ Ƙ	[ƨ ǿ κ a ƨ Ř	t- ± l· f (
{ Ŝ È	y			л Ф (
C Ŝ Ƴ	м ф	о с		
a l·	т	н м		
h Ø Ŝ NJ l· f f {	y			л Ф	
[ƛ (	м м	н у		
5 Ŝ Ŏ Ŝ	м р	н ф		
! Ǝ Ŝ	y			Ғ Ғ л (
ғ (	с	о п		
с	н л	н о		
è LJ ¢	y			л Ф у
м	о	у		
н	о	м р		
о	м р	н л		
п	п	м п		
è LJ b	y			л Ф (
л	м м	н н		
м	т	м п		
н	п	м м		
о	п	м л		
è LJ a	y			л Ф ı
л	н с	р р		
м	л	н		
5 ƛ Ŧ Ŧ Ŝ NJ Ŝ ƴ ű	y			л Ф
l ƛ	м о	н р		
a ƨ Ř Ŝ N	м н	о л		
[ƨ	м	н		
[l· dz NJ Ŝ ƴ / f	y			л Ф (
L ƴ ű Ŝ	м т	о о		
5 ƛ Ŧ Ŧ dz ă	ф	н н		
[ƨ Ŏ l· ű ƛ ƨ ƴ	y			л Ф (
h Ŝ ă ƨ LJ Ƙ l· Ξ	м о	н н		
{ ű ƨ Ƴ	м о	о р		
l 9 w o t ƨ ă ƛ	o			Ғ л Ф
[ƨ	т	о		
l ƛ	с	м п		

W ! - ƛ 9 È LJ NJ Ŝ ă ă ƛ ƨ ƴ Ƴ н Ɐ [l ƛ ǿ Ƙ a ƨ Ř Ŝ N LJ ƨ ű ă Ŝ N LJ l·
¢ dz Ƴ ƨ dz NJ D NJ l· Ř - ƨ Ŝ l Ɔ Ŝ N È LJ l· Ƙ ƛ Ø Ŝ L ƛ ƴ ǿ ű ƨ f Ø Ŝ Ƴ - Ŝ ƴ ű
ƨ LJ Ŝ NJ l· ű ƛ Ø Ŝ Ƴ Ŝ ű l· ă ű l· ă ƛ ă
l 9 w o 9 È LJ NJ Ŝ - ă ƛ ƅ Ƶ ƨ ƴ Ƴ ƛ Ǝ [Ƙ ƨ ǿ o e ƅ Ƶ Ŝ ă ƨ ƨ LJ Ɔ K 9 l· Ŵ Ŝ l

Table 6.1: Tissue Microarray Analysis of JAM-A in gastro-oesophageal cancers with known HER3 expression state outcome. *A TMA of 166 primary tumours from gastro-oesophageal cancer patients was stratified based on either High or Low/Moderate JAM-A staining established on intensity and completeness of JAM-A membranous staining. Statistical analysis was carried out using χ^2 test comparing JAM-A expression with clinicopathological parameters on SPSS version 24 software. Comparisons were considered significant if p<0.05.*

Consistent with observations in our previous TMA, there was no correlation between JAM-A expression and overall survival, TMN staging (post-operatively assessed in this TMA), differentiation, location or Lauren classification in this cohort of gastro-oesophageal cancers. However, χ^2 testing revealed a correlation between JAM-A expression and patient age, where patients under 65 were more likely to demonstrate low/moderate JAM-A staining. Further analysis using a two-tailed unconfirmed Fisher's exact test confirmed that statistical significance was retained for high JAM-A expression in older patients **(Figure 6.2**; p<0.01**).** Surprisingly, we also noted a statistically significant correlation between JAM-A and HER3 expression by χ^2 test **(Table 6.1)**. However post-test analysis of test revealed that the Fisher's exact correlation was no longer statistically significant. However there was nonetheless a trend for cases high in HER3 levels to have low/moderate JAM-A expression **(Figure 6.2).** Importantly, the number of patient cases that could be appropriately correlated for HER3 and JAM-A expression was only 30,and hence may not offer a wide enough scope to accurately correlate JAM-A and HER3 expression in gastro-oesophageal cancers.

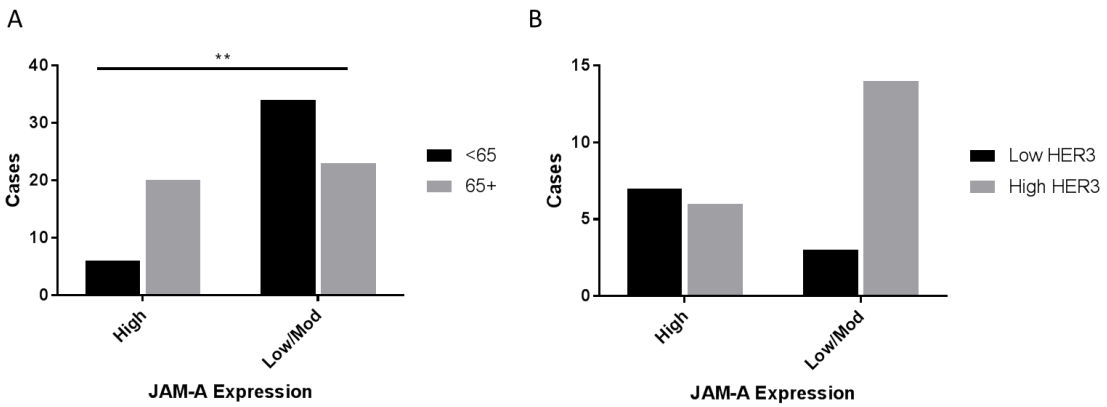

Figure 6.2: High JAM-A expression in gastro-oesophageal cancers correlates with age and trends towards low HER3 expression. *A gastro-oesophageal cancer TMA of 166 patients was stained for JAM-A expression. The association between JAM-A expression and clinicopathological variables was determined by* χ^2 *testing. Asymptotic significant correlations were further tested by Fisher's exact test for both age of patients (<65/65+)* ***(A)****, and HER3 expression* ***(B).*** *Statistical significance **p<0.01.*

6.3.3 Elucidating whether JAM-A regulates HER3 in gastro-oesophageal cancer cell lines

In view of HER3 overexpression correlating best with low/moderate JAM-A and a lack of correlation between JAM-A/HER3 patient gene expression data, it seemed unlikely that JAM-A was regulating HER3. Nonetheless, to complete the story, we examined whether HER3 levels were regulated by those of JAM-A (as in breast cancer cells). We first established the expression levels of HER3 in our panel of three gastro-oesophageal cancer cell lines using immunohistochemistry of cell pellets. As illustrated in **Figure 6.3**, ESO26, N87 and OE19 expressed similar levels of HER3 (3+).

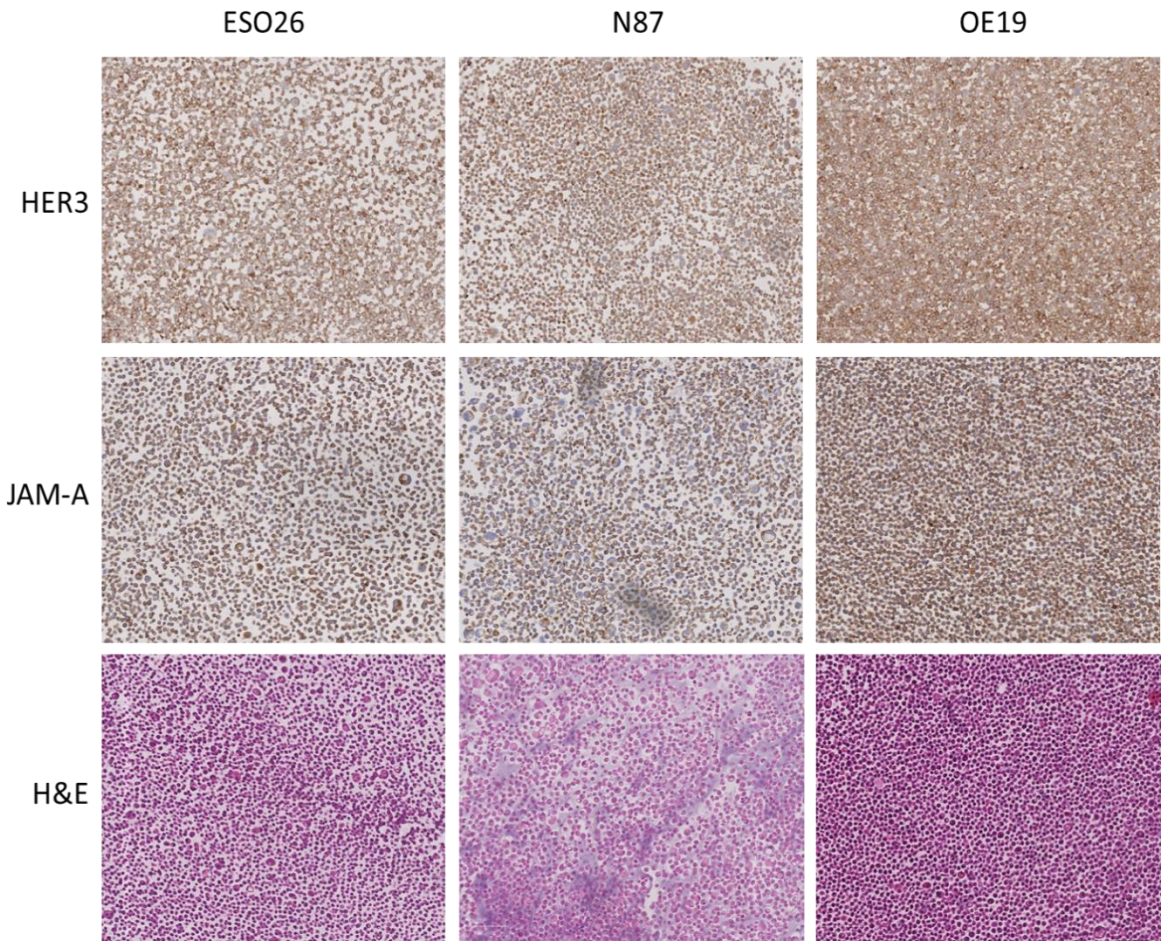

Figure 6.3: JAM-A and HER3 expressed in panel of gastro-oesophageal cancer cell lines. *Formalin fixed cell pellets from five gastro-oesophageal cell lines were embedded in paraffin and underwent immunohistochemistry staining for JAM-A and HER3 to assess expression (n=1). Stained sections were imaged and formatted using Qupath software at 9.66x magnification.*

Since our gastro-oesophageal cell lines had strong HER3 expression, we next sought to examine whether JAM-A silencing could alter HER3 expression in gastro-oesophageal cancer cell lines, mirroring the work carried out in breast cancer cell lines.

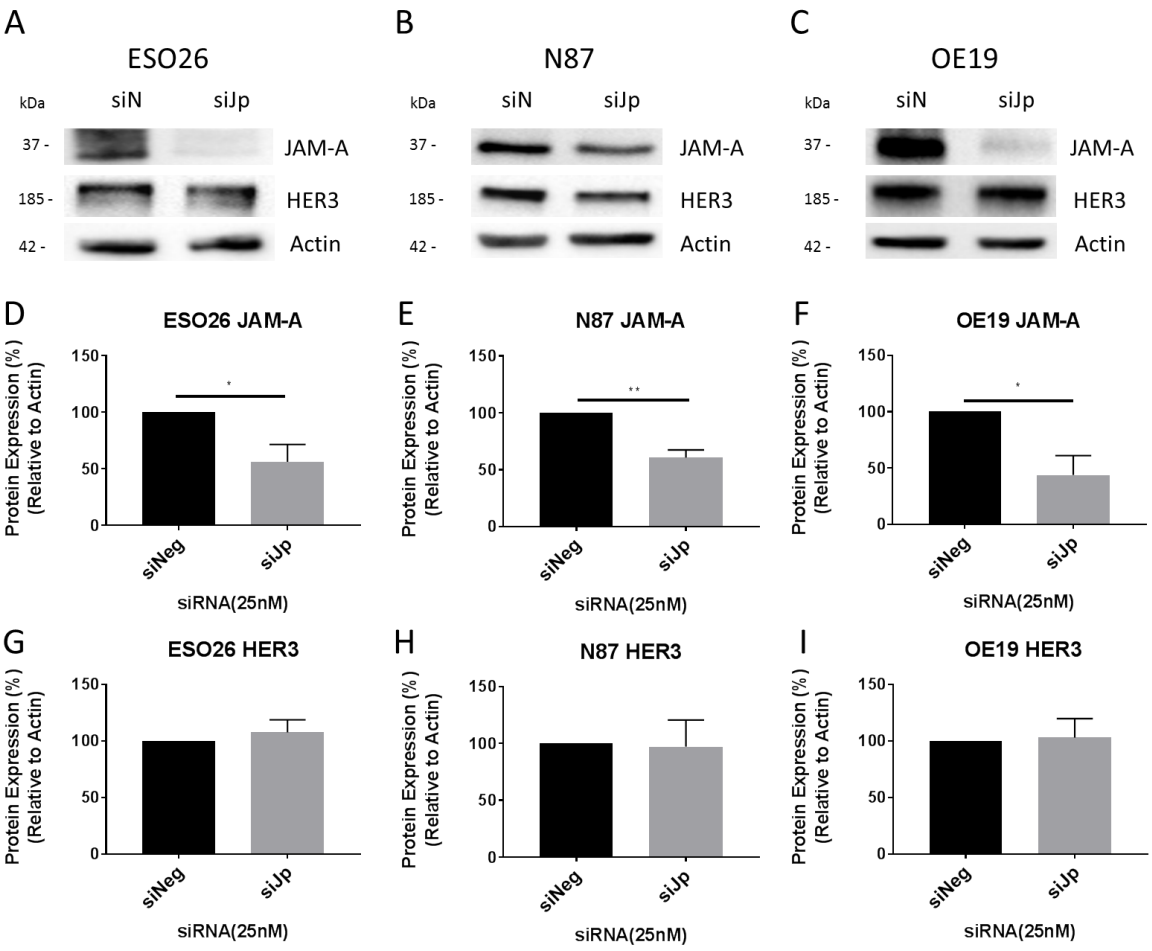

Figure 6.4: JAM-A silencing does not alter HER3 protein expression. *Gastro-oesophageal cancer cell lines were plated at 2x10^5 in 6-well plates. Following one doubling time, cells were transiently transfected for 96h with either control, non-targeting siRNA (siNeg) or a pool of siRNA targeting JAM-A (siJp). Samples were immunoblotted as follows: ESO26* ***(A)****, N87* ***(B)****, and OE19* ***(C)****. Densitometry was performed relative to actin as a loading control; and graphs displayed are shown relative to siNeg: ESO26* ***(D,G)****, N87* ***(E,H)****, OE19* ***(F,I)****. Experimental data (n=3 independent experiments) are shown as mean ± SEM. Statistical analysis was completed using two-tailed unpaired Student's t-test (*p<0.05, **p<0.01, ***p<0.001).*

Since breast cancer cell lines used for the initial study of this mechanism have faster growth rates, we extended the transfection time from 72h to 96h to account for the slower growth of gastro-oesophageal cancer cell lines. Despite significant reductions to JAM-A across all three JAM-silenced cell lines (ESO26 by 44 ± 16%, $p<0.05$; N87 39 ± 7%, $p<0.01$; OE19 56 ± 17%, $p<0.05$) there were no significant changes induced in HER3 protein expression **(Figure 6.4)**. Considering the slow growth of these cells, and their preference for clustering, we speculate that changes would not be demonstrated at protein level following transfections at this early stage. We therefore examined mRNA expression of HER3 at the same timepoint across all three gastro-oesophageal cell lines following JAM-A silencing.

We saw no significant changes in HER3 mRNA levels secondary to JAM-A silencing, despite large increases in HER3 mRNA levels in some ESO26 replicates **(Figure 6.5)**. The outcome of this mirrored result in previous chapters; where the modulation of JAM-A levels induced variable results across biological replicates and cell lines, a feature we ascribe to a predicted "molecular switch" threshold levels of residual JAM-A expression remaining after gene silencing.

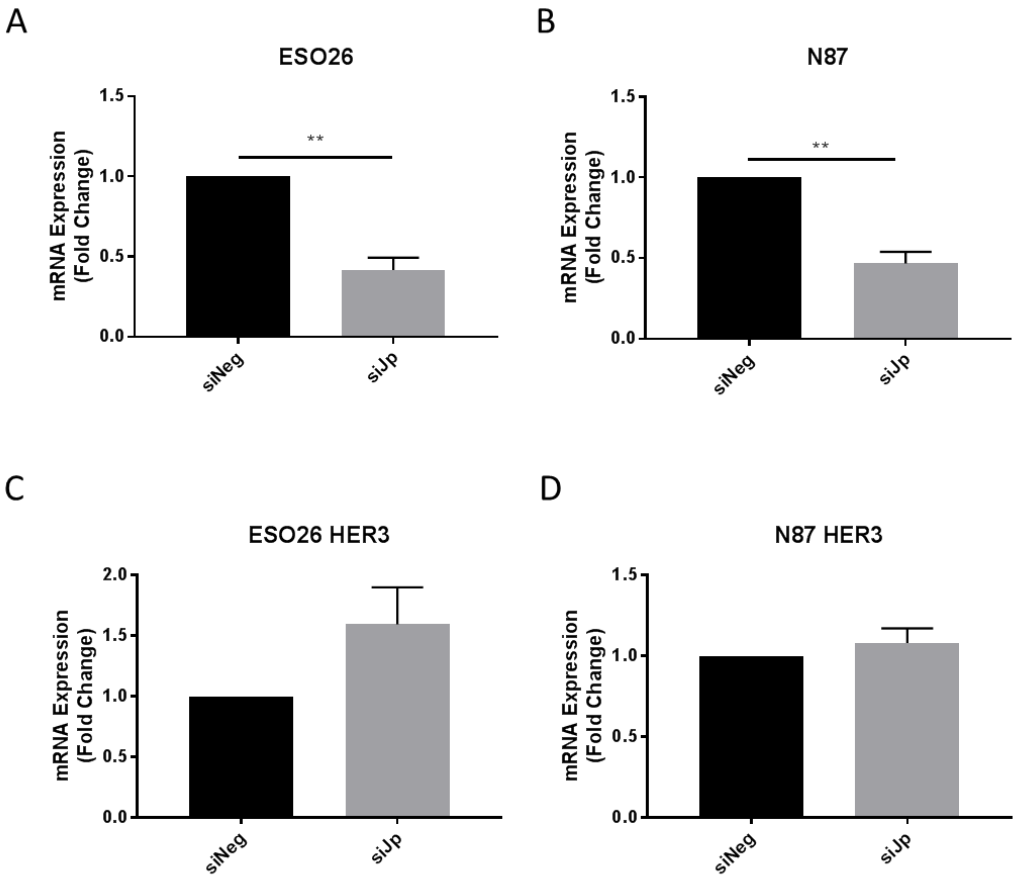

Figure 6.5: JAM-A silencing does not alter HER3 mRNA expression. *Gastro-oesophageal cancer cell lines were plated at 2x10^5 cells/well in 6-well plates. Following one doubling period, cells were transiently transfected for 96h with either control, non-targeting siRNA (siNeg) or a pool of siRNA targeting JAM-A (siJp) siRNA. Quantitative real time PCR was then performed as follows: ESO26* ***(A,C)****, N87* ***(B,D)****. Ct values of samples were set relative to matched Ct values of the housekeeping gene RPLP0. Data from three independent experiments are shown (displayed as mean ± SEM), and unpaired, two-tailed Student's t-tests were used to test for statistical significance. (*p<0.05, **p<0.01, ***p<0.001).*

6.3.4 JAM-A and FOXA1 overexpression predicts poor outcomes for gastro-oesophageal cancers

Since the unpublished linear relationship between JAM-A and HER3 in breast cancer involved intermediary proteins FOXA1 and β-catenin (Rodrigo Cruz, personal communication), we next sought to establish whether JAM-A could influence their expression or localisation as a way of regulating protein pathways beyond the HER family.

First we therefore tested a correlation between FOXA1 and JAM-A gene expression in gastric cancers (140).

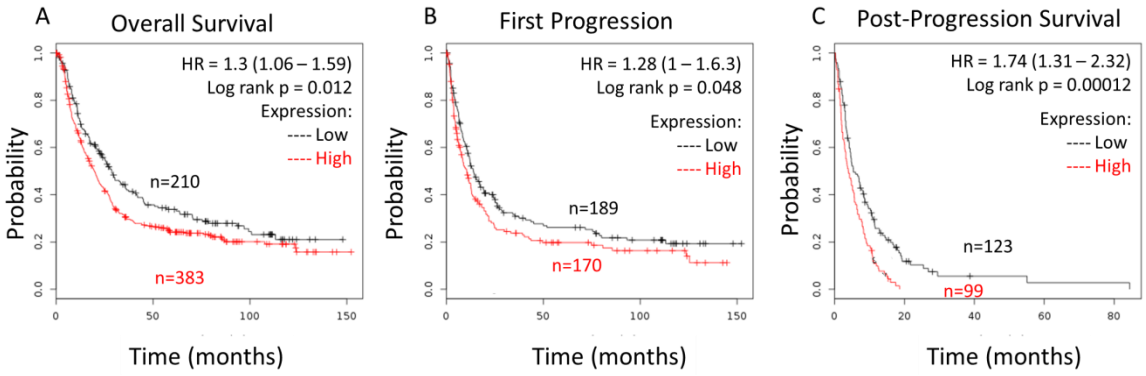

Figure 6.6: High co-expression of JAM-A and FOXA1 mRNA predicts worsened survival in gastric cancer patients. *Kaplan-Meier Plot platform (http://kmplot.com/analysis/) was used to generate survival curves correlating JAM-A and FOXA1 expression in gastric cancer patients. Using F11R and FOXA1 jetset probe (excluding GSE62254 as recommended) revealed no significant correlations between F11R and FOXA1 mRNA expression with worsened overall survival* ***(A),*** *risk of progression* ***(B)*** *or post-progression* ***(C).***

As shown in **Figure 6.6,** concurrent high gene expression of both JAM-A and FOXA1 significantly correlated with poorer overall survival, shorter time to first progression and shorter post-progression survival in gastric cancer patients. Since JAM-A/HER3 regulation did not appear to exist in gastro-oesophageal

cancers, we hypothesised that the correlation between JAM-A and FOXA1 may be indicative of a regulatory role beyond the scope of HER3 signalling.

To investigate this in gastro-oesophageal cancers, we set out to explore whether JAM-A silencing impacted FOXA1 gene expression as it does in breast cancer cells.

6.3.5 JAM-A silencing does not influence FOXA1 expression in GE cancer cell lines

Having hypothesised that JAM-A levels in cells determined those of FOXA1 in gastro-oesophageal cancer cells, we examined the gene expression levels of FOXA1 in two gastro-oesophageal cancer cell lines following JAM-A silencing. As shown in **Figure 6.7**, JAM-A silencing did not significantly alter FOXA1 mRNA expression in either ESO26 or N87 cells. Interestingly, however, FOXA1 levels were greatly increased (with large standard deviations) in ESO26 cells, suggesting that the linear relationship highlighted in the breast cancer setting is not valid in the gastro-oesophageal cancer setting. Since FOXA1 increases were demonstrated in one cell line, we hypothesised that FOXA1 may increase as a compensatory mechanism following JAM-A loss, rather than via direct JAM-A-mediated regulation of FOXA1. Either way, it suggests that specifically targeting JAM-A to reduce FOXA1 in gastro-oesophageal cancers would prove to be unreliable in this cancer type.

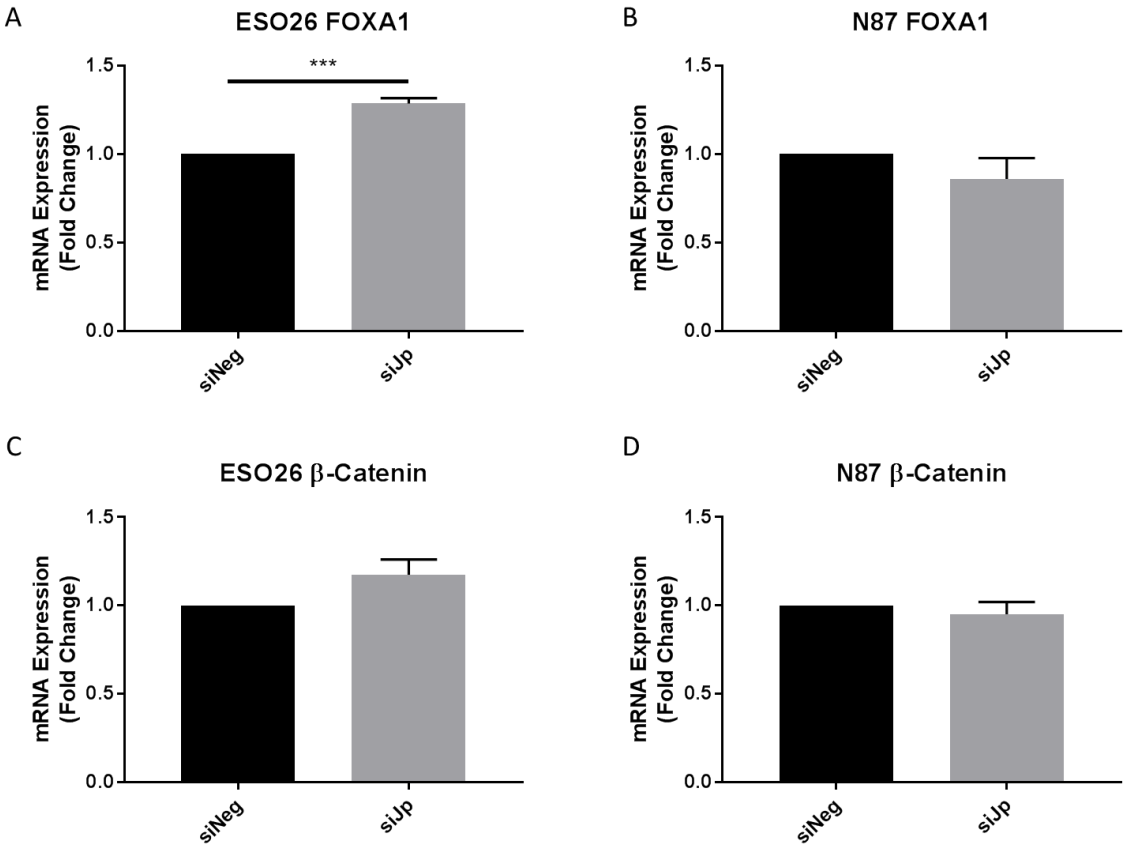

Figure 6.7: JAM-A silencing increases FOXA1 mRNA expression. *Gastro-oesophageal cancer cells were plated at 2x10^5 in 6-well plates and allowed to undergo one doubling time before cells were transiently transfected with either non-targeting siRNA (siNeg) or JAM-A targeting siRNA pool (siJp) (final concentration 25nM). RNA was extracted, cDNA generated and qRT-PCR performed to determine HER2 expression for ESO26* ***(A)*** *N87* ***(B)*** *and OE19* ***(C)*** *cells. Ct values of samples were set relative to matched Ct values of the housekeeping control gene (RPLP0). Analysis of three independent experiments was displayed as mean ± SEM and statistically compared using unpaired, two-tailed Student's t-test (*p<0.05, **p<0.01, ***p<0.001).*

To further validate this, we tested to see whether the next protein in the proposed regulatory pathway; β-catenin; was also impacted by JAM-A silencing in gastro-oesophageal cancer cells. As shown in **Figure 6.7**, significant JAM-A mRNA reductions in both ESO26 and N87 cell lines did not impact β-catenin levels.

6.3.6 JAM-A does not alter β-catenin localisation in gastro-oesophageal cancer cells

Since β-catenin localisation is more important than expression levels for influencing gene transcription, we also wanted to uncover whether JAM-A silencing could change influence β-catenin localisation within gastro-oesophageal cells. We wanted to ensure that, since JAM-A was not directly influencing FOXA1 levels, another transcription factor was not being favoured over FOXA1 in gastro-oesophageal cancers.

There was no evidence to suggest that JAM-A was regulating pathways in the same manner demonstrated previously in breast cancer cell lines, therefore we ruled out any regulation of FOXA1 or β-catenin by JAM-A. If JAM-A loss could increase FOXA1 protein levels in some, but not all, gastro-oesophageal cancers, it may not attenuate the proliferative natures of gastro-oesophageal tumours as we had hoped.

Since our work involving HER family members had evidently highlighted a differential role for JAM-A in gastro-oesophageal cancers compared to the one our group has played a part in establishing for breast cancer, we finally examined another RTK known to be upregulated in some cancers with some preliminary evidence of crosstalk with JAM-A in the breast cancer setting.

6.3.7 JAM-A and EphB4 overexpression correlates in pilot study of gastro-oesophageal cancer cases

Using the same 11 gastro-oesophageal cancer cases discussed previously in this thesis **(Chapter 5.3.12)**, full-face sections were stained for EphB4 and correlated with both clinicopathological features and with JAM-A staining.

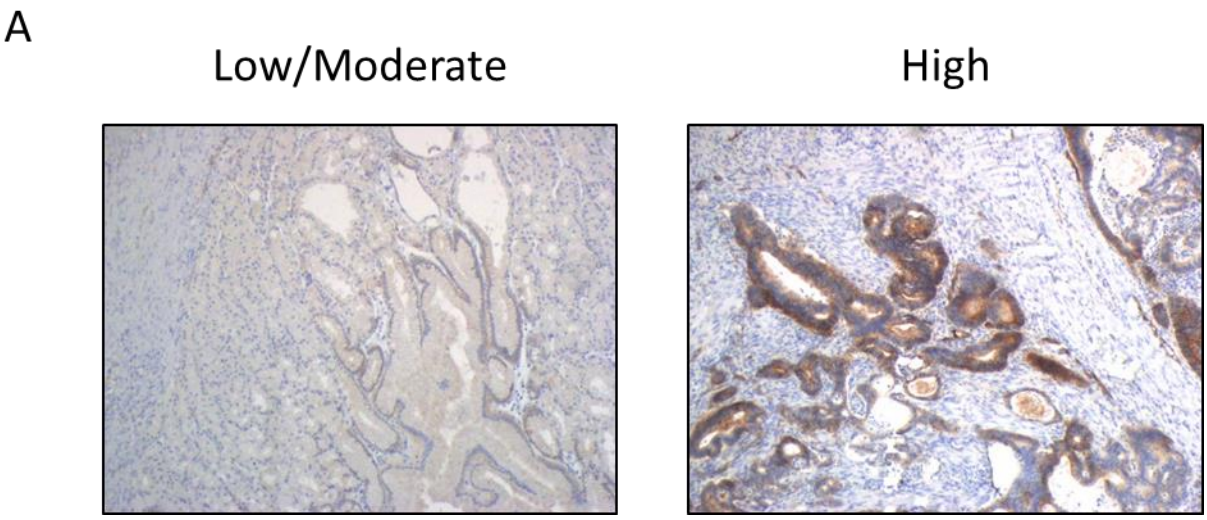

Figure 6.10: EphB4 immunohistochemical staining in gastro-oesophageal cancer. *EphB4 immunohistochemistry (IHC) was performed on 4µm full-face sections across a series of gastro-oesophageal cancers totalling 11 primary tumour cases. Membranous EphB4 expression was scored 0, 1+, 2+, 3+ based on completeness and intensity of staining with each score given % for each section. JAM-A results were scored in conjunction with a histopathologist.*

Sections were scored in the same way previously described for JAM-A IHC, with either no (0) weak and incomplete (1+), weak and complete (2+), or strong and complete (3+) staining being categorised into either Low/Moderate (0-2+) or High (3+) EphB4 staining. Scores were then correlated with the limited clinicopathological data available for the cohort.

As illustrated in **Table 6.2,** no significant correlations were noted between EphB4 staining and T or N staging, differentiation, Lauren classification or tumour location. Intriguingly, however, each case correlated identically with JAM-A expression for both low/moderate and high scoring cases. While this may be a coincidental upregulation of aggressive tumour-promoting proteins with no direct causation, the 100% overlap was nonetheless interesting. Furthermore, as had been demonstrated with the JAM-A expression, EphB4 staining also correlated significantly with HER2 positivity in this small 11-patient cohort.

Table 6.2: EphB4 expression correlated with JAM-A expression and HER2 positivity in gastro-oesophageal cancer. *Full-face sections of gastro-oesophageal cancer patients (n=11) were stratified based on either High or Low/Moderate EphB4 expression. Statistical analysis was* ^{2} *test comparing EphB4 expression with clinicopathological parameters on SPSS version 24 software. Comparisons were considered significant at* $p<0.05$.

± l· NJ ƛ l· ō f Ŝ	b	l ƛ ∃ K	[ƨ ø к a ƨ Ř	t- ± l· f
¢ { ű l· ∃ Ŝ	м			л Ф
м	м	л		
н	л	л		
с	о	п		
г	м	н		
b- { ű l· ∃ Ŝ	м			л Ф
л	о	н		
м	м	м		
н	л	о		
с	м	л		
5 ƛ Ŧ Ŧ Ŝ NJ Ŝ ƴ ű ƛ l· ű ƛ	м			л Ф
l ƛ	м	о		
a ƨ Ř Ŝ N	м	л		
[ƨ	о	о		
[l· dz NJ Ŝ ƴ / f l· ă ă ƛ	м			л Ф
L ƴ ű Ŝ	н	о		
5 ƛ Ŧ	н	н		
a ƛ È	л	м		
[ƨ Ŏ l· ű ƛ ƨ ƴ	м			лФ л
h D Wdz ƴ Ŏ ű ƛ ƨ ƴ ь	л	п		
D l· ă ű NJ	н	л		
D l· ă ű NJ ƛ Ŏ . ƨ Ř è	м	л		
h D Wdz	м	л		
h D Wdz ƴ Ŏ ű ƛ ƨ	л	м		
D l· ă ű NJ ƛ	л	м		
D l· ă ű NJ ƛ	м	л		
l 9 w н t ƨ ă ƛ ű ƛ Ø ƛ	м			Ғ Ғ л
b Ŝ ∃ l·	л	p		
t ƨ ă	p	м		
				Ғ Ғ Ғ
W ! -ȡ 9 È LJ NJ Ŝ ă ă ƛ ƨ	м			м
l ƛ	p	л		
[ƨ ø к a ƨ	л	с		
W ! -ȡ ȝ 9 LJ Ƙ . п 9 È LJ NJ Ŝ ă -ă н ƛ ь ƨ ƴ Ƴ Ƴ ƛ ∃ [Ƙ ƨ ø Ґ к a o ƨ ь Ř Ŝ NJ				
l 9 w н t ƨ ă ƛ ű ƛ Ø Ŝ L l / o ь Σ h D Ґ h Ŝ ă ƨ LJ Ƙ l· ∃				

We next extracted the significantly correlated data sets and conducted further analysis using Fisher's exact test (**Figure 6.11**). In support of **Table 6.2**, JAM-A and EphB4 expression correlated significantly with each other (**Figure 6.11;** $p<0.01$); suggesting a possible mirrored response in gastro-oesophageal cancers to the emerging relationship our group has noted in breast cancer cells. Furthermore, significant correlations were highlighted between HER2 positivity and EphB4 expression **(Figure 6.11;** $p<0.05$**)**.

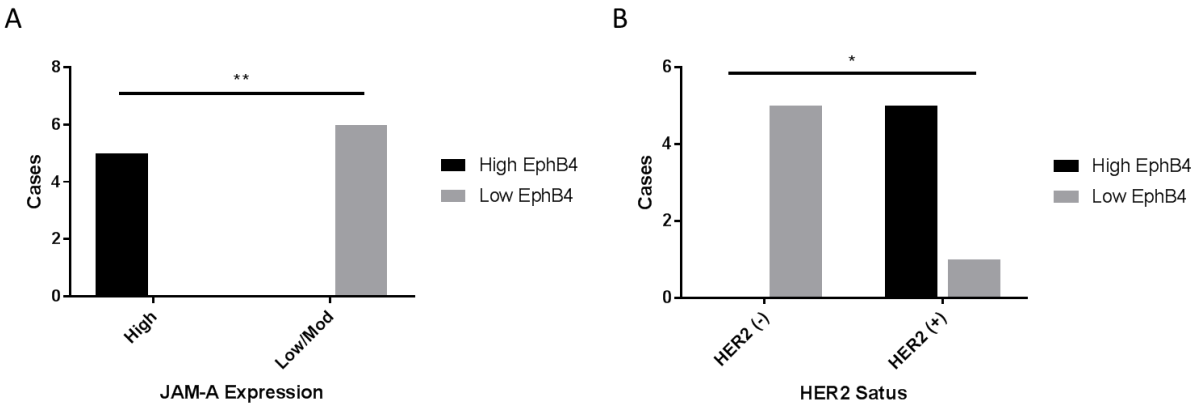

Figure 6.11: High EphB4 expression in gastro-oesophageal cancers correlates with JAM-A and HER2 expression. *Gastro-oesophageal cancer full-face sections (n=11) were stained for EphB4 expression. The association between EphB4 expression and clinicopathological variables was determined by χ^2 testing. Asymptotic significant correlations were further tested by Fisher's exact test. Association between EphB4 expression and JAM-A expression **(A)**, and between EphB4 and HER2 positivity **(B).** Statistical significance *p<0.05 **p<0.01*

6.3.8 JAM-A increases EphB4 mRNA expression

In an attempt to establish whether this correlation was directly related to JAM-A expression levels, we silenced JAM-A as previously described and assessed downstream consequences for EphB4 expression in gastro-oesophageal cancer cell lines. Surprisingly, we did not see results that supported our earlier work in tissues for gastro-oesophageal cancer patients **(Figure 6.12)**. There were no significant changes to EphB4 mRNA expression following JAM-A reductions.

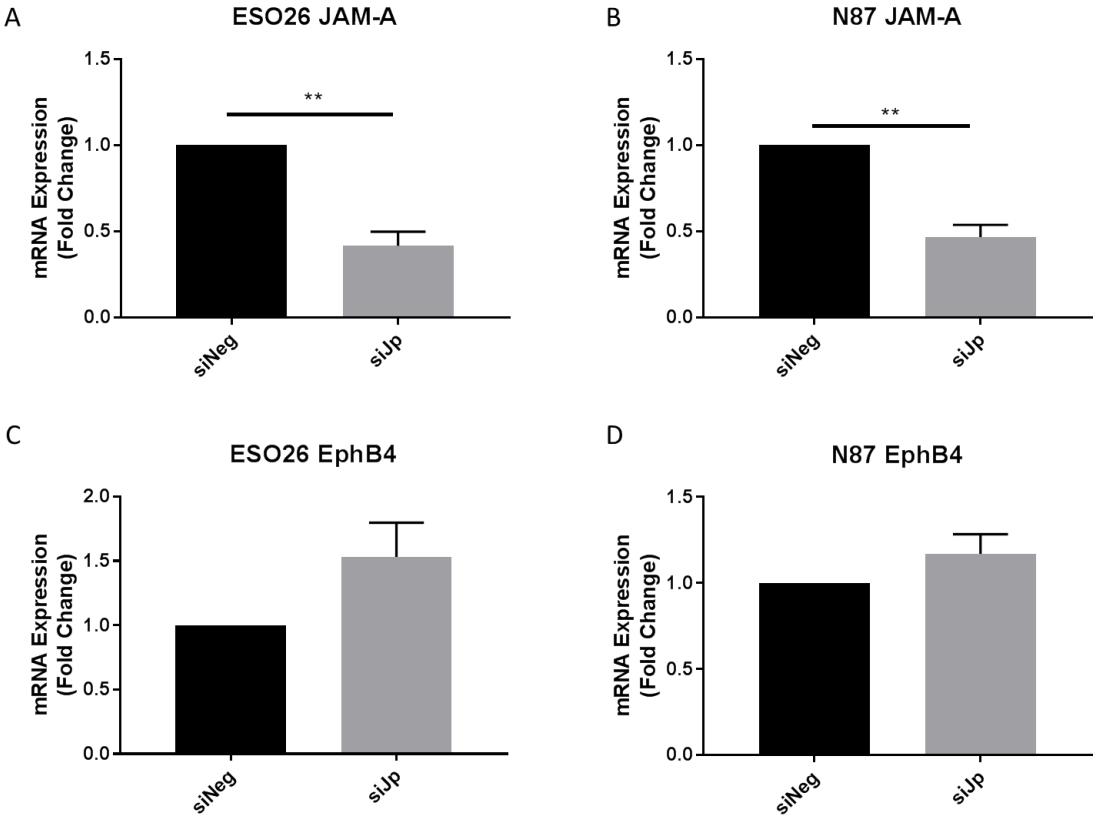

Figure 6.12 JAM-A silencing does not significantly alter EphB4 mRNA expression. *Gastro-oesophageal cancer cell lines were plated at 2x10^5 cells/well n 6-well plates. Following one doubling period, cells were transiently transfected for 96h with either control, non-targeting siRNA (siNeg) or a pool of siRNA targeting JAM-A (siJp) siRNA. Quantitative real time PCR was then performed as follows: ESO26* ***(A,C)****, N87* ***(B,D)****. Ct values of samples were set relative to matched Ct values of the housekeeping gene RPLP0. Data from three independent experiments are shown (displayed as mean ± SEM), and unpaired, two-tailed Student's t-tests were used to test for statistical significance. (*p<0.05, **p<0.01, ***p<0.001).*

6.4 Discussion

RTKs have been shown to play key roles in tumorigenesis (243). In breast cancer models, our group has uncovered an emerging regulatory role for the tight junction protein JAM-A, where its loss or increase can correspondingly impact several proteins including those belonging to the HER and Eph receptor families, via both transcriptional and post-translational mechanisms. Since targeting JAM-A has shown promising efficacy *in vivo* (Yvonne Smith, personal communication), JAM-A could offer a potential alternative target in cancers overexpressing downstream regulated RTKs.

JAM-A has been shown to play varying roles in different cancer settings and has been reported as varying within cancer types themselves (122, 124-128, 131, 133). However, the clinical significance of JAM-A in gastro-oesophageal cancers remains unclear. The work in this chapter centred on the hypothesis that the controversial role of JAM-A in gastro-oesophageal cancers may reflect its ability to regulate oncogenic signalling through downstream effects on various RTKs. Expression of JAM-A in gastro-oesophageal tumours was first examined in a cohort of 144 patients, post treatment analysed by Hedner et al.(251). Tissue microarrays are commonly utilised for establishing molecular profiling of potential or known markers in various cancers (269, 270) (271). We hypothesised that high expression of JAM-A in these cases would correlate with HER3 positivity, however the results in a small subset of the cohort suggested the opposite. Our method for assessing JAM-A expression across the TMA was robust, and all scoring was moderated by a clinical histopathologist. However, since JAM-A expression appears to be heterogeneous in nature, it is possible that a TMA did not appropriately capture all the relevant information in order to effectively establish JAM-A expressional profiles across these cases. Therefore, we suggest that going forward, full-face sections, although more costly and labour-intensive, would assure researchers are provided with accurate representations of tumours, so that sound clinical significance could be generated. Another method that might offer insight into protein expression in heterogeneous proteins is reverse

phase protein arrays (RPPA) analysis, which can examine at total overall protein expression in patient tumours which have been flash-frozen on removal (271).

Nonetheless, the TMA revealed a potential correlation between high JAM-A expression and higher patient age (over 65 years old). Interestingly, it is already known that age-related disruption to epithelial barriers is common occurrence, with research showing regular aberrant expressional changes to tight junction proteins across the gastrointestinal tract (272-274), and hence the correlation with JAM-A overexpression in older patients may reflect a natural aging process occurring irrespective of cancer development. In contrast, work in breast cancer models had demonstrated the opposite, with JAM-A overexpression more likely to occur in younger breast cancer patients (100, 131). We hypothesise that these differences may reflect the physiological role of JAM-A in the specific tissues and hence, basal levels across tissues and cohorts of patients should be considered.

Since a linear regulation pathway involving JAM-A, FOXA1, β-catenin and HER3 had been established *in vitro* and in patient tissues of breast cancer patients (Rodrigo Cruz, personal communication), we wanted to investigate whether JAM-A silencing could influence HER3 in the same manner in gastro-oesophageal cancer cell lines. The evidence presented in this chapter showed no significant decreases to HER3 protein or mRNA expression following JAM-A silencing. However there was a trend that JAM-A silencing *increased* HER3 expression, mirroring previous chapters in which JAM-A silencing induced increased HER2 expressions. Since JAM-A appears to impact diverse protein pathways in this cancer setting, we suggest that the increases to HER3 may be as a result of JAM-A loss from the cells and compensatory mechanisms activating to ensure cell survival. Another possible explanation is that JAM-A expression maintains tightly regulated homeostasis in gastro-oesophageal cancers and, depending on the cancer s
scale' towards oncogenesis through JAM-A. Either way, it appears as though JAM-A is critical for maintaining cellular homeostasis; and hence targeting it in as a

regulator of HER protein family members may cause more harm than benefit to gastro-oesophageal cancer patients.

Transcription regulation/dysregulation is an important mechanism in driving pathogenesis, and targeting transcriptional factors activating oncogenes has offered promising therapeutic potential (275, 276). FOXA1, a transcription factor with many known gene targets, changed in parallel with expression changes in JAM-A in unpublished breast cancer work (Rodrigo Cruz, personal communication). Furthermore, reductions in either JAM-A and FOXA1 induced downstream reductions in HER3 mRNA and protein levels. We hypothesised that JAM-A may regulate FOXA1, and that phenotypical changes discussed previously in this thesis were as a result of losses to an important transcription factor. However, the results demonstrated that this was not the case, and in fact JAM-A silencing significantly *increased* FOXA1 expression in one of the gastro-oesophageal cancer cell lines. At this juncture it is important to note that JAM-A-silencing also capable of influencing the expression of classic housekeeping or cytoskeletal proteins. Since both protein and mRNA samples were analysed pre-assessment via either BCA or Nanodrop (respectively) to ensure equal loading, we expected to see equivalent loading of our loading controls (Actin or RPLP0). During qRT-PCR, siJp samples had consistently higher raw Ct values. This suggests that JAM-A silencing may actually decrease a myriad of genes and, if the housekeeping gene RPLP0 was impacted by JAM-A reductions, the results may not reflect the true expressional levels of genes in those samples. Given that we observed potential changes to HER2 localisation in gastro-oesophageal cells (Chapter 5) and suggested that this may be due to cytoskeletal changes, it may be worth future exploration to test whether JAM-A reduces cytoskeletal protein expression in some cell lines. Firstly, this would support our theory that JAM-A maintains tightly regulated homeostasis of cells in gastro-oesophageal cancer cells. Secondly, if JAM-A truly impacts the expression of cytoskeletal proteins, this may offer insight into the why JAM-A removal induces a possible apoptotic priming across all cell lines tested (Chapter 5).

In parallel, a pilot study of 11 gastric cancer patients (previously described for JAM-A/HER2 correlations), was utilised to assess whether JAM-A expression correlated with that of another RTK, EphB4, recently reported to associate with worsened survival and risk of progression in gastro-oesophageal cancers (268). Since the upregulation of EphB4 remained unclear in this setting and our group had previously highlighted JAM-A as a potential regulator of this RTK in breast cancer settings, we hypothesised that JAM-A may be responsible for EphB4 stabilisation, driving the associated pathogenesis. Correlation of JAM-A and EphB4 staining was significantly evident in the 11 gastro-oesophageal cancer cases. The use of full face sections ensured that JAM-A had been accurately scored across a larger field compared to the TMA scoring of JAM-A discussed previously (Chapter 5).We developed a novel weighted ranking system for scoring JAM-A expression. When we correlated JAM-A expression with EphB4 expression, cases correlated perfectly for Low/Moderate JAM-A and EphB4 or High JAM-A and EphB4 expression. Given the limitations of the size of this cohort, expanding this would prove extremely beneficial, especially since this work has established an effective, working grading system for heterogeneous JAM-A expression in gastro-oesophageal cancers.

JAM-A silencing was also utilised to examine whether any direct regulation between JAM-A and EphB4 could be demonstrated *in vitro.* However EphB4 appeared to be *upregulated* following reductions in JAM-A levels. Since correlation of EphB4 and JAM-A in gastric cancer tissues may represent an aggressive tumour type, and mRNA changes were not correlated to the evidence presented in tissue, we suggest that JAM-A may not confer direct regulation in this setting. It is possible that both proteins are present in aggressive tumours, and that the paired correlation is coincidental rather than causative. To validate this, we suggest future work of a larger cohort of full faced sections from gastro-oesophageal cancer patients, as well as supportive RPPA data.

Taken together, it appears that the regulatory role for RTKs by JAM-A established in breast cancer models does not seem to occur in gastro-

oesophageal cancer models. However, JAM-A may still play an important role in maintaining cellular homeostasis since loss of JAM-A induced inconsistent downstream alterations to RTKs and cytoskeletal proteins.

Chapter 7 General Discussion

Gastro-oesophageal cancers remain associated with poor survival in the western world (36, 37, 44, 45). While a multipronged approach is often taken towards treatment, late-stage diagnosis often requires radical interventions and mortality remains clinically challenging (63, 65-68). Both gastric and oesophageal cancers are heterogeneous in nature, with very few common mutations that can be pharmacologically targeted (277, 278). Furthermore, given the late stage of diagnosis, patients often have locally advanced or metastatic disease by the time they receive their diagnosis (279, 280). Hence, new universal therapies with broad specificities would be valuable in improving survival rates.

Given the 'difficult-to-treat' nature of gastro-oesophageal cancers, this thesis first tested the efficacy of a novel natural compound in gastro-oesophageal cancer cell models (Chapter 3). Promisingly, the IC_{50} for Crassin in viability assays across several gastro-oesophageal cancer cell lines was found to be in the low micromolar range. Furthermore, Crassin reduced colony-forming potential in all cell lines tested; a surrogate for clonogenic ability (281) and therefore a positive indicator that Crassin may merit investigation for its capacity to prevent tumour development *in vivo.*

As a first step towards that goal, and in an effort to translate this work into a clinically relevant model, we tested the efficacy of Crassin in an *in ovo* / semi-*in vivo* chick embryo xenograft model. This model, which uses the chicken egg chorioallantoic membrane (CAM) as a host site for tumour xenograft development, is emerging as an extremely useful pre-clinical tool in cancer therapeutics. Several publications have reported that tumour establishment and invasion can be measured accurately between control and treated groups (172, 187); and that the model is ideally suited for the study of novel therapeutics in cancer research (187). Furthermore, CAM models are now showing promise as models for patient derived xenograft (PDX) studies (282). Utilising the chick embryo model, we were able to highlight the ability of Crassin to effectively inhibit tumour establishment of gastro-oesophageal cancer cells. However, given a limited number of replicates in our study, we

suggest expanding the scale in addition to using higher *in vivo* models to bring Crassin further along the regulatory pathway in this setting.

A further indication of the potential of Crassin as a novel cancer therapeutic was highlighted in a recent publication arising directly from this thesis (205), where Crassin induced cytostasis in triple-negative breast cancer (TNBC) cell models. Like gastro-oesophageal cancers, TNBC are notoriously difficult to treat', since they lack markers (26, 27). Crassin exerted ROS-dependent cytostatic reductions in metabolism and proliferation in a panel of TNBC cell lines. Interestingly, we showed cells shifted from G1 to G2/M, which was indicative of induced senescence in treated cells. Protein expression analysis revealed increases in the cell survival proteins pAKT and pERK, which were inhibited in the presence of an antioxidant. Furthermore, Crassin synergised with a common chemotherapeutic drug, Doxorubicin to reduce TNBC cell viability (205). Since current therapies are often accompanied by undesirable toxic side effects (141-143), it is exciting to speculate that co-administration of natural compounds like Crassin may in the future have potential in reducing the doses of highly-toxic conventional chemotherapies. In summary, we have highlighted promising *in vitro* and semi-*in vivo* efficacy of Crassin in targeting cancer cell proliferation and survival, and suggest that this novel natural compound warrants further investigation to explore the therapeutic efficacy of Crassin in higher *in vivo* models. There is already excellent precedent for using compounds of the diterpenoid chemical class, based on the success of Taxol as a chemotherapeutic drug (283-285). Crassin holds considerable potential as a platform for the popularly-coined "one-two punch" strategy, described in both patients, two pronged approach, one to induce senescence and the other to eradicate senescent cells, increasing patient responsiveness to therapies (286-288).

While treatment options are limited in gastro-oesophageal cancers, a few common mutations have nonetheless been established. These include E-cadherin and HER family members (289-291). E-cadherin is an adherens junction protein that regulates migration and differentiation of epithelial cells (292). Loss of E-cadherin is considered to be a hallmark for epithelial

mesenchymal transition (EMT) (293), and its aberrant expression has been associated with aggressive phenotypes in gastric cancers, including increased migration and association with advanced stages of the disease (290, 291). E-cadherin offers insight into how adhesion molecules can play important roles in maintaining homeostasis and hence, and accordingly how their dysregulation may contribute to the pathogenesis of cancer progression. Our group and others have also shown the importance of adhesion protein regulation in the breast cancer setting (100, 111, 125, 126, 131, 133, 206, 208, 294, 295), but there is accumulating evidence that adhesion proteins play key roles in many other cancers too (reviewed by Leech et al) (106).

The adhesion protein of most interest in our group has been Junctional Adhesion Molecule-A (JAM-A), a protein found at epithelial and endothelial tight junctions which plays important physiological roles in cell polarity and migration (121). In pathophysiological contexts, however, JAM-A has been found to be overexpressed in breast cancers and to increase cell proliferation and migration (131, 206). However, the role of JAM-A in gastro-oesophageal cancers is unclear, with contradictory results surrounding the aberrant expression of JAM-A in this setting (122, 127). In Chapter 4 we highlighted high JAM-A expression in gastro-oesophageal cancers in a small, commercially available tissue microarray. Furthermore, using an online tool (140) we demonstrated an association between high JAM-A gene expression and poor survival in gastric cancer patients. Having established gastro-oesophageal cancer cell line models suitable for the study of JAM-A expression in this setting, we then observed differential outcomes of JAM-A silencing across gastro-oesophageal cancer cells *in vitro.* Reductions to JAM-A expression impaired cell viability and colony-forming ability in two gastro-oesophageal cell lines; whereas both cell viability and colony-forming ability were paradoxically *increased* in another cell line. Furthermore, overexpression of JAM-A in the same cell lines had no impact on either proliferation or colony forming abilites. Interestingly, we demonstrated in later chapters that JAM-A silencing elicited an apoptotic 'primed' state across all their initial response to JAM-A silencing. Thus it is possible that, in this

instance, loss of JAM-A reduces the stabilisation of cellular homeostasis and increases gastro-oesophageal susceptibility to apoptosis. This was an important finding, as it suggests that JAM-A targeting, in combination with apoptosis-inducing chemotherapeutics, may warrant further investigation for its potential to offer clinical benefit across all gastro-oesophageal cancers.

We also set out to study the tumour growth and invasion of gastro-oesophageal cells in a more clinically relevant model. While JAM-A silencing across xenografts from the *in ovo* chick embryo model elicited extremely heterogeneous JAM-A expressional reductions, it is extremely promising that we have made some progress in reducing JAM-A levels in an emerging (and valuable) model. However, we saw no reduction to the invasive nature of xenograft tumours compared to control treated (siNeg) tumours in the focal regions where there was real evidence of JAM-A loss. As discussed previously (Chapter 4), it is conceivable that a threshold level of JAM-A may be crucial for the transition between physiological and pathophysiological functions of JAM-A; with JAM-A in effect performing as This would suggest that neither loss nor overexpression singularly define the role of JAM-A in gastro-oesophageal cancers. Instead, JAM-A aberrant expression should be considered as oncogenic, and defining the regulatory points of the 'molecular switch' could in this cancer setting. Of course, it is also possible that JAM-A can exert either oncogenic or tumour suppressive functions depending on the tissue of origin, like many other proteins that have been so-established (296). However, given the role mentioned in this thesis and in other cancer research (100, 125, 127) for JAM-A in restraining apoptosis, we would suggest that JAM-A has oncogenic properties and that an expressional threshold scenario appears more likely.

Cancers in gastro-oesophageal locations are associated with a very high risk of thrombosis and other clotting issues in patients; in fact being reported as carrying the highest risk for both deep vein thrombosis (DVT) and pulmonary embolism (PE) (297). Gastro-related cancers were shown to have increased rates of thromboembolic events of ~9% compared to ~3% in non-gastro-

related cancers (298). Interestingly, cleaved JAM-A (cJAM-A) is associated with cardiovascular disease and hypertension, with higher circulating levels in serum of patients (210, 212). It is tempting to speculate that higher expression levels of JAM-A in gastro-oesophageal patients may translate into increased circulating levels of cJAM-A, and an increased risk of thromboembolic events. We recently reviewed the role of cJAM-A in HER2 therapy resistance in breast cancers and suggested correlations between cJAM-A in cancer and cardiovascular disease (299). In Chapter Four, recombinant cJAM-A (rcJAM-A) was demonstrated to have little effect on gastro-oesophageal cell viability *in vitro*. Surprisingly however we observed that rcJAM-A reduced clonogenic potential of the same cell lines. It is possible that, in this *in vitro* setting, cJAM-A confers no advantage to cancer cells survival and perhaps that rcJAM-A was even toxic to gastro-oesophageal cells. We propose that testing of cJAM-A in an *in vivo* model, while monitoring angiogenic properties and clotting factors, would be a valuable approach. Furthermore, studying the serum of gastro-oesophageal patients who have suffered DVT or PE might offer valuable insight into whether this cJAM-A protein acts as a novel biomarker for patients at risk of cardio-associated events.

Previous work in our lab has placed both JAM-A and cJAM-A as players in the regulation of HER2 expression and in resistance to HER2-targeted therapies (100, 208). Given that JAM-A is an easily accessible cell surface target expressed at increased levels in gastro-oesophageal cancers, there may be potential for JAM-A targeting in gastro-oesophageal cancers. Hence, we sought to define whether JAM-A could offer an alternative target in HER2-overexpressing gastro-oesophageal cancers, particularly those which have developed resistance to HER2-targeted therapies (70, 227, 247, 300, 301). Using gastro-oesophageal cell lines, we reduced or increased JAM-A expressional levels and examined their impact on HER2 expression. However, there was great variability between both biological replicates and across cell lines; and in some instances JAM-A silencing even *increased* HER2 expression. The lack of consistency in these cases suggested that JAM-A

may not be directly regulating HER2 as had been previously described in breast cancer cell lines (100).

Given the discrepancies, we sought to visualise the localisation of HER2 on cellular membranes following JAM-A silencing. Interestingly, we noted disruption to HER2 staining, which appeared fragmented and punctate across gastro-oesophageal cancer cells when JAM-A was reduced. Initially, we believed that this represented a possible mechanism for JAM-A stabilisation of HER2, where JAM-A loss increased HER2 recycling. However, given previously-highlighted issues around aberrant expression of even cytoskeletal and other housekeeping proteins in gastro-oesophageal cancer cells following JAM-A silencing (Chapters 4, 5, 6), it is possible that the disruption to HER2 results from disrupted cellular structures. Notably, JAM-A has previously been shown to disrupt the cytoskeleton of epithelial cells other than gastro-oesophageal (302), and hence could play a similar a role here. Targeting both JAM-A and HER2 in parallel may therefore induce cytoskeletal disruption and induce apoptotic priming in a manner that would enhance HER2 therapy efficacy. This would offer the potential for a (sim288) style of treatment for gastro-oesophageal cancers.

In the consideration of any new therapy regimens, there needs to be a method for clinically assessing patients who would benefit. IHC for JAM-A could provide this opportunity. Histological correlation is often utilised to establish patterns of overexpression or loss in cancer patients (303, 304). We utilised both tissue microarray (TMA) and full face tissue sections from gastro-oesophageal cancer patients, and searched for correlations between JAM-A and HER2 expression. While the TMA represented a larger cohort, significant variation in JAM-A staining was observed between duplicate cores of the same cases which negated the possibility of uncovering an expressional correlation between JAM-A and HER2. Given the extremely heterogeneous nature of JAM-A expression in these tissues, we postulated that small TMA cores were insufficient to meaningfully study JAM-A expressional patterns in this complex setting. A small pilot-study of gastro-oesophageal cancer full face sections supported this postulate. JAM-A staining was extremely

heterogeneous and, with the help of a clinical histopathologist, we developed a novel, weighted ranking system which accurately captured the expression levels of JAM-A across all cases. Interestingly, the small study revealed a correlation between JAM-A and HER2 protein expression. Since we saw large variability in HER2 expression following JAM-A modulation (Chapter 5), it is possible that JAM-A and HER2 co-expression is indicative of an aggressive tumour type rather than being evidence of a linear regulatory pathway. However, a larger cohort of full face sections with known HER2 status, stained for JAM-A expression and assessed using the established weighted ranking system, would be important in future studies to conclude whether JAM-A overexpression is correlated with HER2 positivity.

Our group has previously highlighted a linear mechanism of regulation by JAM-A of other receptor tyrosine kinases (RTKs) in breast cancer cell line models (Rodrigo Cruz, Sri Vellanki, personal communications). Hence, in Chapter Six we sought to determine whether a similar regulatory role for JAM-A existed in gastro-oesophageal cancers. Previous work in our laboratory has highlighted how JAM-A loss alters the location of β-catenin within cells, reducing its capacity to travel to the nucleus and switch on FOXA1 expression, in turn reducing levels of HER3. Since HER3 has been placed at the centre of acquired resistance to HER2-targeted therapies (248, 255, 261, 262), it seemed conceivable that if JAM-A were to regulate HER3 in gastro-oesophageal settings it may offer a novel target for therapy-resistant patients. We examined the levels of both HER3 and FOXA1 in gastro-oesophageal cancer cell lines following JAM-A silencing. JAM-A expression reductions had a similarly-variable influence on both HER3 and FOXA1 expression that was previously noted for HER2 following JAM-A silencing. Furthermore, analysis of JAM-A expression in a TMA revealed no correlation with HER3 expression in this setting. Of course, the same limitation of JAM-A expression across very small TMA cores still remains, given that gastro-oesophageal tumours tend to be large and very variable. However, given the lack of an unequivocal response across many *in vitro* datasets, we conclude that JAM-A is unlikely to regulate HER3 expression in this setting.

Since the regulation of HER family members by JAM-A appeared unlikely in gastro-oesophageal cell lines, we examined whether JAM-A had the ability to regulate non-HER RTKs. Previous work by our group has uncovered a potential mechanism of JAM-A-dependent regulation of EphB4 in breast cancer cell lines (Sri Vellanki, personal communication). Since EphB4 has recently been shown to associate with unfavourable outcomes for gastric cancer patients (268), we tested to see whether any correlation between JAM-A and EphB4 was evident across our small cohort of gastro-oesophageal cancer full faced tissue sections. Surprisingly, we saw a complete positive correlation between cases. However, when we examined whether JAM-A had the ability to regulate EphB4 *in vitro*, JAM-A silencing in fact *increased* EphB4 mRNA levels. Since both JAM-A and EphB4 appear to associate with aggressive gastro-oesophageal cases, as shown through available gene datasets (www.kmplot.com) (140), we believe that the correlation in tissues may represent a coincidental co-expression demonstrating aggressive tumour behaviour, rather than an indication of direct JAM-A regulation of EphB4 in this setting.

To summarize, this body of work has highlighted two potential mechanisms of 'one-two punch' therapeutic cancers: (1) Gas1 as a senescence inducer and (2) JAM-A antagonists as an 'a **(Figure 7.1)**. We suggest that, while JAM-A may offer some promise in priming apoptotic cells in gastro-oesophageal cancers, its it does not play the same regulatory role demonstrated in breast cancer models. Specifically, RTKs known to be regulated by JAM-A in breast cancer models were unaffected by JAM-A loss or overexpression in gastro-oesophageal models. However, the ability of JAM-A loss to prime cells for apoptosis appears to supersede the oncogenic or tumour suppressive basal role of JAM-A in cell lines; and hence may offer a novel target in gastro-oesophageal cancers when considered in the scope of 'multiple hit

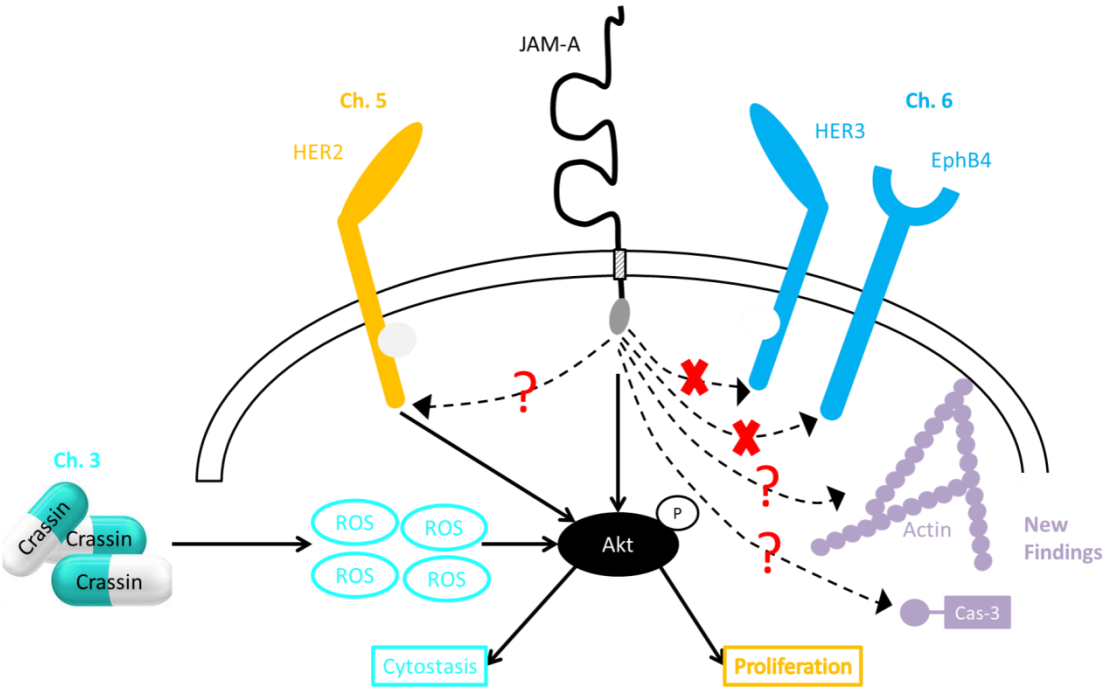

Figure 7.1 Summary of thesis. *Crassin treatments induce ROS, which in turn increase pAkt, driving cytostasis in cancer cells. JAM-A was shown to correlate with HER2 expression in full-face sections and the relationship requires further elucidation. JAM-A was shown not to regulate RTKs HER3 and EphB4 in gastro-oesophageal cancers in vitro. JAM-A has been highlighted as potentially destabilising cells through potential cytoskeleton disruption and JAM-A protein reductions via siRNA silencing prime cells to undergo apoptosis.*

Chapter 8 Future Works

Since the work presented here was sometimes limited in scale by both samples and resources, there are several suggestions for continued investigation of both Crassin treatment and JAM-A in gastro-oesophageal cancers.

1) Expand Crassin treatment study into a larger scale, higher *in vivo* model and test both the efficacy and toxicity of Crassin treatment in other cancer types.
2) Establish both CRISPR-Cas9 JAM-A-silenced and JAM-A-overexpressed stably expressing JAM-A cell lines to:
    a. Uncover effects, if any, on protein and mRNA levels of RTKs
    b. Examine the morphology of cells to elucidate any structural changes following JAM-A modulation.
    c. Uncover any protein and mRNA expressional changes of both cytoskeletal and ribosomal proteins.
3) Since JAM-A heterogeneity was an issue across TMAs, we suggest using a larger cohort of full-face sections to correlate JAM-A expression with RTKs, specifically HER2, HER3 and EphB4. We also suggest utilising the novel weighted ranking system for JAM-A expression (Chapter 5) as a method for all future scoring of JAM-A staining in gastro-oesophageal tissues.
4) To complement the larger tissue study, we suggest using RPPA analysis of JAM-A expression from patients with known HER2 status. This will help elucidate whether any correlation between JAM-A and HER2 exists.
5) Can JAM-A expression reductions prime cells to undergo apoptosis *in vivo*? We suggest targeting JAM-A expression in gastro-oesophageal cells with JAM-A inhibitors (such as small peptide inhibitor developed by our group, termed JBS2) and miRNA miR-145, in combination with apoptotic inducing chemotherapies (i.e Doxorubicin) in *in vivo* models. This would highlight whether JAM-A reductions can increase the efficacy of chemotherapy treatments against tumours.
6) Can JAM-A expressional reductions re-sensitise gastro-oesophageal cells resistant to HER2-targeted therapies? As above, we suggest testing

whether JAM-A expression reductions in combination with HER2-targeted therapies (Trastuzumab or Pertuzumab and Lapatinib) has the ability to re-sensitise gastro-oesophageal cancer cell lines induced to become conditionally resistant to HER2-targeted therapies.

7) Finally, can cJAM-A foster invasive behaviour of gastro-oesophageal cancers *in vivo*? We hypothesise that cJAM-A may play a role in driving invasion *in vivo*, which does not occur *in vitro*. Hence, we suggest a two-pronged approach to study cJAM-A *in vivo* in gastro-oesophageal cancer settings
    a. Since ADAM-10/-17 are responsible for JAM-A cleavage, their inhibition (with consequent reductions to cJAM-A) may offer insight into the role of cJAM-A in tumour invasion. Using ADAM-10/-17 inhibitors as treatments in *in vivo* tumour invasion models should be analysed.
    b. rcJAM-A treatments given *in vivo* could help elucidate whether cJAM-A plays a role in priming metastatic niches *in vivo.* Tumour invasion and angiogenic properties should then be assessed.

Further delineation of the different spatiotemporal roles of JAM-A is crucial in our understanding of this pathophysiology. This thesis has merely scratched the surface - there remains much to be elucidated in this complex and fascinating field.

Bibliography

1. Hassanpour SH, Dehghani M. Review of cancer from perspective of molecular. Journal of Cancer Research and Practice. 2017;4(4):127-9.

2. Hanahan D, Weinberg RA. Hallmarks of cancer: the next generation. Cell. 2011;144(5):646-74.

3. Vineis P, Fecht D. Environment, cancer and inequalities-The urgent need for prevention. Eur J Cancer. 2018.

4. Lee EY, Muller WJ. Oncogenes and tumor suppressor genes. Cold Spring Harb Perspect Biol. 2010;2(10):a003236.

5. Luo J, Solimini NL, Elledge SJ. Principles of cancer therapy: oncogene and non-oncogene addiction. Cell. 2009;136(5):823-37.

6. Lodish H, Berk A, Zipursky S. Molecular Cell Biology. 4th ed. New York: W. H. Freeman; 2000.

7. Michor F, Iwasa Y, Nowak MA. Dynamics of cancer progression. Nat Rev Cancer. 2004;4(3):197-205.

8. Webber C, Gospodarowicz M, Sobin LH, Wittekind C, Greene FL, Mason MD, et al. Improving the TNM classification: findings from a 10-year continuous literature review. Int J Cancer. 2014;135(2):371-8.

9. Ludwig JA, Weinstein JN. Biomarkers in cancer staging, prognosis and treatment selection. Nat Rev Cancer. 2005;5(11):845-56.

10. Elston CW, Ellis IO. Pathological prognostic factors in breast cancer. I. The value of histological grade in breast cancer: experience from a large study with long-term follow-up. Histopathology. 1991;19(5):403-10.

11. Carriaga MT, Henson DE. The histologic grading of cancer. Cancer. 1995;75(1 Suppl):406-21.

12. Christgen M, Langer F, Kreipe H. [Histological grading of breast cancer]. Pathologe. 2016;37(4):328-36.

13. Institute NC. Cancer Staging 2015 [Available from: https://www.cancer.gov/about-cancer/diagnosis-staging/staging.

14. NCRI. Cancer Factsheet. National Cancer Regsitry Ireland; 2016 29th April 2016.

15. Ireland NCR. Cancer Factsheet Female Breast: NCRI; 2018 [Available from: https://www.ncri.ie/sites/ncri/files/factsheets/Factsheet%20Female%20breast.pdf.

16. Kalager M, Haldorsen T, Bretthauer M, Hoff G, Thoresen SO, Adami HO. Improved breast cancer survival following introduction of an organized mammography screening program among both screened and unscreened women: a population-based cohort study. Breast cancer research : BCR. 2009;11(4):R44.

17. DeSantis CE, Lin CC, Mariotto AB, Siegel RL, Stein KD, Kramer JL, et al. Cancer treatment and survivorship statistics, 2014. CA: a cancer journal for clinicians. 2014;64(4):252-71.

18. Zucca-Matthes G, Urban C, Vallejo A. Anatomy of the nipple and breast ducts. Gland Surg. 2016;5(1):32-6.

19. Fu D, Zuo Q, Huang Q, Su L, Ring HZ, Ring BZ. Molecular Classification of Lobular Carcinoma of the Breast. Scientific reports. 2017;7:43265.

20. Yu X, Zhu W, Di Y, Gu J, Guo Z, Li H, et al. Triple-functional albumin-based nanoparticles for combined chemotherapy and photodynamic therapy of pancreatic cancer with lymphatic metastases. International journal of nanomedicine. 2017;12:6771-85.

21. Cheang MC, Chia SK, Voduc D, Gao D, Leung S, Snider J, et al. Ki67 index, HER2 status, and prognosis of patients with luminal B breast cancer. Journal of the National Cancer Institute. 2009;101(10):736-50.

22. Tran B, Bedard PL. Luminal-B breast cancer and novel therapeutic targets. Breast cancer research : BCR. 2011;13(6):221.

23. Slamon DJ, Leyland-Jones B, Shak S, Fuchs H, Paton V, Bajamonde A, et al. Use of chemotherapy plus a monoclonal antibody against HER2 for metastatic breast cancer that overexpresses HER2. The New England journal of medicine. 2001;344(11):783-92.

24. Drakaki A, Hurvitz S. HER2-Positive Breast Cancer: Update on New and Emerging Agents American Journal of Hematology / Oncology®. 2015;11(4):17-23.

25. Slamon DJ, Clark GM, Wong SG, Levin WJ, Ullrich A, McGuire WL. Human breast cancer: correlation of relapse and survival with amplification of the HER-2/neu oncogene. Science. 1987;235(4785):177-82.

26. Chacon RD, Costanzo MV. Triple-negative breast cancer. Breast cancer research : BCR. 2010;12 Suppl 2:S3.

27. Foulkes WD, Smith IE, Reis-Filho JS. Triple-negative breast cancer. The New England journal of medicine. 2010;363(20):1938-48.

28. Wahba HA, El-Hadaad HA. Current approaches in treatment of triple-negative breast cancer. Cancer biology & medicine. 2015;12(2):106-16.

29. Mina A, Yoder R, Sharma P. Targeting the androgen receptor in triple-negative breast cancer: current perspectives. Onco Targets Ther. 2017;10:4675-85.

30. Lumachi F, Brunello A, Maruzzo M, Basso U, Basso SM. Treatment of estrogen receptor-positive breast cancer. Curr Med Chem. 2013;20(5):596-604.

31. Brufsky AM. Long-term management of patients with hormone receptor-positive metastatic breast cancer: Concepts for sequential and combination endocrine-based therapies. Cancer Treat Rev. 2017;59:22-32.

32. Ahmed S, Sami A, Xiang J. HER2-directed therapy: current treatment options for HER2-positive breast cancer. Breast Cancer. 2015;22(2):101-16.

33. Goyal RK, Chaudhury A. Physiology of normal esophageal motility. J Clin Gastroenterol. 2008;42(5):610-9.

34. Ramsay PT, Carr A. Gastric acid and digestive physiology. Surg Clin North Am. 2011;91(5):977-82.

35. Jin RU, Mills JC. Are Gastric and Esophageal Metaplasia Relatives? The Case for Barrett's Stemming from SPEM. Dig Dis Sci. 2018;63(8):2028-41.

36. Carcas LP. Gastric cancer review. Journal of carcinogenesis. 2014;13:14.

37. Ang TL, Fock KM. Clinical epidemiology of gastric cancer. Singapore Med J. 2014;55(12):621-8.

38. Sitarz R, Skierucha M, Mielko J, Offerhaus GJA, Maciejewski R, Polkowski WP. Gastric cancer: epidemiology, prevention, classification, and treatment. Cancer Manag Res. 2018;10:239-48.

39. Karimi P, Islami F, Anandasabapathy S, Freedman ND, Kamangar F. Gastric cancer: descriptive epidemiology, risk factors, screening, and prevention. Cancer Epidemiol Biomarkers Prev. 2014;23(5):700-13.

40. Pharoah PD, Guilford P, Caldas C, International Gastric Cancer Linkage C. Incidence of gastric cancer and breast cancer in CDH1 (E-cadherin) mutation carriers from hereditary diffuse gastric cancer families. Gastroenterology. 2001;121(6):1348-53.

41. Corso G, Marrelli D, Roviello F. Familial gastric cancer and germline mutations of E-cadherin. Ann Ital Chir. 2012;83(3):177-82.

42. Corso G, Marrelli D, Pascale V, Vindigni C, Roviello F. Frequency of CDH1 germline mutations in gastric carcinoma coming from high- and low-risk areas: metanalysis and systematic review of the literature. BMC cancer. 2012;12:8.

43. Park KJ, Choi HJ, Suh SP, Ki CS, Kim JW. Germline TP53 Mutation and Clinical Characteristics of Korean Patients With Li-Fraumeni Syndrome. Ann Lab Med. 2016;36(5):463-8.

44. Napier KJ, Scheerer M, Misra S. Esophageal cancer: A Review of epidemiology, pathogenesis, staging workup and treatment modalities. World journal of gastrointestinal oncology. 2014;6(5):112-20.

45. Huang FL, Yu SJ. Esophageal cancer: Risk factors, genetic association, and treatment. Asian J Surg. 2018;41(3):210-5.

46. Whiteman DC, Sadeghi S, Pandeya N, Smithers BM, Gotley DC, Bain CJ, et al. Combined effects of obesity, acid reflux and smoking on the risk of adenocarcinomas of the oesophagus. Gut. 2008;57(2):173-80.

47. O'Sullivan KE, Phelan JJ, O'Hanlon C, Lysaght J, O'Sullivan JN, Reynolds JV. The role of inflammation in cancer of the esophagus. Expert Rev Gastroenterol Hepatol. 2014;8(7):749-60.

48. Aleman JO, Eusebi LH, Ricciardiello L, Patidar K, Sanyal AJ, Holt PR. Mechanisms of obesity-induced gastrointestinal neoplasia. Gastroenterology. 2014;146(2):357-73.

49. Kern PA, Ranganathan S, Li C, Wood L, Ranganathan G. Adipose tissue tumor necrosis factor and interleukin-6 expression in human obesity and insulin resistance. Am J Physiol Endocrinol Metab. 2001;280(5):E745-51.

50. Huo X, Juergens S, Zhang X, Rezaei D, Yu C, Strauch ED, et al. Deoxycholic acid causes DNA damage while inducing apoptotic resistance through NF-kappaB activation in benign Barrett's epithelial cells. American journal of physiology Gastrointestinal and liver physiology. 2011;301(2):G278-86.

51. Lynam-Lennon N, Connaughton R, Carr E, Mongan AM, O'Farrell NJ, Porter RK, et al. Excess visceral adiposity induces alterations in mitochondrial function and energy metabolism in esophageal adenocarcinoma. BMC cancer. 2014;14:907.

52. Rakoff-Nahoum S. Why cancer and inflammation? Yale J Biol Med. 2006;79(3-4):123-30.

53. Zhang Y. Epidemiology of esophageal cancer. World J Gastroenterol. 2013;19(34):5598-606.

54. Dunne MR, Michielsen AJ, O'Sullivan KE, Cathcart MC, Feighery R, Doyle B, et al. HLA-DR expression in tumor epithelium is an independent prognostic indicator in esophageal adenocarcinoma patients. Cancer Immunol Immunother. 2017;66(7):841-50.

55. Kavanagh ME, O'Sullivan KE, O'Hanlon C, O'Sullivan JN, Lysaght J, Reynolds JV. The esophagitis to adenocarcinoma sequence; the role of inflammation. Cancer letters. 2014;345(2):182-9.

56. Picardo SL, Maher SG, O'Sullivan JN, Reynolds JV. Barrett's to oesophageal cancer sequence: a model of inflammatory-driven upper gastrointestinal cancer. Dig Surg. 2012;29(3):251-60.

57. Hampel H, Abraham NS, El-Serag HB. Meta-analysis: obesity and the risk for gastroesophageal reflux disease and its complications. Ann Intern Med. 2005;143(3):199-211.

58. Doyle SL, Donohoe CL, Finn SP, Howard JM, Lithander FE, Reynolds JV, et al. IGF-1 and its receptor in esophageal cancer: association with adenocarcinoma and visceral obesity. Am J Gastroenterol. 2012;107(2):196-204.

59. Alexandre L, Long E, Beales IL. Pathophysiological mechanisms linking obesity and esophageal adenocarcinoma. World J Gastrointest Pathophysiol. 2014;5(4):534-49.

60. Siewert JR. Adenocarcinoma of the esophago-gastric junction. Gastric cancer : official journal of the International Gastric Cancer Association and the Japanese Gastric Cancer Association. 1999;2(2):87-8.

61. Lauren P. The Two Histological Main Types of Gastric Carcinoma: Diffuse and So-Called Intestinal-Type Carcinoma. An Attempt at a Histo-Clinical Classification. Acta pathologica et microbiologica Scandinavica. 1965;64:31-49.

62. Ma J, Shen H, Kapesa L, Zeng S. Lauren classification and individualized chemotherapy in gastric cancer. Oncol Lett. 2016;11(5):2959-64.

63. Smyth EC, Verheij M, Allum W, Cunningham D, Cervantes A, Arnold D, et al. Gastric cancer: ESMO Clinical Practice Guidelines for diagnosis, treatment and follow-up. Annals of oncology : official journal of the European Society for Medical Oncology / ESMO. 2016;27(suppl 5):v38-v49.

64. Lu M, Yang Z, Feng Q, Yu M, Zhang Y, Mao C, et al. The characteristics and prognostic value of signet ring cell histology in gastric cancer: A retrospective cohort study of 2199 consecutive patients. Medicine (Baltimore). 2016;95(27):e4052.

65. Cunningham D, Allum WH, Stenning SP, Thompson JN, Van de Velde CJ, Nicolson M, et al. Perioperative chemotherapy versus surgery alone for resectable gastroesophageal cancer. The New England journal of medicine. 2006;355(1):11-20.

66. van Hagen P, Hulshof MC, van Lanschot JJ, Steyerberg EW, van Berge Henegouwen MI, Wijnhoven BP, et al. Preoperative chemoradiotherapy for esophageal or junctional cancer. The New England journal of medicine. 2012;366(22):2074-84.

67. Park SC, Chun HJ. Chemotherapy for advanced gastric cancer: review and update of current practices. Gut Liver. 2013;7(4):385-93.

68. Ajani JA, D'Amico TA, Almhanna K, Bentrem DJ, Chao J, Das P, et al. Gastric Cancer, Version 3.2016, NCCN Clinical Practice Guidelines in Oncology. J Natl Compr Canc Netw. 2016;14(10):1286-312.

69. Repka M, C. The Role of Radiotherapy in the Management of Gastric Cancer. The American Journal of Hematology/Oncology. 2017;13(5):8-15.

70. Gravalos C, Jimeno A. HER2 in gastric cancer: a new prognostic factor and a novel therapeutic target. Annals of oncology : official journal of the European Society for Medical Oncology / ESMO. 2008;19(9):1523-9.

71. FDA. Herceptin (trastuzumab) Label. FDA; 2010 Nov 2010.

72. Bang YJ, Van Cutsem E, Feyereislova A, Chung HC, Shen L, Sawaki A, et al. Trastuzumab in combination with chemotherapy versus chemotherapy alone for treatment of HER2-positive advanced gastric or gastro-oesophageal junction cancer (ToGA): a phase 3, open-label, randomised controlled trial. Lancet. 2010;376(9742):687-97.

73. Keller SZ, G. Ebert, K. Hasenauer, J. Wasmuth, J. Maier, D. Haffner, I. Schierle, K. Weirich, G. Luber, B. Effects of trastuzumab and afatinib on kinase activity in gastric cancer cell lines. Molecular Oncology. 2018;12(4):441-62.

74. Janjigian YY, Viola-Villegas N, Holland JP, Divilov V, Carlin SD, Gomes-DaGama EM, et al. Monitoring afatinib treatment in HER2-positive gastric cancer with 18F-FDG and 89Zr-trastuzumab PET. J Nucl Med. 2013;54(6):936-43.

75. Kasper S, Schuler M. Targeted therapies in gastroesophageal cancer. European journal of cancer. 2014;50(7):1247-58.

76. Galon J, Pages F, Marincola FM, Angell HK, Thurin M, Lugli A, et al. Cancer classification using the Immunoscore: a worldwide task force. J Transl Med. 2012;10:205.

77. Jiang Y, Zhang Q, Hu Y, Li T, Yu J, Zhao L, et al. ImmunoScore Signature: A Prognostic and Predictive Tool in Gastric Cancer. Ann Surg. 2018;267(3):504-13.

78. Zeng D, Zhou R, Yu Y, Luo Y, Zhang J, Sun H, et al. Gene expression profiles for a prognostic immunoscore in gastric cancer. Br J Surg. 2018;105(10):1338-48.

79. Duan J, Xie Y, Qu L, Wang L, Zhou S, Wang Y, et al. A nomogram-based immunoprofile predicts overall survival for previously untreated patients with esophageal squamous cell carcinoma after esophagectomy. J Immunother Cancer. 2018;6(1):100.

80. Hynes CF, Kwon DH, Vadlamudi C, Lofthus A, Iwamoto A, Chahine JJ, et al. Programmed Death Ligand 1: A Step Toward Immunoscore for Esophageal Cancer. Ann Thorac Surg. 2018;106(4):1002-7.

81. Moasser MM. The oncogene HER2: its signaling and transforming functions and its role in human cancer pathogenesis. Oncogene. 2007;26(45):6469-87.

82. Gutierrez C, Schiff R. HER2: biology, detection, and clinical implications. Archives of pathology & laboratory medicine. 2011;135(1):55-62.

83. Chakrabarty A, Rexer BN, Wang SE, Cook RS, Engelman JA, Arteaga CL. H1047R phosphatidylinositol 3-kinase mutant enhances HER2-mediated transformation by heregulin production and activation of HER3. Oncogene. 2010;29(37):5193-203.

84. Dey N, Williams C, Leyland-Jones B, De P. A critical role for HER3 in HER2-amplified and non-amplified breast cancers: function of a kinase-dead RTK. American journal of translational research. 2015;7(4):733-50.

85. Yan M, Schwaederle M, Arguello D, Millis SZ, Gatalica Z, Kurzrock R. HER2 expression status in diverse cancers: review of results from 37,992 patients. Cancer Metastasis Rev. 2015;34(1):157-64.

86. Iqbal N, Iqbal N. Human Epidermal Growth Factor Receptor 2 (HER2) in Cancers: Overexpression and Therapeutic Implications. Mol Biol Int. 2014;2014:852748.

87. Liu P, Cheng H, Roberts TM, Zhao JJ. Targeting the phosphoinositide 3-kinase pathway in cancer. Nat Rev Drug Discov. 2009;8(8):627-44.

88. Wee P, Wang Z. Epidermal Growth Factor Receptor Cell Proliferation Signaling Pathways. Cancers (Basel). 2017;9(5).

89. Ruiz-Saenz A, Dreyer C, Campbell MR, Steri V, Gulizia N, Moasser MM. HER2 Amplification in Tumors Activates PI3K/Akt Signaling Independent of HER3. Cancer Res. 2018;78(13):3645-58.

90. Gusscott S, Jenkins CE, Lam SH, Giambra V, Pollak M, Weng AP. IGF1R Derived PI3K/AKT Signaling Maintains Growth in a Subset of Human T-Cell Acute Lymphoblastic Leukemias. PLoS One. 2016;11(8):e0161158.

91. Fruman DA, Rommel C. PI3K and cancer: lessons, challenges and opportunities. Nat Rev Drug Discov. 2014;13(2):140-56.

92. Fruman DA, Chiu H, Hopkins BD, Bagrodia S, Cantley LC, Abraham RT. The PI3K Pathway in Human Disease. Cell. 2017;170(4):605-35.

93. Dillon LM, Miller TW. Therapeutic targeting of cancers with loss of PTEN function. Curr Drug Targets. 2014;15(1):65-79.

94. Chalhoub N, Baker SJ. PTEN and the PI3-kinase pathway in cancer. Annu Rev Pathol. 2009;4:127-50.

95. Oda K, Stokoe D, Taketani Y, McCormick F. High frequency of coexistent mutations of PIK3CA and PTEN genes in endometrial carcinoma. Cancer Res. 2005;65(23):10669-73.

96. Huang J, Manning BD. The TSC1-TSC2 complex: a molecular switchboard controlling cell growth. Biochem J. 2008;412(2):179-90.

97. Manning BD, Toker A. AKT/PKB Signaling: Navigating the Network. Cell. 2017;169(3):381-405.

98. Zhang W, Liu HT. MAPK signal pathways in the regulation of cell proliferation in mammalian cells. Cell research. 2002;12(1):9-18.

99. McCain J. The MAPK (ERK) Pathway: Investigational Combinations for the Treatment Of BRAF-Mutated Metastatic Melanoma. P T. 2013;38(2):96-108.

100. Brennan K, McSherry EA, Hudson L, Kay EW, Hill AD, Young LS, et al. Junctional adhesion molecule-A is co-expressed with HER2 in breast tumors and acts as a novel regulator of HER2 protein degradation and signaling. Oncogene. 2013;32(22):2799-804.

101. Nava P, Capaldo CT, Koch S, Kolegraff K, Rankin CR, Farkas AE, et al. JAM-A regulates epithelial proliferation thro u g h Akt/β-catenin signalling. EMBO Rep. 2011;12(4):314-20.

102. Tian Y, Tian Y, Zhang W, Wei F, Yang J, Luo X, et al. Junctional adhesion molecule-A, an epithelial-mesenchymal transition inducer, correlates with metastasis and poor prognosis in human nasopharyngeal cancer. Carcinogenesis. 2015;36(1):41-8.

103. Zihni C, Mills C, Matter K, Balda MS. Tight junctions: from simple barriers to multifunctional molecular gates. Nat Rev Mol Cell Biol. 2016;17(9):564-80.

104. Gunzel D, Yu AS. Claudins and the modulation of tight junction permeability. Physiol Rev. 2013;93(2):525-69.

105. Oxford. Dictionary of Biology (7 ed.). 7th ed. Martin RHaE, editor: Oxford University Press; 2015.

106. Leech AO, Cruz RG, Hill AD, Hopkins AM. Paradigms lost-an emerging role for over-expression of tight junction adhesion proteins in cancer pathogenesis. Annals of translational medicine. 2015;3(13):184.

107. Balda MS, Matter K. Tight junctions at a glance. Journal of cell science. 2008;121(Pt 22):3677-82.

108. Chiba H, Osanai M, Murata M, Kojima T, Sawada N. Transmembrane proteins of tight junctions. Biochim Biophys Acta. 2008;1778(3):588-600.

109. González-Mariscal L, Betanzos A, Nava P, Jaramillo BE. Tight junction proteins. Prog Biophys Mol Biol. 2003;81(1):1-44.

110. Bazzoni G. The JAM family of junctional adhesion molecules. Current opinion in cell biology. 2003;15(5):525-30.

111. Vellanki SR, C.E. Smith, Y.E. Hopkins, A.M. The Contribution of Ig-Superfamily and MARVEL D Tight Junction Proteins to Cancer Pathobiology. Cancer Pathobiology. 2016;Current Pathology Reports 2016(2):37-46.

112. Ebnet K, Schulz CU, Meyer Zu Brickwedde MK, Pendl GG, Vestweber D. Junctional adhesion molecule interacts with the PDZ domain-containing proteins AF-6 and ZO-1. The Journal of biological chemistry. 2000;275(36):27979-88.

113. Kahle KT, Macgregor GG, Wilson FH, Van Hoek AN, Brown D, Ardito T, et al. Paracellular Cl- permeability is regulated by WNK4 kinase: insight into normal physiology and hypertension. Proc Natl Acad Sci U S A. 2004;101(41):14877-82.

114. Wilson FH, Disse-Nicodème S, Choate KA, Ishikawa K, Nelson-Williams C, Desitter I, et al. Human hypertension caused by mutations in WNK kinases. Science. 2001;293(5532):1107-12.

115. Wilcox ER, Burton QL, Naz S, Riazuddin S, Smith TN, Ploplis B, et al. Mutations in the gene encoding tight junction claudin-14 cause autosomal recessive deafness DFNB29. Cell. 2001;104(1):165-72.

116. Riazuddin S, Ahmed ZM, Fanning AS, Lagziel A, Kitajiri S, Ramzan K, et al. Tricellulin is a tight-junction protein necessary for hearing. Am J Hum Genet. 2006;79(6):1040-51.

117. Bazzoni G, Martinez-Estrada OM, Mueller F, Nelboeck P, Schmid G, Bartfai T, et al. Homophilic interaction of junctional adhesion molecule. J Biol Chem. 2000;275(40):30970-6.

118. Ebnet K, Aurrand-Lions M, Kuhn A, Kiefer F, Butz S, Zander K, et al. The junctional adhesion molecule (JAM) family members JAM-2 and JAM-3 associate with the cell polarity protein PAR-3: a possible role for JAMs in endothelial cell polarity. Journal of cell science. 2003;116(Pt 19):3879-91.

119. Ebnet K, Suzuki A, Ohno S, Vestweber D. Junctional adhesion molecules (JAMs): more molecules with dual functions? Journal of cell science. 2004;117(Pt 1):19-29.

120. Ebnet K. JAM-A and aPKC: A close pair during cell-cell contact maturation and tight junction formation in epithelial cells. Tissue barriers. 2013;1(1):e22993.

121. Ebnet K, Suzuki A, Horikoshi Y, Hirose T, Meyer Zu Brickwedde MK, Ohno S, et al. The cell polarity protein ASIP/PAR-3 directly associates with junctional adhesion molecule (JAM). EMBO J. 2001;20(14):3738-48.

122. Huang JY, Xu YY, Sun Z, Wang ZN, Zhu Z, Song YX, et al. Low junctional adhesion molecule A expression correlates with poor prognosis in gastric cancer. J Surg Res. 2014;192(2):494-502.

123. Gutwein P, Schramme A, Voss B, Abdel-Bakky MS, Doberstein K, Ludwig A, et al. Downregulation of junctional adhesion molecule-A is involved in the progression of clear cell renal cell carcinoma. Biochem Biophys Res Commun. 2009;380(2):387-91.

124. Naik UP, Naik MU. Putting the brakes on cancer cell migration: JAM-A restrains integrin activation. Cell Adh Migr. 2008;2(4):249-51.

125. Murakami M, Giampietro C, Giannotta M, Corada M, Torselli I, Orsenigo F, et al. Abrogation of junctional adhesion molecule-A expression induces cell apoptosis and reduces breast cancer progression. PloS one. 2011;6(6):e21242.

126. Gotte M, Mohr C, Koo CY, Stock C, Vaske AK, Viola M, et al. miR-145-dependent targeting of junctional adhesion molecule A and modulation of fascin expression are associated with reduced breast cancer cell motility and invasiveness. Oncogene. 2010;29(50):6569-80.

127. Ikeo K, Oshima T, Shan J, Matsui H, Tomita T, Fukui H, et al. Junctional adhesion molecule-A promotes proliferation and inhibits apoptosis of gastric cancer. Hepatogastroenterology. 2015;62(138):540-5.

128. Zhang M, Luo W, Huang B, Liu Z, Sun L, Zhang Q, et al. Overexpression of JAM-A in non-small cell lung cancer correlates with tumor progression. PloS one. 2013;8(11):e79173.

129. Lathia JD, Li M, Sinyuk M, Alvarado AG, Flavahan WA, Stoltz K, et al. High-throughput flow cytometry screening reveals a role for junctional adhesion molecule a as a cancer stem cell maintenance factor. Cell Rep. 2014;6(1):117-29.

130. Naik MU, Naik TU, Suckow AT, Duncan MK, Naik UP. Attenuation of junctional adhesion molecule-A is a contributing factor for breast cancer cell invasion. Cancer research. 2008;68(7):2194-203.

131. McSherry EA, McGee SF, Jirstrom K, Doyle EM, Brennan DJ, Landberg G, et al. JAM-A expression positively correlates with poor prognosis in breast cancer patients. International journal of cancer. 2009;125(6):1343-51.

132. Murakami M, Francavilla C, Torselli I, Corada M, Maddaluno L, Sica A, et al. Inactivation of junctional adhesion molecule-A enhances antitumoral immune response by promoting dendritic cell and T lymphocyte infiltration. Cancer research. 2010;70(5):1759-65.

133. Goetsch L, Haeuw JF, Beau-Larvor C, Gonzalez A, Zanna L, Malissard M, et al. A novel role for junctional adhesion molecule-A in tumor proliferation: modulation by an anti-JAM-A monoclonal antibody. International journal of cancer. 2013;132(6):1463-74.

134. Amieva MR, Vogelmann R, Covacci A, Tompkins LS, Nelson WJ, Falkow S. Disruption of the epithelial apical-junctional complex by Helicobacter pylori CagA. Science. 2003;300(5624):1430-4.

135. Cover TL, Peek RM, Jr. Diet, microbial virulence, and Helicobacter pylori-induced gastric cancer. Gut Microbes. 2013;4(6):482-93.

136. Wroblewski LE, Peek RM, Jr. "Targeted disruption of the epithelial-barrier by Helicobacter pylori". Cell Commun Signal. 2011;9(1):29.

137. Donatello S, Hudson L, Cottell DC, Blanco A, Aurrekoetxea I, Shelly MJ, et al. An imbalance in progenitor cell populations reflects tumour progression in breast cancer primary culture models. Journal of experimental & clinical cancer research : CR. 2011;30:45.

138. Feoktistova M, Geserick P, Leverkus M. Crystal Violet Assay for Determining Viability of Cultured Cells. Cold Spring Harb Protoc. 2016;2016(4):pdb prot087379.

139. Gyorffy B, Lanczky A, Eklund AC, Denkert C, Budczies J, Li Q, et al. An online survival analysis tool to rapidly assess the effect of 22,277 genes on breast cancer prognosis using microarray data of 1,809 patients. Breast cancer research and treatment. 2010;123(3):725-31.

140. Szasz AM, Lanczky A, Nagy A, Forster S, Hark K, Green JE, et al. Cross-validation of survival associated biomarkers in gastric cancer using transcriptomic data of 1,065 patients. Oncotarget. 2016;7(31):49322-33.

141. Dasari S, Tchounwou PB. Cisplatin in cancer therapy: molecular mechanisms of action. Eur J Pharmacol. 2014;740:364-78.

142. Longley DB, Harkin DP, Johnston PG. 5-fluorouracil: mechanisms of action and clinical strategies. Nature reviews Cancer. 2003;3(5):330-8.

143. Tacar O, Sriamornsak P, Dass CR. Doxorubicin: an update on anticancer molecular action, toxicity and novel drug delivery systems. J Pharm Pharmacol. 2013;65(2):157-70.

144. Greenlee H. Natural products for cancer prevention. Seminars in oncology nursing. 2012;28(1):29-44.

145. Amin AR, Kucuk O, Khuri FR, Shin DM. Perspectives for cancer prevention with natural compounds. Journal of clinical oncology : official journal of the American Society of Clinical Oncology. 2009;27(16):2712-25.

146. Khanna C, Rosenberg M, Vail DM. A Review of Paclitaxel and Novel Formulations Including Those Suitable for Use in Dogs. Journal of veterinary internal medicine. 2015;29(4):1006-12.

147. Yuan QQ, Tang S, Song WB, Wang WQ, Huang M, Xuan LJ. Crassins A-H, Diterpenoids from the Roots of Croton crassifolius. Journal of natural products. 2017;80(2):254-60.

148. Galluzzi L, Bravo-San Pedro JM, Vitale I, Aaronson SA, Abrams JM, Adam D, et al. Essential versus accessory aspects of cell death: recommendations of the NCCD 2015. Cell death and differentiation. 2015;22(1):58-73.

149. Kaufmann SH, Earnshaw WC. Induction of apoptosis by cancer chemotherapy. Exp Cell Res. 2000;256(1):42-9.

150. Joo MW, Kang YK, Yoo CY, Cha SH, Chung YG. Prognostic significance of chemotherapy-induced necrosis in osteosarcoma patients receiving pasteurized autografts. PloS one. 2017;12(2):e0172155.

151. Guo J, Xu B, Han Q, Zhou H, Xia Y, Gong C, et al. Ferroptosis: A Novel Anti-tumor Action for Cisplatin. Cancer Res Treat. 2018;50(2):445-60.

152. Huang C, Luo Y, Zhao J, Yang F, Zhao H, Fan W, et al. Shikonin kills glioma cells through necroptosis mediated by RIP-1. PloS one. 2013;8(6):e66326.

153. Elmore S. Apoptosis: a review of programmed cell death. Toxicol Pathol. 2007;35(4):495-516.

154. Yuan S, Yu X, Topf M, Ludtke SJ, Wang X, Akey CW. Structure of an apoptosome-procaspase-9 CARD complex. Structure. 2010;18(5):571-83.

155. Srinivasula SM, Ahmad M, Fernandes-Alnemri T, Alnemri ES. Autoactivation of procaspase-9 by Apaf-1-mediated oligomerization. Mol Cell. 1998;1(7):949-57.

156. Denecker G, Vercammen D, Declercq W, Vandenabeele P. Apoptotic and necrotic cell death induced by death domain receptors. Cell Mol Life Sci. 2001;58(3):356-70.

157. Ouyang L, Shi Z, Zhao S, Wang FT, Zhou TT, Liu B, et al. Programmed cell death pathways in cancer: a review of apoptosis, autophagy and programmed necrosis. Cell Prolif. 2012;45(6):487-98.

158. Glick D, Barth S, Macleod KF. Autophagy: cellular and molecular mechanisms. J Pathol. 2010;221(1):3-12.

159. Darzynkiewicz Z, Juan G, Li X, Gorczyca W, Murakami T, Traganos F. Cytometry in cell necrobiology: analysis of apoptosis and accidental cell death (necrosis). Cytometry. 1997;27(1):1-20.

160. Rock KL, Kono H. The inflammatory response to cell death. Annu Rev Pathol. 2008;3:99-126.

161. Christofferson DE, Yuan J. Necroptosis as an alternative form of programmed cell death. Current opinion in cell biology. 2010;22(2):263-8.

162. Dhuriya YK, Sharma D. Necroptosis: a regulated inflammatory mode of cell death. J Neuroinflammation. 2018;15(1):199.

163. Chen D, Yu J, Zhang L. Necroptosis: an alternative cell death program defending against cancer. Biochimica et biophysica acta. 2016;1865(2):228-36.

164. Dixon SJ, Stockwell BR. The role of iron and reactive oxygen species in cell death. Nature chemical biology. 2014;10(1):9-17.

165. Stockwell BR, Friedmann Angeli JP, Bayir H, Bush AI, Conrad M, Dixon SJ, et al. Ferroptosis: A Regulated Cell Death Nexus Linking Metabolism, Redox Biology, and Disease. Cell. 2017;171(2):273-85.

166. Xie Y, Hou W, Song X, Yu Y, Huang J, Sun X, et al. Ferroptosis: process and function. Cell death and differentiation. 2016;23(3):369-79.

167. Imai H, Matsuoka M, Kumagai T, Sakamoto T, Koumura T. Lipid Peroxidation-Dependent Cell Death Regulated by GPx4 and Ferroptosis. Curr Top Microbiol Immunol. 2017;403:143-70.

168. Rixe O, Fojo T. Is cell death a critical end point for anticancer therapies or is cytostasis sufficient? Clinical cancer research : an official journal of the American Association for Cancer Research. 2007;13(24):7280-7.

169. Mervin LH, Cao Q, Barrett IP, Firth MA, Murray D, McWilliams L, et al. Understanding Cytotoxicity and Cytostaticity in a High-Throughput Screening Collection. ACS chemical biology. 2016;11(11):3007-23.

170. Reuter S, Gupta SC, Chaturvedi MM, Aggarwal BB. Oxidative stress, inflammation, and cancer: how are they linked? Free radical biology & medicine. 2010;49(11):1603-16.

171. Visconti R, Grieco D. New insights on oxidative stress in cancer. Curr Opin Drug Discov Devel. 2009;12(2):240-5.

172. Deryugina EI, Quigley JP. Chick embryo chorioallantoic membrane model systems to study and visualize human tumor cell metastasis. Histochem Cell Biol. 2008;130(6):1119-30.

173. Yamaguchi H, Wang HG. The protein kinase PKB/Akt regulates cell survival and apoptosis by inhibiting Bax conformational change. Oncogene. 2001;20(53):7779-86.

174. Song G, Ouyang G, Bao S. The activation of Akt/PKB signaling pathway and cell survival. Journal of cellular and molecular medicine. 2005;9(1):59-71.

175. Datta SR, Brunet A, Greenberg ME. Cellular survival: a play in three Akts. Genes & development. 1999;13(22):2905-27.

176. Brunet A, Bonni A, Zigmond MJ, Lin MZ, Juo P, Hu LS, et al. Akt promotes cell survival by phosphorylating and inhibiting a Forkhead transcription factor. Cell. 1999;96(6):857-68.

177. Dolado I, Nebreda AR. AKT and oxidative stress team up to kill cancer cells. Cancer cell. 2008;14(6):427-9.

178. Hou YQ, Yao Y, Bao YL, Song ZB, Yang C, Gao XL, et al. Juglanthraquinone C Induces Intracellular ROS Increase and Apoptosis by Activating the Akt/Foxo Signal Pathway in HCC Cells. Oxidative medicine and cellular longevity. 2016;2016:4941623.

179. Liu Q, Qiu J, Liang M, Golinski J, van Leyen K, Jung JE, et al. Akt and mTOR mediate programmed necrosis in neurons. Cell death & disease. 2014;5:e1084.

180. Peyssonnaux C, Eychene A. The Raf/MEK/ERK pathway: new concepts of activation. Biology of the cell. 2001;93(1-2):53-62.

181. Kirsch DG, Doseff A, Chau BN, Lim DS, de Souza-Pinto NC, Hansford R, et al. Caspase-3-dependent cleavage of Bcl-2 promotes release of cytochrome c. The Journal of biological chemistry. 1999;274(30):21155-61.

182. Porter AG, Janicke RU. Emerging roles of caspase-3 in apoptosis. Cell death and differentiation. 1999;6(2):99-104.

183. Fulda S. Regulation of necroptosis signaling and cell death by reactive oxygen species. Biological chemistry. 2016;397(7):657-60.

184. Guo GC, Wang JX, Han ML, Zhang LP, Li L. microRNA-761 induces aggressive phenotypes in triple-negative breast cancer cells by repressing TRIM29 expression. Cellular oncology. 2017;40(2):157-66.

185. Robles-Escajeda E, Das U, Ortega NM, Parra K, Francia G, Dimmock JR, et al. A novel curcumin-like dienone induces apoptosis in triple-negative breast cancer cells. Cellular oncology. 2016;39(3):265-77.

186. Fkih M'hamed I, Privat M, Lorca F, Kerdraon A, Bignon Y-J, Penault Identification of miR-10b, miR-26a, miR-146a and miR-153 as potential triple-negative breast cancer biomarkers. Cellular oncology. 2015;38(6):433-42.

187. Lokman NA, Elder AS, Ricciardelli C, Oehler MK. Chick chorioallantoic membrane (CAM) assay as an in vivo model to study the effect of newly identified molecules on ovarian cancer invasion and metastasis. Int J Mol Sci. 2012;13(8):9959-70.

188. Tufan AC, Satiroglu-Tufan NL. The chick embryo chorioallantoic membrane as a model system for the study of tumor angiogenesis, invasion and development of anti-angiogenic agents. Curr Cancer Drug Targets. 2005;5(4):249-66.

189. Gerdes J, Lemke H, Baisch H, Wacker HH, Schwab U, Stein H. Cell cycle analysis of a cell proliferation-associated human nuclear antigen defined by the monoclonal antibody Ki-67. J Immunol. 1984;133(4):1710-5.

190. Sawaf MH, Ouhayoun JP, Shabana AH, Forest N. [Cytokeratins, markers of epithelial cell differentiation: expression in normal epithelia]. Pathol Biol (Paris). 1992;40(6):655-65.

191. Nowak-Sliwinska P, Segura T, Iruela-Arispe ML. The chicken chorioallantoic membrane model in biology, medicine and bioengineering. Angiogenesis. 2014;17(4):779-804.

192. Franke TF, Hornik CP, Segev L, Shostak GA, Sugimoto C. PI3K/Akt and apoptosis: size matters. Oncogene. 2003;22(56):8983-98.

193. Zhou H, Li XM, Meinkoth J, Pittman RN. Akt regulates cell survival and apoptosis at a postmitochondrial level. The Journal of cell biology. 2000;151(3):483-94.

194. Ray PD, Huang BW, Tsuji Y. Reactive oxygen species (ROS) homeostasis and redox regulation in cellular signaling. Cellular signalling. 2012;24(5):981-90.

195. Son Y, Cheong YK, Kim NH, Chung HT, Kang DG, Pae HO. Mitogen-Activated Protein Kinases and Reactive Oxygen Species: How Can ROS Activate MAPK Pathways? Journal of signal transduction. 2011;2011:792639.

196. Cagnol S, Chambard JC. ERK and cell death: mechanisms of ERK-induced cell death--apoptosis, autophagy and senescence. The FEBS journal. 2010;277(1):2-21.

197. Keshari RS, Verma A, Barthwal MK, Dikshit M. Reactive oxygen species-induced activation of ERK and p38 MAPK mediates PMA-induced NETs release from human neutrophils. Journal of cellular biochemistry. 2013;114(3):532-40.

198. Lobo V, Patil A, Phatak A, Chandra N. Free radicals, antioxidants and functional foods: Impact on human health. Pharmacognosy reviews. 2010;4(8):118-26.

199. Turrens JF. Mitochondrial formation of reactive oxygen species. The Journal of physiology. 2003;552(Pt 2):335-44.

200. Valencia A, Moran J. Reactive oxygen species induce different cell death mechanisms in cultured neurons. Free radical biology & medicine. 2004;36(9):1112-25.

201. Choi YH, Yoo YH. Taxol-induced growth arrest and apoptosis is associated with the upregulation of the Cdk inhibitor, p21WAF1/CIP1, in human breast cancer cells. Oncol Rep. 2012;28(6):2163-9.

202. Ciardiello F, Caputo R, Bianco R, Damiano V, Pomatico G, De Placido S, et al. Antitumor effect and potentiation of cytotoxic drugs activity in human cancer cells by ZD-1839 (Iressa), an epidermal growth factor receptor-selective tyrosine kinase inhibitor. Clinical cancer research : an official journal of the American Association for Cancer Research. 2000;6(5):2053-63.

203. Villasana M, Ochoa G, Aguilar S. Modeling and optimization of combined cytostatic and cytotoxic cancer chemotherapy. Artificial intelligence in medicine. 2010;50(3):163-73.

204. Bacus SS, Gudkov AV, Lowe M, Lyass L, Yung Y, Komarov AP, et al. Taxol-induced apoptosis depends on MAP kinase pathways (ERK and p38) and is independent of p53. Oncogene. 2001;20(2):147-55.

205. Richards CE, Vellanki SH, Smith YE, Hopkins AM. Diterpenoid natural compound C4 (Crassin) exerts cytostatic effects on triple-negative breast cancer cells via a pathway involving reactive oxygen species. Cell Oncol (Dordr). 2018;41(1):35-46.

206. McSherry EA, Brennan K, Hudson L, Hill AD, Hopkins AM. Breast cancer cell migration is regulated through junctional adhesion molecule-A-mediated activation of Rap1 GTPase. Breast cancer research : BCR. 2011;13(2):R31.

207. Severson EA, Parkos CA. Structural determinants of Junctional Adhesion Molecule A (JAM-A) function and mechanisms of intracellular signaling. Current opinion in cell biology. 2009;21(5):701-7.

208. Leech AO, Vellanki SH, Rutherford EJ, Keogh A, Jahns H, Hudson L, et al. Cleavage of the extracellular domain of junctional adhesion molecule-A is associated with resistance to anti-HER2 therapies in breast cancer settings. Breast cancer research : BCR. 2018;20(1):140.

209. Koenen RR, Pruessmeyer J, Soehnlein O, Fraemohs L, Zernecke A, Schwarz N, et al. Regulated release and functional modulation of junctional adhesion molecule A by disintegrin metalloproteinases. Blood. 2009;113(19):4799-809.

210. Cavusoglu E, Kornecki E, Sobocka MB, Babinska A, Ehrlich YH, Chopra V, et al. Association of plasma levels of F11 receptor/junctional adhesion molecule-A (F11R/JAM-A) with human atherosclerosis. Journal of the American College of Cardiology. 2007;50(18):1768-76.

211. Azari BM, Marmur JD, Salifu MO, Cavusoglu E, Ehrlich YH, Kornecki E, et al. Silencing of the F11R gene reveals a role for F11R/JAM-A in the migration of inflamed vascular smooth muscle cells and in atherosclerosis. Atherosclerosis. 2010;212(1):197-205.

212. Ong KL, Leung RY, Babinska A, Salifu MO, Ehrlich YH, Kornecki E, et al. Elevated plasma level of soluble F11 receptor/junctional adhesion molecule-A (F11R/JAM-A) in hypertension. Am J Hypertens. 2009;22(5):500-5.

213. Menyhart O, Harami-Papp H, Sukumar S, Schafer R, Magnani L, de Barrios O, et al. Guidelines for the selection of functional assays to evaluate the hallmarks of cancer. Biochimica et biophysica acta. 2016;1866(2):300-19.

214. Schaefer MH, Serrano L. Cell type-specific properties and environment shape tissue specificity of cancer genes. Sci Rep. 2016;6:20707.

215. Wang M, Zhao J, Zhang L, Wei F, Lian Y, Wu Y, et al. Role of tumor microenvironment in tumorigenesis. J Cancer. 2017;8(5):761-73.

216. Oliver AJ, Lau PKH, Unsworth AS, Loi S, Darcy PK, Kershaw MH, et al. Tissue-Dependent Tumor Microenvironments and Their Impact on Immunotherapy Responses. Front Immunol. 2018;9:70.

217. van't Veer LJ, Bernards R. Enabling personalized cancer medicine through analysis of gene-expression patterns. Nature. 2008;452(7187):564-70.

218. Gil J, Laczmanska I, Pesz KA, Sasiadek MM. Personalized medicine in oncology. New perspectives in management of gliomas. Contemp Oncol (Pozn). 2018;22(1A):1-2.

219. Mroz EA, Rocco JW. The challenges of tumor genetic diversity. Cancer. 2017;123(6):917-27.

220. Liu Y, Cao X. Characteristics and Significance of the Pre-metastatic Niche. Cancer cell. 2016;30(5):668-81.

221. Deryugina EI, Quigley JP. Chapter 2. Chick embryo chorioallantoic membrane models to quantify angiogenesis induced by inflammatory and tumor cells or purified effector molecules. Methods Enzymol. 2008;444:21-41.

222. Okines AF, Cunningham D. Trastuzumab in gastric cancer. European journal of cancer. 2010;46(11):1949-59.

223. Barok M, Tanner M, Koninki K, Isola J. Trastuzumab-DM1 is highly effective in preclinical models of HER2-positive gastric cancer. Cancer letters. 2011;306(2):171-9.

224. Pietrantonio F, Fuca G, Morano F, Gloghini A, Corso S, Aprile G, et al. Biomarkers of Primary Resistance to Trastuzumab in HER2-Positive Metastatic Gastric Cancer Patients: the AMNESIA Case-Control Study. Clinical cancer research : an official journal of the American Association for Cancer Research. 2018;24(5):1082-9.

225. Kim HP, Han SW, Song SH, Jeong EG, Lee MY, Hwang D, et al. Testican-1-mediated epithelial-mesenchymal transition signaling confers acquired resistance to lapatinib in HER2-positive gastric cancer. Oncogene. 2014;33(25):3334-41.

226. Feldinger K, Generali D, Kramer-Marek G, Gijsen M, Ng TB, Wong JH, et al. ADAM10 mediates trastuzumab resistance and is correlated with survival in HER2 positive breast cancer. Oncotarget. 2014;5(16):6633-46.

227. Bedard PL, de Azambuja E, Cardoso F. Beyond trastuzumab: overcoming resistance to targeted HER-2 therapy in breast cancer. Curr Cancer Drug Targets. 2009;9(2):148-62.

228. Miller KD. The role of ErbB inhibitors in trastuzumab resistance. Oncologist. 2004;9 Suppl 3:16-9.

229. Cortese K, Howes MT, Lundmark R, Tagliatti E, Bagnato P, Petrelli A, et al. The HSP90 inhibitor geldanamycin perturbs endosomal structure and drives recycling ErbB2 and transferrin to modified MVBs/lysosomal compartments. Mol Biol Cell. 2013;24(2):129-44.

230. Kleeff J, Kornmann M, Sawhney H, Korc M. Actinomycin D induces apoptosis and inhibits growth of pancreatic cancer cells. International journal of cancer. 2000;86(3):399-407.

231. Lu DF, Wang YS, Li C, Wei GJ, Chen R, Dong DM, et al. Actinomycin D inhibits cell proliferations and promotes apoptosis in osteosarcoma cells. Int J Clin Exp Med. 2015;8(2):1904-11.

232. Mauthe M, Orhon I, Rocchi C, Zhou X, Luhr M, Hijlkema KJ, et al. Chloroquine inhibits autophagic flux by decreasing autophagosome-lysosome fusion. Autophagy. 2018;14(8):1435-55.

233. Mizushima N, Yoshimori T. How to interpret LC3 immunoblotting. Autophagy. 2007;3(6):542-5.

234. Valabrega G, Montemurro F, Aglietta M. Trastuzumab: mechanism of action, resistance and future perspectives in HER2-overexpressing breast cancer. Annals of oncology : official journal of the European Society for Medical Oncology / ESMO. 2007;18(6):977-84.

235. Henson ES, Hu X, Gibson SB. Herceptin sensitizes ErbB2-overexpressing cells to apoptosis by reducing antiapoptotic Mcl-1 expression. Clinical cancer research : an

official journal of the American Association for Cancer Research. 2006;12(3 Pt 1):845-53.

236. Nahta R, Yuan LX, Du Y, Esteva FJ. Lapatinib induces apoptosis in trastuzumab-resistant breast cancer cells: effects on insulin-like growth factor I signaling. Mol Cancer Ther. 2007;6(2):667-74.

237. Huang HL, Chen YC, Huang YC, Yang KC, Pan H, Shih SP, et al. Lapatinib induces autophagy, apoptosis and megakaryocytic differentiation in chronic myelogenous leukemia K562 cells. PloS one. 2011;6(12):e29014.

238. Hedner C, Tran L, Borg D, Nodin B, Jirstrom K, Eberhard J. Discordant human epidermal growth factor receptor 2 overexpression in primary and metastatic upper gastrointestinal adenocarcinoma signifies poor prognosis. Histopathology. 2016;68(2):230-40.

239. Allison KH, Sledge GW. Heterogeneity and cancer. Oncology (Williston Park). 2014;28(9):772-8.

240. Stepanenko AA, Heng HH. Transient and stable vector transfection: Pitfalls, off-target effects, artifacts. Mutat Res. 2017;773:91-103.

241. Kim TK, Eberwine JH. Mammalian cell transfection: the present and the future. Anal Bioanal Chem. 2010;397(8):3173-8.

242. Thurtle-Schmidt DM, Lo TW. Molecular biology at the cutting edge: A review on CRISPR/CAS9 gene editing for undergraduates. Biochem Mol Biol Educ. 2018;46(2):195-205.

243. Du Z, Lovly CM. Mechanisms of receptor tyrosine kinase activation in cancer. Molecular cancer. 2018;17(1):58.

244. Schlessinger J. Cell signaling by receptor tyrosine kinases. Cell. 2000;103(2):211-25.

245. Lemmon MA, Schlessinger J. Cell signaling by receptor tyrosine kinases. Cell. 2010;141(7):1117-34.

246. Begnami MD, Fukuda E, Fregnani JH, Nonogaki S, Montagnini AL, da Costa WL, Jr., et al. Prognostic implications of altered human epidermal growth factor receptors (HERs) in gastric carcinomas: HER2 and HER3 are predictors of poor outcome. Journal of clinical oncology : official journal of the American Society of Clinical Oncology. 2011;29(22):3030-6.

247. Boku N. HER2-positive gastric cancer. Gastric cancer : official journal of the International Gastric Cancer Association and the Japanese Gastric Cancer Association. 2014;17(1):1-12.

248. de Melo Gagliato D, Jardim DL, Marchesi MS, Hortobagyi GN. Mechanisms of resistance and sensitivity to anti-HER2 therapies in HER2+ breast cancer. Oncotarget. 2016;7(39):64431-46.

249. Escriva-de-Romani S, Arumi M, Bellet M, Saura C. HER2-positive breast cancer: Current and new therapeutic strategies. Breast. 2018;39:80-8.

250. Hayashi M, Inokuchi M, Takagi Y, Yamada H, Kojima K, Kumagai J, et al. High expression of HER3 is associated with a decreased survival in gastric cancer. Clinical cancer research : an official journal of the American Association for Cancer Research. 2008;14(23):7843-9.

251. Hedner C, Borg D, Nodin B, Karnevi E, Jirstrom K, Eberhard J. Expression and prognostic significance of human epidermal growth factor receptors 1, 2 and 3 in oesophageal and gastric adenocarcinomas preneoadjuvant and postneoadjuvant treatment. J Clin Pathol. 2018;71(5):451-62.

252. Hedner C, Borg D, Nodin B, Karnevi E, Jirstrom K, Eberhard J. Expression and Prognostic Significance of Human Epidermal Growth Factor Receptors 1 and 3 in Gastric and Esophageal Adenocarcinoma. PloS one. 2016;11(2):e0148101.

253. Koltz BR, Hicks DG, Whitney-Miller CL. HER2 testing in gastric and esophageal adenocarcinoma: new diagnostic challenges arising from new therapeutic options. Biotechnic & histochemistry : official publication of the Biological Stain Commission. 2012;87(1):40-5.

254. Mishra R, Alanazi S, Yuan L, Solomon T, Thaker TM, Jura N, et al. Activating HER3 mutations in breast cancer. Oncotarget. 2018;9(45):27773-88.

255. Mishra R, Patel H, Alanazi S, Yuan L, Garrett JT. HER3 signaling and targeted therapy in cancer. Oncol Rev. 2018;12(1):355.

256. Reichelt U, Duesedau P, Tsourlakis M, Quaas A, Link BC, Schurr PG, et al. Frequent homogeneous HER-2 amplification in primary and metastatic adenocarcinoma of the esophagus. Modern pathology : an official journal of the United States and Canadian Academy of Pathology, Inc. 2007;20(1):120-9.

257. Tokunaga A, Onda M, Okuda T, Teramoto T, Fujita I, Mizutani T, et al. Clinical significance of epidermal growth factor (EGF), EGF receptor, and c-erbB-2 in human gastric cancer. Cancer. 1995;75(6 Suppl):1418-25.

258. Gala K, Chandarlapaty S. Molecular pathways: HER3 targeted therapy. Clinical cancer research : an official journal of the American Association for Cancer Research. 2014;20(6):1410-6.

259. Jaiswal BS, Kljavin NM, Stawiski EW, Chan E, Parikh C, Durinck S, et al. Oncogenic ERBB3 mutations in human cancers. Cancer cell. 2013;23(5):603-17.

260. Chiu CG, Masoudi H, Leung S, Voduc DK, Gilks B, Huntsman DG, et al. HER-3 overexpression is prognostic of reduced breast cancer survival: a study of 4046 patients. Ann Surg. 2010;251(6):1107-16.

261. Ebbing EA, Medema JP, Damhofer H, Meijer SL, Krishnadath KK, van Berge Henegouwen MI, et al. ADAM10-mediated release of heregulin confers resistance to trastuzumab by activating HER3. Oncotarget. 2016;7(9):10243-54.

262. Sato Y, Yashiro M, Takakura N. Heregulin induces resistance to lapatinib-mediated growth inhibition of HER2-amplified cancer cells. Cancer science. 2013;104(12):1618-25.

263. Bernardo GM, Bebek G, Ginther CL, Sizemore ST, Lozada KL, Miedler JD, et al. FOXA1 represses the molecular phenotype of basal breast cancer cells. Oncogene. 2013;32(5):554-63.

264. Lin L, Miller CT, Contreras JI, Prescott MS, Dagenais SL, Wu R, et al. The hepatocyte nuclear factor 3 alpha gene, HNF3alpha (FOXA1), on chromosome band 14q13 is amplified and overexpressed in esophageal and lung adenocarcinomas. Cancer research. 2002;62(18):5273-9.

265. Castano J, Davalos V, Schwartz S, Jr., Arango D. EPH receptors in cancer. Histol Histopathol. 2008;23(8):1011-23.

266. Davalos V, Dopeso H, Castano J, Wilson AJ, Vilardell F, Romero-Gimenez J, et al. EPHB4 and survival of colorectal cancer patients. Cancer research. 2006;66(18):8943-8.

267. Wu Q, Suo Z, Risberg B, Karlsson MG, Villman K, Nesland JM. Expression of Ephb2 and Ephb4 in breast carcinoma. Pathol Oncol Res. 2004;10(1):26-33.

268. Yin J, Cui Y, Li L, Ji J, Jiang WG. Overexpression of EPHB4 Is Associated with Poor Survival of Patients with Gastric Cancer. Anticancer research. 2017;37(8):4489-97.

269. Skacel M, Skilton B, Pettay JD, Tubbs RR. Tissue microarrays: a powerful tool for high-throughput analysis of clinical specimens: a review of the method with validation data. Appl Immunohistochem Mol Morphol. 2002;10(1):1-6.

270. Jawhar NM. Tissue Microarray: A rapidly evolving diagnostic and research tool. Ann Saudi Med. 2009;29(2):123-7.

271. Boellner S, Becker KF. Reverse Phase Protein Arrays-Quantitative Assessment of Multiple Biomarkers in Biopsies for Clinical Use. Microarrays (Basel). 2015;4(2):98-114.

272. Man AL, Bertelli E, Rentini S, Regoli M, Briars G, Marini M, et al. Age-associated modifications of intestinal permeability and innate immunity in human small intestine. Clin Sci (Lond). 2015;129(7):515-27.

273. Ren WY, Wu KF, Li X, Luo M, Liu HC, Zhang SC, et al. Age-related changes in small intestinal mucosa epithelium architecture and epithelial tight junction in rat models. Aging Clin Exp Res. 2014;26(2):183-91.

274. Parrish AR. The impact of aging on epithelial barriers. Tissue barriers. 2017;5(4):e1343172.

275. Bradner JE, Hnisz D, Young RA. Transcriptional Addiction in Cancer. Cell. 2017;168(4):629-43.

276. Darnell JE, Jr. Transcription factors as targets for cancer therapy. Nature reviews Cancer. 2002;2(10):740-9.

277. de Aretxabala X, Yonemura Y, Sugiyama K, Hirose N, Kumaki T, Fushida S, et al. Gastric cancer heterogeneity. Cancer. 1989;63(4):791-8.

278. Testa U, Castelli G, Pelosi E. Esophageal Cancer: Genomic and Molecular Characterization, Stem Cell Compartment and Clonal Evolution. Medicines (Basel). 2017;4(3).

279. Wu SG, Zhang WW, He ZY, Sun JY, Chen YX, Guo L. Sites of metastasis and overall survival in esophageal cancer: a population-based study. Cancer Manag Res. 2017;9:781-8.

280. Turkoz FP, Solak M, Kilickap S, Ulas A, Esbah O, Oksuzoglu B, et al. Bone metastasis from gastric cancer: the incidence, clinicopathological features, and influence on survival. J Gastric Cancer. 2014;14(3):164-72.

281. Hoffman RM. In vitro sensitivity assays in cancer: a review, analysis, and prognosis. J Clin Lab Anal. 1991;5(2):133-43.

282. DeBord LC, Pathak RR, Villaneuva M, Liu HC, Harrington DA, Yu W, et al. The chick chorioallantoic membrane (CAM) as a versatile patient-derived xenograft (PDX) platform for precision medicine and preclinical research. Am J Cancer Res. 2018;8(8):1642-60.

283. Perez EA. Paclitaxel in Breast Cancer. Oncologist. 1998;3(6):373-89.

284. Long HJ. Paclitaxel (Taxol): a novel anticancer chemotherapeutic drug. Mayo Clin Proc. 1994;69(4):341-5.

285. Long BH, Fairchild CR. Paclitaxel inhibits progression of mitotic cells to G1 phase by interference with spindle formation without affecting other microtubule functions during anaphase and telephase. Cancer research. 1994;54(16):4355-61.

286. Wang L, Leite de Oliveira R, Wang C, Fernandes Neto JM, Mainardi S, Evers B, et al. High-Throughput Functional Genetic and Compound Screens Identify Targets for Senescence Induction in Cancer. Cell Rep. 2017;21(3):773-83.

287. Leite de Oliveira R, Bernards R. Anti-cancer therapy: senescence is the new black. EMBO J. 2018;37(10).

288. Pardo A, Selman M. Fibroblast Senescence and Apoptosis. "One-Two Punch" to Slow Down Lung Fibrosis? American journal of respiratory cell and molecular biology. 2017;56(2):145-6.

289. Guilford P, Hopkins J, Harraway J, McLeod M, McLeod N, Harawira P, et al. E-cadherin germline mutations in familial gastric cancer. Nature. 1998;392(6674):402-5.

290. Graziano F, Humar B, Guilford P. The role of the E-cadherin gene (CDH1) in diffuse gastric cancer susceptibility: from the laboratory to clinical practice. Annals of oncology : official journal of the European Society for Medical Oncology / ESMO. 2003;14(12):1705-13.

291. Torabizadeh Z, Nosrati A, Sajadi Saravi SN, Yazdani Charati J, Janbabai G. Evaluation of E-cadherin Expression in Gastric Cancer and Its Correlation with Clinicopathologic Parameters. Int J Hematol Oncol Stem Cell Res. 2017;11(2):158-64.

292. van Roy F, Berx G. The cell-cell adhesion molecule E-cadherin. Cell Mol Life Sci. 2008;65(23):3756-88.

293. Adhikary A, Chakraborty S, Mazumdar M, Ghosh S, Mukherjee S, Manna A, et al. Inhibition of epithelial to mesenchymal transition by E-cadherin up-regulation via repression of slug transcription and inhibition of E-cadherin degradation: dual role of scaffold/matrix attachment region-binding protein 1 (SMAR1) in breast cancer cells. The Journal of biological chemistry. 2014;289(37):25431-44.

294. Vellanki SH, Cruz RGB, Richards CE, Smith YE, Hudson L, Jahns H, et al. Antibiotic Tetrocarcin-A Down-regulates JAM-A, IAPs and Induces Apoptosis in Triple-negative Breast Cancer Models. Anticancer research. 2019;39(3):1197-204.

295. Vellanki SH, Cruz RGB, Jahns H, Hudson L, Sette G, Eramo A, et al. Natural compound Tetrocarcin-A downregulates Junctional Adhesion Molecule-A in conjunction with HER2 and inhibitor of apoptosis proteins and inhibits tumor cell growth. Cancer letters. 2019;440-441:23-34.

296. Shen L, Shi Q, Wang W. Double agents: genes with both oncogenic and tumor-suppressor functions. Oncogenesis. 2018;7(3):25.

297. Khorana AA, Kuderer NM, Culakova E, Lyman GH, Francis CW. Development and validation of a predictive model for chemotherapy-associated thrombosis. Blood. 2008;111(10):4902-7.

298. Tetzlaff ED, Cheng JD, Ajani JA. Thromboembolism in gastrointestinal cancers. Gastrointest Cancer Res. 2008;2(6):267-72.

299. Richards CE, Rutherford EJ, Hopkins AM. Cleaved JAM-A - connecting cancer and vascular disease? Oncotarget. 2019;10(39):3831-2.

300. Wang YK, Chen Z, Yun T, Li CY, Jiang B, Lv XX, et al. Human epidermal growth factor receptor 2 expression in mixed gastric carcinoma. World J Gastroenterol. 2015;21(15):4680-7.

301. Nahta R, Esteva FJ. HER2 therapy: molecular mechanisms of trastuzumab resistance. Breast cancer research : BCR. 2006;8(6):215.

302. Mitchell LA, Ward C, Kwon M, Mitchell PO, Quintero DA, Nusrat A, et al. Junctional adhesion molecule A promotes epithelial tight junction assembly to augment lung barrier function. The American journal of pathology. 2015;185(2):372-86.

303. Campbell RJ, Pignatelli M. Molecular histology in the study of solid tumours. Mol Pathol. 2002;55(2):80-2.

304. He L, Long LR, Antani S, Thoma GR. Histology image analysis for carcinoma detection and grading. Comput Methods Programs Biomed. 2012;107(3):538-56.

Appendices

Appendix A ï Antibodies for Western Blot

Antibody	Brand	Species	Dilution	Conc. (µg/mL)	Diluent	Product Code
Actin	Abcam	Rabbit	1:5000	0.02	Milk	Ab8227
HER2	Cell Signalling	Rabbit	1:1000	-	BSA	2165
HER3	Cell Signalling	Rabbit	1:1000	-	Milk	12708
JAM-A	BD	Mouse	1:1000	0.25	Milk	612120
LC3B	Cell Signalling	Rabbit	1:1000	-	BSA	2775
pAKT	Cell Signalling	Rabbit	1:1000	-	BSA	4060
Total Akt	Cell Signalling	Mouse	1:1000	-	BSA	2920
pERK	Cell Signalling	Rabbit	1:1000	-	BSA	4370
Total ERK	Cell Signalling	Rabbit	1:1000	-	BSA	2920
Cleaved Cas-3	Cell Signalling	Rabbit	1:1000	-	BSA	9661
Total Caspas-3	Cell Signalling	Rabbit	1:1000	-	BSA	14220

Appendix B ï Antibodies for IHC

Antibody	Brand	Species	Dilution	Conc. (µg/mL)	Retrieval Solution	Product Code
JAM-A	Abnova	Mouse	1:1000	0.4	Leica ER 1	H00050848-M01
HER2	Cell Signalling	Rabbit	Ready-to-use	-	CC1	2165
HER3	Cell Signalling	Rabbit	1:50	-	Leica ER 2	12708
Ki67	Agilent Dako	Mouse	1:75	-	Leica ER 2	M7240
EphB4	Cell Signalling	Rabbit	1:100	-	Leica ER 2	14960
Cytokeratin	BD	Mouse	1:10	-	Leica ER 1	BD345779

Appendix C ï Antibodies for IF

Antibody	Brand	Species	Dilution	Conc. (µg/mL)	Diluent	Product Code
JAM-A	Santa Cruz	Mouse	1:500	0.4	Goat Serum	Sc-53623
HER2	Cell Signalling	Rabbit	1:200	-	Goat Serum	2165
B-catenin	Cell Signalling	Rabbit	1:100	-	Goat Serum	8480

Appendix D ï Solutions

1.5M Tris-Cl pH 8.8 (Running Gel) ï Store at 4°C

- 90.83g Trizma base
- 300mL dd$H_2$0
- pH to 8.8 with v. concentrated HCl (~8mL)
- ddH_2O up to 500mL

1M Tris-Cl pH 6.8 (Stacking Gel) ï Store at RT

- 60.55g Trizma base
- 300mL dd$H_2$0
- pH to 6.8 with v. concentrated HCl (~10mL)
- ddH_2O up to 500mL

10X Tris Glycine ï Store at 4°C

- 30.3g Tris base
- 144g Glycine
- ddH_2O up to 1L

check if pH = 8.3

10X TBS ï Store at 4°C

- 80g NaCl
- 2g KCl
- 30g Trizma base
- 800mL dd$H_2$0
- pH to 7.4 with concentrated HCl
- ddH_2O up to 1L

10X PBS ï Store at RT

- 80g NaCl
- 2g KCl
- 14.4g Na_2HPO_4

- 2.4g KH_2PO_4
- 800mL ddH_20
- pH to 7.4
- ddH_2O up to 1L

Relax Buffer ï Store at 4°C

- 1.4912g KCl
- 0.0351g NaCl
- 0.0666g MgCl2 (anhydrous)
- 2mL 1M HEPES
- 100mL ddH_2O
- pH to 7.4
- ddH_2O up to 200mL

RIPA Buffer ï Store at 4ºC

- 0.877g 150mM NaCl
- 1mL 1% Triton-X 100
- 0.5g 5% Sodium Deoxycholate
- 0.1g SDS
- 0.606g 50mM Tris-Cl pH8
- ddH_2O up to 100mL

Stripping Buffer ï Store at RT

- 80mL 10% SDS
- 25mL 1M Tris-Cl pH 7
- ddH_2O up to 400mL

* A d d 7 -0mmL captβethanol per 10mL **IN FUME HOOD**

10% SDS ï Store at RT

- 10g SDS
- ddH_2O up to 100mL

* 100% = 1g/mL

Running Buffer (For 2 Gels)

- 100mL 10X Tris-Glycine
- 900mL dH2O
- 5mL 10% SDS

Transfer Buffer (For 2 Gels)

- 140mL methanol
- 70 mL 10X Tris-Glycine
- ddH_2O up to 700mL

Ponceau S

- 1mg Ponceau
- 0.1mL Acetic acid
- 1mL ddH_2O

Laemelli Buffer 6x

- 3.75mL 1M Tris-Cl pH 6.8 (0.375M)
- 4mL Glycerol (40%)
- 1.2g SDS (12%)
- 10mg Bromophenol Blue
- 0.93g DTT
- ddH_2O up to 10mL

Appendix E ï Resolving Gel Recipes

Resolving Gel:

	9%	10%	12%	13%	15%
ddH20 (mL)	8.6	7.9	6.6	5.9	4.6
30% Acrylamide (mL)	6	6.7	8	8.7	10
Tris-Cl pH8.8 (mL)	5	5	5	5	5
10% SDS (µ L)	200	200	200	200	200
APS (µ L)	200	200	200	200	200
TEMED (µ L)	8	8	8	8	8

Stacking Gel:

	5%
ddH20 (mL)	6.8
30% Acrylamide (mL)	1.7
Tris-Cl pH8.8 (mL)	1.25
10% SDS (µ L)	100
APS (µ L)	100
TEMED (µ L)	10

Appendix F ï Primary Cell Cultre Media Recipe

Supplement	Concentration Stock	Volume to Add (500mL)	Final Concentration
EGF	100µg/mL	50µL	10ng/mL
Hydrocortisone	1mg/mL	250µl	0.5µg/mL
Insulin	1mg/mL	2.5mL	5µg/mL
BPE	14mg/mL (as bought)	2.5mL	70µg/mL
Transferrin	10mg/mL	250µl	5µg/mL
Ethanolamine	$1x10^{-1}$ M	500µl	$1x10^{-4}$ M
O-phosphoethanolamine	$1x10^{-1}$ M	500µl	$1x10^{-4}$ M

Appendix G ï siRNA

siRNA	Brand	Product Code	Sequence
siJAM11	Dharmacon	Designed	CGGGGGUCGCAGGAAUCUG

Appendix H ï Primer Sequences

siRNA	Sequence
JAM-A Forward	CTC TCA GTC CCC TCG CTG TA
JAM-A Reverse	AAT GCC AGG GAG CAC AAC AG
RPLP0 Forward	GGC AGC ATC TAC AAC CCT GA
RPLP0 Reverse	GGC AGC ATC TAC AAC CCT GA
HER2 Forward	ACG TTT GAG TCC ATG CCC AA
HER2 Reverse	AGG TAG TTG TAG GGA CAG GCA
HER3 Forward	GTG GTG AAG GAC AAT GGC AG
HER3 Reverse	CAC AGA TGG TCT TGG TCA ATG TC
FOXA1 Forward	AGG GCT GGA TGG TTG TAT TG
FOXA1 Reverse	GCT CGT AGT CAT GGT GTT CAT
B-catenin Forward	CCT TCA ACT ATT TCT TCC ATG CG
B-catenin Reverse	CTA GTT CAG TTG CTT GTT CGT G
EphB4 Forward	TAT GAG AGC GAT GCG GAC AC
EphB4 Reverse	CGT GTC CAC CTT GAT GTA GGG

Appendix I ï Clinocpathological Features of Full-Face Gastro-oesophageal Cancer Cases

Patient	Tumour type	Grade	Location	HER2 status	T stage	N stage
1	adenocarcinoma, intestinal type	moderate and poorly differentiated	OG junction and lesser curve	Negative	pT3	N0
2	adenocarcinoma, diffuse type	poorly differentiated	gastric body	Positive	pT3	N0 (i+)
3	adenocarcinoma, intestinal type	moderate and poorly differentiated	gastric body	Positive	ypT3	N0
4	adenocarcinoma intestinal and diffuse	poorly differentiated	gastric cardia	Negative	pT4a	N2
5	adenocarcinoma, intestinal type	moderately differentiated	gastric body lesser curve	Positive	pT3	N1
6	adenocarcinoma, diffuse type	poorly differentiated	gastric body	Negative	pT4a	N0
7	adenocarcinoma, intestinal type	moderate and poorly differentiated	gastric body	Positive	pT3	N2
8	adenocarcinoma, NOS	poorly differentiated	gastric pylorus	Positive	pT4a	N3a
9	adenocarcinoma, diffuse type	poorly differentiated	gastric body	Negative	ypT3	N1
10	adenocarcinoma, diffuse type	poorly differentiated	OG junction	Positive	ypT1b	N0
11	adenocarcinoma, intestinal type	moderate and poorly differentiated	OG junction and gastric	Negative	pT3	N2

Appendix J ï Supplementary Data

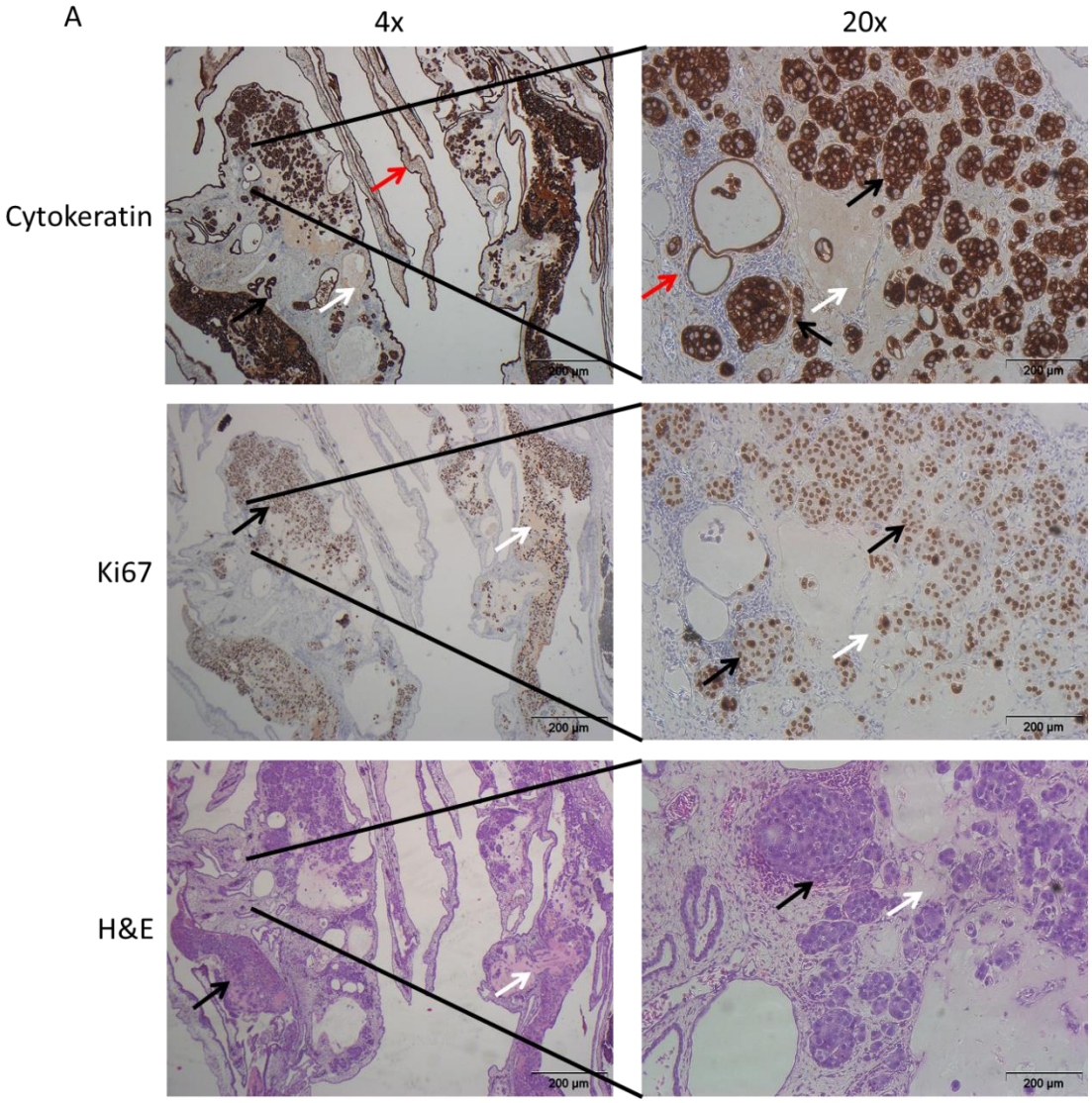

Supplementary Figure 1: Crassin-treated Xenografts showed evidence of tumour growth and proliferation. 2 x ^{6} E1SOO 2 6 w e r e s i m p l a n o n t t d h C E A M o f f e r t i l i s e d b e n d e g g s a n d m e d a y a t 8 w i t h e i t h (e 1 r . K M C 5 o a s s e h i c l e c , o r 0 t . r 0 o l V 0 (6 D M S O on days 10 and sliced rings and surrounding areas of the CAM were excised, formalin fixed and stained for cytokeratin, Ki67 or haematoxylin and eosin (H&E). Stained sections were then imaged on Olympus CKx41 microscope at 4x or 20x with Cell B imaging software. Areas of tumour are denoted by black arrows, areas of Matrigel are denoted by white arrows and areas of CAM are denoted by red arrows. All images were obtained using an Olympus CKx41 microscope with Cell B imaging software at 20x magnification.

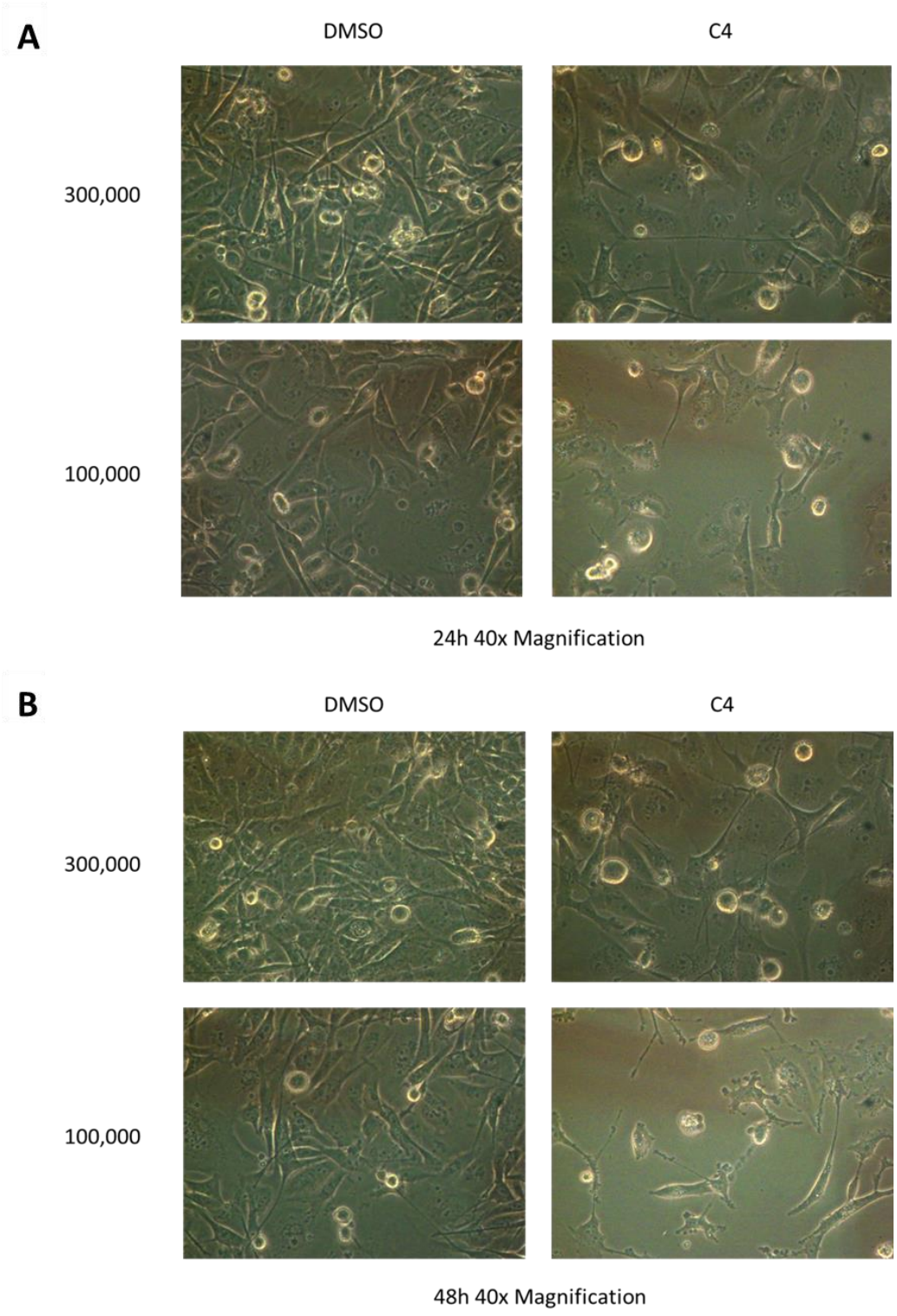

Supplementary Figure 2: C4 alters cellular morphology in MDA-MB-231 cells. *MDA-MB-231 cells were plated at either 300,000 or 100,000 per well and treated 48h later with C4 (5μM) or vehicle control (DMSO) for either 24h* ***(A)*** *or 48h* ***(B)*** *for 48h. Cells were then imaged at 40x magnification on an Olympus CKX41 microscope using Cell B imaging software.*

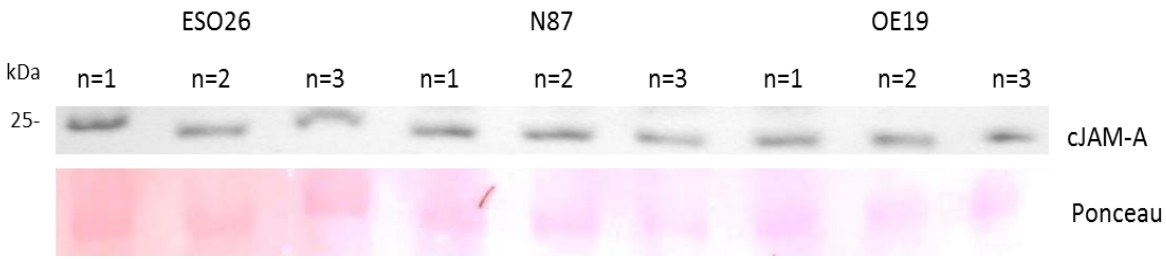

Supplementary Figure 3: Levels of cJAM-A across gastro-oesophageal cell lines ESO26, N87 and OE19. *Gastro-oesophageal cells were plated 2x10^5 cells/per well and supernatants collected after 72h. Cell debris was removed from supernatant by centrifugation (300rcf/3min) and remaining the supernatant concentrated. Samples were western blotted for basal levels of cJAM-A* ***(A)*** *across the cell lines.*

Appendix K ï Manuscripts

(Attached at rear of Thesis)

Published:

Richards CE, Vellanki SH, Smith YE, Hopkins AM. Diterpenoid natural compound C4 (Crassin) exerts cytostatic effects on triple-negative breast cancer cells via a pathway involving reactive oxygen species. Cell Oncol (Dordr). 2018;41(1):35-46.

Richards CE, Rutherford EJ, Hopkins AM. Cleaved JAM-A - connecting cancer and vascular disease? Oncotarget. 2019;10(39):3831-2.

Vellanki SH, **Richards CE**, Smith, YE, Hopkins, AM The Contribution of Ig-Superfamily and MARVEL D Tight Junction Proteins to Cancer Pathobiology. Cancer Pathobiology. 2016;Current Pathology Reports 2016(2):37-46.

Vellanki SH, Cruz RGB, **Richards CE**, Smith YE, Hudson L, Jahns H, et al. Antibiotic Tetrocarcin-A Down-regulates JAM-A, IAPs and Induces Apoptosis in Triple-negative Breast Cancer Models. Anticancer research. 2019;39(3):1197-204.

In Preperation:

Richards CE, Rutherford EJ, Sheehan K, Fay J, Hudson L, Hopkins AM. Junctional Adhesion Molecule-A: A novel role in gastro-oesophageal combination drug treatments

(Editorial) **Richards CE,** Sheehan K, Hopkins AM. Tissue Microarrays: friend or foe when assessing heterogeneous proteins in gastro-oesophageal cancers?

Appendix L ï Presentations

Awards

- Irish Association of Cancer Research annual meeting- Professor Patrick Johnston Award for Excellence in cancer outreach (2018) Time for a new Taxol? Promising anti-cancerous properties of a natural compound 'C4' in triple-negative breast cancer cells – **Overall winner, Oral Poster Award**
- Beaumont Translational Research Awards annual meeting (2017) Time for a new Taxol? Promising anti-cancerous properties of a natural compound 'C4' in triple-negative breast cancer cells - **Overall winner, Scientific Display Poster Award**
- Irish Association of Cancer Research annual meeting (2018) Time for a new Taxol? Promising anti-cancerous properties of a natural compound 'C4' in triple-negative breast cancer cells - **Shortlisted Display Poster**
- RCSI Research Day annual meeting - (2018) A novel role for Junctional Adhesion Molecule-A (JAM-A) in HER2-positive gastro-oesophageal cancers - **Shortlisted Display Poster**

Oral Presentations

- RCSI Research Day (Thesis-in-three) (2017) Natural compound 'C4' as a novel therapeutic in triple-negative breast cancers
- Irish Epithelial Physiology Group annual meeting (2017) Novel natural compound with anti-cancerous properties in triple-negative breast cancers
- Irish Association of Cancer Research annual meeting - Professor Patrick Johnston Award for Excellence in cancer outreach (2018) Outreach in Cancer Research
- Irish Association of Cancer Research annual meeting- Science communication (2019) Junctional Adhesion Molecule-A (JAM-A): a novel role for cell adhesion protein in HER2-positive in gastro-oesophageal cancers?

- RCSI Research Day (Thesis-in-three) (2019) Junctional Adhesion Molecule-A (JAM-A): a novel role for cell adhesion protein in HER2-positive in gastro-oesophageal cancers?

Display Poster Presentations

- Irish Association of Pharmacologists annual meeting (2016) Natural compound 'C4' as a novel therapeutic in triple-negative breast cancers
- Irish Association of Cancer Research annual meeting (2017) Investigating the anti-cancerous properties of a natural compound 'C4' in triple-negative breast cancers
- European Association of Cancer Research annual meeting (2018) A novel role for Junctional Adhesion Molecule-A (JAM-A) in HER2-positive gastro-oesophageal cancers
- Beaumont Translational Research Awards annual meeting (2018) Gastro-oesophageal Cancers: A novel role for Junctional Adhesion Molecule-A (JAM-A) in HER2-positive cases?
- Irish Association of Cancer Research annual meeting (2019) Junctional Adhesion Molecule-A (JAM-A): a novel role for a cell adhesion protein inn HER2-positive gastro-oesophageal cancers?

Media Engagement

- Irish Association of Cancer Research (2018) Media Workshop in Cancer Outreach – **Selected for Presentation**
- Irish Times (2018) What is the postgrad experience like and how will you cope?'
- Irish Association of Cancer Research (2019) Patient Advocate Workshop in Cancer Outreach